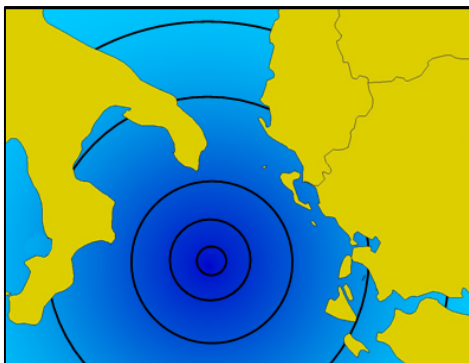


“ex duobus oculis pars unica”

Foreword



We would like to extend a warm welcome to all the participants of the 2nd International Tsunami Field Symposium Puglia - Ionian Islands 2008. This is the second important tsunami meeting organised within the framework of the IGCP Project n. 495 "Quaternary Land-Ocean Interactions: Driving Mechanisms and Coastal Responses" which is led by Anthony Long from Durham University, United Kingdom, and Shahidul Islam, University of Chittagong, Bangladesh.

The 1st International Tsunami Field Symposium was organised by Dieter Kelletat, Anja and Sander Scheffers in March 2006 when the participants enjoyed an interesting scientific week along the coasts of Bonaire, Netherland Antilles.

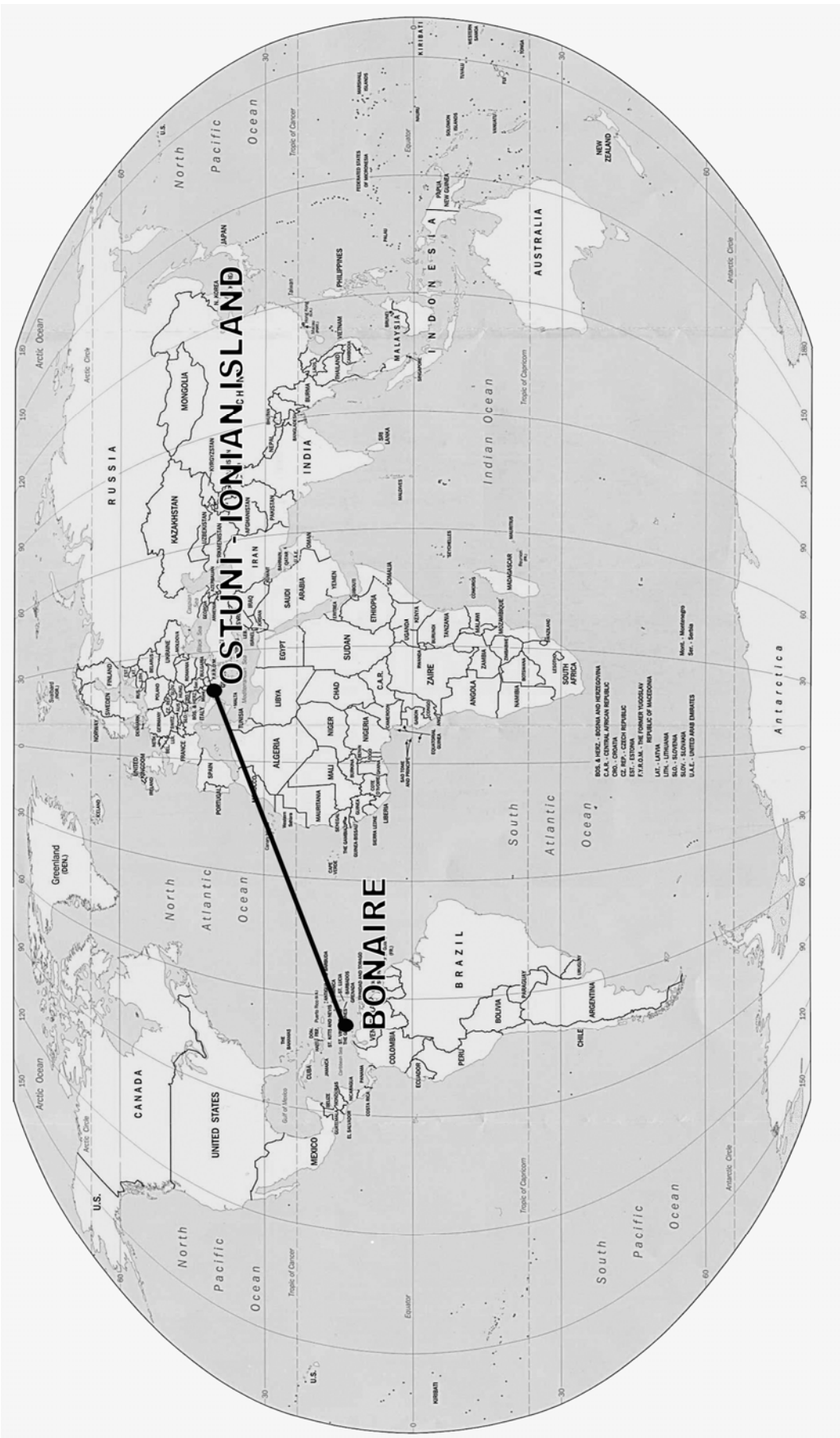
Only about one year before, the most horrific and deadly tsunami in human history occurred on December 26th, 2004. About 300.000 persons died in Indonesia, Thailand, and other countries facing the Indian Ocean in Asia and Africa. The tsunami waves caused also tremendous damage of infrastructure facilities and the environment. Unfortunately, the cause for the incredibly long list of casualties seems to be related to the little knowledge of the tsunamigenic areas and also of the tsunami propagation and its effects on the coasts. Surely, the waves were even more destructive due to the ignorance of the tsunami hazard as a consequence of underrating tsunami risk and vulnerability. There are numerous other tsunami that occurred in the past and killed thousands of people along many coasts of the world. During the past ten years the number of scientific studies consecrated to different aspects of tsunami-related research has impressively increased including geological and geomorphological, geophysical and modelling approaches as well as biological and ecological, social and human, economic and juridical and also engineering and warning aspects. This is all the more important as the scientific community, the local and national administrations and the potentially affected coastal population must not be unprepared for the next event.

This is the first time that an international multi-disciplinary official meeting on tsunami science is to be held both in Italy and Greece. These two countries, both of them facing the Ionian Sea, were affected by two (palaeo-) tsunami which are considered to belong to the most impressive ones in the Mediterranean area: the eruption of the Santorini volcano around 1620 B.C. caused a tremendous tsunami which destroyed many ancient settlements in northern Crete. There are also mythological approaches combining eruption, earthquake and tsunami as potential triggers for the decline of the Minoan civilisation and even for the exodus of the Israelites passing through the Red Sea. The tsunami which destroyed Messina in Sicily and Reggio in Calabria was caused by strong earthquakes along the Malta fault scarp not far from the coast in the Ionian Sea on December 28, 1908. Numerous coastal villages were destroyed by tsunami inundation; in Reggio, the run-up reached 13 m high and the tsunami killing some thousands of people.

Recent tsunami studies carried out along the Italian and Greek coasts revealed geomorphological and sedimentological findings of several tsunami that occurred since the mid-Holocene. In the Mediterranean basin, around three hundred events have been found by modern research techniques within the framework of sedimentological, morphological, biological, archaeological and historical investigations. During the forthcoming symposium, the participants will be introduced to the most significant sites of tsunami landfall in Apulia and the Lefkada-Preveza coastal zone (Ionian Islands).

The book at hand presents extended abstracts of about 50 scientific communications which will certainly improve our overall knowledge on tsunami dynamics. The book may also provide some references useful for the management of coastal areas. There is and, in the future, will be a lot of progress in science. This is all the more true for the last ten years which provided an impressive improvement in tsunami sciences. So, even if we must admit that we are far from considering as final all of our statements, it is necessary that the results of our work will be considered in all administrative affairs.

We would like to thank the INQUA Commission on Coastal and Marine Processes, the INQUA Neotectonics Subcommission, the AIGeo – Italian Association of Physical Geography and Geomorphology, the AMK – German Working Group on the Geography of Coasts and Seas, and the SIGEA – Italian Society of Environmental Geology for the scientific support of this meeting.



Finally, we gratefully acknowledge the technical assistance and financial support by the Administration of the Regione Puglia, by the “Fondazione Cassa di Risparmio di Puglia”, by the Municipality of Ostuni, by the Provinces of Brindisi, Lecce and Taranto, by GAL – Alto Salento, by the Dipartimento di Geologia e Geofisica and the Central Administration of the University of Bari and by the Dipartimento di Scienza dei Materiali the Central Administration of the University of Lecce, by Leica Geosystems S.p.A., Colacem S.p.A. and Geo Data Service s.r.l. without which this symposium would not have been possible.

The Conference Organizers

Giuseppe Mastronuzzi

Paolo Sansò

Helmut Brückner

Andreas Vött



Department of Geography, Philipps Universität zu Marburg, Germany



Department of Geography, Universität zu Köln, Germany



Dipartimento di Geologia e Geofisica, Università degli Studi “Aldo Moro”, Bari, Italy



Dipartimento di Scienza dei Materiali, Università del Salento, Lecce, Italy



Introduction

Welcome to this, the Second International Tsunami Symposium of IGCP 495 “Quaternary land-ocean interactions: driving mechanisms and coastal responses”.

IGCP UNESCO PROJECT 495

Previous IGCP projects have been highly successful in improving our understanding of the patterns of sea-level change and coastal evolution over a wide range of timescales. Indeed, Project 495 has evolved from several previous IGCP programmes including Project 61 “Sea-level change during the last deglacial hemicycle” directed by A.L. Bloom (1974-1982), Project 200 “Sea-level correlation and application” directed by Paolo Antonio Pirazzoli (1983-1987), Project 274 “Coastal evolution in the Late Quaternary” directed by Orson van de Plassche (1988-1993), Project 367 “Late Quaternary coastal records of rapid change” directed by D.B. Scott (1994-1998) and Project 437 “Coastal environmental change during sea-level highstands” directed by C.V. Murray-Wallace (1999-2003). The final meeting of the latter project included a superb meeting and fieldtrip to the Puglia region of Italy, organized by two of the current hosts of this meeting – Giuseppe Mastronuzzi and Paolo Sansò.

Thirty years on from the first IGCP coastal project, the global sea-level community is now well-equipped to develop local, regional and global records of relative sea-level (RSL) change. It is also increasingly able to describe linkages between terrestrial, coastal and marine environments through the application of new techniques of sediment finger-printing, dating, as well as quantitative models of coastal change, sea-level change and sediment flux. The aim of IGCP495 is to focus attention on establishing the driving mechanisms of the patterns we observe and reconstruct. The work has two main dimensions: the vertical component of RSL change and the lateral dimension of changing shoreline position.

IGCP 495 has several working groups, one of the most active of which is the Tsunami working group. This group held its first international field meeting on the island of Bonaire (Netherlands Antilles) in March 2006, organised by Anja Scheffers and Dieter Kelletat, University of Duisburg-Essen, Germany and attended by 21 participants from 10 countries. A special issue including papers from the meeting has been published (Scheffers and Kelletat, 2006) and a report is available on the IGCP495 web site (see below).

As in previous projects, IGCP 495 has strong links with other international research programmes, notably the INQUA Coastal and Marine Processes group and, with particular relevance to this meeting, the working groups that include the Mediterranean Basin (Chair - Ahuva Almogi-Labin), North West Europe (Chair - Roland Gehrels) and Short-term sea level changes and coastal vulnerability (Chair - Fabrizio Antonioli).

Since the inception of IGCP 495, there have been four international meetings of the project:

The inaugural meeting was held in Maine, USA, organized by Joe Kelley and Dan Belknap (University of Maine). The trip provided a wonderful start to the project with a focus on climate-driven sea-level change along the east coast of North America. The second meeting in 2005 was in the Anyer-Carita, Banten-Sunda Strait area of Indonesia, organized by Wahyoe Hantoro and colleagues from the Research Centre for Geotechnology, Indonesian Institute of Sciences (LIPI). The timing of the meeting, so shortly after the Indian Ocean tsunami, provided an opportunity to review recent research associated with this event and a special issue of Marine Geology followed (Gehrels and Long 2007).

The third international meeting of IGCP495 in 2006 was held in Balneário Camboriú, Santa Catarina, Brazil, organized by Rodolfo Angulo and Maria Cristina de Souza (Universidade Federal do Paraná) and Dr. Antônio Klein (Universidade do Vale do Itajaí). The fourth international meeting was held jointly with the INQUA Congress in Cairns. IGCP 495 and the INQUA Commission on Coastal and Marine Processes held the largest session of the entire conference, spreading across three full days of the meeting. Dr. Sarah Woodroffe and Dr.

Scott Smithers (Durham University and James Cook University) ran an excellent field trip along the north Queensland coast. The fifth international meeting will be held in Faro, Portugal by Tomasz Boski, Delminda de Jesus Moura, João M. A. Dias, Cristina Veiga-Pires and Oscar Ferreira in September 2008. The final meeting of project 495 is likely to be held in South Carolina, USA in late June 2009, organized by David Scott and Paul Gayes.

Details of all of the meetings detailed above, including many downloadable copies of field guides, abstracts volumes and trip reports, as well as other information about the project in general, are available from its web site at:

<http://www.geography.dur.ac.uk/projects/igcp495/Home/tabid/333/Default.aspx>

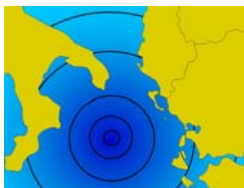
We wish all those attending the Second international Tsunami Symposium an enjoyable and stimulating meeting and would like to take this opportunity to thank the organizers, Giuseppe Mastronuzzi, Paolo Sansò, Andreas Vött and Helmut Brückner for all their hard work in organizing what promises to be a superb meeting.

Antony J. Long^{1*}, Shahidal Islam^{2*}

* Project leaders, IGCP 495

¹Department of Geography, Durham University, Durham DH1 3LE, UK,
e-mail: A.J.Long@Durham.ac.uk

²Department of Geography, University of Chittagong, Bangladesh, e-mail: shahidulbd@gononet.com



Armigliato A.¹, Tinti S.¹, Tonini R.¹, Pagnoni G.¹, Gallazzi S.¹, Manucci A.¹, Zaniboni F.¹,
Mastronuzzi G.², Pignatelli C.², Sansò P.³

The 20th February 1743 tsunamigenic earthquake in Apulia, Italy: investigation on the source from numerical tsunami modelling and geological evidences

¹Università di Bologna, Dipartimento di Fisica, Bologna (Italy), e-mail: alberto.armigliato@unibo.it;

²Dipartimento di Geologia e Geofisica, Università degli Studi "Aldo Moro", Bari (Italy),
e-mail: g.mastrozz@geo.uniba.it; c.pignatelli@geo.uniba.it;

³Osservatorio di Chimica, Fisica e Geologia ambientale, Dipartimento di Scienza dei Materiali,
Università degli Studi del Salento, Lecce (Italy), e-mail: paolo.sanso@unile.it;

Keywords: *historical tsunamis, numerical modelling, boulders, coastal morphology, Apulia*

On 20th February 1743 a strong earthquake (M=6.9 according to the CPTI04 Catalogue) severely hit the Salento peninsula (Apulia, southern Italy) and the Greek Ionian Islands (Fig. 1). It was felt in a very large area, including Calabria, the Messina Straits and Naples.

The maximum macroseismic intensity (IX MCS) was recorded in the towns of Nardò and Francavilla Fontana in southern Apulia, where most buildings were ruined, and in the village of Amaxichi, in the Lefkada island.



Figure 1. Geographical position of studied area. The black star indicates the 1743 epicentre position according to CPTI04. Intensities in the most affected sites are taken from Stucchi et al. (2007).

The earthquake was responsible for more than 160 victims in Apulia and about 100 in the Ionian islands, Greece. The earthquake generated a tsunami, the historical accounts on which are quite scarce. The only available report describes some tsunami effects in the harbour of Brindisi, where the sea withdrew (see the Italian Tsunami Catalogue, Tinti et al., 2004).

The impact of the tsunami waves generated by the 1743 earthquake along the Ionian and Adriatic coasts of Apulia appears to be well documented from the geomorphological point of view. The morphological evidences are particularly recognizable along the coastal tract comprised approximately between Capo Santa Maria di Leuca (S.M.Leuca) and Brindisi (Fig. 2). It is a ~200 km long stretch of microtidal coast, where the morphographic features can vary significantly

depending on the outcropping lithological units and on the wave climate. Moving from North to South along this coastal segment, three different sites are found that preserve the most evident signatures (mostly boulders) of the impact of tsunami waves and in a couple of sites the deposits can be reasonably attributed to the 1743 event. The sites are Torre Santa Sabina, Torre Sant'Emiliano and Torre Sasso (Fig. 2).

In the first one, boulders are arranged either in small groups or rows composed of a few imbricated elements coming from the intertidal area; their sizes suggest weights up to 8 tons. The boulders, that have been recognized up to 1.5 m above biological sea level (b.s.l.) and at about 15 m inland, were probably accumulated due to the superimposed effects of two distinct tsunamis as well as of storm waves (Mastronuzzi & Sansò, 2004).

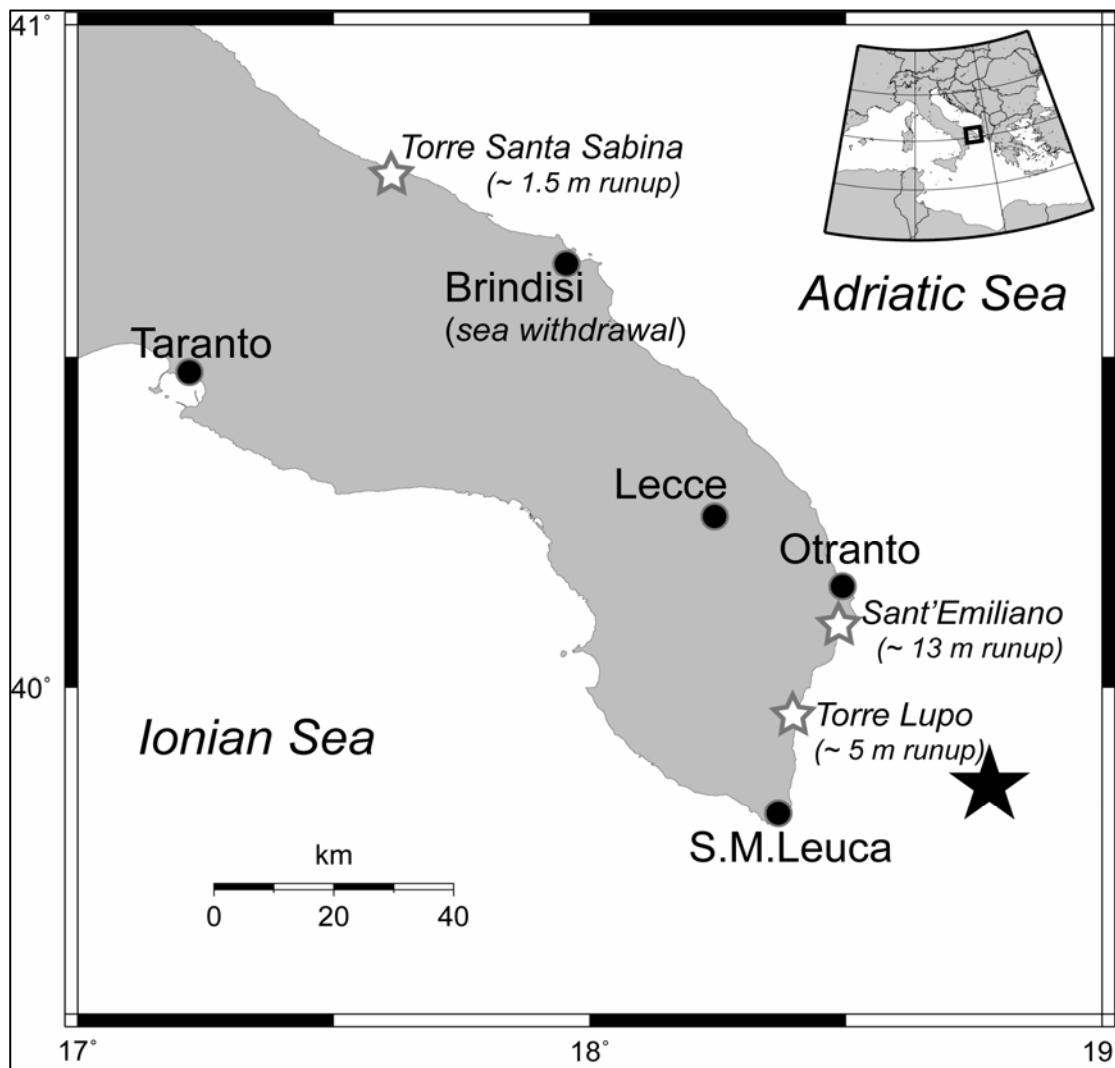


Figure 2. Position of the places (white stars) where the boulder accumulations imputable to the 1743 tsunami have been observed and characterised. As in Fig. 1, the black star indicates the 1743 epicentre position according to CPTI04.

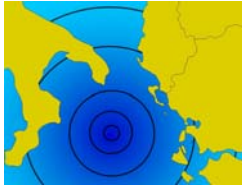
At Torre Sant'Emiliano the best evidences of the February 20, 1743 tsunami impact are recognizable: two almost continuous boulder ridges, about 40 m wide, can be observed, with the innermost placed at a height of about 10 m above b.s.l. and the seaward one exposed up to 11.5 m above b.s.l.. Boulders are up to 75 tons in weight and are placed at about 13 m above b.s.l. (Mastronuzzi et al., 2007). Finally, at Torre Sasso two almost continuous boulder ridges, about 40 m wide, are present, with the innermost placed at a height of about 10 m above b.s.l. and the seaward one exposed up to 11.5 m above b.s.l.. A maximum weight of about 31 tons was estimated.

The main goal of this study is to put some constraints on the source of the 1743 tsunamigenic earthquake by numerical modelling of the tsunami itself and comparing the results with the above mentioned geomorphological evidences. To do this, based on some basic information coming from local tectonics, we take into account a small number of seismic sources and for each of them we simulate numerically the ensuing tsunami, trying to reproduce the data on runup and inundation length. More specifically, for each studied fault (basically chosen from the FAUST database, see Valensise et al., 2002) we compute the coseismic deformation of the sea bottom and take it to be identical to the tsunami initial condition. The subsequent tsunami wave propagation is computed by means of a finite-differences numerical code, UBO-TSUF, developed at the Department of Physics of the University of Bologna, which implements and solves the Navier-Stokes equations in the shallow-water approximation and includes the computation of the tsunami inundation on the coasts. For each run, we compare the numerical results with the available geological and historical evidences: attention is posed especially on the tsunami wave propagation direction, on the polarity of the first wave arrivals in some selected coastal stations in southern Apulia and on the spatial distribution of

the extreme water elevations along the coastlines. The results are discussed in order to draw some preliminary conclusions on the most probable source area and geometry for the 1743 tsunamigenic earthquake.

References

- Gruppo di Lavoro CPTI04 (2004). *Catalogo Parametrico dei Terremoti Italiani, versione 2004 (CPTI04)*. INGV, Bologna.
<http://emidius.mi.ingv.it/CPTI04>
- Mastronuzzi G., Sansò P. (2004). *Large Boulder Accumulations by Extreme Waves along the Adriatic Coast of southern Apulia (Italy)*. Quaternary International, 120, 173-184.
- Mastronuzzi G., Pignatelli C., Sansò P., Selleri G. (2007). *Boulder Accumulations Produced by the 20th of February, 1743 Tsunami Along the Coast of Southeastern Salento (Apulia Region, Italy)*. Marine Geology, 242, 191-205.
- Stucchi M. et al. (2007). *DBMI04, il database delle osservazioni macrosismiche dei terremoti italiani utilizzate per la compilazione del catalogo parametrico CPTI04*.
<http://emidius.mi.ingv.it/DBMI04/>
- Tinti S., Maramai A., Graziani L. (2004). *The New Catalogue of Italian Tsunamis*. Natural Hazards, 33, 439-465.
- Valensise G., Basili R., Mucciarelli M., Pantosti, D. (2002). *Database of potential sources for earthquakes larger than M 5.5 in Europe, a compilation of data collected by partners of the EU project FAUST*.
http://legacy.ingv.it/roma/banche/catalogo_euro_pao/index.html
- Ambraseys N.N. (1962). *Data for investigation of seismic sea waves in the Eastern Mediterranean*. Bulletin Seismology Society American, 52, 895-913.



Bahlburg H.^{1*}, Spiske M.¹, Amijaya H.³, Weiss R.², Piepenbreier J.¹

Sedimentological characteristics

of the July 17, 2006 tsunami in South Java

¹Westfälische Wilhelms-Universität, Geologisch-Paläontologisches Institut, Münster, Germany

²JISAO, University of Washington - NOAA Center for Tsunami Research, Seattle, USA

³Department of Geological Engineering, Gadjah Mada University, Indonesia

*corresponding author: bahlbur@uni-muenster.de

Keywords: *tsunami, sedimentary structures, grain size analysis, Java*

With the help of tsunami deposits, tsunami run-up characteristics and tsunami depositional processes can be inferred in order to understand tsunami as a geological process, but also to recognise tsunami deposits within sedimentary deposits of different sedimentary environments.

Unique features of such deposits have not been identified to distinguish them from, for example, storm or other deposits indicating high-energy regimes within sandy beach deposits. It is still unresolved in which water depths and environments tsunami entrain sediment during run-up.

We report the initial results of a study of the deposits of the July 17, 2006 Java tsunami (Fig. 1). The Java tsunami was caused 200 km off the south coast of Java by a ca. 10 km deep M_w 7.8

earthquake at 15:19 local time. The quake caused a ca. 200 km trench-parallel rupture and struck the coast 20 minutes later (Ammon et al., 2006). Depending on the geometry of coast and beaches, run-up heights exceeded 20 m at headlands, and were significantly lower, less than 2 m, along many straight beaches. The flow depth reached c. 165 cm at a distance of 150 m from the swash zone.

We surveyed beaches along the central south coast of Java between Pandangaran and Parangtritis south of Yogyakarta (Fig. 1), sampled the tsunami deposits, and measured the maximum run-up distance of 700 m to the west of Pandangaran. Quasi-linear debris accumulations document up to three waves of decreasing inundation and run-up.

The tsunami deposits consist of sand, reach

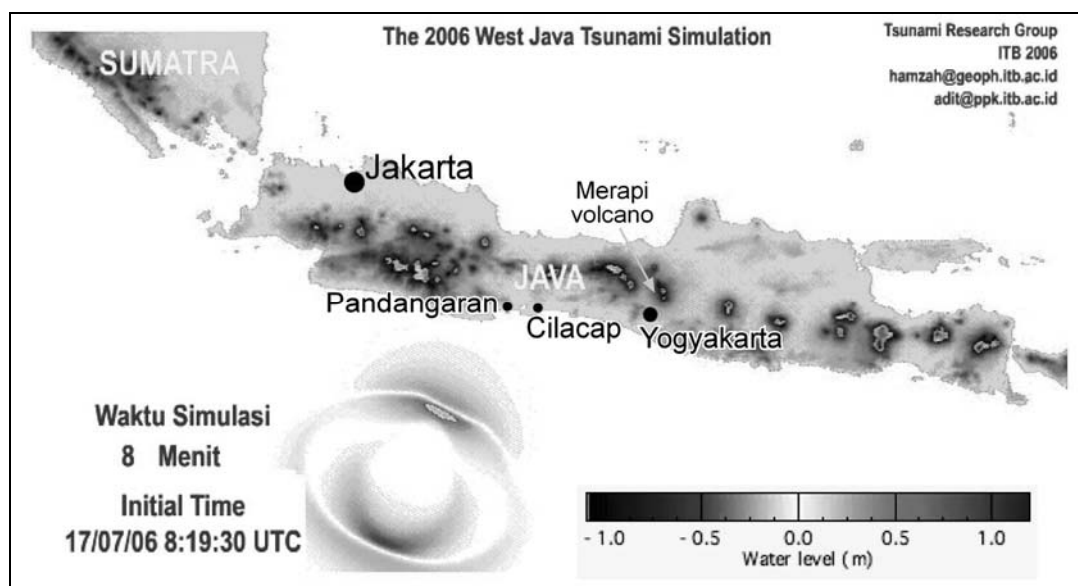


Figure 1. Screen shot of simulation of the July 17, 2006 Java tsunami 8 minutes after tsunami initiation (Latif, 2006). The tsunami caused damages mainly between Pandangaran and the coast south of Yogyakarta. Deposits are best preserved along the same part of the coast.

maximum thicknesses of 10 cm, display a weakly developed fining-inland trend, and taper out approximately at half the run-up distance.

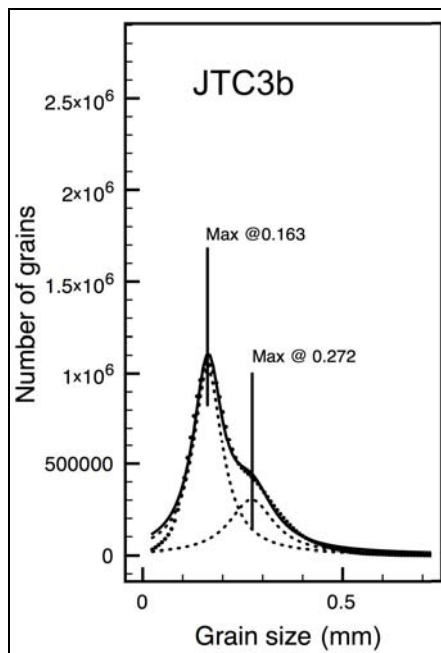


Figure 2. Grain-size distribution of the basal lamina of tsunami sample JTC3b near Cilacap (Fig. 1), measured by digital-optical analysis (solid line). Deconvolution of the grain-size distribution (dashed lines) indicates the presence of two-grain populations with modes differing by approximately between 0.05 and 0.1 mm.

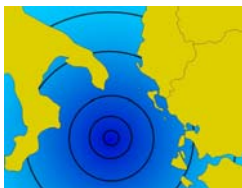
They commonly have erosive bases and consist of one to five parallel-laminated and in some cases graded layers. Bottom layers may contain soil rip-up clasts eroded from inundated agricultural fields. Sedimentary structures include small current ripples produced by backwash flow in morphological depressions. Larger palm trees were bent inland during tsunami run-up whereas the less energetic backwash bent smaller palm trees seaward.

The beach sands underlying the tsunami deposits are rich in detrital magnetite. Deconvolution of grain-size distributions of both beach and tsunami deposits revealed that most tsunami deposits consist of at least two well-sorted sandy, normal grain populations, the modes of which differ by between 0.05 and 0.1 mm (Fig. 1).

Separate grain-size analysis of magnetic and non-magnetic detritus demonstrates that the two normal distributions correspond to the magnetic and non-magnetic fractions. As the composition of tsunami sands is similar to beach and near shore marine sands, we conclude that the detritus constituting the tsunami deposits was derived locally.

References

- Ammon C.J., Kanamoori H., Lay T., Velasco A.A. (2006). *The 17 July 2006 Java tsunami earthquake*. Geophysical Research Letters 33, L24308.
- Latif H. (2006). <http://www.ppk.itb.ac.id/tsunami2006/jabar.gif>.



Belousov A.¹, Belousova M.¹

Deposits and effect of tsunamis generated by the 1996 underwater explosive eruption in Karymskoye Lake, Kamchatka, Russia

¹*Institute of Volcanology and Seismology, Petropavlovsk-Kamchatsky, Russia. e-mail: belousov@mail.ru*

Keywords: tsunami deposits, underwater explosion, Kamchatka

The 1996 underwater explosive eruption in Karymskoye Lake generated multiple tsunamis up to 30 m high, which strongly eroded shores of the lake and left various deposits. This event provided a unique opportunity to study the effect of tsunami of explosive origin.

Karymskoye Lake and course of the 1996 eruption

Karymskoye caldera lake is located in an uninhabited region of the Eastern Volcanic Belt of

Kamchatka Peninsula (Fig. 1). The lake has almost circular shape with diameter ~4 km, maximum depth 65m, and contains ~ 0.5 cub. km of fresh water. The lake is drained by the Karymskaya River. The surface of the lake has an altitude of 624 m above sea-level. From November to June the lake is covered by ice (up to 1 m thick) and snow (up to several metres thick). The shores of the lake are heavily vegetated by alder bushes. Before the eruption there were no well-developed beaches around the lake.

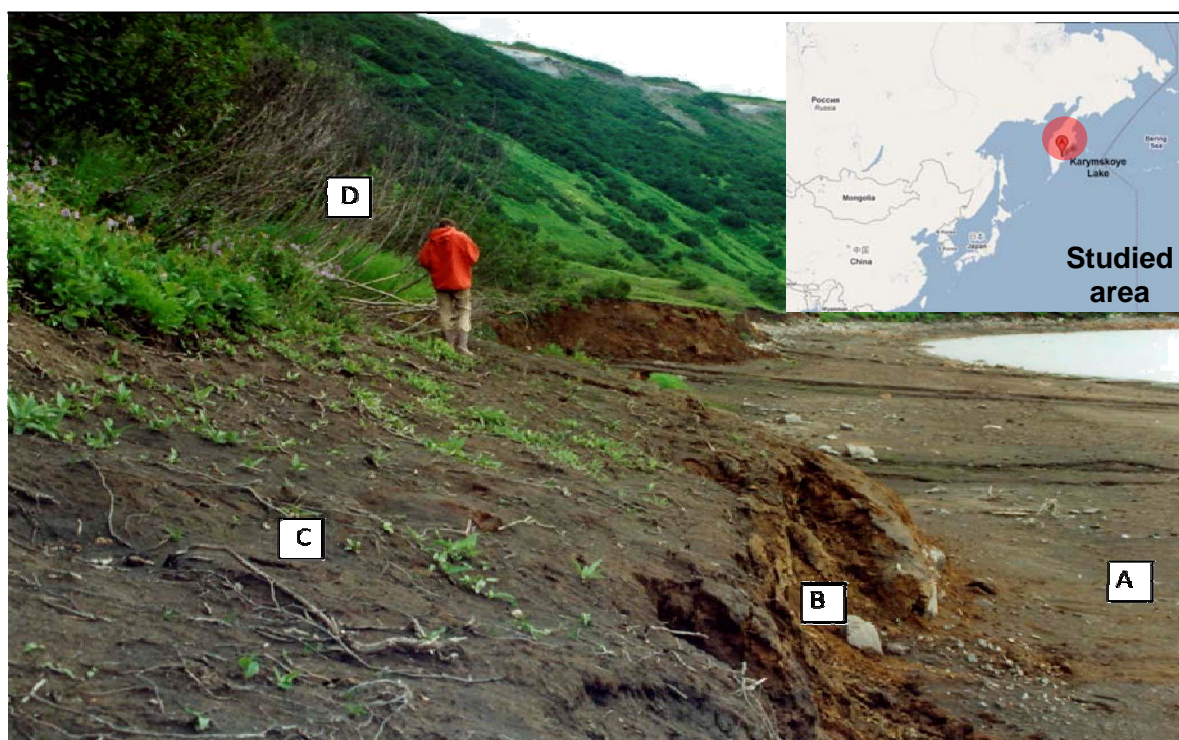


Figure 1. Shore of the lake affected by the 1996 tsunamis. The beach, (A) cliff; (B) and area with stripped vegetation; (C) were formed by tsunami erosion. Limit of the tsunami invasion marked by dry bushes; (D) (See text for details).

The 1996 underwater eruption in Karymskoye caldera lake started early in the morning on January 2. The total duration of the eruption is estimated as 10-20 hours. The only observation of the eruptive processes in the lake was made during an overflight at 15²⁰-16²⁰ LT. By the time of the overflight, the ice cover of the lake had melted, and an eruption of Surtseyan type was in progress from a vent ~400 m off the northern shore. Initial water depth above the vent is estimated as ~50 m.

Underwater explosions represented separate vertical outbursts of water-gas-pyroclastic mixture with initial velocities of 110 m/s. The ejected material reached heights up to 1 km above the lake surface, and then collapsed back into the lake producing base surges (runout up to 1.3 km; average velocity 12.5 m/s). The eruptive cloud rose to a convective height of 3 km. Underwater explosions generated tsunamis, which periodically forced water from the lake into the canyon of Karymskaya River, forming pulsing lahars. Underwater explosions occurred every 4-12 min; in total about 6 explosions were observed during the overflight with an average interval of 6 min. Taking the average observed interval between the explosions as 6 min, we estimate that 100-200 explosions in all occurred in the lake in the course of eruption.

Tsunamis

The effect and deposits of the tsunamis were studied in 7 months after the eruption. The area affected by tsunamis is marked around the lake by strong erosion of the shore line, water-damaged bushes and the tsunami deposits. The degree of the erosion of the shoreline declines with distance from the eruption crater. In proximal area the strongest erosion occurred on the steep northern shore of the lake adjacent to the crater. The slope was eroded up to 30 m above the level of the lake, with all plants and soil more than 1.5 m thick stripped so as to expose poorly consolidated bedrock. No deposits of the eruption were found in the eroded area. We suppose that the shore here was eroded by both tsunamis and flows of water-pyroclastic mixture ejected from the crater by the explosions. Pyroclastic deposit of the eruption adjacent to the base of the eroded slope is repeatedly interbedded with layers, 10-20 cm thick, which are rich in clasts of yellow, altered rock, and pieces of plants eroded from the slope. Such layers are interpreted as backwash deposits of the tsunamis.

The action of the multiple tsunamis in many places around the lake formed new beaches up to 50 m wide (area A on Fig. 1), which are terminated by new cliffs up to 2-3 m high (area B).

Further from the lake (inland, behind the cliff) is an area C, up to 50 m wide, where the upper layer of soil up to 1.5 m thick was eroded and all plants were washed back into the lake. Along the outer boundary of the area inundated by the tsunamis (area D), soil was not eroded and bushes with some broken branches remained standing, but were killed by the action of the lake water (warm and acidic due to eruption). Later they dried and served as a good marker of the inundation limit. The width of area D ranges from 1 m to 100 m.

Deposits left by the tsunamis can be divided into two main classes: those composed of non-floating material, which was deposited near the place where it was mobilised, and those represented by floating objects, which before final deposition could drift considerable distances.

Two types of deposits of the first class were discovered: individual blocks of poorly consolidated old tuff and patches of sand. The tuff blocks 0.1-4 m across originate from newly eroded cliffs. They are abundant on the NE shore of the lake, and are almost entirely absent on the southern shore, which is composed mostly of hard, unerodible rocks. Blocks are scattered on the surface of the beaches or incorporated into the beach deposits below the cliffs (area A). Some blocks with volumes up to 1.3 m³ were transported by the tsunamis from their source up to 60 m inland (into areas C and D). Patches of sand are common in area D, but sometimes can be found in area C. The patches are usually meters to tens of meters across and up to 35 cm thick. The sand with scattered pebbles, fragments of plants and clots of soil is well sorted (0.7 to 2.1 phi). Sometimes up to 4 parallel layers with thickness 2-6 cm can be distinguished, which reflect the multiple waves of tsunami runup and backwash. The composition and grain size of the deposit reflects the material mobilised by the tsunami. In the zone near the crater the deposit comprises mostly fresh basaltic pyroclasts of the eruption. Further from the crater the deposit is composed of picked up beach sand.

Deposits of floated material are represented in areas C and D by scattered well rounded pebbles of pumice, 2-10 cm in diameter, and branches of bushes, which are oriented mostly perpendicular to the direction of tsunami runup. They are most abundant on the SE shore, which is the result of a NW wind that blew during the eruption. Here pumice pebbles comprise patches and bands up to 3 m across and up to 20 cm thick, with openwork fabric. These resemble deposits of the much larger scale tsunamis that accompanied the 1883 Krakatau eruption. Unlike Krakatau, pumice deposited by the 1996 tsunamis was not fresh, but was eroded by the tsunamis from old pyroclastic deposits.

In both cases the floating pumice formed “pumice rafts”, which were cast ashore. In Karymskoye Lake the rafts also contained abundant floating bushes.

After deposition on the SE shore, interlaced branches of bushes formed “wooden rampart” up to 2 m high, 10-15 m wide and several hundred meters long. Branches of the ramparts are completely debarked with rounded or splintered, brush-like ends, that indicates their prolonged beating by tsunami waves before final deposition.

There are two lines of evidence suggesting that the largest of the tsunamis occurred at the end of the eruption. First, the areas eroded by tsunamis are not covered by ash fall of the eruption. Second, the composition of floated material deposited on the SE shore shows that it originates mostly from the northern shore. Thus several hours during the eruption were needed for the floating material washed off from the northern shore to drift across the lake to be deposited on the SE shore.

The distinctive band of devastation, and the tsunami deposits, allowed us to measure the runup height of the tsunamis at 24 points around the lake (Fig. 2).

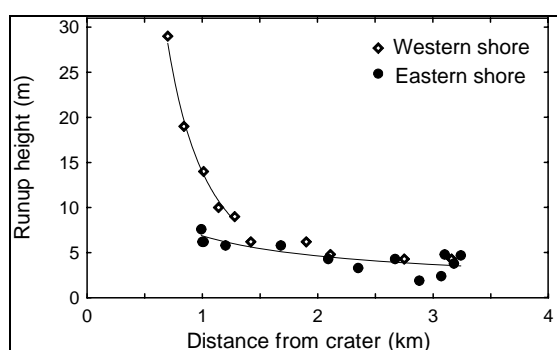


Figure 2. Tsunami runup versus distance from the crater. Note change in trend ~ 1.3 km from the crater.

Because there were several tsunamis, the measurements represent the runup of the strongest

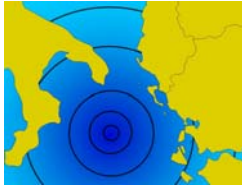
event. The highest runup (20-30 m) occurs on the shore immediately adjacent to the crater.

For the proximal zone, to radial distances (r) up to 1.3 km, the runup height (R) shows rapid attenuation with distance as $\log R = -1.98 \log[r] + 2.6$. For the distal zone, $r > 1.3$ km, R decays more slowly as $\log R = -0.56 \log[r] + 1.9$. For the most distant points, tsunami runup was 2-3 m.

Tsunami, a Japanese term that usually describes extraordinary water waves generated in seas or large lakes by earthquakes, volcanic eruptions, landslides and so on. The fast decay of the runup of the Karymskoye's tsunamis in the proximal zone can be a sign that they were not only water waves, but also flows of water or/and water-pyroclastic mixture ejected by underwater explosions. In the distal zone, however, evidence indicates that they were conventional tsunami waves.

References

- Belousov A., Voight B., Belousova M., Muraviev Y. (2000). *Tsunamis generated by subaquatic volcanic explosions: unique data from 1996 eruption in Karymskoye lake, Kamchatka, Russia*. Pure Applied Geophysics, 157, 1135-1143.
- Belousov A., Belousova M. (2001). *Eruptive process, effects and deposits of the 1996 and ancient basaltic phreatomagmatic eruptions in Karymskoye lake, Kamchatka, Russia*. In Lacustrine Volcanoclastic Sedimentation (ed. by White J.D., Riggs N.R. (eds) IAS Special Volume, 30, 235-260
- Latter J. (1981). *Tsunamis of volcanic origin: summary of causes, with particular reference to Krakotoa, 1883*. Bulletin Volcanology, 44, 467-490.



2nd International Tsunami Field Symposium

IGCP Project 495

Quaternary Land-Ocean Interactions:
Driving Mechanisms and Coastal Responses

Ostuni (Italy) and Ionian Islands (Greece) 22-28 September 2008



Project 495

Costa P.¹, Andrade C.¹, Freitas M. C.¹, Oliveira M. A.¹, Taborda R.², da Silva C. M.¹

High energy boulder deposition in Barranco and Furnas lowlands, western Algarve (south Portugal)

¹Centro de Geologia, Universidade de Lisboa, Faculdade de Ciências, Departamento de Geologia, Lisboa, Portugal

²LATTEX-IDL, Universidade de Lisboa, Faculdade de Ciências, Departamento de Geologia, Lisboa, Portugal,

e-mail: ppcosta@fc.ul.pt; candrade@fc.ul.pt; cfreitas@fc.ul.pt; maoliveira@fc.ul.pt;
rtaborda@fc.ul.pt; paleocarlos@fc.ul.pt

Keywords: *Tsunami, storms, boulders, sediment transport, bioerosion, southern Portugal*

Introduction

The south Algarve coast of Portugal is an area rarely subjected to extreme storms or tsunamis, though both types of events have been recurrent. The most devastating tsunami that affected the Portuguese coast in historical times took place in AD 1755 and several studies discussed sandy sedimentation associated to that event in Portugal and elsewhere, in contrast with few reports on deposition of larger particles. Here, we present first results obtained in the scope of Project NEAREST (*integrated observations from nearshore sources of*

tsunamis: towards an early warning system), on the characterization of boulder-sized clasts from two coastal lowlands (Barranco and Furnas) of the western section of the south Algarve coast and discuss entrainment and depositional mechanisms and the location of their source area.

The westernmost section of the southern Algarve coast is high (*circa* 40m above mean sea level) and rocky, sea cliffs cutting resistant Jurassic limestones and dolomites (Fig. 1).

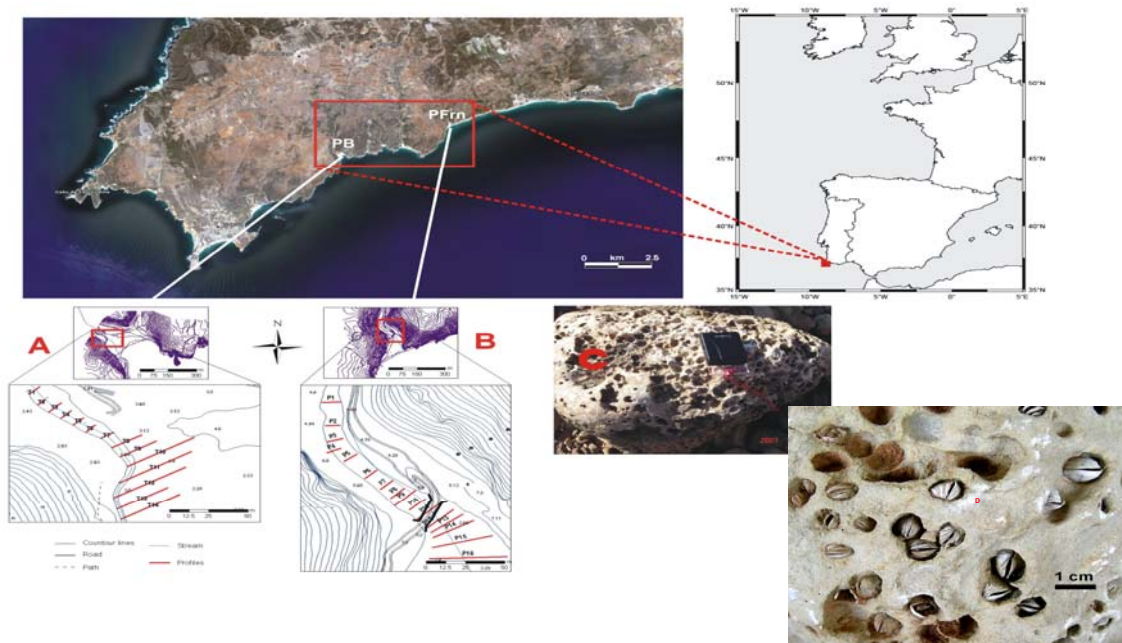


Figure 1. General overview of the study areas. PB - Praia do Barranco. PFrn - Praia das Furnas. Red lines in [A] and [B] indicate profiles where boulders have been measured; [C] and [D] – perforated boulders; note endolithic shells (photos: Google Earth, P.J.M. Costa, C. M. Silva).

The drainage system consists of few ephemeral rivulets running in deeply incised canyon-shaped valleys. In their downstream sections the valleys are flat-floored and choked with alluvial mud, the valley bottom resting some 2-3m above mean sea level. The narrow alluvial floodplains are limited seawards by beaches, usually made of a thin veneer of sand covering shingle, in agreement with the sand-starved character of this coast, and backed by overwash fans, essentially made of sand and eventually including scattered boulders, reaching up to 100m in width.

Barranco and Furnas are narrow flat-floored canyons, the stream flowing across small floodplains, which consist of sandy mud and abundant heterometric angular pebbles, cobbles and occasional boulders, mixed with lithic and quartz grit. Towards the beach the stream deposits spread into a thin discontinuous gravely fan, resting upon the alluvial mud and merging with backbeach sand. Here, the gravel is a mixture of fluvial and marine-sourced pebbles to boulders bearing macrobioerosion features.

Marine boulder deposits

Marine-borne pebbles, cobbles and boulders found in Barranco and Furnas extend up to 250-300m inland from the berm crest (Tab.1) above the spring high-tide line; they were not found at higher elevations, namely in the confining valley slopes.

Their marine source is evidenced by well developed macrobioerosion sculpturing that includes ichnofossils produced by marine organisms such as clionid sponges (*Entobia* isp. bioerosion structures) and boring bivalves (*Gastrochaenolites* isp. bioerosion structures) as well as numerous *in situ* and extremely well preserved skeletal remains of the endolithic shallow marine *Petricola lithophaga* bivalve inside their original borings (Fig. 1D). These features indicate that each of these clasts has been originally sculptured and bored in a very shallow, infra- to low meso-littoral, non depositional and rocky marine environment, preceding its entrainment and redeposition inland and also suggest a recent date for its emplacement. Today, environments with these characteristics can be found along the western Algarve littoral.

Most of the endolithic bivalve shells preserved *in situ* within the boulders showed both valves still articulated and clearly protruding outside their borings, sticking out above the host-rock surface. Given their fragile nature, this implies the absence of prolonged activity of downwearing of the boulders during transport and redeposition. This suggests simultaneous entrainment of coarse lithic particles from the shallow sea floor, rapid shoreward transport as suspended load (with minimum particle-particle and particle-bottom interaction, therefore excluding sliding, rolling and frequent saltation) followed by deposition inland.

Profile	A-axis (m)	B-Axis (m)	C-axis (m)	Distance to coast (m)	Volume (m ³)	Weight (kg)	Ht (m)	Hw (m)
P1	0.44	0.30	0.23	253	0.030	78.94	0.19	0.77
P2	0.40	0.33	0.16	234	0.021	54.91	0.29	1.16
	0.27	0.26	0.23	234	0.016	41.98	0.16	0.64
	0.56	0.30	0.18	234	0.030	78.62	0.23	0.92
P3	0.75	0.55	0.30	221	0.124	321.75	0.40	1.61
	0.44	0.33	0.28	221	0.041	105.71	0.19	0.77
P4	0.48	0.25	0.24	212	0.029	74.88	0.15	0.59
P5	0.60	0.30	0.17	203	0.031	79.56	0.24	0.96
	0.60	0.40	0.30	203	0.072	187.20	0.24	0.96
P6	0.60	0.50	0.30	183	0.090	234.00	0.34	1.37
	0.35	0.25	0.20	183	0.018	45.50	0.17	0.66
P7	0.40	0.18	0.15	171	0.011	28.08	0.13	0.53
P8	0.29	0.22	0.22	162	0.014	36.49	0.13	0.54
P9	1.60	1.00	0.50	156	0.800	2080.00	0.74	2.95
P11	0.48	0.36	0.15	140	0.026	67.39	0.35	1.41
P12	0.45	0.40	0.25	132	0.045	117.00	0.28	1.11
P13	0.76	0.40	0.40	127	0.122	316.16	0.19	0.78
P14	0.90	0.46	0.40	121	0.166	430.56	0.24	0.96
P15	0.80	0.54	0.25	109	0.108	280.80	0.45	1.82
P16	1.15	0.60	0.55	95	0.379	986.70	0.28	1.13

Table 1. Characteristics of boulders of Furnas and minimum height of tsunami (Ht) and wind (Hw) waves required to exceed the threshold of movement (see text for explanation).

In order to search for a pattern of spatial distribution in size, a number of regularly spaced cross valley profiles were surveyed upstream of the beach at each site; the number of clasts bearing macrobioerosion features in each profile was noted and the largest boulders measured (Fig. 1A, B, Table 1). The results showed that there is no clear trend in size variation with distance, whereas the number of bored clasts is higher in the vicinity of the beach and rapidly drops further inland. These results are consistent with their lifting from the shallow marine zone and inland transportation excluding size selection and suggest that deposition was essentially a non-gradational process.

Entrainment and transport of boulders

Noormets et al. (2004) indicated that tsunamis as well as large swell waves are capable of quarrying large boulders from the rocky shore, provided that sufficient initial fracturing is present. However, wind waves are seldom capable of emplacing large blocks onto the emerged platform (due to the rapid disintegration of the waves after breaking) in contrast with tsunamis, which have longer duration and attain higher velocities (Goto et al., 2007 indicate $8-15\text{ms}^{-1}$ for the 2004 tsunami in Thailand).

Nott (1997, 2003) presented a set of equations relating the forces involved in the transport of submerged boulders in coastal areas. Application of these equations to the boulders of Barranco and Furnas indicate that low energy storms have the capacity to move them. The heaviest particle detected at Furnas could be moved by a storm with H_w of only 2.94m (Table 1). Moreover, all boulders could have been moved by wind waves smaller than 3m.

Komar and Miller (1974) and Soulsby (1997) addressed the issue of threshold wave height required to induce motion of particles resting in the sea floor and compared computed results with experimental data. Application of Airy wave theory in combination with the latter solutions to the most frequent boulder size (B-axis~0.3m) in both Algarve field sites indicates a threshold wave height of about 5m at depths of 3m (the same depth implied in Nott's approach) and the height should increase to at least 8m in the case of the largest boulder (B-axis~1m). This set of results practically rules out a wind-generated wave origin for the boulder deposits, in clear contrast with the former conclusion. The large discrepancies found between results yielded by the two approaches may reside in different assumptions on the mode of particle threshold (sliding or rolling) and on the length scales of particles and of sea bottom roughness, issues that are not clearly discussed in those papers, but that Wiberg and Smith (1987) indicate as

governing significant changes in near-bottom critical shear stress.

Regardless the physical aspects, it is worth to note that the wave climate in the Algarve is one of low-energy. On average, once every winter a SW storm raises waves with significant height of about 3m and mean period of 7-8s (Capitão, 1992). Taking exceedance of threshold of movement according to Nott's solutions as implying the entrainment and landward transport of gravel particles from the nearshore during storms, formation of boulder storm-ridges and washovers with abundant perforated clasts containing *in situ* shells of endolithic marine bivalves and other bioerosion structures should be quite common during winter along the rocky coast of Algarve, and this is clearly not the case. In addition, there is a substantial difference between attaining the threshold of particle movement under waves and sustaining its continuous transportation upslope in the direction of wave travel for a distance exceeding several wavelengths. Based on the results and discussion stated above, we hypothesize a tsunami origin for the Barranco and Furnas boulders.

Conclusions

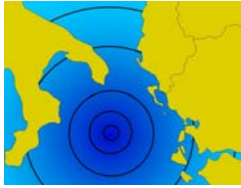
Boulders accumulated at Barranco and Furnas lowlands were entrained from the sea floor and rapidly transported without significant wearing out before redeposition up to 300m inland by an exceptionally high energy inundation episode. The deposit includes numerous bored particles with *in situ* shells of endolithic marine bivalves and other bioerosion structures, that show no trend in size variation with distance to the shore, though the number of bored clasts is higher in the vicinity of the beach and rapidly drops inland. These results are consistent with their lifting from the shallow marine zone and inland transportation excluding size selection and suggest that deposition was essentially a non-gradational process.

Application of two distinct threshold criteria resulted in contrasting values of minimum wave height required for particle entrainment and in different driving mechanisms (storm *versus* tsunami). The low-energy wave regime and nature of storm washovers in the Algarve coast suggest a tsunami as the most probable cause for the emplacement of these boulders.

References

- Capitão R. (1992). *Wave climatology of the Portuguese coast. Clima de agitação marítima na costa portuguesa*. Unp. Tech. Rep. NATO PO-Waves TFOM 10/92, Instituto Hidrográfico, Lisboa, 14 pp.

- Goto K., Chavanich S., Imamura F., Kunthasap P., Matsui K., Minoura K., Sugawara D., Hideaki Y. (2007). *Distribution, origin and transport process of boulders deposited by the 2004 Indian Ocean tsunami at Pakarang Cape, Thailand*. *Sedimentary Geology*, 202, 821-837.
- Komar P., Miller M. C. (1975). *On the comparison of the threshold of sediment motion under waves and unidirectional currents with a discussion of the practical evaluation of the threshold*. *Journal of Sedimentary Petrology*, 45, 362-367.
- Noormets R., Crook K.A.W., Felton E.A. (2004). *Sedimentology of rocky shorelines: 3. Hydrodynamics of megaclasts emplacement and transport on a shore platform, Oahu, Hawaii*. *Sedimentary Geology*, 172, 41-65.
- Nott J.F. (1997). *Extremely high-energy wave deposits inside the Great Barrier Reef, Australia: determining the cause — tsunami or tropical cyclone*. *Marine Geology*, 141, 193-207.
- Nott J.F. (2003). *Waves, coastal boulders and the importance of the pre-transport setting*. *Earth and Planetary Science Letters*, 210, 269-276.
- Soulsby R. (1997). *Dynamics of marine sand. A manual for practical applications*. Thomas Telford, London, 249 pp.
- Wiberg P. Smith J. D. (1987). *Calculations of the critical shear stress for motion of uniform and heterogeneous sediments*. *Water Resources Research*, 23, 8, 1471-1480.



De Martini P. M.¹, Burrato P.¹, Pantosti D.¹, Maramai A.¹, Graziani L.¹, Abramson H.²
**Identification of tsunami deposits and liquefaction features in the
Gargano area (Italy): paleoseismological implication**

¹Istituto Nazionale di Geofisica e Vulcanologia, Sezione di Roma 1, Italy, e-mail: demartini@ingv.it;

burrato@ingv.it; pantosti@ingv.it; maramai@ingv.it; graziani@ingv.it;

²Geomatrix Consultants, Ca, USA, e-mail: habramson@geomatrix.com

Keywords: *tsunami, liquefaction, 1627 earthquake, Gargano, Italy*

Introduction

The Gargano promontory and surrounding sea have been the objects of several recent geological and seismological studies. The promontory is clearly differentiated both geographically and as seismic activity rate from the foreland of the Apennines chain that bounds it to the west. Historical accounts from the 1627 earthquake, $I_{max}=X$, describe extensive destruction with formation of cracks and liquefaction features from the Lesina area to San Severo and a strong tsunami

that inundated the northern Gargano coastland, also observed at the city of Manfredonia, to the east (Fig. 1).

Evidence of these effects may be preserved in coastal lowlands around Gargano. Reliable historical records of large earthquakes ($M > 6$) there reach ~1,000 years into the past, but the geologic record preserved in coastal marshes and lakes may cover much of the late Holocene.

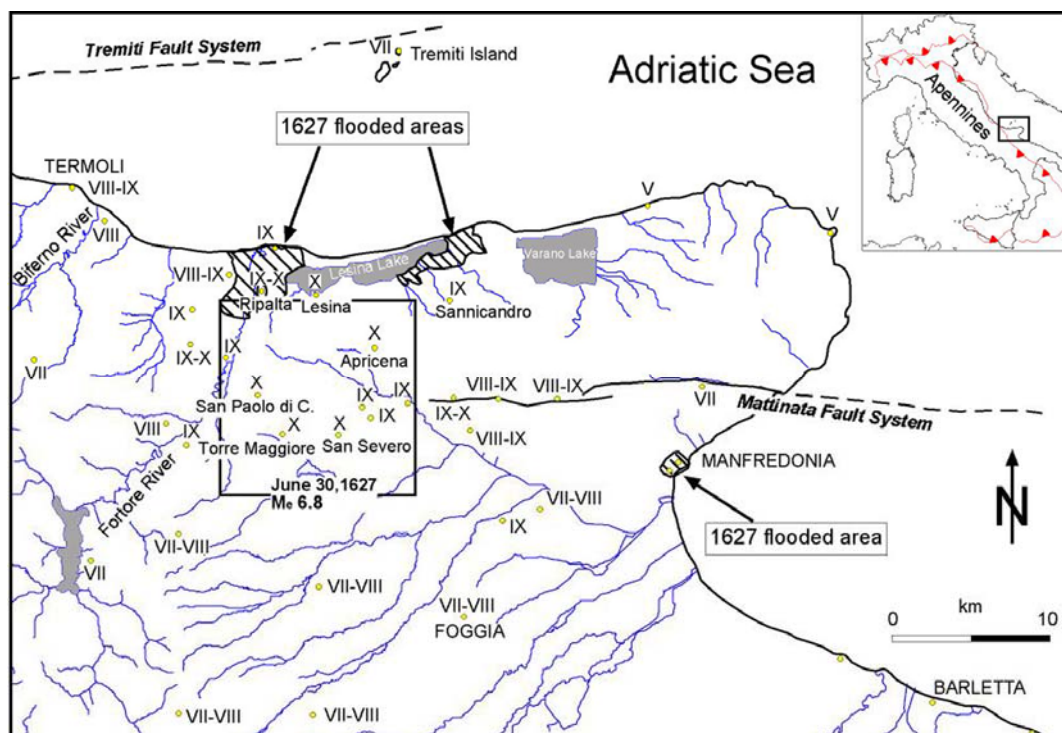


Figure 1. Damage distribution of the June 30, 1627 earthquake. Intensities are plotted in roman numbers (Boschi et al., 2000). Areas inundated by the 1627 tsunami are also shown.

Based on geology, we could provide a longer time frame to assess the tsunami recurrence and hazard of the study areas, an assessment now based on historical information only. We studied the stratigraphy of coastal wetlands to characterize better the recurrence and distribution of tsunamis and liquefaction in the Gargano region. These features could likely be the result of the 1627 earthquake and previous Holocene events. In doing this, we studied the upper 5 meters of stratigraphy in three marshes located on the northern and southeastern coast of the promontory (Fig. 1). Preliminary micropalaeontological analysis has also been performed to describe the depositional environment of anomalous sand layers. Radiocarbon dating of nine samples helped us reconstruct the inundation history of the studied areas.

Seismotectonic framework

Geological-structural setting

The Gargano promontory is located on the southern Adriatic coast of the Italian peninsula and is considered part of the Adriatic block (Adria): one of the microplates identified in the central Mediterranean at the collisional border of the European and African plates. The Gargano promontory, a structural high area where Mesozoic strata rise to about 1000 m above sea level (a.s.l.), is characterized by the presence of several marine terraces indicating substantial Quaternary uplift of the promontory. Structural and geomorphic analyses show that the dominant deformation structures are the regional E-W strike slip Mattinata Fault system together with secondary NW-SE strike slip and dip slip faults.

Historical and instrumental seismicity

Despite its location in the supposedly inactive foreland of the southern Apennine fold and thrust belt, the Gargano promontory has been affected by strong local earthquakes in the past. Historical seismic catalogues (Boschi et al., 2000) include a large number of earthquakes in the last millennium. Some earthquakes, in particular those in 1223 (Imax IX), 1627 (Imax X), 1646 (Imax IX-X), 1731 (Imax IX), 1875 (Imax VII-VIII) and 1948 (Imax VII-VIII), were characterized by significant damage. Two of them (1627 and 1731 eqs) were also followed by tsunami waves. The Italian seismic network, implemented in the past twenty years, shows seismic activity offshore near Gargano localized along ~ E-W trending structures. Detailed studies of three seismic sequences in the southern Adriatic sea between 1986 and 1990 suggest their

association with the Tremiti fault. Thus, both the Tremiti fault and the Mattinata fault system should be considered major candidates for the location of large earthquakes and related tsunamis.

The July 30, 1627 earthquake

On July 30, 1627 around midday a disastrous earthquake (Imax=X MCS) hit the Gargano promontory, with the strongest shaking concentrated in the northern coastal area between Lesina and Ripalta (Fig. 1). The shock was followed by a strong tsunami and four large aftershocks. Many contemporary sources described the event, providing a detailed picture of extensive destruction and many casualties. Fig. 1 shows the distribution of the macroseismic intensities (Boschi et al., 2000), and the location of the flooded areas. The earthquake left more than 5,000 victims and was felt in a very broad area, as far as the central Apennines and Sicily. It caused cracks on the ground surface, subsidence, flooding, and gas emissions. However no clear evidence for surface faulting was found. The damage distribution does not help resolving the ambiguity of the earthquake source location and leaves open the possibility of an offshore source. A significant tsunami, intensity 5 on the Sieberg-Ambraseys scale (Ambraseys, 1962) which means “very strong tsunami”, occurred after the main shock. The tsunami was particularly violent on the northern coast of Gargano, between the Fortore river and the Lesina and Varano lakes.

Observation and data collection

The 1627 contemporary chronicles clearly state that the July 30 earthquake produced a tsunami wave that flooded the northern coast of the Gargano promontory and the Manfredonia harbor to the east, along with liquefaction features over a wide area. We identified marshes at the Fortore river mouth in the eastern part of the Lesina Lake and in the Siponto farmlands (Fig. 1) where the features that formed during the 1627 and possibly older earthquakes may have been preserved in the stratigraphic sequence.

Fortore mouth area

The Fortore river flows, with a NNE direction, from the southern Apennines and abuts the Adriatic sea just west of the Gargano promontory (Fig. 1). At Le Casette 2 site distinct sand dikes and ball and pillar structures in a stratigraphy of interbedded sand, silt, and clay signify earthquake-induced liquefaction. One convoluted layer is exposed at depths from 25 to 40 cm in a 50-meter reach of the cut-banks of an abandoned channel. It consists primarily of very

fine to medium grained sand with thin silty layers, and presents a total thickness ranging from 10 to 20 cm. Clasts of gray clay, that are sometimes angular and sometimes stretched parallel to the convoluted upper and lower contacts, are entrained in the sand and silt. This layer is graded to finest material both toward its top and bottom. The presence of coarsest material in the middle suggests flow of liquefied sand within it. Both the upper and lower contacts of this layer are contorted into “ball and pillar structures”, common in liquefied sand (Obermeier, 1996; Obermeier & Pond, 1999). The most convincing evidence for liquefaction, however, are the vertical sand dikes that extrude from the top of this layer, crosscut bedding and rising to within 5-10 cm of the marsh surface where they are overprinted by bioturbation and modern loamy soil. These dikes are very thin (up to 3 cm thick) and planar but locally are thicker (5-10 cm) and bulbous. Taking into account that the upper termination of the sand dikes reaches the modern soil, we suggest that this liquefaction is related to the 1627 earthquake, the local best candidate for inducing strong shaking and high peak ground acceleration values.

Lesina Lake area

At the lake's northeastern edge (Fig. 1) we studied five sites located as far as 1 km inland from the modern shoreline. A convoluted layer shows evidence of either liquefaction or syn-depositional soft-sediment deformation at this site. This very fine, tan silty sand layer locates from 40 to 60 cm below the modern ground surface. It contains stretched and broken clay clasts in a matrix of fine grained sand with horizontal flow structures around them. The sand is finer on the upper and lower edges of the layer and coarser in the middle, features common in liquefied sand deposits (Obermeier, 1996; Obermeier & Pond, 1999). Radiocarbon dating of a piece of charcoal from the top of this layer yields an age of 1450-1640 AD, providing a limiting maximum age for the disruption. Moreover, we collected 18 gouge cores that penetrated up to 5 meters deep. The general stratigraphy observed consists primarily of peat and mud with a few thicker clayey and sandy silt intervals. This stratigraphy is punctuated by 3 anomalous sandy or coarse silty layers. The uppermost disturbance layer, found at a depth of 70-90 cm, is ~10 cm thick, light brown, medium to fine sand, with shell fragments concentrated at the bottom. The second is ~3-5 cm thick, gray, fine sand with abundant shell fragments, lying approximately 270 cm deep. The third layer is ~3-5 cm thick, sandy silt that is normally graded (coarser at the bottom, where shell fragments have been found) and lies about 340 cm below the surface

(Fig. 2). Each disturbance stratum has a sharp lower contact, contains shell detritus and sediments coarser than that above and below it. Four radiocarbon dates constrain the time of deposition of two disturbance layers. Dating suggests that the uppermost disturbance layer (L1) is younger than 1440-1890 AD, with the older age statistically preferred, and the lowermost sand (L3) was deposited in the interval 3630-3350 BC.

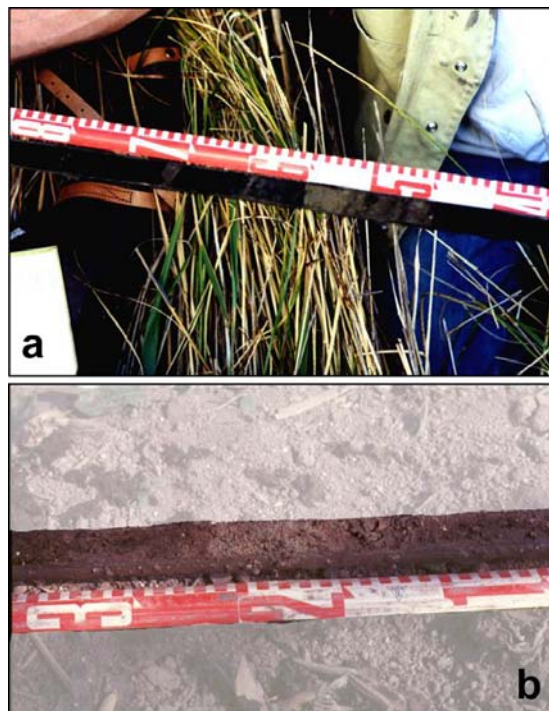


Figure 2. (a) Picture of the event L3 sand found at Black Panther site; (b) picture of event S3 sand collected at Mr. Paolo's site.

Siponto area

The area South of Siponto (south of Manfredonia in Fig. 1), that was once the seaport of the ancient Roman town of Siponto, was naturally filled with sediment and is today represented by a low lying area extending inland roughly 1.0-1.3 km. As exposed in irrigation ditches and in gouge cores, the observed stratigraphy consists almost entirely of brownish black peat. The 5 meters of fine-grained muddy and peaty deposits are interrupted by 3 coarse-grained layers indicative of high-energy deposition. The upper layer (“Event S1 layer”) occurs at depths of 40-60 cm and it consists of mixed pockets of tan fine-grained sand, silt, blackish muddy peat. It most commonly has sharp lower and gradational upper contacts. In 15 of the 27 ditches examined this layer is clearly distinguishable. Radiocarbon dating of a charcoal collected just below this sand indicates that it is younger than 240-420 AD.

The next layer (“Event S2 layer”) typically occurs at depths of 70-90 cm and it consists of a

discontinuous 1-3 cm layer of fine- to medium-grained, gray sand in sharp contact with the surrounding black peat.

This stratum is visible in 5 of the 9 sections studied. Two charcoal samples, collected above and below this deposit yield radiocarbon dates that bracket its age between 320 and 420 AD. At the Siponto site two fragments of pottery lie at a depth of 70 cm and were dated between 400 and 1200 AD based on the style of pottery, with the older part of the interval preferred. The third layer ("Event S3 layer", Fig. 2) consists of normally graded fine- to medium-grain tan sand. It sharply overlies brown peat and underlies peaty mud in a gradational contact. This layer occurs at about 250 cm below the surface and is only visible in gouge cores. It is found in all 8 cores that penetrated to this depth. Dating of charcoal fragments collected above and below it constrains its age to the interval 2130-1430 BC.

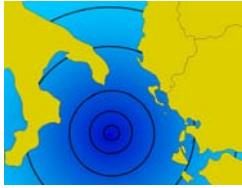
Conclusions

The recurrence and distribution of tsunami deposits and liquefaction features in the Gargano region have been explored through field surveys of irrigation ditch walls and gouge cores. We identified clear evidence of liquefaction near the mouth of the Fortore river and close to the eastern edge of Lesina Lake. Based on the upper termination of sand dikes and the age of a charcoal sample collected from the top of a liquefied sand layer, we claim to have found features related to the 1627 earthquake. Based on field observations and the constraints given by radiocarbon dating of selected samples, we believe we have identified evidence in the gouge cores for three tsunamis that inundated Lesina Lake and three that submerged the town of Siponto. We must emphasize that while detritus of marine macrofossils have been found in

the coarse sand samples, micropalaeontological analysis does not provide unequivocal constraints to a tsunamigenic cause. In the Lesina Lake area, radiocarbon datings suggest an origin from the 1627 tsunami for the uppermost sand layer and constrain the deposition of the oldest sand between 3630-3350 BC. Thus, a conservative interpretation provides a minimum average recurrence interval of about 1700 yr for tsunami inundation in this area. In the Siponto area, archeological and radiocarbon ages indicate that the two upper disturbance layers were deposited in historical time. Dating of charcoal fragments constrains the age of the oldest sand layer to the interval 2130-1430 BC. Accordingly, the average recurrence time for violent sea inundation at this site is approximately 1200 yr.

References

- Ambraseys N. N. (1962). *Data for the investigation of the seismic sea-waves in the eastern Mediterranean*. Bulletin Seismology Society American, 52 (4), 895-913.
- Boschi E., Guidoboni E., Ferrari G., Mariotti D., Valensise G., Gasperini P. (2000). *Catalogue of Strong Italian Earthquakes from 461 B. C. to 1997*. Annali di Geofisica, 43 (4), 607-868, with Database on CD-ROM.
- Obermeier S. F. (1996). *Using Liquefaction-Induced Features for Paleoseismic Analysis*. In Paleoseismology, edited by J.P. McCalpin, 331-396. Academic. San Diego, CA.
- Obermeier S.F., Pond E.C. (1999). *Issues in using liquefaction features for paleoseismic analysis*. Seismology Research Letters, 70, 34-58.



Didenkulova I.¹, Pelinovsky E.²

Analysis and modeling of the 1883 Krakatau volcanic tsunami

¹Institute of Cybernetics, Tallinn University of Technology, Tallinn (Estonia), e-mail: ira@cs.ios.ee;

²Department of Nonlinear Geophysical Processes, Institute of Applied Physics, Nizhny Novgorod (Russia), e-mail: Pelinovsky@hydro.appl.sci-nnov.ru

Keywords: *global tsunami, Krakatau Volcano, tide-gauge data*

The 1883 Krakatau volcanic eruption has generated the giant tsunami waves reached heights of 40 m above sea level (Verbeek, 1885; Symons, 1888; Murty, 1977; Simkin & Fiske, 1983; Bryant, 2001). Sea level oscillations related with this event have been reported in the Indian, Atlantic and Pacific Oceans. Main goal of this study is to analyze all available tide-gauge records (35) of this event. The location of the tide-gauges is presented in Fig. 1, and, especially, for Europe – in Fig. 2. All the records are digitized with time step 2 min and processed. First of all, the tidal components are calculated and eliminated from the records. records are available through the web (Pelinovsky et al, 2004). Filtered tide-gauge records are used to re-

determine the observed tsunami characteristics (positive and negative amplitudes, wave heights). Description of data can be found in the paper (Pelinovsky et al, 2005). Digitized tide-gauge The results of given analysis are compared with the results of the direct numerical simulation of the tsunami wave propagation in the framework of the linear shallow-water theory using the ETOPE2 bathymetry. Mathematical model and details of numerical simulations are given in (Choi et al, 2003).

Instrumental data of the 1883 Krakatau tsunami are compared with instrumental data of the last 2004 tsunami occurred in the same region in Indian Ocean.

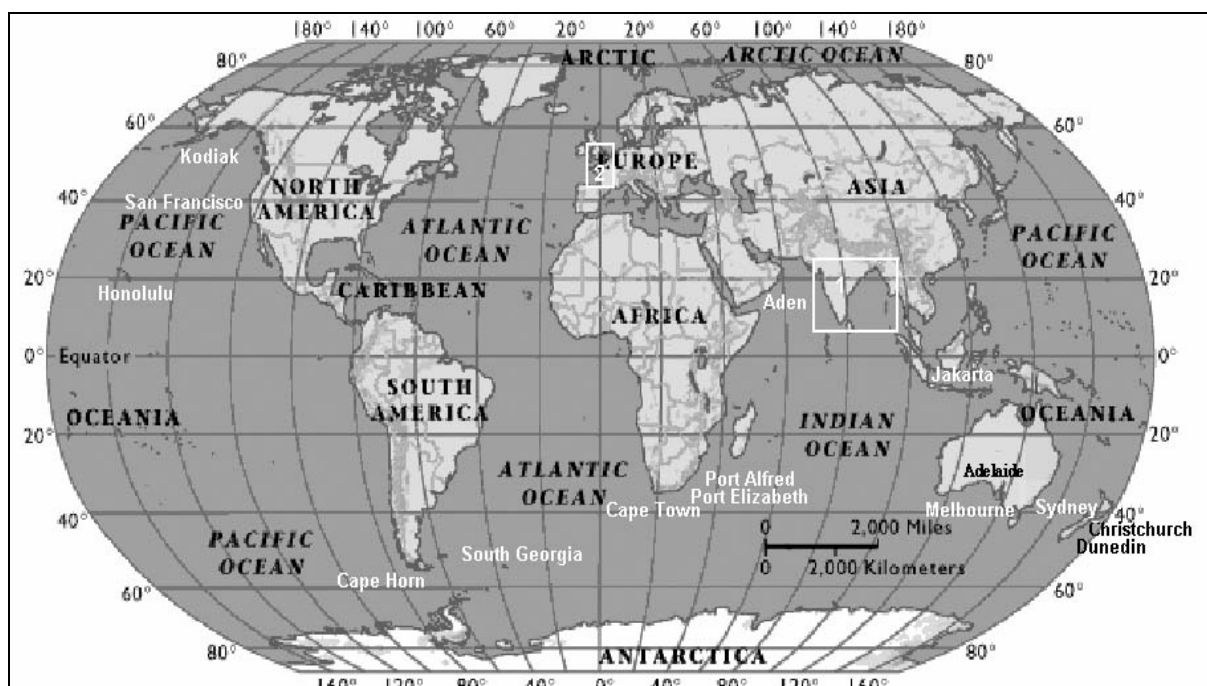


Figure 1. Locations of the tide-gauge registration of the Krakatau tsunami.

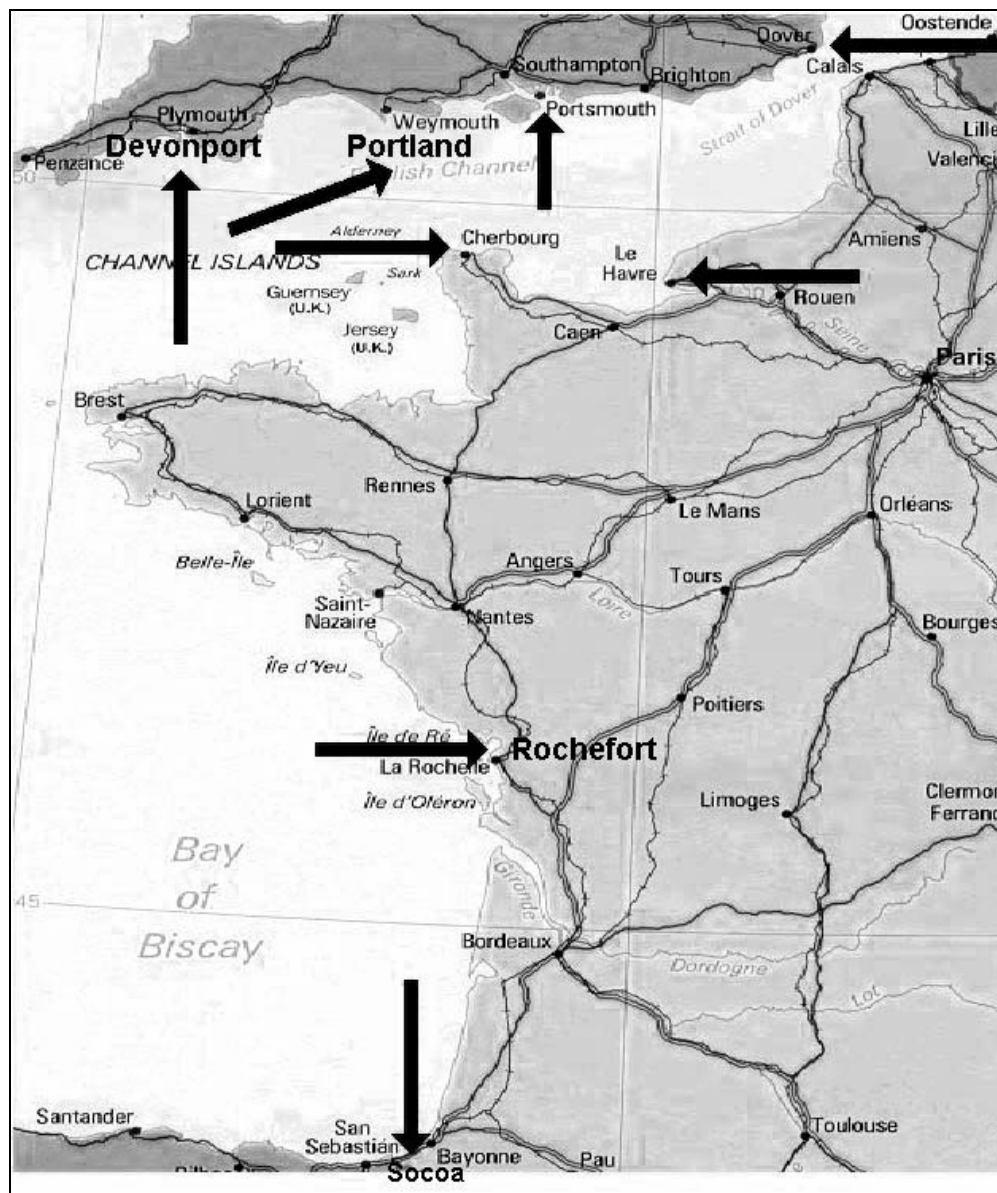
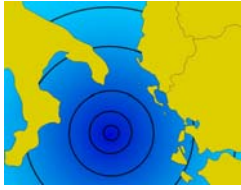


Figure 2. Registration of the 1883 tsunami in Europe

References

- Bryant T. (2001). *Tsunamis*. Cambridge University Press, 342 pp.
- Choi B.H., Pelinovsky E., Kim K.O., Lee J.S. (2003). *Simulation of the trans-oceanic tsunami propagation due to the 1983 Krakatau volcanic eruption*. Natural Hazards and Earth System Sciences, 3, 321–332.
- Murty T. (1977). *Seismic Sea Waves – Tsunamis*. Bulletin Department. Fisheries, Canada, 337 pp.
- Pelinovsky E., Stromkov A., Didenkulova I. (2004). *Tide-gauge records of the 1883 Krakatau tsunami*. <http://www.ipfran.ru/pp/Pelinovsky/krakatau/>
- Pelinovsky E., Choi B.H., Stromkov A., Didenkulova I., Kim H.S. (2005). *Analysis of tide-gauge records of the 1883 Krakatau tsunami*. *Tsunamis: case studies and recent developments*. Advances in Natural and Technological Hazards Research, 23, Springer, 57-77.
- Simkin T., Fiske R.S. (1983). *Krakatau 1883 - the volcanic eruption and its effects*. Smithsonian Institution Press, Washington, D.C. 464 pp.
- Symons G.J. (1888). *The eruption of Krakatoa and subsequent phenomena*. Report of the Krakatoa committee of the Royal Society, London: Trubner & Co. 494 pp.
- Verbeek R.D.M. (1884). *Krakatau*. Nature 30, 10-15.



2nd International Tsunami Field Symposium

IGCP Project 495

Quaternary Land-Ocean Interactions:
Driving Mechanisms and Coastal Responses

Ostuni (Italy) and Ionian Islands (Greece) 22-28 September 2008



Project 495

Engel M.¹, Brückner H.¹, Kelletat D.², Schäbitz F.³, Scheffers A.⁴, Vött A.²,
Wille M.³, Willershäuser T.¹

Traces of Holocene extreme wave events within sediment traps along the coast of Bonaire (Netherlands Antilles)

¹Department of Geography, Philipps-Universität Marburg, Marburg (Germany),
email: max.engel@staff.uni-marburg.de;

²Department of Geography, Universität zu Köln, Cologne (Germany)

³Seminar for Geography and Education, Universität zu Köln, Cologne (Germany)

⁴School of Environmental Science and Management, Southern Cross University, Lismore (Australia)

Keywords: *tsunami, hurricanes, fine deposits, Holocene, Bonaire, southern Caribbean*

According to the results of extensive geomorphologic research by Scheffers (2002; 2004; 2005) and Scheffers and Scheffers (2006) the coasts

of Bonaire (Netherlands Antilles) have undergone several major wave events during the Holocene (Fig. 1).

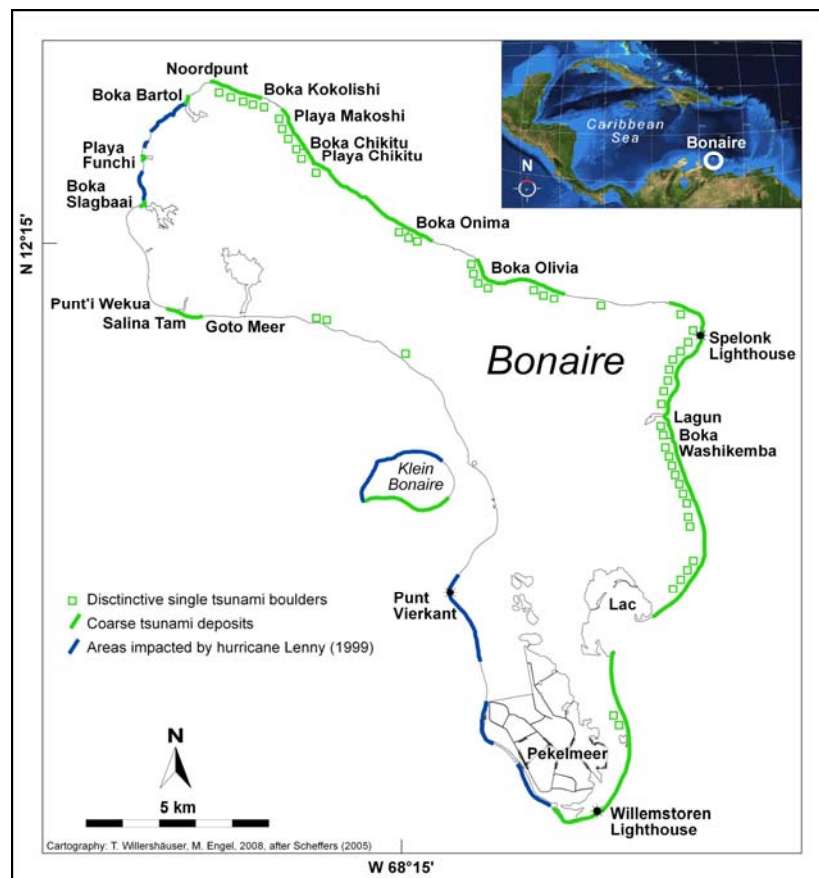


Figure 1. Map of Bonaire displaying important littoral landmarks including sampling sites Lagun, Salina Tam and Boka Bartol. The positions of tsunamigenic deposits and geomorphologic influence of hurricane Lenny (1999) were mapped by Scheffers (2005). The overview of the Caribbean is based on a NASA World Wind image.

Obviously several high energy wave impacts such as tsunami and hurricanes significantly altered the littoral morphology and left traces in form of boulders and allochthonous coral deposits. Our new project combines existing evidence of coarse accumulations with new data of the fine sedimentary record. By deciphering the Holocene palaeogeographies of Bonaire's coastal embayments, we aim to elaborate the contribution of extreme wave events to nearshore morphodynamics. New datings from within the stratigraphic context will improve the chronology of mid- to late Holocene extreme wave events in the southern Caribbean and will also contribute to a first local relative sea level

terraces during Pleistocene sea level lowstands (Alexander, 1961; Jackson & Robinson, 1994) and today act as traps for terrestrial and marine sediments. The locations of Salina Tam, Boka Bartol and Lagun (Fig. 1) were chosen for sampling by means of the vibration coring technique (on land) and gravity coring (on water). At Lagun, a coring transect was established along the narrow alluvial plain separated from the embayment by a fringe of mangroves. Core Bon 4 (Fig. 2), chronostratigraphically comprising at least the past 7 ka, clearly reflects a fluctuating sedimentation regime, implying abrupt changes between continuous and episodic morphodynamics.

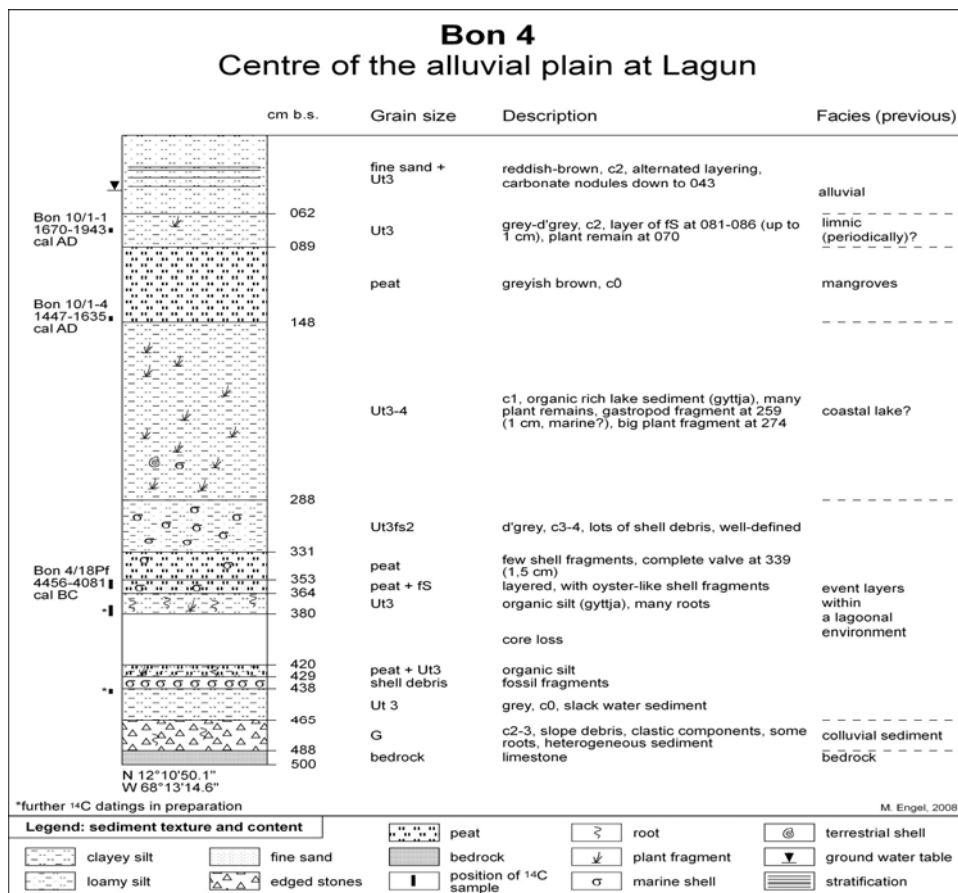


Figure 2. Stratigraphic profile of coring Bon 4 on the distal floodplain at Lagun. ¹⁴C datings are displayed within the 2σ range. Calibration was carried out according to Reimer et al. (2004).

curve for Bonaire with implications for the entire Leeward Islands. The study presented here takes its cue from the sedimentological and geomorphological approach of Vött et al. (2007), with modifications through the application of high-resolution geochemical analyses. Characteristic features of Bonaire's coastline are the so-called *bokas* or *salinas* that are – in some cases – separated from the sea by large dams of coral rubble. These coastal embayments are drowned creek valleys, cut into the lower *in-situ* limestone

The first unit overlying the MIS 5e-bedrock consists of proximal coarse terrestrial facies, referring to a significantly lowered sea level.

High rates of sea level rise during early and mid-Holocene times (Fairbanks, 1989) – greatly overcompensating the late Quaternary moderate net uplift of the island (Jackson & Robinson, 1994) – initiated the elevation of the base level as well as the formation of a nearshore environment with fine grained and organic-rich sedimentation. Well-defined intercalations of marine shell debris start at

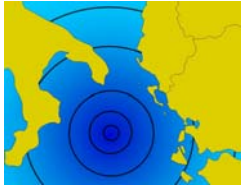
438 cm b.s. (below surface) interrupting the continuous lagoonal sedimentation pattern. Up to 288 cm b.s. the partly interbedded strata seem to reflect a large number of extreme wave events. Whether these sandy carbonate layers are due to tsunami or hurricane impacts still has to be determined.

Since nearshore peat accumulations strongly correlate to isochronic sea level stands (Vött, 2007) radiocarbon datings of plant remains from Bon 4 at 360-353 (4456-4081 cal BC) and 145-144 cm bs. (1447-1635 cal BC) are evidence of decelerated late Holocene sea level rise at an average of 35-40 cm/ka compared to more than 1 cm/a during late Pleistocene/early Holocene times (Fairbanks, 1989). An expanded data set will be necessary for setting up a reliable local relative sea level curve. Similar to the sedimentary pattern of Bon 4, the stratigraphic columns of lagoonal and terrestrial sites at Boka Bartol and Saliña Tam also reveal intercalations of well-rounded carbonatic sands and shell hash of varying thickness within a matrix of lagoonal mud, redistributed from sublittoral

environments during short periods of high energy wave action. Especially the case of the latter location emphasizes the relevance of wave refraction since palaeo-tsunami are assumed to have hit the island from easterly directions (Scheffers, 2004).

References

- Alexander C.S. (1961). *The marine terraces of Aruba, Bonaire and Curaçao, Netherlands Antilles*. Annals AAG 51/1, 102-123.
- Fairbanks R.G. (1989). *A 17,000 year glacio-eustatic sea level record: influence of glacial melting rates on the Younger Dryas event and deep ocean circulation*. Nature 342, 637-642.
- Jackson T.A., E. Robinson (1994). *The Netherlands and Venezuelan Antilles*. In: Donovan S.K., Jackson T.A. (eds.). *Caribbean Geology: an introduction*. UWI Publishers Association/UWI Press, Kingston, 249-263.



Etienne S.¹, Paris R.¹

Boulder accumulations related to storms on the south coast of the Reykjanes Peninsula (Iceland)

¹Géolab UMR 6042 CNRS – Université Blaise Pascal Clermont-Ferrand, France

Contact author: e-mail: samuel.etienne@univ-bpclermont.fr

Keywords: Coastal geomorphology, volcanic rock coast, storm deposits, boulder ridge, cliff-top boulders, tsunami, Iceland

Coastal boulder accumulations were often mentioned in the literature (e.g. Oak, 1984; McKenna, 2005; Felton & Crock, 2003), even though their interpretation remains difficult, especially along rock coast affected both by storms and tsunamis. Studies on the geomorphic impact of such high-energy events are actually of great interest, since their intensity and frequency are key issues for the future evolution of coasts in the framework of the global change.

The west coast of Iceland faces the powerful storms of the North Atlantic Ocean, with wave's heights more than 15 m. A powerful storm

destroyed a Danish trading centre at Básendar in 1799. The probability for past and present tsunamis to hit this coast is very low. Thus, the boulder accumulations along the volcanic rock coast of the Reykjanes Peninsula (southwest Iceland, Fig. 1), which are described in this paper, are clearly related to storms. They consist in cliff-top boulders, clusters and ridges, beaches, and boulder fields. Plurimetric boulders, up to 80 tons in weight, were transported and deposited until 65 m inland (6 m a.s.l.). The maximum limit of boulder deposition and driftwood were found respectively 210 m and 550 m inland (Fig. 1).

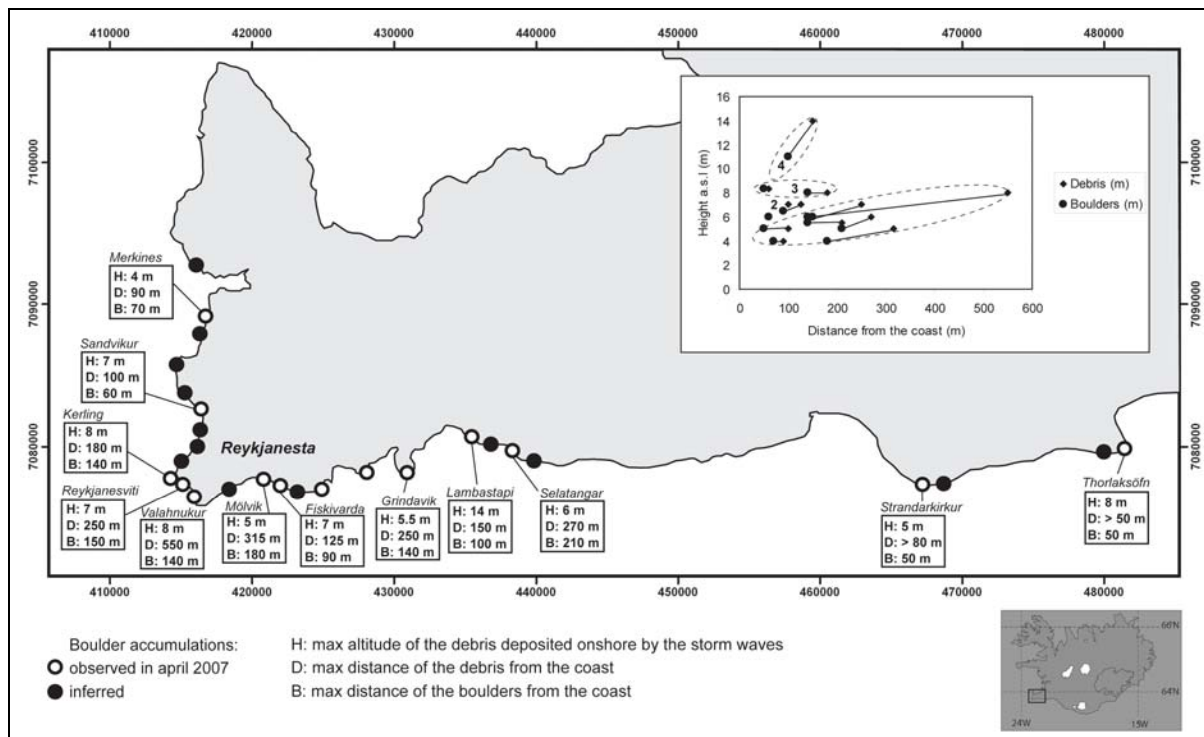


Figure 1. Location, altitude and distance from the shoreline of the boulder accumulations.

We could not detect any granulometric trend along the boulder beaches of the Reykjanes except for the smaller ones.

Several typical associations between storm deposit type and coastal landform (morphotypes) can be recognized (Fig. 2).

Coastal morphology is predominant in the distribution of storm boulder accumulations. Nevertheless, the heterogeneity of the estimated minimum wave heights and transport figures suggests that storm intensity is also important. For instance, the foreshore slope of the boulder beaches displays evidences of fresh impacts and boulder movements, whereas the deposition of plurimetric mega-clasts requires centennial waves. The influence of the morphology on the nature and distribution of storm deposits will differ from one storm to another. Highest storm waves (> 15 m) are higher than the cliffs and break on cliff-top platforms. Thus, the most powerful storms may also rework the deposits of less intensity storms (e.g.

moderate storms erode the cliff and deposit cliff-top clasts, then transported landward and laid down as ridges or clusters by severe storms). Thus, storms appear as a predominant factor in the geomorphic evolution of Reykjanes coasts.

These observations also give new insight for the interpretation of coastal boulder accumulations. Processes of erosion and deposition by tsunamis are a rising topic in the literature, and the effects of recurrent and powerful storms appear neglected. Indeed, the maximum transport figures of the largest mega-clasts in Reykjanes (2700-32.000) are in the range of values estimated for past-tsunamis on the coasts of Italy (1456 Ionian tsunami: Mastronuzzi & Sansó, 2000), Spain (1755 Lisbon tsunami: Whelan & Kelletat, 2005) and Hawaii (1946 Aleutian tsunami: Noormets et al., 2002). Paris et al. (2008) reported transport figures

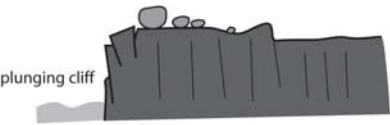
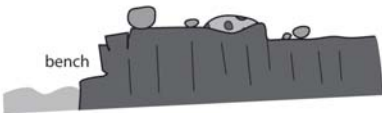
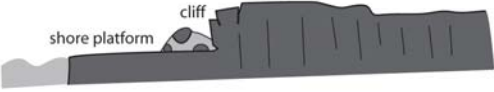




Sea/land contact		Morphotype	Deposit	Example
CLIFF	plunging cliff		cliff-top deposits only	Reykjanesta, Thorlaskhöfn
	bench		cliff-top deposits & boulder ridge	Thorlaskhöfn, Fiskivardha, Lambastapi
	shore platform		boulder beach	Kerling, Reykjanesviti
	embayment & inland cliff		boulder beach	Karl, Lambastapi
NO CLIFF	structural ramp (lava flow)		boulder ridge (& wash-over boulders)	Sandvikur, Reykjanesviti, Grindavik
	embayment		boulder beach & wash-over boulders	Valahnukur, Merkines, Selatangar
				

Figure 2. Storm boulder accumulations and their geomorphological setting along rocky coasts of the Reykjanes Peninsula (Iceland). There is no scale. Slopes might vary from place to place.

respectively less than 13.000 and 45.000 for shore platform mega-clasts and coral boulders transported by the 2004 tsunami in Sumatra.

Transport figures exceeding 70,000 and 100,000 were calculated for coastal boulders in the Netherlands Antilles and in Australia (Scheffers & Kelletat, 2003), but their actual elevation and distance from the coastline could have been different at the time of deposition.

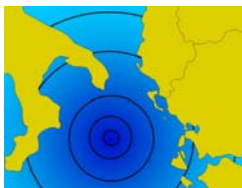
A fundamental distinction between storm and tsunamis could be their capability of forming ridges. Indeed, the organisation of coarse clasts into ridges requires repeated reworking by waves rather than the single impact of a tsunami front wave (Williams & Hall, 2004). As far as we know, observed tsunamis did not leave boulder ridges. Pleistocene tsunami conglomerates described in the Canary Islands by Pérez Torrado et al. (2006) are lenticular patches attached to the valley walls, rather than well-formed ridges. The extensive cobble-to-boulder ridges and ramparts described by Scheffers (2004) in the Leeward Netherlands Antilles are the only ridge-like features attributed to tsunamis so far studied. Finally, more data need to be collected about the effects of storms along coasts also affected by tsunamis.

Storm intensity trend is then a key issue in the future evolution of coasts. After Kushnir et al. (1997), northeast Atlantic wave heights during cold season have increased at a rate of up to 0.3 m per decade since 1962. Wang and Swail (2001) found highly significant increase of wave heights in the North Atlantic, especially in winter (10%–35%, i.e. 40–204 cm over the last 40 years), a trend found to be associated with an intensified Azores high and a deepened Icelandic low. Alexander et al. (2005) found a global decrease in average intensity of each severe storm event in whole Iceland since 1983. In details, northeastern Iceland shows a large decrease, and northwestern to southwestern parts show an increase in ‘storminess’, although the statistical

significance of the trend is not strong (Alexander, pers. comm., 2007). Nevertheless, even if storminess shows a global decrease, the mean number of severe events recorded at the coast is increasing: 4.7 storms per year during the 1959–1982 (n = 107) period and 5.3 storms per year during the period 1983–2003 (n = 111). Facing the future global climate evolution and the reinforcement of atmospheric gradient between high and low latitudes, storm-induced geomorphic processes might have even greatest impacts on the coasts.

References

- Alexander L.V., Tett S.F.B., Jonsson T. (2005). *Recent observed changes in severe storms over the United Kingdom and Iceland*. Geophysical Research Letters, 32(13), L13704.
- Felton E.A., Crook K.A.W. (2003). *Evaluating the impact of huge waves on rocky shorelines: an essay review of the book 'Tsunami – The Underrated Hazard*. Marine Geology, 197, 1–12.
- Kushnir Y., Cardone V. J., Greenwood J. G., Cane M. A. (1997). *The recent increase in North Atlantic wave heights*. Journal of Climate 10, 2107–2113.
- Mastronuzzi G., Sansò P. (2000). *Boulders transport by catastrophic waves along the Ionian coast of Apulia (southern Italy)*. Marine Geology, 170, 93–103.
- McKenna J. (2005). *Boulder beaches*. In: Schwartz, M.L. (ed.), Encyclopedia of Coastal Science. Springer, 206–208.
- Noormets R., Felton E.A., Crook K.A.W. (2002). *Sedimentology of rocky shorelines: 2 – Shoreline megaclasts on the north shore of Oahu, Hawaii – origins and history*. Sedimentary Geology, 150, 31–45.



Federici P. R.¹, Rodolfi G.²

Traces of an ancient tsunami event on the Archangelos coast (Southern Peloponnese, Lakonia, Greece)

¹Dipartimento di Scienze della Terra, Università degli Studi, Pisa (Italy) e-mail: federici@dst.unipi.it;

²Dipartimento di Scienza del Suolo e Nutrizione della Pianta, Università degli Studi, Firenze (Italy)
e-mail: giuliano.rodolfi@unifi.it

Keywords: boulders, pumice, tsunamis, Santorini explosion, Archangelos, Lakonia, Greece

During the geomorphological survey of a coastal stretch of the South-western Peloponnese Lakonia, Greece (Federici, Rodolfi & Stocker, 2002, located about 1 km south of the Archangelos village, Authors brought out the presence of some signs of a likely exceptional event that affected the area. This event can be explained only taking into account very high levels of the wave energy reached not so far in the past.

The surveyed costal stretch is characterized by the presence of an abrasion platform cutting an outcrop of strongly dipping stratified dolomite, as the result of a marine ingression (Kowalczyk *et al.*, 1992). It is composed mainly of Triassic dolomites and Jurassic - Lower Cretaceous limestones and dolomitic limestones (Jacobshagen, 1986).

A scattered and partly submerged beachrock, probably of Thyrrenian age, lies discordant on it.



Figure 1. Studied area.



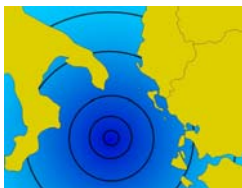
Figure 2. Traces of an ancient tsunami along the Archangelos coast.

Isolated boulders of this beachrock, the volume of which can reach 2 m³, are found to form an arch broadly parallel to the actual shoreline, about a hundred metres from it. Moreover, just out of the actual abrasion platform, some rounded fragments of pumice have been found, sometimes enrobed in the red soil formed on the colluvial deposits at the foot of the carbonate reliefs hanging over the coast.

Waiting for the results from the dating of pumice elements, the Authors propose the hypothesis that the surveyed situation could be put in relationship with the catastrophic volcanic eruption of Santorini, around the 1500 b.C.

References

- Federici P.R, Rodolfi G., Stocker E (2002). *Geomorphological mapping and relief evolution of the Dokali River catchment near Démonia (South-western Lakonia, Greece)*. Géomorphologie, 3, 2002, 223-238.
- Jacobshagen V. (1986). *Einführung, Bau und Entwicklung griechischer Gebirge - Westgriechenland und Peloponnes*. In: Jacobshagen V. (Ed.). *Geologie von Griechenland*. Beiträge zur regionalen Geologie der Erde, Bd. 19, 1-53, Berlin, Stuttgart.
- Kowalczyk G., Winter K.P, Steinich G., Reisch H. (1992). *Jungpleistozäne Strandterrassen in SE-Lakonien (Peloponnes, Griechenland)*. Schriftenreihe für Geowissenschaften, 1 (1), 1-72, Berlin, Stuttgart.



Gelfenbaum G.¹, Jaffe B.², Morton R.³, Moore A.⁴

Variations in tsunami deposit thickness: the role of pre-existing topography

¹U.S. Geological Survey, Menlo Park, CA, USA; e-mail: ggelfenbaum@usgs.gov;

²U.S. Geological Survey, Santa Cruz, CA USA; e-mail: bjaffe@usgs.gov;

³U.S. Geological Survey, St. Petersburg, FL USA; e-mail: rmorton@usgs.gov;

⁴Earlham College, Richmond, IN USA; email: moorean@earlham.edu

Keywords: *Tsunami, sandy deposits, coastal morphology, sediment transport, Sumatra, Indonesia*

Sedimentary deposits left by tsunamis are important indicators of extreme wave inundation. At a minimum, tsunami deposits record the existence of the extreme event, and research is underway to determine whether some characteristics of the waves, such as height, speed, or flow history, can also be interpreted from the deposits. With this goal in mind, there has been extensive examination of the deposits left after recent large tsunamis at several sites around the world. Detailed measurements and observations of onshore sandy deposits along shore-perpendicular transects collected soon after the 1998 Papua New Guinea (Gelfenbaum & Jaffe, 2003) and the 2004 Sumatra (Jaffe et al., 2006; Moore et al., 2006; Morton et al., 2008) tsunamis have been used to characterize these tsunami deposits. The deposits typically begin several tens of meters from the

shoreline and extend hundreds to over a thousand meters inland. Commonly, the deposits are tabular in shape, averaging about 10 cm in thickness, and thinning at the seaward and landward extents. At many sites, deposit thickness varies with pre-existing topography, with thicker deposits in pre-existing lows and thinner deposits at pre-existing highs (Fig. 1).

To better understand the relationship between tsunami deposit thickness and pre-existing topography we use a process-based morphological model to simulate the hydrodynamics and sediment transport of a tsunami inundation. The model is initialized with offshore bathymetry and onshore topography measured at Kuala Meurisi on the west coast of Sumatra and a time series of offshore water levels (Gelfenbaum et al., 2007).

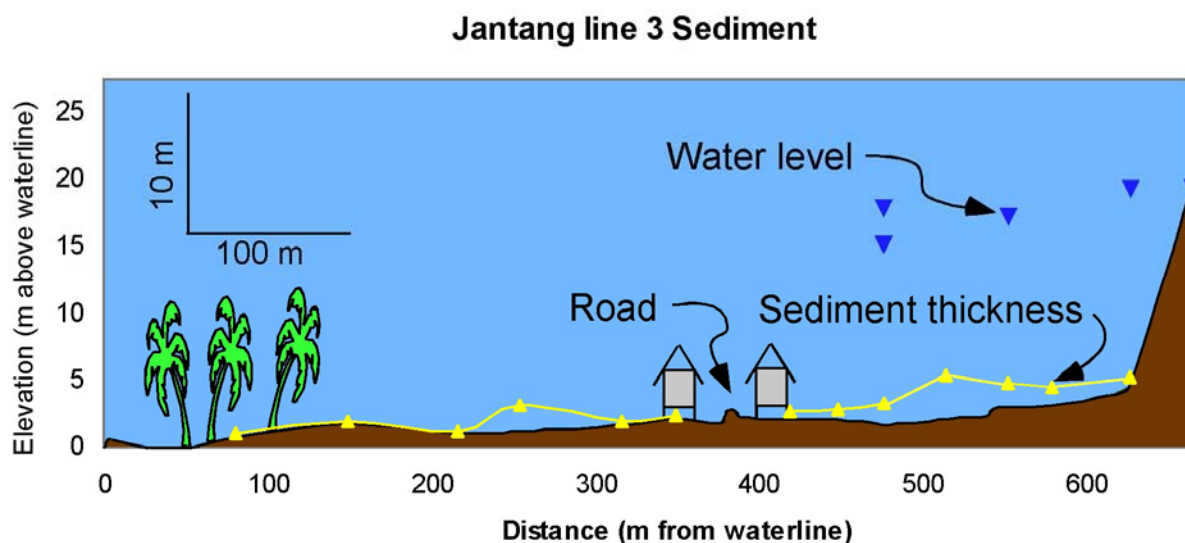


Figure 1. Shore-perpendicular transect of topography and tsunami deposit thickness (exaggerated by 10 times) at Jantang along the west coast of Sumatra, Indonesia

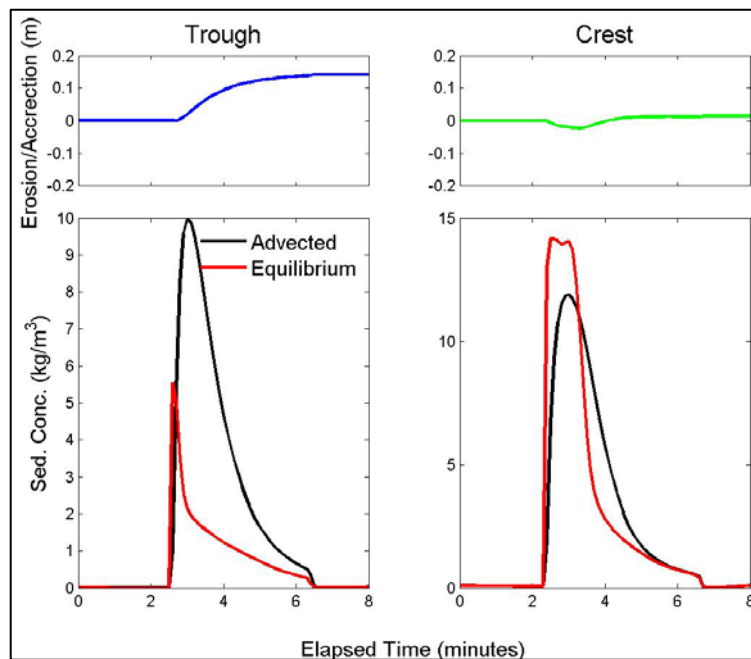
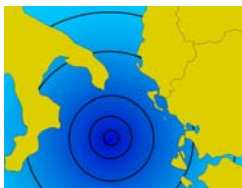


Figure 2. Time series of modeled suspended-sediment concentration and bed-elevation change (erosion or deposition) at a topographic low (trough) and adjacent high (crest) along a shore-perpendicular transect.

The topography along a shore-perpendicular transect at this site is undulating, with several ridges and swales with elevation changes of about 0.5 m between crests and adjacent troughs 15-m apart. Simulated maximum water depths of 12-15 m at this site coincide reasonably well with measured values taken in the field. Despite the subtle topographic changes and large tsunami water depths, the model correctly predicts the observed variations in deposit thickness, with thicker deposits in the troughs and thinner deposits at the crests. These variations in deposit thickness result from the minor, yet sufficient, accelerations and decelerations in the tsunami flowing over the pre-existing topography. The flow accelerates over the topographic highs, increasing its capacity to carry more sediment in suspension, thus eroding the bed. The flow decelerates over the topographic lows, reducing capacity to carry sediments, thus depositing sand on the bed (Fig. 2). The variation in deposit thickness with topography also depends on the sediment grain size. Finer sediment will tend to de-emphasize the effect of the pre-existing topography, whereas coarser sediment will tend to emphasize the effect. Results from this study provide useful insights for interpreting variations in tsunami deposit thickness that may ultimately help in the interpretation of tsunami hazards from geologic evidence.

References

- Gelfenbaum G., Jaffe B. (2003). *Erosion and sedimentation from the 17 July 1998 Papua New Guinea tsunami*. Pure and Applied Geophysics, 160, 10-11, 1969-1999
- Gelfenbaum G., Vatvani D., Jaffe B., Dekker, F. (2007). *Tsunami inundation and sediment transport in vicinity of coastal mangrove forest*. Proceedings of Coastal Sediments 07 May 2007, New Orleans, LA, 1117-1128
- Jaffe B. E., Borrero J. C., Prasetya G. S., Dengler L., Gelfenbaum G., Hidayat R., Higman B., Kingsley E., Lukiyanto McAdoo, B., Moore A., Morton R., Peters R., Ruggiero P., Titov V., Kongko W. Yulianto, E. (2006). *The December 26, 2004 Indian Ocean Tsunami in Northwest Sumatra and Offshore Islands*. Earthquake Spectra, 22, S3, S105-S136.
- Moore A., Nishimura Y., Gelfenbaum G., Kamataki T., Triyono R. (2006). *Sedimentary deposits of the 26 December 2004 tsunami on the northwest coast of Aceh, Indonesia*. Earth, Planets and Space, 58, 253-258.
- Morton R.A., Goff J.R., Nichol S.L. (2008). *Hydrodynamic implications of textural trends in sand deposits of the 2004 tsunami in Sri Lanka*. Sedimentary Geology, in press.



Gerardi F.¹, Barbano M. S.¹, De Martini P. M.², Pantosti D.²

Discrimination of tsunami sources (earthquake or landslide) on the basis of historical data in Eastern Sicily and Southern Calabria

¹Dipartimento di Scienze Geologiche, Università degli Studi, Catania (Italy),

e-mail: f.gerardi@unict.it, barbano@unict.it;

²Istituto Nazionale di Geofisica e Vulcanologia, Sezione Sismologia e Tettonofisica, Gruppo di Tettonica Attiva, Roma (Italy), e-mail: paolomarco.demartini@ingv.it, pantosti@ingv.it

Keywords: *historical earthquakes, tsunamis, run-up, seismic dislocations, landslides, southern Italy*

Coastal areas of southern Calabria and eastern Sicily have been affected by large destructive earthquake-related tsunamis in historical times. As described in the historical reports, devastating anomalous waves followed the 1908, 5 and 6 February 1783, 1693 and 1169 earthquakes (Fig. 1).

Some of these events occurred along mapped, crustal, normal faults; whereas the source of the older events, either offshore or inland, is still debated. The uncertainties in the location of the sources originated also a debate on the origin of the tsunamis and in particular whether these

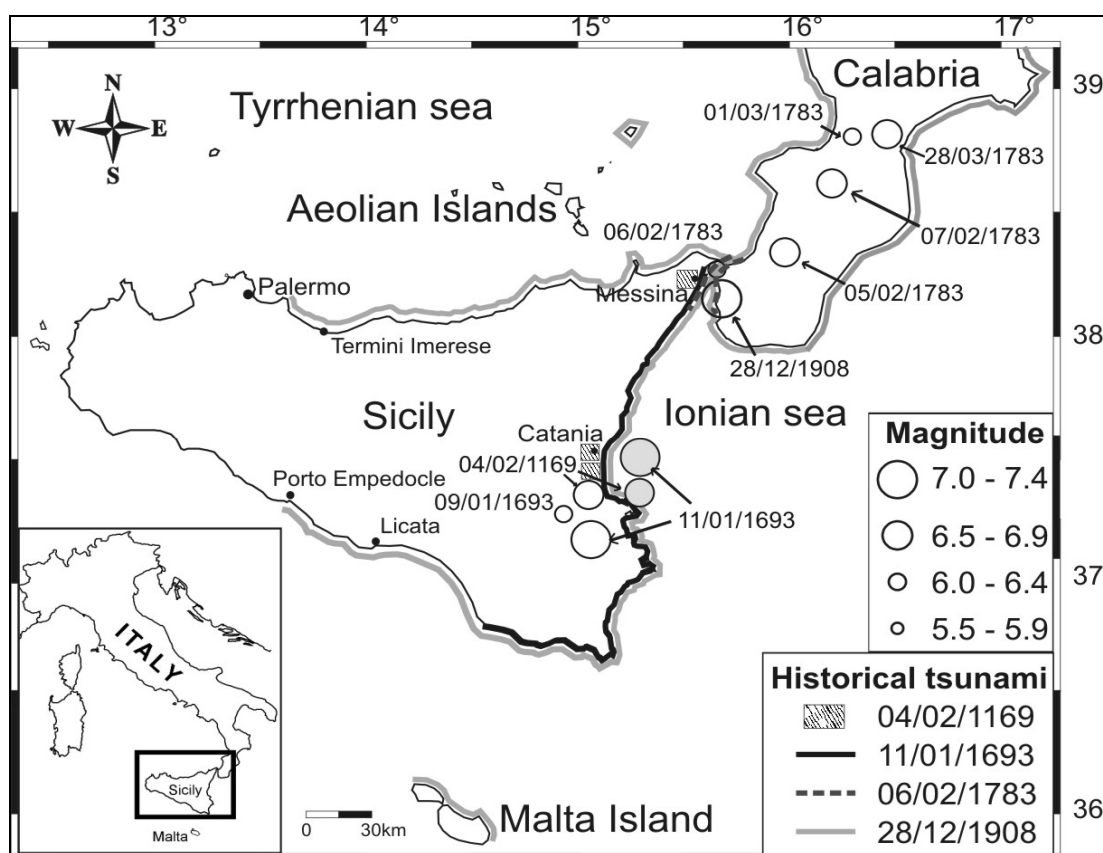


Figure 1. Historical earthquakes followed by tsunamis analysed in this work; epicentres (unfilled circles) from the CPTI4 catalogue (Working group CPTI, 2004) and (filled circles) from the NT4.1 catalogue (Camassi & Stucchi, 1997).

were related to a seismic dislocation or to a submarine landslide (e.g. Tinti & Armigliato, 2003; Ortolani et al., 2005; Tinti et al., 2007; Billi et al., 2008). We try to contribute to this debate by applying the method proposed by Okal and Synolakis (2004) to the 1908, 6 Feb 1783, and 1693 tsunamis. This method has the potential to discriminate the nature of the tsunami source by using run-up amplitude distribution in the near field. The Okal and Synolakis (2004) approach was initially developed for a rectilinear coastline and for open oceans; it can be applied also to the southern Calabria and eastern Sicilian coasts because the method is for near-field tsunamis and although the Ionian basin (1-3000m) is not as deep as oceanic depths, the impact of depths on the model is negligible on the results as demonstrated by the Okal and Synolakis (2004).

As a first step in this study, we compiled a database storing information on the effects of tsunamis through a detailed analysis of coeval accounts. Available historical reports for the 1908 event illustrate in detail hit localities, maximum run-up (Fig. 2a) and inundation areas (Gerardi et al., 2006); conversely, data for the 1169 and 5 Feb 1783 are so scanty that they could not be used in the analysis. For the 1693 and 6 February 1783 tsunamis, coeval accounts describe mainly inundation values. Therefore, we computed the tsunami run-up values through the Hills and Mader (1997) equation:

$$X_{\max} = (H_s)^{1.33} \cdot n^{-2} \cdot k \quad (1)$$

where X_{\max} is the limit of landward incursion (m); H_s is the run-up heights; k a constant and the Manning's coefficient n represents the roughness of land, that equals 0.015 for very smooth topography, 0.03 for urbanized/built land, and 0.07 for densely treed landscape. We used the 1908 observations of both inundation and run-up in the Hills and Mader (1997) equation (1) to define the best Manning's coefficient n for each sites.

The Manning's n , so obtained for the localities affected by the 1693 (Fig. 2b) and 1783 (Fig. 2c) tsunamis, have been used to compute run-ups from observed inundation data. Furthermore, to take in account the large topographic variability along the coast, we computed maximum and minimum run-ups by using the two end-members 0.03 and 0.07, considering that all 1908 data fall into this interval. As a second step, we sketched an linear profile, which exemplifies the real shoreline, and plotted perpendicularly on it run-up observed at individual locations. The origin of tsunami on the profile is set at the nearest point with respect to the tsunami source. In our plotting, we used historical and computed run-ups values and more linear profile to

take into account of the different strike characterizing the Calabrian and Sicilian coasts around the Messina Straits (Fig. 2 a, b, c).

For each investigated events, we tried the empirically best-fit run-up distribution along the coast using the formula proposed by Okal and Synolakis (2004):

$$\zeta(y) = b / \{[(y-c)/a]^2 + 1\} \quad (2)$$

where ζ are run-up values, "a" is the lateral extent of sustained run-up along the beach, "b" is the maximum amplitude run-up on the fitted curve and "c" is the distance of "b" from the 0, along the idealized linear shoreline.

We work out several sets of parameters (a, b, c), in the Okal and Synolakis (2004) equation (2) in order to find the theoretical best-fit curve of historical and computed run-up values.

The values "a" and "b", obtained from the best-fit curves, are used to calculate the dimensionless parameter $I_2 = b/a$, the ratio of the maximum run-up to its lateral extent along beach. According to Okal and Synolakis (2004), I_2 value discriminates the nature of the source: I_2 less than 10^{-4} is characteristic of a seismic dislocation source; whereas, I_2 is usually greater than 10^{-4} in case of underwater landslides.

To test the influence of the amplitude distribution of run-up on the coast, we have used a variety of sources and of idealized linear shorelines (Gerardi et al., 2008). We present here only the boundary results derived from this analysis (Fig. 2a,b,c).

From the best-fit to the data set of 1908 tsunami, we obtained $I_2 = 6.3 \cdot 10^{-5}$ (Fig. 2a). The same procedure has been applied to the 1783 and 1693 tsunamis; this yielded for the 1783 tsunami $I_2 = 3.6 \cdot 10^{-3}$ (Fig. 2c) and for the 1693 tsunami $I_2 = 6.6 \cdot 10^{-5}$ (Fig. 2b).

Summarizing, for the 1908 and 1693 run-up data, the obtained I_2 values suggest that the tsunami source is a seismic dislocation (I_2 smaller than 10^{-4}). On the other hand, the I_2 value obtained for 1783 data suggests that its tsunami source is a landslide triggered by earthquake shaking (I_2 larger than 10^{-4}).

To model different sources Okal and Synolakis (2004) also consider other two dimensionless quantities I_1 and I_3 . $I_1 = b/\Delta u$ scales the maximum run-up ("b") on the beach to the amplitude of seismic slip on the fault (Δu). $I_3 = -b/\eta$ scales the maximum run-up ("b") on the beach to the amplitude of initial depression (η) on the sea surface. To compute I_1 and I_3 , the slip Δu and depression η are inferred from published values. For the 1908 earthquake we used $\Delta u = 2.07 \pm 0.83$ (Pino et al., 2000) and for the 1693 earthquake we used $\Delta u = 2$ m (Gutscher et al., 2006);

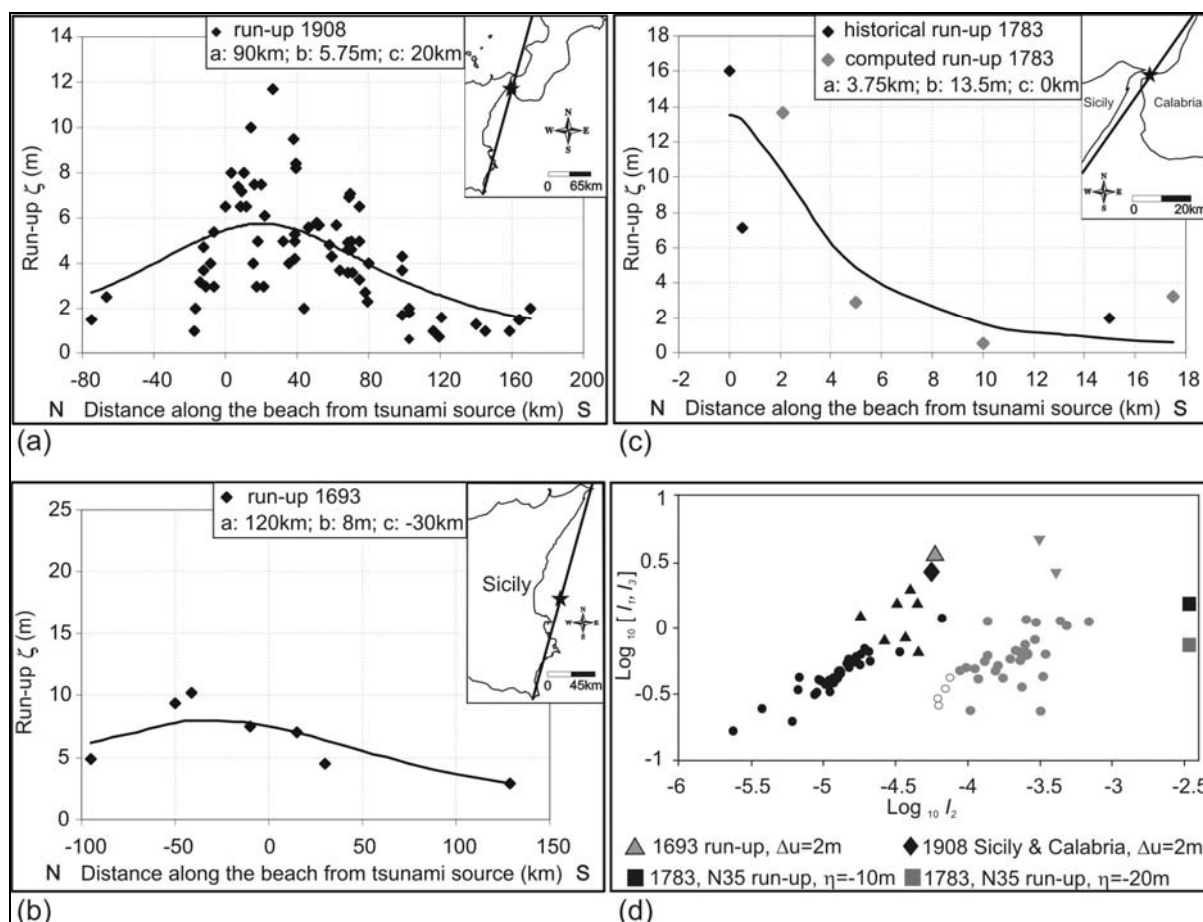


Figure 2 (a) Run-up profile obtained for the 1908 tsunami using observed run-up data from both the Calabrian and Sicilian coasts. (b) Run-up profile for the 1693 tsunami obtained by using observed and computed data with different n Manning's values. (c) Run-up profiles for the 1783 Feb 6 tsunami obtained by using observed and computed run-ups with different n Manning's values, coastline N35°E. The idealised coastlines used to construct the profiles are reported in the insets. Stars represent the closest point of the profile to the source. The curves are the best-fit of the Okal and Synolakis (2004) equation (2). (d) I_1 or I_3 vs. I_2 modified after Okal and Synolakis (2004): black dots are from dislocation models, grey dots from landslide models, whereas black and grey triangles refer to worldwide observed dislocation and landslide tsunami data, respectively. Results from the present work are plotted too. It is clear that this representation confirms that the 1693 and 1908 tsunamis are related to a seismic dislocation and that the 1783 6 Feb is referable to an earthquake triggered landslide.

for the 6 Feb 1783 tsunami, we have used an amplitude of depression $\eta = 10$ -20 m (Bosman et al., 2006).

Plotting the I_1 and I_3 values in the logarithmic diagram obtained by Okal and Synolakis for the simulations performed in their study, the combined values I_1 and I_2 confirm that the run-up distribution for 1908 and 1693 data is compatible with tsunamis generated by a seismic dislocation, as also shown by numerical modelling (Tinti & Armigliato, 2003; Gutscher et al., 2006) (Fig. 2d).

On the contrary, combined values of I_1 and I_3 prove that a submarine landslide is the source of the 1783 tsunami, in agreement with historical accounts describing a huge earthquake-induced rockfall in the south-western side of Scilla cliff that collapsed into the sea. Recent off-shore investigations have also shown off-shore evidence of submarine

landslide just in the area of the sub-aerial one (Bosman et al., 2006; Bozzano et al., 2006).

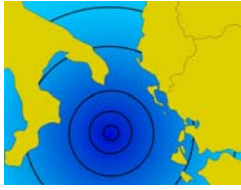
Acknowledgments

This work was funded by the Italian Dipartimento della Protezione Civile in the frame of the 2004-2006 agreement with Istituto Nazionale di Geofisica e Vulcanologia - INGV.

References

- Billi A., Funiciello R., Minelli L., Faccenna C., Neri G., Orecchio B., Presti D. (2008). *On cause of the 1908 Messina tsunami, Southern Italy*. Geophysical Research Letters, 35, L06301, doi:10.1029/2008GL033251.

- Bosman A., Bozzano F., Chiocci F. L., Mozzanti P. (2006). *The 1783 Scilla tsunami: evidences of a submarine landslide as a possible (con?) cause*. Geophysical Research Abstracts, 8, 10558, EGU 2006.
- Bozzano F., Chiocci F.L., Mozzanti P., Bosman A., Casalbore D., Giuliani R., Martino S., Prestininzi A. Scarascia Mugnozza, G. (2006). *Subaerial and submarine characterization of the landslide responsible for the 1783 Scilla tsunami*. Geophysical Research Abstracts, Vol. 8, 10422, EGU 2006.
- Camassi R., Stucchi M. (Ed.) (1997): NT4.1 – *un catalogo parametrico di terremoti di area italiana al di sopra della soglia del danno (ver. NT4.1.1)*. GNDT-CNR, rapporto interno, Milano, 93 pp.
(<http://www.emidius.itim.mi.cnr.it/NT/CONSN T.html>).
- Gerardi F., De Martini P. M., Barbano M. S., Pantosti D. (2006). *Nature of tsunami sources (earthquake or landslide) in eastern Sicily and southern Calabria as inferred from historical data*. XXV Convegno del Gruppo Nazionale di Geofisica della Terra Solida. Roma, 28-30 Novembre 2006.
- Gutscher M.-A., Roger J., Baptista, M.-A., Miranda J.M., Tinti S. (2006). *Source of the 1693 Catania earthquake and tsunami (southern Italy): new evidence from tsunami modelling of a locked subduction fault plane*. Geophysical Research Letters, 33, 1-4, L08309.
- Hills J. G. Mader C.L (1997). *Tsunami produced by the impact of small asteroids*. Annals of New York Academy of Sciences 882, 381-394.
- Ortolani F., Pagliuca S., D'Agostino G. (2005). *Terremoti, frane sottomarine e tsunami lungo le coste italiane: l'esempio di Messina-Reggio Calabria del 1908*. 24° Convegno Nazionale GNGTS, Abstract, pp. 311-313.
- Okal E. A., Synolakis C.E. (2004). *Source discriminants for near-field tsunamis*. Geophys. J. Int., 158, 899-912.
- Pino N. A., Giardini D., Boschi E. (2000). *The December 28, 1908, Messina Straits, southern Italy, earthquake: Waveform modelling of regional seismograms*. Journal of Geophysical Research, 105, B11, 25473-25492.
- Tinti S., Artigliato A. (2003). *The use of scenarios to evaluate the tsunami impact in southern Italy*. Marine Geology, 199, 221-243.
- Tinti S., Argnani A., Zaniboni F., Pagnoni G., Armigliato A. (2007). *Tsunamigenic potential of recently mapped submarine mass movements offshore eastern Sicily (Italy): numerical simulations and implications for the 1693 tsunami*. Abstract n. 8235, IUGG XXIV General Assembly.
- Working Group CPTI (2004). *Catalogo Parametrico dei Terremoti Italiani, versione 2004 (CPTI04)*. INGV, Bologna. <http://emidius.mi.ingv.it/CPTI/>



Goff J.¹

Local, regional, and nationwide palaeotsunamis – a comprehensive database refocuses ongoing and future palaeotsunami research (New Zealand)

¹National Institute of Water & Atmospheric Research, Christchurch (New Zealand)

e-mail: j.goff@niwa.co.nz

Keywords: *Tsunamis, geology, geomorphology, archaeology, anthropology, sources, New Zealand*

A palaeotsunami database has been developed for New Zealand. It is the most comprehensive palaeotsunami database of its kind because it not only contains physical evidence from geological studies, but also data from archaeological and geomorphological sources, and cultural information from anthropological research and prehistoric Māori oral recordings (Goff, 2006). From a geological perspective there are what have been termed primary (geological) and secondary (non-geological) data sources, all of which have varying degrees of validity or reliability. The reliability of any single piece of data, however, is enhanced by

cross-referencing with other related lines of evidence from the same time period or area. The database currently contains about 320 items of evidence (Fig. 1), relating to between 35 and 40 palaeotsunamis.

These data are now being used to improve our understanding of tsunami sources, inundation, event magnitude and frequency, and to guide future research.

For example, in 2005 a local government agency stated that “*in the wake of the Indian Ocean tsunami residents will be glad to know that we do not have a tsunami hazard on our coast*”.

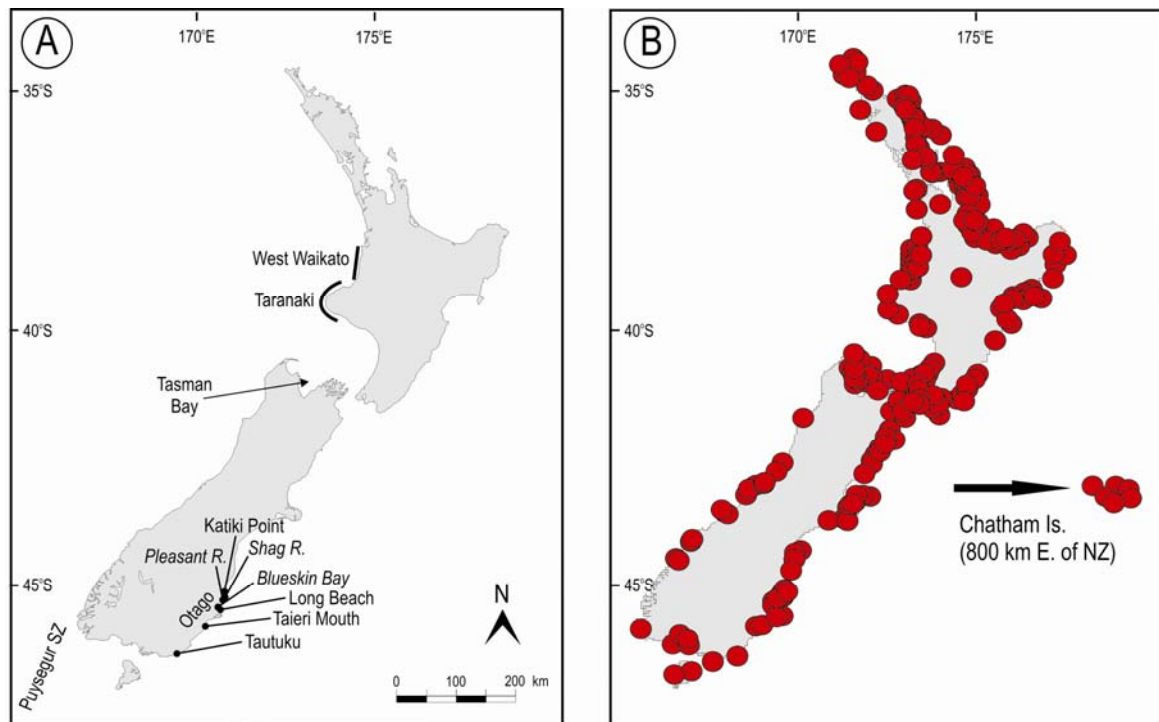


Figure 1. Maps of New Zealand, A) Sites mentioned in the text; B) Existing coverage of the New Zealand Palaeotsunami Database (each site record noted as an item in the database is indicated by a dot on the map).

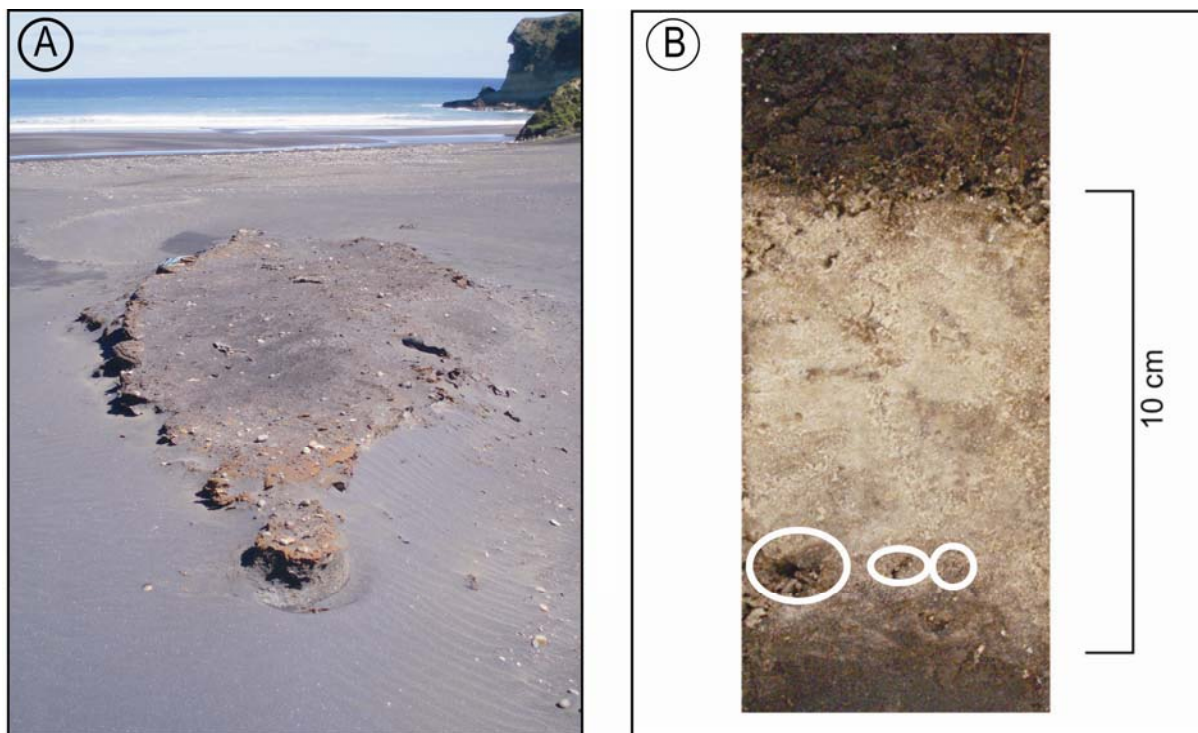


Figure 2. Photographs of recent findings. A) West Waikato coast – discontinuous pebble veneer overlying eroded soil/root mat dated to 13th Century. This provides a maximum age for inundation. B) Chatham Islands - fining-upwards sand unit with marine diatom assemblage and elemental geochemistry indicative of saltwater inundation (rip-up clasts indicated by white ovals).

Geological evidence for palaeotsunamis, however, record that the coastline in question – Tasman Bay - has been struck by several large tsunamis over the past 1000 years (Fig. 1). A paucity of useful palaeoseismic data meant that suggested possible palaeotsunami sources were thought to be less than convincing, thus casting doubt on the original palaeotsunami interpretations. Reference to the recently completed database indicated numerous archaeological and anthropological lines of evidence that added value to earlier palaeotsunami interpretations. The combined evidence for just one of the events is now sufficiently compelling to strongly argue for a region-wide palaeotsunami striking the region's coast about 500 years ago. The addition of new archaeological and anthropological information has changed scepticism of the interpretation of geological data into recognition of a region-wide tsunami hazard. It has also shifted the search for a potential tsunami source from a less convincing fault scenario between the two main islands to more realistic local origins to the west of the area. These findings also add further credence to the interpretation of earlier events in the region.

A search of the database indicated that the SE corner of the South Island, the Otago region, may have also experienced palaeotsunami inundation during the last 1000 years or so (Fig. 1). The data in this case were limited to some poor primary and secondary information from Long Beach and Katiki

Point. In the former location archaeologists noted that a prehistoric coastal Māori settlement had been abandoned in the 15th Century (radiocarbon dated to AD 1460+/-58) and that many of the artefacts on the surface appeared to have been “washed by the sea” (Leach & Hamel, 1981). In the latter location, a discontinuous pebble layer overlies an abandoned prehistoric coastal Māori settlement. Abandoned occurred sometime in the 15th Century (Trotter, 1967). Similar discontinuous pebble layers have been recognised in numerous New Zealand sites as being one of a suite of criteria indicative of past tsunami inundation (e.g. Nichol et al., 2003). A preliminary study was therefore carried out to assess the palaeotsunami record for the region. Examination of the Otago coastline revealed a geomorphology consistent with tsunami inundation. This tsunami geomorphology consisted of a number of elements including dune pedestals, hummocky topography, parabolic dune systems, and post-tsunami features resulting from changes in the nearshore sediment budget (Goff et al., 2007).

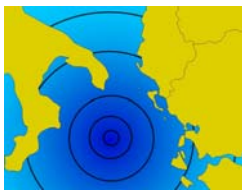
Additional geological, geomorphological, archaeological, and anthropological data were also gathered. A similar discontinuous pebble veneer was evident at Long Beach. It has long been hypothesised that these veneers represent a remnant lag of the original deposit (Nichol et al., 2003). In the case of Long Beach much of the original deposit remains as a predominantly sandy unit with pebble “floaters” overlying the prehistoric Maori

occupation site and adjacent land (Goff et al., in press). This geological evidence sits within the wider geomorphological evidence mentioned above (Goff & Lane, in press). Similar geomorphological evidence was also noted at sites such as Tautuku, Taieri Mouth, Shag River, Pleasant River and Blueskin Bay (Anderson, 1981; Goff et al., 2007). Archaeological evidence for site abandonment either as a result of inundation (e.g. Pleasant River) or probable co-seismic subsidence (e.g. Shag Point) have also been reported (Goff et al., 2007; McFadgen, 2007) (Fig. 1). There are several Māori oral recordings from the region, one of which refers to a wise man's guardian whale called *Matamata* or *Tu-te-raki-hua-noa*. One day the whale appeared off Moeraki (Katiki Point) (Fig. 1) and the children cursed it. Angry at this insult, its owner sent a tidal wave which drowned them. The creek they were standing by had been fresh water till then but it has been brackish ever since (Beattie, 1919). Genealogical estimates place this event around the 15th Century. Recent numerical modelling has determined that the most probable tsunami source for this event is the Puysegur subduction zone to the SW of the South island (Fig. 1). In this instance geological and geomorphological data validate the numerical model output (Lane et al., 2007; Goff & Lane, in press).

Ongoing and future research in New Zealand is now focused on two key areas. First, studies are being carried out in regions not conventionally believed to be exposed to a significant tsunami hazard, but which have numerous secondary data citations. In particular this includes sites on the western side of the North Island such as Taranaki and west Waikato (Fig. 1). Second, there are several areas with a high historical tsunami hazard that have little representation in the palaeotsunami database. This includes the Chatham Islands, 800 km E of the main islands. Preliminary results from both sites have produced notable geological evidence for palaeotsunami inundation (Goff, 2007; Goff, unpublished data) (Fig. 2).

References

- Anderson A.J. (1981). *A fourteenth-century fishing camp at Purakanui Inlet, Otago*. Journal of the Roy Society of New Zealand, 11, 201-221.
- Beattie J.H. (1919). *Nature-lore of the Southern Maori*. Transactions and proceedings of the New Zealand Institute, 52, 53-77.
- Goff J.R. (2006). *Draft palaeotsunami database*. NIWA Internal Report.
- Goff J.R. (2007). *New Plymouth District – tsunami risk*. NIWA Report CHC2007-119, 32pp.
- Goff J.R. Lane E. M. (in press) *The tsunami geomorphology of coastal dunes*. Marine and Freshwater Research.
- Goff J. R., Hicks D. M., Hurren H. (2007) *Tsunami geomorphology in New Zealand*. NIWA Technical Report No. 128, 67 pp.
- Goff J. R., McFadgen B. G., Wells A., Hicks M. (in press) *Seismic signals in coastal dune systems*. Earth Science Reviews.
- Lane E., Walters R., Wild M., Arnold J., Mountjoy J. (2007). *Otago region hazards management investigation: tsunami modelling study*. NIWA Report CHC2007-030.
- Leach H. M., Hamel J. (1981) *Archaic and Classic Maori relationships at Long Beach, Otago: the artifacts and activity areas*. New Zealand Journal of Archaeology, 3, 109-141.
- McFadgen B. G. (2007). *Hostile Shores: Catastrophic events in pre-historic New Zealand and their impact on Maori coastal communities*. Auckland University Press, New Zealand.
- Nichol S. L., Lian O. B., Carter C. H. (2003) *Sheet-gravel evidence for a late Holocene tsunami run-up on beach dunes, Great Barrier Island, New Zealand*. Sedimentary Geology, 155, 129-145.



2nd International Tsunami Field Symposium

IGCP Project 495

Quaternary Land-Ocean Interactions:
Driving Mechanisms and Coastal Responses

Ostuni (Italy) and Ionian Islands (Greece) 22-28 September 2008



Project 495

Graziani L.¹, Maramai A.¹, Tinti S.², Brizuela B.³

Four tsunami events in the Euro-Mediterranean region: analysis and reconstruction of the effects

¹Istituto Nazionale di Geofisica e Vulcanologia, Rome (Italy) e-mail: graziani@ingv.it, maramai@ingv.it;

²Dip. di Fisica, Settore Geofisica, Università di Bologna, Bologna (Italy) e-mail: stefano.tinti@unibo.it

Keywords: *Tsunami, Euro-Mediterranean region, ICG/NEAMTWS*

The Euro-Mediterranean region has been affected along the time by several strong tsunamis (Maramai et al, 2004). The analysis of tsunami catalogues allow to establish the main tsunamigenic sources and reveal that most of the events were local, nevertheless there are some important tsunamis that propagated regionally, involving more than one country. In this study we analysed four tsunami events, the best documented for each one of the most prone areas and to be considered as benchmarks in the Euro-Mediterranean region in the frame of the work carried out by the ICG/NEAMTWS group.

For all the four events a careful analysis of bibliographical and historical sources has been performed in order to obtain a detailed picture of the effects and, where possible, a reconstruction of the inundation and runup values.

The selected events are one for each of these regions, namely AT (eastern Atlantic Ocean), M3 (western Mediterranean, including Spanish and north African events), M2 (central Mediterranean that is Italy, France and eastern Adriatic coasts) and M1 (eastern Mediterranean, including Greek, Turkish and Marmara Sea coasts). They are the most representative and can be either the strongest, the best documented or the most remarkable, considering the extension of its propagation. All of them were generated by earthquakes.

In particular, the case study representative for the NE Atlantic area (AT) is the Lisbon 1755 event, one of the most destructive tsunami ever occurred in the European region, causing severe damage and a lot of victims and propagated as far as the south-eastern coast of England (Andrade, 1992; Baptista et al., 1997, 1998, 1998a). For this event travel time, run-up and wave height distribution have been reconstructed both in the near and in the far-field.

The May 21, 2003 Algerian event is representative for the Western Mediterranean region (M3). This is a strong earthquake located in

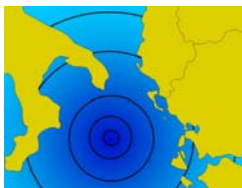
the sea very close to the Algerian coasts, generating a tsunami not destructive but propagated regionally with effects observed along the Balearic islands coast (Alasset et al, 2006; Bounif et al., 2004; Meghraoui et al., 2004). Run-up and inundation values reported at the Balearic islands and travel time at the Italian and French coasts are presented. For the central Mediterranean (M2) the representative event is the December 28, 1908 Messina tsunami, definitely the most important Italian tsunami which caused destruction and many victims along the Sicily and Calabria coasts. In most places the first sea movement was a withdrawal followed by an inundation with two or three waves (Baratta, 1909, 1910; Martinelli, 1909; Platania, 1909; Tinti et al, 2001). Measured run-up and inundation values along the Sicilian, Calabrian and Maltese coasts are reported. The July 9, 1956 Cyclades tsunami, locally very strong affecting all the Aegean islands and propagating as far as Crete, has been selected as representative for the eastern Mediterranean area (M1) (Ambraseys, 1960; Dominey-Howes, 1996; Galanopoulos, 1957; Papadopoulos et al., 2005). Reconstructed run-up and wave height distribution are presented.

For some localities struck by the selected tsunamis a reconstruction of the inundated areas was performed and, where possible, an hypothetical inundation lines was superimposed to the present day territory maps in order to identify vulnerable structures.

References

- Alasset P. J., Hébert H., Maoche S., Calbini V., Meghraoui M., 2006. *The tsunami induced by the 2003 Zemmouri earthquake (Mw=6.9), Algeria): modelling and results*. Geoph. Jour. Intern., doi:10.1111/j.1365-246X.2006.02912.x.
- Ambraseys N. N. (1960). *The seismic sea wave of July 9, 1956, in the Greek Archipelago*. Journal

- Geophysical Research, vol.65, n.4, pp1257-1265.
- Andrade C. (1992). *Tsunami Generated Forms in the Algarve Barrier Islands (South Portugal)*. Science of Tsunami Hazards, 10 (1), 21-34
- Baptista M. A., Heitor S., Miranda J. M., Miranda P., Mendes Victor L. (1997). *The 1755 Lisbon Tsunami: Evaluation of the Tsunami parameters*, - Journal of Geodynamics, vol 25, n° 2, pp 143-157. 1997
- Baptista M. A., Miranda P. M. A., Miranda J. M. Victor L.M. (1998). *Constraints on the source of the 1755 Lisbon tsunami inferred from numerical modelling of historical data*. Journal of Geodynamics, 25, 159-174, Pergamon.
- Baratta M., 1909. *Alcuni risultati ottenuti dallo studio del terremoto calabro messinese del 28.XII.1908*. Bollettino Società Geografica Italiana, Vol. X, Fasc. 11.
- Baratta M. (1910). *La catastrofe sismica calabro messinese*. Biblioteca di Sismologia, Roma.
- Bounif A., Dorbath C., Ayadi A., Meghraoui M., Beldjoudi H., Laouami N., Frogneux M., Slimani A., Alasset P. J., Kharroubi A., Ousadou F., Chikh M., Harbi A., Larbes S., Maouche S. (2004). *The 21 May 2003 Zemmouri (Algeria) earthquake Mw 6.8 : relocation and aftershock sequence analysis*. Geophysical. Research Letters, 31, 1-4
- Dominey-Howes D.T.M. (1996). *Sedimentary deposits asociated with the July 9, 1956 Aegean sea tsunami*. Physical and Chemistry of the Earth, 21, pp.51-55.
- Galanopoulos A.G. (1957). *The seismic sea wave of July 9, 1956*. Prakt. Acad.Athens, 32, pp. 90-101.
- Maramai A., Graziani L., Tinti S. (2003). *Updating and revision of the European Tsunami Catalogue*. NATO Sciences Series: "Submarine Landslides and Tsunamis", Kluwer Academic Publishers, (Editors: Yalciner A.C., Pelinovsky E. , Okal E and Sinolakis C.), 25-32.
- Martinelli G. (1909). *Osservazioni preliminari sul terremoto calabro messinese del mattino del 28 dicembre 1908*. Bollettino Bimensuale della Società Meteorologica Italiana, Ser. III, Vol. XXVIII, pp.3-11.
- Meghraoui M. et al, (2004). *Coastal uplift and thrust faulting associated with the Mw=6.8 Zemmouri (Algeria) earthquake of 21 May, 2003*. Geophysical Research Letters, 31, L19605 1-4.
- Papadopoulos G.A., Imamura F., Minoura K., Takahashi T., Karakatsanis S., Fokaefs A., Orfanogiannaki K., Daskalaki E., Diakogianni G. (2005). *The 9 July 1956 large tsunami in the South Aegean sea: compilation of a data basis and re-evaluation*. Proceeding 22nd IUGG International tsunami Symposium, Chania, Crete, pp.173-180.
- Platania G. (1909). *Il maremoto dello Stretto di Messina del 28 dicembre 1908*. Bollettino Società Sismologica. Italiana, XIII, pp.369-458.
- Tinti S. Armigliato A. (2001). *Impact of large tsunamis in the Messina Straits, Italy: the case of the 28 December 1908 tsunami*. Tsunami research at the end of a Critical Decade, Hebenstrait, G.T. Editor, Kluwer, pp.139-162.



2nd International Tsunami Field Symposium

IGCP Project 495

Quaternary Land-Ocean Interactions:
Driving Mechanisms and Coastal Responses

Ostuni (Italy) and Ionian Islands (Greece) 22-28 September 2008



Project 495

Khomarudin M. R.^{1,2}, Strunz G.¹, Ludwig R.³, Zoßeder K.¹,

Post J.¹, Kongko W.^{2,4}, Pranowo S. W.^{2,5}

People exposure and land use damage estimation caused by tsunami using numerical modelling and GIS approaches (Case study: South Coast of Java – Indonesia)

¹German Aerospace Center (DLR), e-mail: rokhis.khomarudin@dlr.de; guenter.strunz@dlr.de; kai.zosseder@dlr.de; joachim.post@dlr.de;

²United Nation University-Environment and Human Security (UNU-EHS), email: khomarudin@ehs.unu.edu;

³Department of Geography-Ludwig Maximilian University Munich, e-mail: r.ludwig@lmu.de;

⁴Danish Hydrological Institute (DHI), e-mail: liawid@yahoo.com;

⁵Alfred Wegener Institute (AWI), e-mail: Widodo.Pranowo@awi.de

Keywords: *Tsunami, modeling, exposed people, land-use, GIS, South Coast of Java*

For tsunami risk analysis information about the number of exposed people and about the land-use in the endangered areas are important input parameters. Data on people distribution could help to manage the evacuation planning and mitigate the people loss by tsunami. Land-use and potential damages are relevant for rehabilitation management.

The aim of the paper is to present methodologies and tools to generate the above mentioned missing information before a disaster happens. Based on this, governmental authorities can prepare and calculate how many people are living in the affected area, how many people could be evacuated, and how to perform adequate land use planning to mitigate the disaster impact. For the disaster response phase, the local government will be supported to plan and manage the evacuation process more efficiently. For the recovery phase, government will be provided by estimates on the amount and type of potential damages.

This research analyzes the estimation of people at risk and potential land-use damage estimation by tsunamis in the South Coast of Java, Indonesia. Combinations of numerical modelling and Geographic Information System (GIS) approaches have been applied in this research. There are three scenarios for tsunami simulations generated by earthquake magnitude Mw 8.5 with different locations of the epicentres.

TUNAMI-N1 model has been applied to determine the tsunami wave height in the coastal area. Validation of tsunami modelling has been performed using Aceh Tsunami 2004 data.

Inundation modelling was applied to the study area and the results were combined with the people distribution map and land-use data to estimate people at risk and land-use damage by tsunami.

People distribution maps during day time and night time were derived.

The results of this research will be integrated in an information system, which in future can be applied on the level of the local government to better mitigate the impact of tsunami disaster and provide tools for an improved tsunami risk assessment for decision makers at the local level.

Method

To reach the described goals four methodological steps have been developed. The first is the tsunami inundation modelling. A combination between Tsunami N1 (Imamura, et al. (2006)) and modification of Federici, et al. (2006) formula was conducted in this research.

This means that tsunami modelling results, which are valid for the calculation of expected wave heights at the coastline, are combined with empirically derived relationships, which are newly developed to calculate the tsunami inundation.

Tsunami wave heights at coastlines have then been used as input in the Federici formula to calculate the inundation area. The modification of the Federici formula is replacing the land use condition as a reducing tsunami wave factor with tsunami wave height and inundation reduction caused by distance from the coast.

The maximum wave heights from TUNAMI-N1 are used as input values (R_u) to inundation modelling using the Federici formula as shown in equation (1):

$$W = \varepsilon \cdot R_u - Z \quad (1)$$

Where,

ε = Roughness parameters
 R_u = Maximum wave height at the coast
 Z = height of the ground (from DEM SRTM)

If $W > 0$ inundation pixel = 1 wet
 If $W < 0$ no inundation pixel = 0 dry

Validation of proposed inundation calculation was done based on inundation mapping using post disaster Landsat data (USGS, 2004). The validated model was then used to calculate the potential inundation area in the study area. The second part is deriving the people distribution maps in study area. Generally population distribution is representative for administrative units, far too coarse to adequately calculate amount of people affected. An improvement of spatial resolution of population database is presented here. The population data from census sources are commonly made available per political or administrative unit (Schneiderbauer,

2007). In Indonesia, the people distributions data is represented at village level. In fact, people are doing activity in certain land uses within the representative census data at village level. The combination of people distribution data from census and detailed land use information (derived from Indonesian topographic map at 1: 25.000 scale) is used to disaggregate and down-scale population distribution. For example, distribution of people in a settlement area in one village will be different than in a paddy field area in that village which is not reflected in census population data. The proportion (weighting) of people in the different land-use areas is needed in this analysis. This is a critical value to estimate people distribution based on detailed land use information (Gallego, 2007). For the south coast of Java, this proportion is calculated based on people activity during day and night time within the assigned land use classes. The distribution factors to calculate population distribution at day and night time per land use is derived from national statistical data (BPS, 2006). Hereof percentages of people working in certain land use classes (e.g. agriculture, industry) are derived and have been used as weighting / distribution factor. This data also will be used to calculate the land use damage estimation.

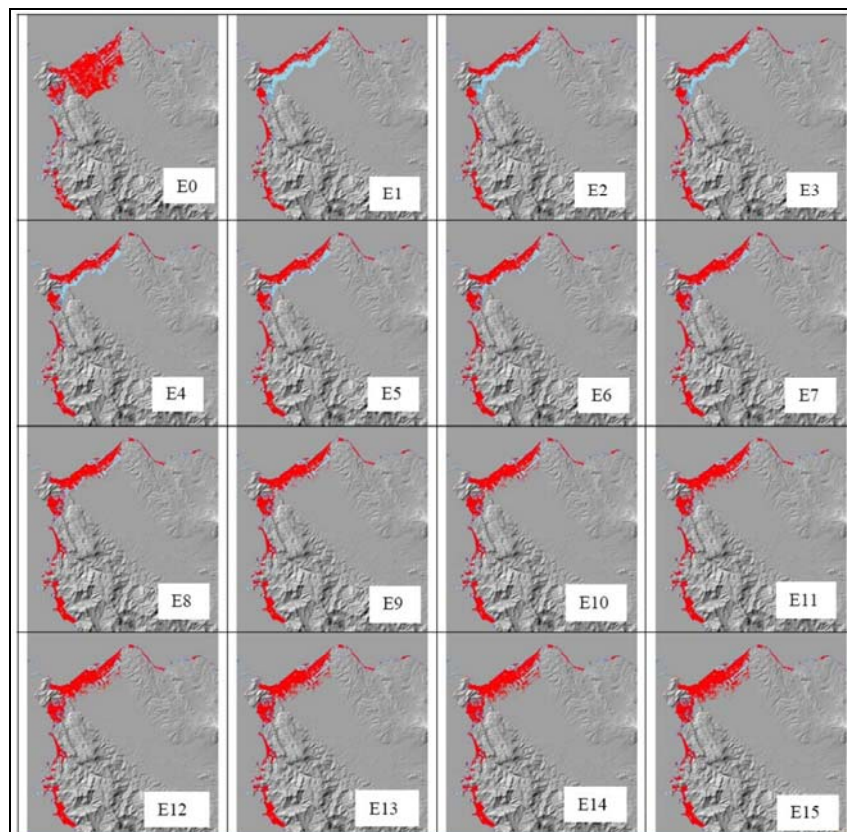


Figure 1. The validation of tsunami inundation base on Federici, et al. (2006) modification.

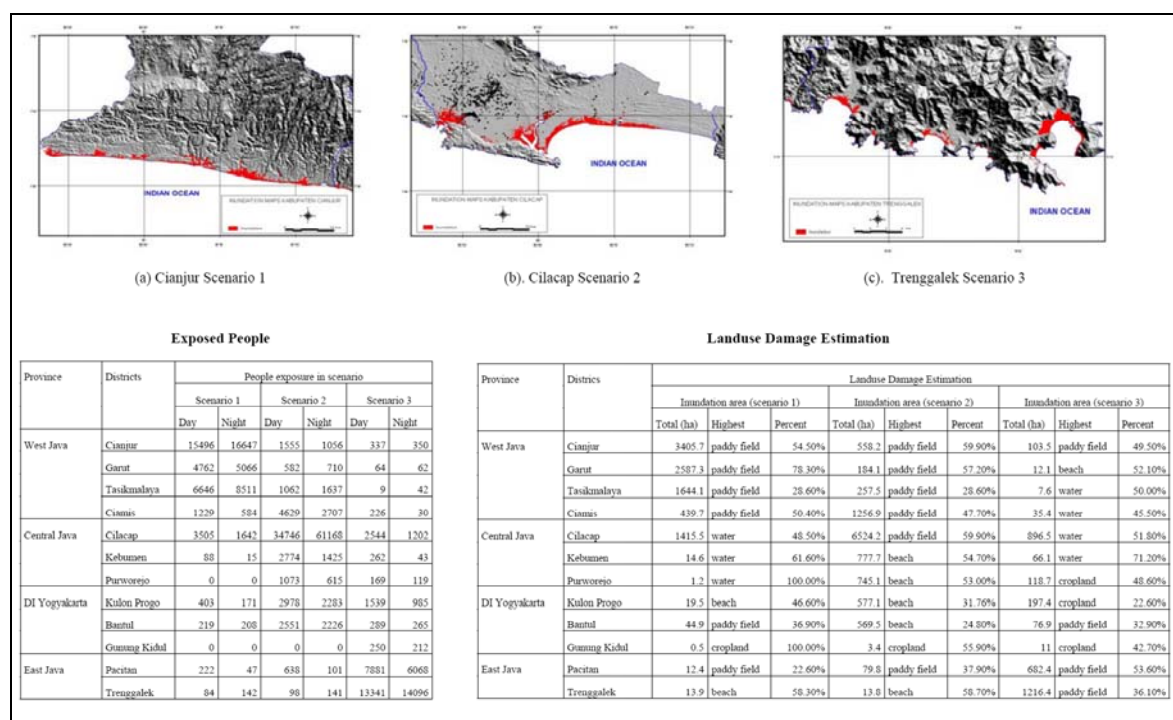


Figure 2. The result of inundation modelling in the most danger districts, total number of exposed people and land damages estimation

In a third step, the newly derived people density information and land use 1: 25.000 scales data were combined (overlaid) with validated tsunami inundation modelling to derive exposed people and estimate land use damaged in 12 districts in South Coast of Java.

The last and fourth step is a conceptual study to design and implement a risk information tool. It is designed to help local government and reflects the needs of local decision makers handling a simple and robust tool. The tool shall deliver the possibility for the local government to extract information relevant for disaster management planning.

The data that were used in this work are the Digital Elevation Model (DEM), which is based on the Shuttle Radar Topography Mission (SRTM), for tsunami inundation modelling. For the exposure analysis the topographic maps of South Coast of Java, scale 1: 25.000 (Bakosurtanal) and statistical data (Statistical Bureau Indonesia, 2006) were used.

Results and Discussion

The result of the validation is shown in Fig. 1. The proposed modifications of Federici formula for the calculation of tsunami inundation deliver a similar pattern compared to the inundation area from USGS.

Based on this result the Tunami N1 software has been run with three scenario of tsunami source in Indian Ocean. There are 3 different epicentre locations used to calculate the used tsunami

scenarios: epicentre's location at 108.192 E, 9.27565 S as scenario 1; at 108.896 E, 9.11123 S as scenario2; and at 109.619 E, 9.02594 S as scenario 3. The result of inundation modeling in the most danger districts, total number of exposed people and land use damage estimation in that three scenarios are shown in the Fig. 2. As can be seen in Fig. 2, the Districts of Cianjur, Cilacap, and Trenggalek are the most affected areas according to estimation results for scenario 1, scenario 2, and scenario 3 respectively. According to the results for scenario 1 the district of Cianjur has 16 villages affected by tsunami inundation.

The village of Jayagiri is showing highest number of people at risk. According to the results presented for scenario 2 the district of Cilacap has 53 villages potentially affected by tsunami inundation with the village of Cilacap at highest risk. In scenario 3 the district of Trenggalek shows 15 villages potentially affected by tsunami inundation with the village of Tasikmadu at highest risk (Fig. 2).

The land-use damage estimation presented here allows quantifying loss of resources and potential monetary losses due to tsunami impact. According to the estimation results from scenario 1, District of Cianjur has 1,858.3 ha paddy field potentially destroyed by tsunami inundation (see Fig. 2). Assuming 4 tons/ha productivity per crop-season, this district will lose 7,433 tons paddy or approximately 7.43 billion rupiah (equal with \$US 826,000) at this moment. The example calculation for paddy field can now be extended to the total

loss from all land use including the budget calculations for its rehabilitation (Fig. 2).

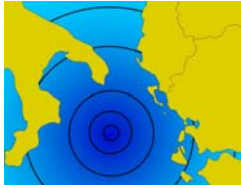
Finally, the integration of the results into a risk information tool for local decision makers was performed. The derived information is supplied to a risk information tool conceptually developed for 12 districts at the south coast of Java.

The tool is user friendly designed and prepared for standard personal computers available at local governmental institutions.

The tool shall help local government to get information of exposed people and land use damages estimation. In a next step, this tool will be further developed based on user requests.

References

- Federici B., Bacino Cosso T., Poggi P., Rebaudengo Landó D. L., Sguerso L. (2006). *Analisi del rischio tsunami applicata ad un tratto della costa Ligure*. Università degli Studi di Genova.
http://www.dimset.unige.it/venti/grass/presentazioni/sessione%205/Tsunami_GrassDay.pdf
- Gallego J. (2007). *Downscaling Population Density with Corine Land Cover. Integrating Socio-Economic and Remote Sensing Information for Food Security and Vulnerability Analyses, Technical Seminar, 12-13 Oktober 2007*. (power point presentation)
- Imamura F., Yalciner A., Ozyurt G. (2006). *Tsunami Modelling Manual*. UNESCO IOC International Training Course on Tsunami Numerical Modelling.
- Schneiderbauer S. (2007). *Population Densities in Zimbabwe. Integrating Socio-Economic and Remote Sensing Information for Food Security and Vulnerability Analyses, Technical Seminar, 12-13 Oktober 2007*. (paper and power point presentation).
- Statistical Bureau Indonesia (2005). *Potensi Desa* 2005.
- Thywissen K. (2006). *Component of Risk a Comparative Glossary*. Source (Studies of The University : Research, Counsel, Education) No. 2/2006. Publication series of UNU-EHS.
- USGS (2004). <http://gisdata.usgs.gov/website/Tsunami>



2nd International Tsunami Field Symposium

IGCP Project 495

Quaternary Land-Ocean Interactions:
Driving Mechanisms and Coastal Responses

Ostuni (Italy) and Ionian Islands (Greece) 22-28 September 2008



Project 495

Kongko W.¹, Lavigne F.², Paris R.³

Investigation on colliding wave of tsunami run-ups in December 26th 2004 Indian Ocean tsunami

¹Coastal Dynamic Research Center BPPT, Jl. Grafika 2, Bulaksumur, Jogjakarta, Indonesia,

e-mail: widjo@webmail.bppt.go.id;

²University Paris 1 and Laboratoire de géographie, Meudon, France, e-mail: lavigne@univ-paris1.fr;

³Géolab, CNRS, Clermont-Ferrand, France

Keywords: *Tsunami run-up, colliding wave, tsunami modelling, bottom roughness*

Huge earthquake on December 26th 2004 which is followed by giant tsunami attacked Nangroe Aceh Darussalam-Indonesia through two directions, namely Uleelheue and Lhoknga. Two directions tsunami run-up collided approximately in Lampisang village, District of Peukan Lambada which has still essentially flow depth and strong

current.

Three weeks after the event, International Tsunami Survey Team (ITST) was formed and performed rapid field survey to record Tsunami wave run-up, flow depth, and its direction in several locations.

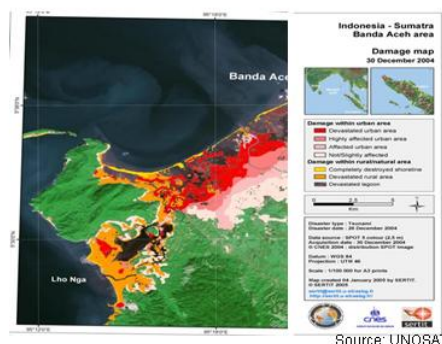
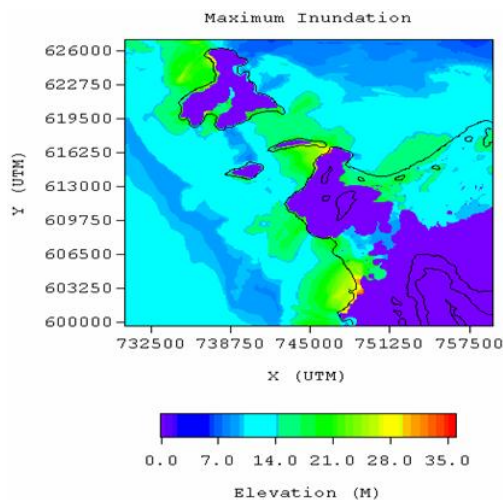


Figure 1. The Focus Study Area and Its Inundation.

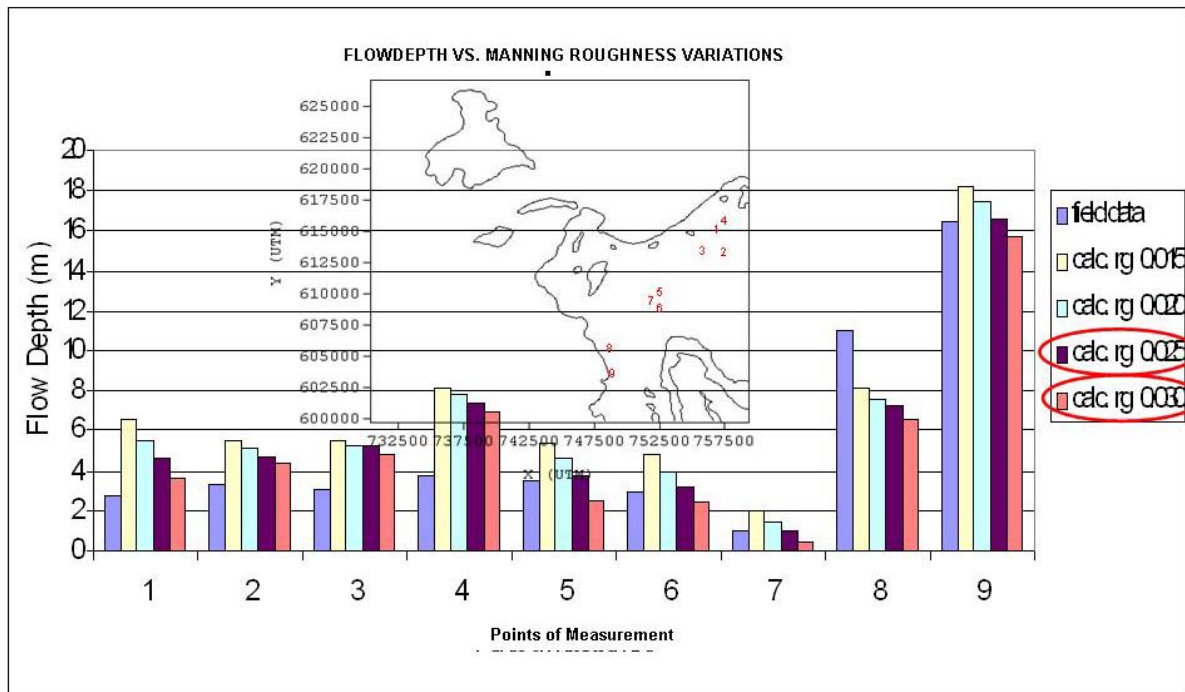


Figure 2. The Flow-depth Vs Roughness Variations.

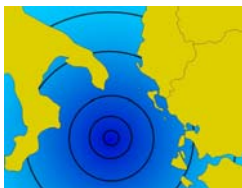
Furthermore, one year later, the small team of local researcher had chance to investigate and make interview witnesses in locations which had tsunami run-up from two directions were met.

This paper will describe the result of the field survey in particularly the event of the colliding two tsunami run-ups and its quantitative parameter, such as flow depth, colliding points, number of incident wave, and arrival time. In addition, by using shallow water wave equation with leap-frog scheme of Tunami N3 model and moving fault of source parameter published by Tanioka, the numerical simulation has been conducted. The result of the numerical simulation namely, tsunami run-up height, travelling time, distance and area penetration were compared with the result of the field survey which was performed.

The comparison of the results show that, however the numerical method has still some problems in determination of bottom roughness value, by giving reasonably value, it has comparatively good agreement with field survey result.

References

- Lavigne F., Paris R. (Eds), 2008. *Rapport scientifique du programme Tsunarisque* (2005-2006), Presses Universitaires de la Sorbonne (in press).
- Kongko W., Istianto D., Hidayat R., Prasetya G. ITST. (2005). *Report of Field Survey on December 26 2004 Indian Ocean Tsunami* (Internal Report, Unpublished).



2nd International Tsunami Field Symposium

IGCP Project 495

Quaternary Land-Ocean Interactions:
Driving Mechanisms and Coastal Responses

Ostuni (Italy) and Ionian Islands (Greece) 22-28 September 2008



Project 495

Lario J.¹, de Luque L.², Zazo C.³, Goy J. L.⁴, Spencer C.⁵, Cabero A.³, Dabrio C.⁶,
Borja F.⁷, Civis J.⁴, González-Delgado J. A.⁴, Borja C.⁸

A review of the high energy events in the Gulf of Cadiz: tsunami vs. storm surges

¹Dep. Ciencias Analíticas, Universidad Nacional de Educación a Distancia, Madrid (Spain),
e-mail: javier.lario@ccia.uned.es;

²Fund.Conjunto Paleontológico - Dinópolis, Teruel (Spain)

³Dep.Geología, Museo Nacional de Ciencias Naturales, Madrid (Spain)

⁴Dep.Geología, Universidad de Salamanca, Salamanca (Spain)

⁵Fac.of the Built Environment, University of West England, Bristol (United Kingdom)

⁶Fac.CC.Geologicas, Universidad Complutense de Madrid, Madrid (Spain)

⁷Fac. Humanidades, Universidad de Huelva. Huelva (Spain)

⁸Facultad de Geografía e Historia, Universidad de Sevilla. Sevilla (Spain)

Keywords: *high energy event, tsunami, storm surge, severe storms, Holocene, Gulf of Cadiz*

During the last decade many papers have appeared devoted to the occurrence of high energy marine episodes associated with sedimentological, palaeontological or geomorphological features.

Currently the most complete record of Holocene high energy marine events comes from the Gulf of Cadiz (SW Iberia) (Fig. 1). These studies focused

on the recognition and description of different deposits from high energy events which have been interpreted as having occurred from tsunamis.

A revision of these data reveal that only few of these events left clear evidence that can be considered of tsunamigenic origin.

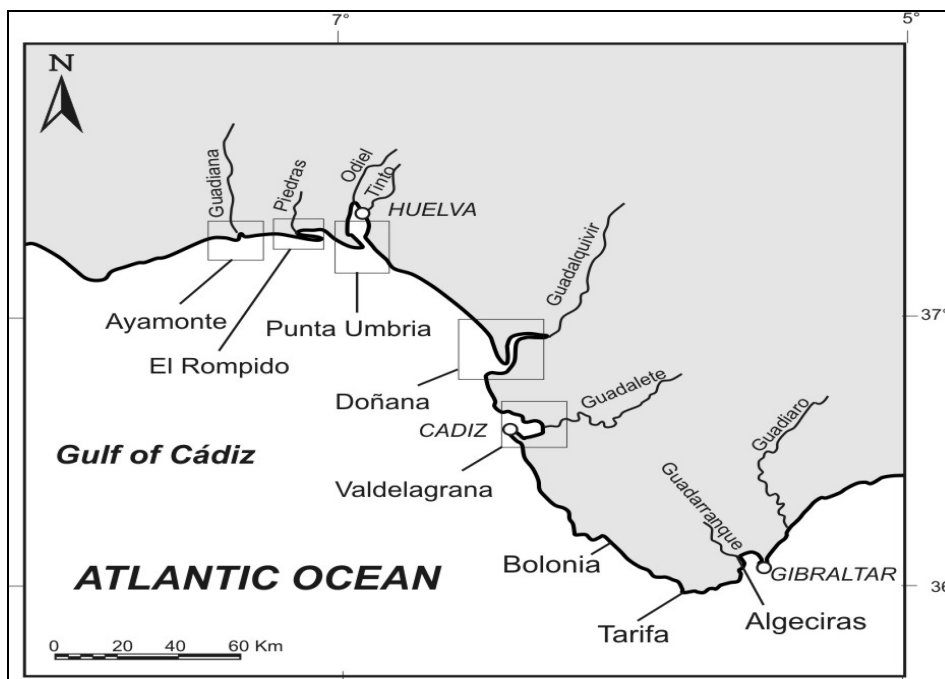


Figure 1. Location of sites cited in text with geological record of high energy event in the Gulf of Cadiz (SW Spain).

Age	Sedim. or geomorphological features	Reference	Interpretation	Data support
Doñana spit barrier / Guadalquivir Marshland				
5500-3500 calBP				
5309 calBP	Fines deposit with shell fragments, breaching of the spit barrier, cherniers development	(Ruiz et al. 2005, Cáceres et al., 2006)	Tsunami	Correlation with others authors
4500-4200 calBP	Spit barrier breaching	(Lario et al., 1995; Lario, 1996)	Storm surge	
4200-4100 calBP	Deposits with marine fauna in the estuary	(Ruiz et al. 2005)	Tsunami & storms	Correlation with others authors
4200-4100 calBP	Cherniers development and fines deposits	(Cáceres et al., 2006)	Tsunami	Correlation with others authors
3900-3700 calBP	Cherniers development and spit barrier breaching + erosion at the bottom of the lagoon and in old cherniers	(Ruiz et al. 2005, Cáceres et al., 2006)	Tsunami	Correlation with others authors
2500-2000 calBP				
2600-2500 calBP	Sand layer with marine fauna between estuarine deposits, erosional limit, high magnetic susceptibility. Spit barrier erosion.	(Lario, 1996; Lario et al., 2001, 2002)	Tsunami	Historical seismic catalogue
2700-2400 calBP	Spit barrier erosion and breaching	(Lario et al., 1995; Lario, 1996)	Storm surges	Climatic instability
2400-2200 calBP	Silt and sand with marine and estuarine fauna. Spit barrier breaching	(Ruiz et al., 2004)	High energy event (storm? tsunami?)	
2400-2250 calBP	Spit barrier erosion and breaching	(Cáceres et al., 2006)	Tsunami	Correlation with others authors or seismic catalogue
ca.2000 calBP	Cherniers development	(Ruiz et al., 2004)	High energy event	
2020-1990 calBP	Erosion at the bottom of the lagoon, marine fauna and cherniers development	(Cáceres et al., 2006)	Tsunami	Correlation with others authors or seismic catalogue
1559-1510 calBP	Bioclastic sandy silts on erosive surface	(Ruiz et al., 2006)	Tsunami	Historical seismic catalogue
Punta Umbria spit barrier/ Tinto-Odiel marshland				
5700 calBP	Sands with micro- and macro- marine shells	(Ruiz et al., 2007)	Storm	
2700-2400 calBP	Spit barrier breaching and reorganisation of the back-barrier drainage system	(Lario, 1996)	Storm surge	
Valdelagrana spit barrier/ Guadalete marshland				
ca.7000 calBP	Input of coarse sediment (sands), marine shells fragments and increase in magnetic susceptibility	(Lario, 1996)	Storm	
ca.5600 calBP	Input of coarse sediment (sands), marine shells fragments and increase in magnetic susceptibility	(Lario, 1996)	Storm	
2700-2400 calBP	Spit barrier breaching and reorganisation of the back-barrier drainage system	(Lario et al., 1995; Lario, 1996; Dabrio et al., 1999)	High energy event	
2300-2200 calBP	Washover fans, repeated fining upward sequence (2 to 3 times), marine shell fragments, armed mounted clasts, erosional lower limit	(Luque et al., 2002)	Tsunami	Concluding characteristics of the deposits
1755	Washover fans, repeated fining upward sequence (3 to 4 times), marine shell fragments, armed mounted clasts, erosional lower limit	(Dabrio et al, 1998; Luque et al., 2001)	Tsunami	Concluding characteristics of the deposits. Dated by historical documents and historical maps
SW coast of Cadiz				
2150-1825 calBP	Bolonia. Coarse sand with bioclast	(Alonso et al., 2004)	Tsunami	Correlation with the Baelo Claudia earthquake
ca.50 AD	Carteia, Algeciras. Coarse sandy layer, fining upward sequence, mounted clast, bioclast, calcareous rodolites, erosional lower limit	(Arteaga Cardineau and González Martín, 2004)	High energy event, probable a tsunami	Dated by roman archaeological remains. Near concluding characteristics of the deposits
1755?	Cabo de Trafalgar. Large orientated rock blocks	(Whelan y Kelletat, 2003, 2005; Alonso et al., 2004)	Tsunami associate with the 1755 Lisbon earthquake	
1755?	Los Lances beach, Tarifa. Washover fans	(Alonso et al., 2004)	Tsunami associate with the 1755 Lisbon earthquake	No sedimentological data
1755	Conil. Washover fans	(Luque et al., 2004)	Tsunami associate with the 1755 Lisbon earthquake	Dated by historical documents and historical maps

Table 1. Geological record of Holocene high energy episodes in the Gulf of Cadiz coast with possible origin of the event

Even though there is evidence of some occurrences of tsunamis in the area during the Holocene, the geological record does not definitely distinguish storm from tsunami events.

There are some geological features common to both types of events such as breaching of the spit barriers with formation of washover fans, fining upward sequences, erosional limit or presence of

marine shell remains. The record of such features indicates only that these deposits have high energy marine origin. There are some other characteristics of the sedimentary record that more definitely attribute the event to a tsunami episode, such as the presence of some fining-upward sequences, presence of mud clast, presence of mud laminae, high variation in grain size (from clays to boulders)

or presence of clay layer on the top (as a cap). Also, there is other geomorphological evidences will be associated with a tsunami event: reorganisation of the barrier-estuary systems with extensive flooding, breaching of the spit barrier, presence of multiple washover fans and complete reorganisation of the drainage system (Andrade, 1992; Goff et al., 2004; Tuttle et al., 2004; Kortekass & Dawson, 2007; Morton et al., 2007).

Data available from Gulf of Cadiz, summarized in Table 1, show that even though there is evidence of some occurrences of tsunamis in the area during the Holocene, the sedimentological and geomorphological record does not definitely distinguish storm from tsunami events. Some of them only will be associated with a high energy event of marine origin that will be also produce by an storm surge episode. In order to calculate recurrence interval both from severe storm surges and from tsunami events more detailed studies should be completed.

For now the occurrence or high energy marine event in this area during the Holocene is summarized as:

ca.7000 calBP: High energy event, storm?

ca.5600-5300 calBP: High energy event, storm?

ca.4200-4000 calBP: High energy event

ca.2700-2400 calBP: High energy events: probably tsunami during climatic instability period with severe storms. The event present features all along the coast. Concluding record of tsunami in Valdelagrana (Luque et al., 2003) probably present in other areas of the Gulf of Cadiz.

ca.2000 calBP: High energy event. Probably tsunami (maybe the same that the last one, problems in dating)

ca.1500 calBP: High energy event 1755 AD: Lisbon earthquake tsunami. Even though historical data describe the occurrence of the tsunami in some sites, there is not always a geological record. Lack in concluding dates from this record in some areas.

References

- Andrade C. (1992). *Tsunami generated forms in the Algarve barrier islands*. Science of Tsunami Hazards, 10, 21-33.
- Alonso C., Gracia F. J., Del Rio L., Anfuso G., Benavente J., Martinez J. A. (2004). *Registro morfosedimentario de eventos históricos de alta energía en el litoral atlántico del Estrecho de Gibraltar (Trafalgar-Tarifa)*. En: Contribuciones recientes sobre Geomorfología (Benito, G. y Diéz herrero, A., Ed.), SEG-CSIC, Madrid, 263-271.
- Cáceres L. M., Rodríguez Vidal J., Ruiz F., Rodríguez Ramírez A., Abad M. (2006). *El registro geológico Holoceno como instrumento para establecer periodos de recurrencia de tsunamis: el caso de la costa de Huelva*. V Asamblea Hispano Portuguesa de Geodesia y Geofísica, Sevilla, 1-4.
- Dabrio C. J., Goy J. L., Zazo C. (1998). *The record of the tsunami produced by the 1755 Lisbon earthquake in Valdelagrana spit (Gulf of Cádiz, S Spain)*. Geogaceta, 23, 31-34.
- Dabrio C. J., Zazo C., Goy J. L., Sierro F. J., Borja F., Lario J., González J. A., Flores J. A. (2000). *Depositional history of estuarine infill during the Last Postglacial transgression (Gulf of Cádiz, Southern Spain)*. Marine Geology, 162, 381-404.
- Goff J., McFadgen B. G., Chagué-Goff C. (2004). *Sedimentary differences between the 2002 Easter storm and the 15th-century Okoropunga tsunami, southeastern North Island, New Zealand*. Marine Geology, 204, 235-250.
- Kortekaas S., Dawson A. G. (2007). *Distinguishing tsunami and storm deposits: An example from Marthinal, SW Portugal*. Sedimentary Geology, 200, 208-221.
- Morton R. A., Gelfenbaum G., Jaffe B. E. (2007). *Physical criteria for distinguishing sandy tsunami and storm deposits using modern examples*. Sedimentary Geology, 200, 184-207.
- Lario J. (1996). *Ultimo y Presente Interglacial en el área de conexión Atlántico – Mediterráneo: Variaciones del nivel del mar, paleoclima y paleoambientes*. Ph.D. Thesis. Universidad Complutense de Madrid: 269 pp.
- Lario J., Zazo C., Dabrio C. J., Somoza L., Goy J. L., Bardají T., Silva P. G. (1995). *Record of recent holocene sediment input on spit bars and deltas of South Spain. In Holocene Cycles; Climate, Sea Levels and Sedimentation*, Journal of Coastal Research, Special Issue, 17, 241-245.
- Lario J., Zazo C., Plater A.J., Goy J.L., Dabrio C., Borja F., Sierro F.J., Luque L. (2001). *Particle size and magnetic properties of Holocene estuarine deposits from the Doñana National Park (SW Iberia): evidence of gradual and abrupt coastal sedimentation*. Zeitschrift fur Geomorphologie 45(1), 33-54.
- Lario J., Spencer C., Plater A.J., Zazo C., Goy J.L., Dabrio C. (2001). *Particle size characterisation of Holocene back-barrier sequences from North Atlantic coasts (SW Spain and SE England)*. Geomorphology 42, 25-42.
- Luque L., Lario J., Zazo C., Goy J.L., Dabrio C. J., Borja F. (2002). *Sedimentary record of historical tsunamis in the Bay of Cádiz (Spain)*. Journal of Quaternary Science, 17: 623-631.
- Luque L., Lario J., Zazo C., Goy J.L., Dabrio C.J., Silva P. G. (2001). *Tsunami deposits as palaeosismic indicators: examples from the spanish coast*. Acta Geológica Hispánica, 36, 197-211.

- Luque L., Zazo C., Lario J., Goy J.L., Civis J., Gonzalez-Hernandez F. M., Silva P. G., Dabrio C. J. (2004). *El efecto del tsunami de 1755 en el litoral de Conil de la Frontera (Cádiz). Zona Arqueológica*, 4. *Miscelánea en Homenaje a Emiliano Aguirre*. V-I, Geología, 72-82.
- Ruiz F., Rodriguez Ramirez A., Caceres L., Rodríguez Vidal J., Carretero M. I., Clemente L., Muñoz J. M., Yañez C., Abad M. (2004). *Late Holocene evolution of the southwestern Doñana Nacional Park (Guadalquivir estuary, SW Spain): a multivariate approach*. *Palaeogeography, Palaeoclimatology, Palaeoecology*, 204, 47-64.
- Ruiz F., Rodriguez Ramirez A., Caceres L., Rodríguez Vidal J., Carretero M. I., Abad M., Olías M., Pozo M. (2005). *Evidence of high-energy events in the geological records: Mid-holocene evolution of the southwestern Doñana Nacional park (SW Spain)*. *Palaeogeography, Palaeoclimatology, Palaeoecology*, 229, 212-229.
- Tuttle M. P., Ruffman A., Anderson T., Jeter H. (2004). *Distinguishing tsunami from storm deposits in eastern North America: the 1929 grand banks tsunami versus the 1991 Halloween storm*. *Seismological Research Letters*, 75, 117-131.
- Whelan F., Kelletat D. (2003). *Analysis of tsunami deposits at Cabo de Trafalgar, Spain, using GIS and GPS technology*. *Essener Geographische Arbeiten*, 35, 11-25.
- Whelan F., Kelletat D. (2004). *Boulder deposits on the Southern Spanish Atlantic Coast: possible evidence for the 1755 AD Lisbon Tsunami?*. *Science of Tsunami Hazards*, 23(3), 25-38.



MacInnes B. T.¹, Bourgeois J.¹, Pinegina T. K.², Kravchunovskaya E. A.²

A comparison of sediment eroded vs. deposited by the 15 Nov 2006 Kuril Island

¹Department of Earth & Space Sciences, University of Washington, Seattle, USA

²Institute of Volcanology and Seismology, Far Eastern Branch Russian Academy of Sciences,
Petropavlovsk-Kamchatskiy, Russia

Corresponding author: Breanyn MacInnes, e-mail: macinneb@u.washington.edu

Keywords: *tsunami, coastal geomorphology, tsunami deposit, tsunami erosion, Kuril Islands*

What effect coastal geomorphology has on tsunami deposition and erosion is an open question in tsunami geology. Although historical accounts suggest that large tsunamis can produce significant geomorphic changes to coastlines (c.f. Konno et al., 1961, Umitsu et al., 2007), these changes are difficult to quantify without pre-tsunami measurement. We were fortunate to have a large

tsunami occur in the midst of a multi-year field project. Our observations allow us to address persistent questions in tsunami geology: What role does geomorphology have on erosion and deposition? How do erosion and deposition compare, e.g., in volume? When during the tsunami does erosion take place? Does a tsunami produce long-term, recognizable geomorphic change?

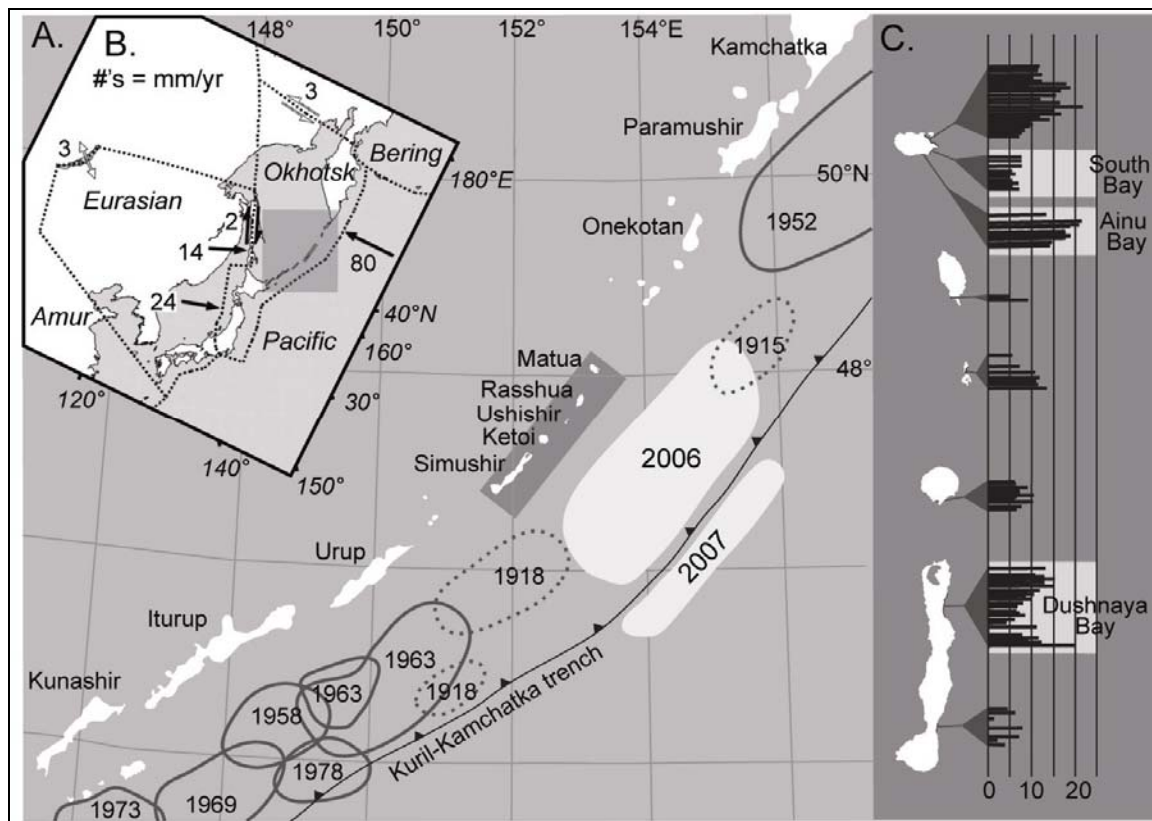


Figure 1. A. Historical seismicity of tsunamigenic earthquakes on the Kuril-Kamchatka trench, after Fedotov et al. (1982). B. Tectonic setting of the region, after Apel et al. (2006). Numbers represent mm/yr motion of the plates. C. Runup measurements from the post-tsunami survey in middle Kuril Islands, 2007. Scale lines are each 5 m elevation.

Herein, we are able to specifically address the relationship between erosion and deposition for sandy coastal plains with high-relief bedforms, such as beach ridges.

The 15 Nov 2006 middle Kurils earthquake (Mw 8.1 – 8.3) occurred in the Kuril-Kamchatka subduction zone (Fig. 1) and produced a large tsunami. Our nearfield measurements of tsunami runup average 10 m and range up to 22 m (Fig. 1). A more recent earthquake and tsunami occurred in the middle Kurils on 13 Jan 2007 (M_w ~8.0), but field evidence indicated the 2007 tsunami was significantly smaller.

In summer 2007, we reoccupied coastal sites we visited in summer 2006, and conducted a post-tsunami survey (Levin et al., 2008). Our colleagues and we documented inundation (local maximum inland distance of the tsunami) and runup (elevation a.s.l. at inundation) at 130 locations over a distance of ~200 km in the nearfield (Fig. 1).

We investigated in detail two areas previously visited— northern Simushir (Dushnaya Bay) and southern Matua islands (South and Ainu bays). We quantified erosion by reoccupying four 2006 topographic profiles as well as reconstructing stripped soil and tephra stratigraphy and comparing before and after photos. We also measured and sampled tsunami deposits on these and other 2007 profiles.

In Dushnaya Bay, a broad, open embayment on the Pacific side of northern Simushir, tsunami effects were closely linked to coastal

geomorphology. One profile, from the central part of the bay (Fig. 2A), illustrates how the tsunami affected broad open regions. This Dushnaya profile recorded a small wave— runup of only 7 m and inundation of 125 m over sandy beach ridges; erosion here was subtle. In general, geomorphic change in Dushnaya Bay was subtle and present mainly near the shoreline. The few examples of erosion are back-beach cliff retreat, superficial sediment removal on sand dunes (which lacked coherent soils), and small-scale scouring associated with focused water withdrawal. Tephra stratigraphy enables an estimate of cliff retreat of ~ 3 m in one section of Dushnaya Bay, suggesting around 10 m³/m volume of sediment loss.

On the unvegetated beach of the Dushnaya profile (Fig. 2A), at least 5-7 m³/m was relocated. Deposition was spatially more extensive than erosion; average extent of deposits throughout the bay was within 8 m of maximum inundation. In general, maximum water inundation and maximum sediment inundation are virtually coincident for sand-dominated profiles. Measurements of the deposits along Dushnaya Bay profiles record 0.4 to 3.0 m³/m of deposition.

The implication of the before and after Dushnaya profile is that there was greater erosion than deposition in total, even though erosion was subtle.

On Matua Island we studied two adjacent bays in detail, each also visited in 2006— South Bay and Ainu Bay.

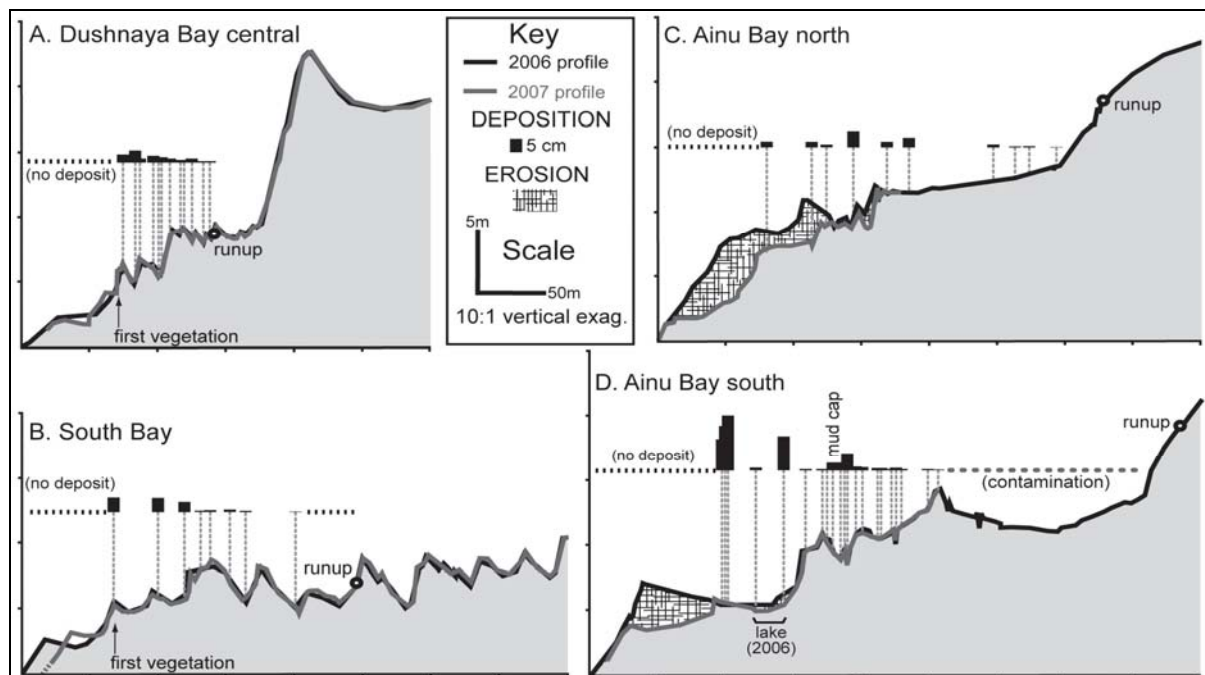


Figure 2. Before and after profiles from Dushnaya Bay, Simushir Island and South Matua Island. A. and B. are cases of low runup and C. and D. of high runup. The zone labeled “contamination” in the deposition survey of D is due to an adjacent dam break that contributed many large cobbles and big zones of soil stripping around 250 m that added large amounts of cinders.

South Bay is a wide beach-ridge plain facing the Pacific Ocean, similar to central Dushnaya Bay but with higher relief beach ridges (Fig. 2A,B). Ainu Bay is about 1 km wide, oriented perpendicular to South Bay, and composed of a few young sandy beach or dune ridges fronting a low-relief marsh (Fig. 2C,D). The scale and effects of the 2006 tsunami were distinctly different in these two bays, with Ainu Bay being much more dramatic. Herein we examine one profiles from South Bay and two in Ainu Bay (Fig. 2B,C,D). In South Bay, runup was low (5-8 m), and inundation of 100-200 m, with little tsunami erosion (similar to Dushnaya Bay). In Ainu Bay, runup was typically 14-20 m, with inundation up to 400 m, generating massive erosion.

Comparison of profiles from 2006 and 2007 in South Bay (Fig. 2B) shows a significant difference in the active beach, but with a similar pattern to Dushnaya Bay. Around 50 m³/m was eroded from the beach, while only a volume of 3.4 m³/m of sand was deposited. The tsunami also ripped turf blocks off the back-beach scarp all along the bay. Erosion otherwise was limited—a few pieces of flagging tape and some blocks of turf from excavations from were virtually undisturbed. Elsewhere in South Bay, the tsunami removed soil locally on seaward-facing sides of beach ridges, though sediment removal was shallow and vegetation generally unaffected.

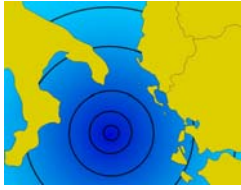
A direct comparison of before and after in Ainu Bay shows that the tsunami removed 30-60 times more sediment than it deposited on land. Approximately 300 m³/m of sediment was removed from North Ainu Bay and only 4.8 m³/m of sediment was deposited. In South Ainu Bay, 175 m³/m of sediment eroded and 6.3 m³/m was deposited. The profiles show that the back-beach eroded landward 25-50 m, with entire beach ridges removed or reduced in size, and troughs between ridges deepened (Fig. 2C,D). Farther landward, there are many zones of soil stripping, both large and small—the tsunami exploited rodent networks and cinder layers to strip the surface. There are also scours and gulying associated with concentrated inflow or outflow, including a dam break. Erosion was slightly more extensive than deposition; erosion could be found up to 5-10 m and deposits up to 10-15 m of maximum inundation.

Our comparison of tsunami deposition and erosion shows that the volume of erosion can far exceed deposition. This is in distinct contrast, for example, to Gelfenbaum and Jaffe's (2003) estimation of twice as much sand deposited as eroded terrestrially from the 1998 Papua New Guinea tsunami. Umitsu et al. (2007) suggests a possible explanation when they theorize that greater elevation differences, such as on beach-ridge plains as compared with lower-lying delta plains, give the

tsunami more power to erode, especially during outflow. Kuril Island geomorphology is much higher-relief than that in Papua New Guinea (although the PNG profiles are no higher than about 3 m, estimates of tsunami flow depth are up to 10 m (Gelfenbaum & Jaffe, 2003) — on the order of Kuril Island runup). Our observations indicate that the assumption that deposits represent a significant fraction of total sediment eroded is not valid for beach ridge plains.

References

- Apel E. V., Burgmann R., Steblov G., Vasilenko N., King R., Prytkov A. (2006). *Independent active microplate tectonics of northeast Asia from GPS velocities and block modeling*, Geophysical Research Letters, v. 33, L11303, doi:10.1029/2006GL026077.
- Fedotov S. A., Chernyshev S. D., Chernysheva G.V. (1982). *The Improved Determination of the Source Boundaries for Earthquakes of $M > 7.75$, of the Properties of the Seismic Cycle, and of Long-term Seismic Prediction for the Kurile-Kamchatka*. Arc: Earthquake Prediction Research, v. 1, p. 153-171.
- Gelfenbaum G., Jaffe B. (2003). *Erosion and Sedimentation from the 17 July 1998 Papua New Guinea Tsunami*, Pure and Applied Geophysics, v. 160, 1969-1999.
- Konno E., Iwai J., Tkayanagi Y., Nakagawa H., Onuki Y., Shiata T., Mii H., Kitamura S., Kodaka T., Kataoka J. (1961). *Geological survey on the Chile Earthquake Tsunami affected areas in the Sanriku coast, northeast Japan*, Contrib. Inst. Geol. Palaeontol. Tohoku Univ. v. 52, p. 1-40 (in Japanese with English abstract).
- Levin B. V., Kaistrenko B. M., Rybin A. B., Nosov M. A., Pinegina T. K., Razhigaeva N. G., Sassorova E. V., Ganzei K. S., Ivelskaya T. N., Kravchenovskaya E. A., Kolesov C. V., Evdokimov Y. V., Bourgeois J., MacInnes B., Fitzhugh B. (2008). *Проявления цунами 15.11.2006 г на центральных Курильских островах и результаты моделирования высот заплесков*. Proceedings of the Russian Academy of Sciences (in Russian), v. 419, p. 1-5.
- Umitsu M., Tanavud C., Patanakanog B. (2007). *Effects of landforms on tsunami flow in the plains of Banda Aceh, Indonesia, and Nam Khem, Thailand*, Marine Geology, v. 242, p. 141-153.



Maouche S.¹, Morhange C.², Meghraoui M.³

Large boulder accumulation on the Algerian Coast evidence catastrophic tsunami events in the Western Mediterranean

¹CRAAG, BP 63 bouzareah Algiers Algeria e-mail: said_maouche@yahoo.fr;

²Aix-Marseille Université CNRS CEREGE UMR Europôle méditerranéen de l'Arbois Aix-en-Provence
France, e-mail : morhange@cerge.fr;

³EOST-Institut de Physique du Globe de Strasbourg, France, e-mail: mustapha@eost.u-strasbg.fr

Keywords: *Coastal morphology, boulders, tsunami, Algeria*

Evidence of catastrophic mega-blocks is presented for the Algerian coastal zone from Tipaza to Dellys including the epicentral area of the 2003 Zemmouri tsunamigenic earthquake (Mw 6.8) (Fig. 1).

Detachment of large boulders from the seashore zone and their deposition inland are among the main morphological effects of tsunami on rocky coasts. The estimated size, weight (volumetric mass) and distance from the shoreline of more than 100 boulders allow us to characterize the nature of the hydrodynamic waves responsible for their transport. The boulders, weighing up to ~200 tons, are scattered along ~150 km of rocky headlands and pocket beaches, isolated or in groups (Fig. 2), and are of subtidal and supratidal origin.

Boulders covered by biogenic encrustations show morphological features which suggest detached, reversed and reworked pieces. We used the formulas of Nott (2003) for the physics of

boulder movement, in particular equations for the joint bound and the submerged scenario, to calculate wave heights responsible for the boulders deposition. Statistical and hydrodynamic analyses indicate that large boulder transport requires either ~30-m-high waves or 5 to 10-m-high waves for catastrophic storm or tsunami events, respectively. Bio-indicators allow us to date these high-energy events to AD 400 – 600 and ~ AD 1700, implying a tsunamigenic origin.

In order to detect other typical geomorphological and hydrological features related to high-energy flooding events along the Algerian coast satellite and aerial images are used. The areas prone to present and past flooding are observed and mapped. The recognition of these areas has been made taking into account the traces of erosion and abrasion. Often these zones are associated with irregular coastal ponds and lakes.

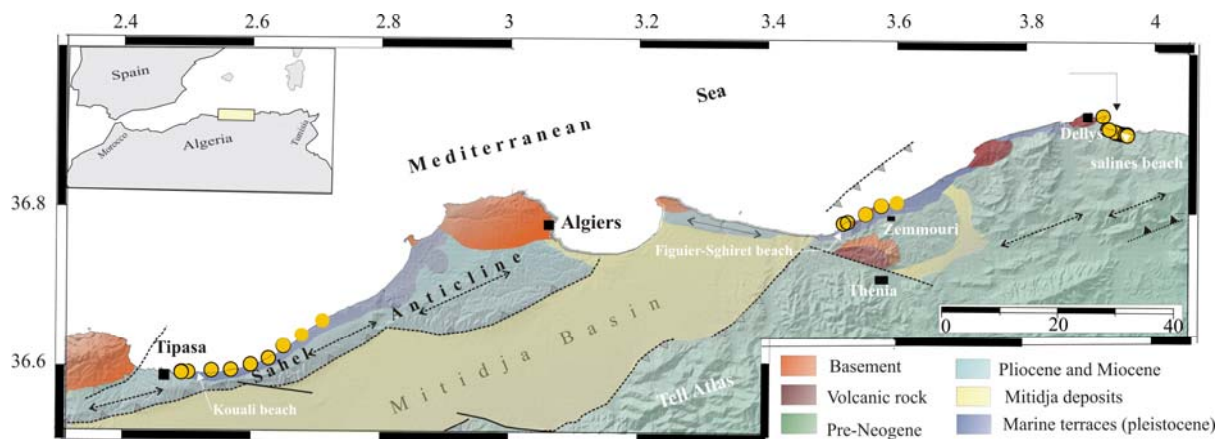


Figure 1. Geographical position and geological context of the studied area, including boulder accumulation sites (yellow circle).

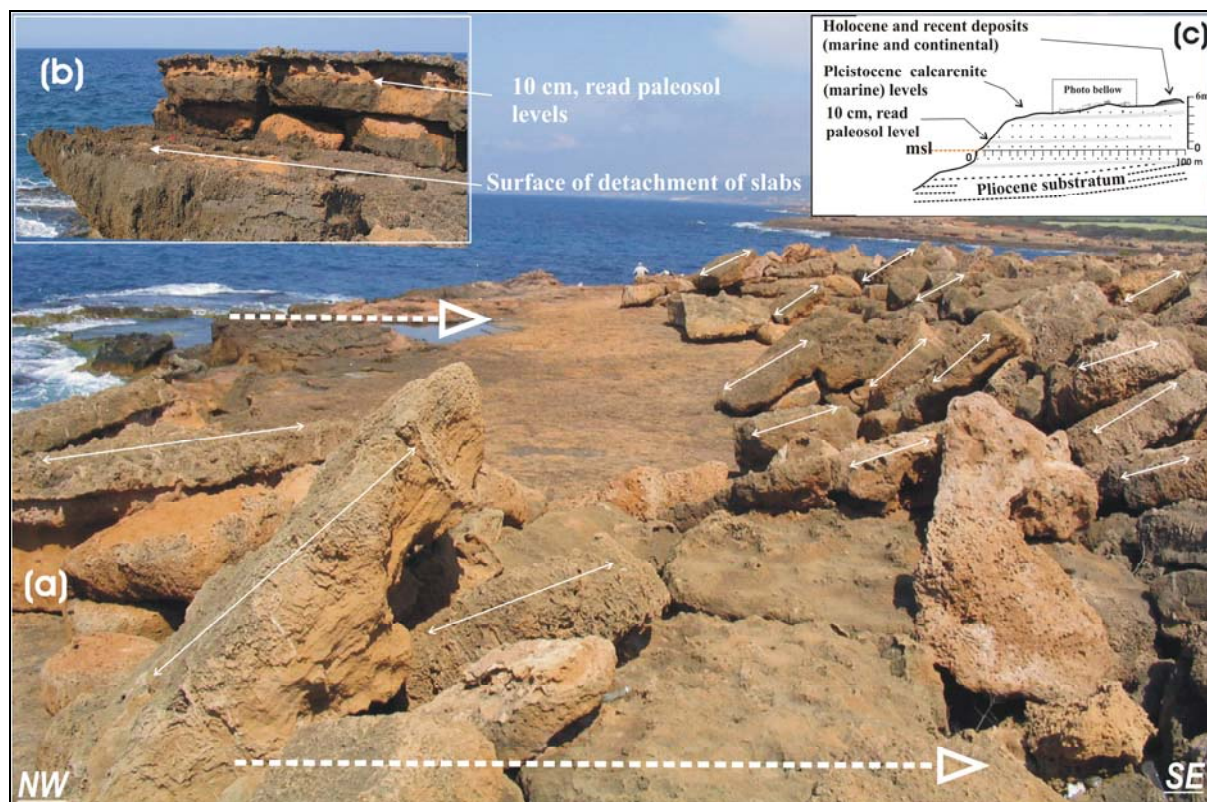


Figure 2. A view of example of boulder accumulation at Tipaza, (A) Boulder accumulation with “a” axes orientation (B) Detachment zone (Subtidal and supratidal) (C) cross section showing the local lithological units.

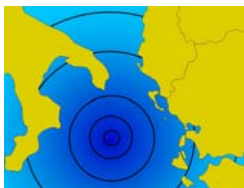
The Algerian coast experienced large earthquakes in the past and some of them are associated with tsunami (Ambraseys 1982, Harbi et al; 2007; Alasset et al; 2006).

Tsunamis derive from either the Algerian offshore area, southern Spain or the Balearic Islands. The historical seismicity induced by active offshore tectonic structures along the Algerian coast explains the origin of tsunamis in southern Europe (Jijel 1856, Gouraya 1891, El Asnam 1980). Bearing in mind the regional seismotectonic context of the western Mediterranean sea, the tsunami events of 1522, 1680 and 1804 might also have been generated in southeast Spain (Soloviev et al., 2000). According to Gracia et al. (2007) the 50-km-long offshore extension of the NE-SW trending Carboneras fault is a potential source of large magnitude earthquakes ($M_w \sim 7.2$), possibly responsible for the 1522 tsunami. Therefore, major earthquakes in the western, Mediterranean sea, particularly in the offshore area of SE Spain, may generate tsunamis responsible for boulder deposition on the North African coast.

In conclusion, this study shows that the scatter of large boulders along the Algerian coastline attests to at least two major tsunamis in the western Mediterranean during the last 1600 years.

References

- Alasset P. J., Hébert H, Maouche S, Calbini V, Meghraoui M (2006). *The tsunami induced by the 2003 Zemmouri earthquake ($M_w=6.9$, Algeria): modelling and results*. Geophys Journal International, doi: 10.1111/j.1365-246X.2006.02912.x.
- Ambraseys N. N. (1982). *The seismicity of North Africa: the earthquake of 1856 at Jijeli, Algeria*. Bollettino Di Geofisica e Teorica ed Applicata, vol XXIV, 93: 31-37.
- Harbi A., Maouche S., F. Vaccari, A. Aoudia, F. Oussadou, G. F. Panza and D. Benouar (2007). *Seismicity, Seismic Input and Site effects in the Sahel-Algiers Region (North Algeria)*. Soil Dynamics and Earthquake Engineering Vol 27, N° 5, 427-447.
- Gracia, E., R. Pallas, J. I. Soto, M. Comas, X. Moreno, E. Masana, P. Santanach, S. Diez, M. Garcia, J. Danobeitia, *Active faulting offshore SE Spain (Alboran Sea): Implications for earthquake hazard assessment in the Southern Iberian Margin*. Earth and Planet. Science Letters 241 (2006) 734–749.
- Nott, J., 2003. *Waves, coastal boulder deposits and the importance of the pre-transport setting*. Earth Planet. Science Letters 210, 269–276.



Marsico A.¹, Pignatelli C.¹

Laser Scanner survey to rebuild large boulder accumulated by extreme event in Torre Squillace (Southern Apulia – Italy)

¹Dipartimento di Geologia e Geofisica, Università degli Studi “Aldo Moro”, Bari, Italy

e-mail: c.pignatelli@geo.uniba.it; a.marsico@geo.uniba.it

Keywords: boulders, Laser Scanner, Apulia, Southern Italy, Tsunami

Along the ionian side of Salento peninsula (Apulia - Southern Italy), the rocky coastal area of Torre Squillace, between the Taranto and Gallipoli towns, is characterized by presence of a boulders field (Fig. 1a).

This singular accumulation was caused by impact of catastrophic wave (Mastronuzzi & Sansò,

2000; Mastronuzzi et al., 2006). This coastal sector is a rocky headland shaped on algal calcarenite units correlable to Tyrrhenian, they overlie Pleistocene clayey sands (Mastronuzzi & Sansò, 2000; Mastronuzzi et al., 2006); here, the boulders are arranged in isolated position and/or embricated in a row of two elements (Fig. 1b).

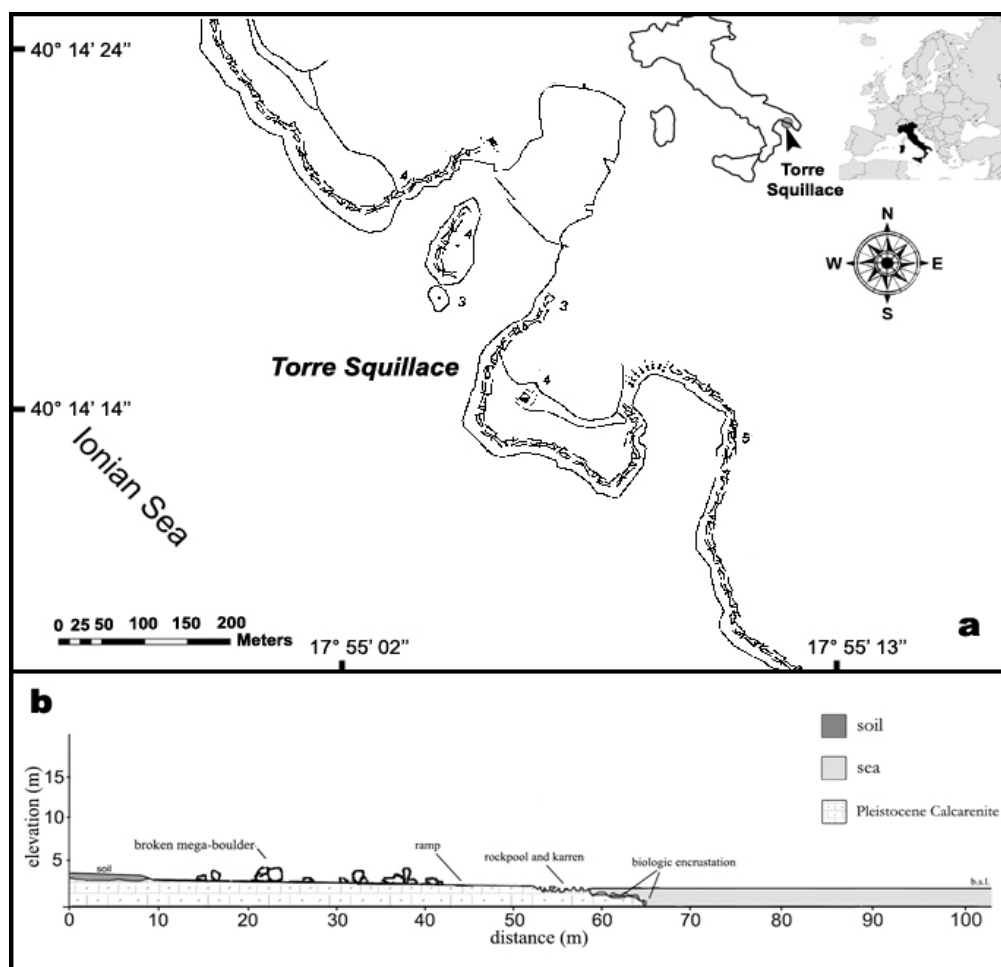


Figure 1. a) Geographical position of studied area; b) Morphological profile of Torre Squillace headlands.

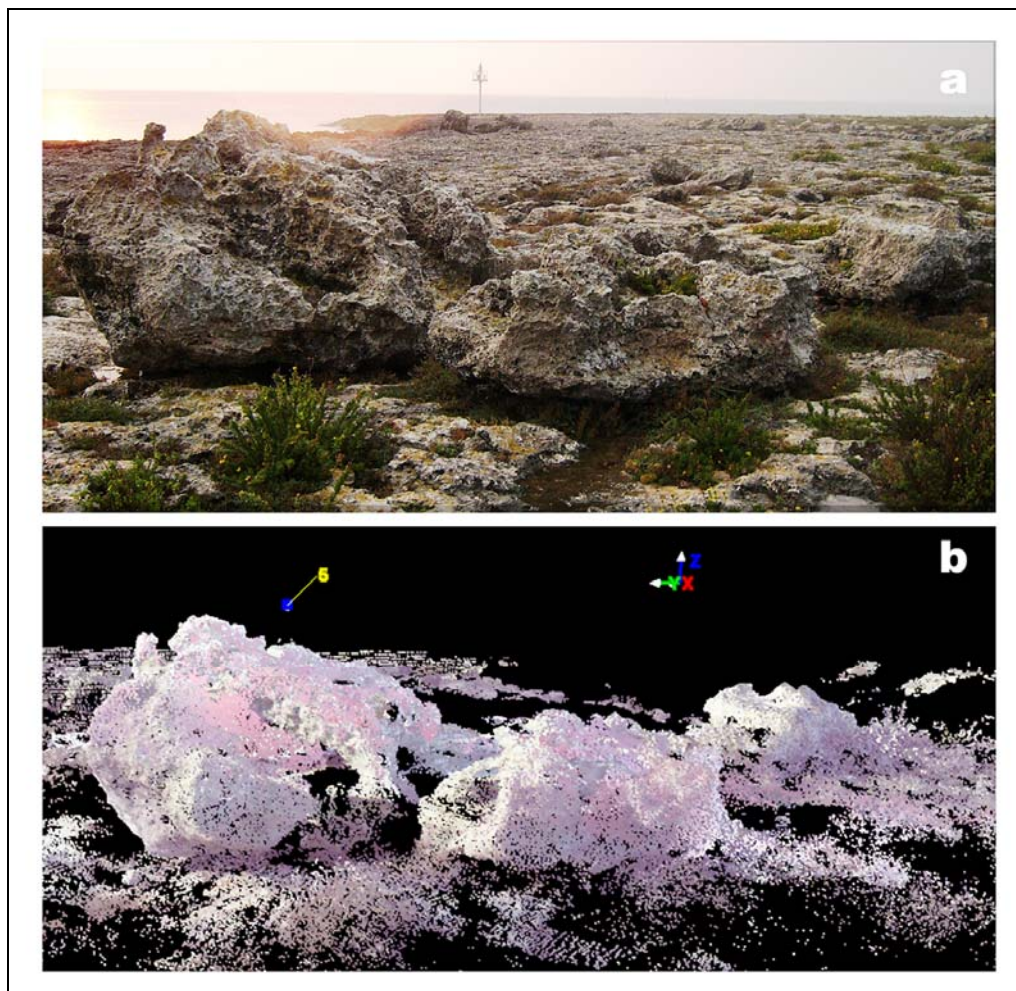


Figure 2. a) biggest boulder in Torre Squillace locality (Southern Apulia, Italy); b) 3D model of biggest boulder.

The biggest boulder (Fig. 2a) of this deposit is located 40 m inland, at 2 m above mean sea level (a.m.s.l.) and surrounded by 3 pieces.

In this work we have performed Laser Scanner surveys (Boehler & Marbs, 2002, 2003) in this coastal area in order to understand the origin of the biggest boulder. Field observation suggest that these four elements constituted a singular unit; their morphology and proximity could be attributed to the bigger boulder breakage. In fact, we suppose the dynamic of the transport of the bigger boulder in three consequently steps:

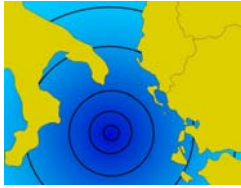
- i) the catastrophic wave detached the boulder from intertidal/adlittoral zone;
- ii) boulder surfing on the wave due to the water turbulence;
- iii) wave energy decreasing due to the bedrock friction and subsequent fell of boulder.

Three-dimensional reconstruction by Laser Scanner (Fig. 2b) was carried out in order to verify our hypothesis. The 3D model allowed to calculate linear distance between the four elements and also the surface morphology of the parts that seem to tie

in. Another result consists in the accuracy in defining shapes and volumes of each boulder.

References

- Mastronuzzi G., Sansò P. (2000). *Boulders transport by catastrophic waves along the Ionian coast of Apulia (Southern Italy)*. Marine Geology 170, 93–103.
- Mastronuzzi G., Pignatelli C., Sansò P. (2006). *Boulder Fields: A Valuable Morphological Indicator of Paleotsunami in the Mediterranean Sea*. Zeitschrift für Geomorphologie, NF Suppl.-Bd. 146, 173-194.
- Boehler W., Marbs A. (2003). *Investigating laser scanner accuracy*. Proceedings of XIX CIPA Symposium (see: <http://scanning.fh-mainz.de/scannertest/result300305.pdf>).
- Boehler W., Marbs A. (2002). *3D scanning instruments*. Proceedings of the CIPA WG6 International Workshop on scanning for cultural heritage recording (see: http://www.i3mainz.fh-mainz.de/publicat/korfu/p05_Boehler.pdf).



2nd International Tsunami Field Symposium

IGCP Project 495

Quaternary Land-Ocean Interactions:
Driving Mechanisms and Coastal Responses

Ostuni (Italy) and Ionian Islands (Greece) 22-28 September 2008



Project 495

Martin M. E.¹, Bourgeois J.¹

Candidate tsunami deposit near Seattle, Washington state, USA

¹Department of Earth and Space Sciences, University of Washington, Seattle, Washington (USA)

email: memartin@u.washington.edu; jbourgeo@u.washington.edu

Keywords: *tsunami deposits, Puget Sound, Seattle fault*

The processes involved in depositing a perplexing sand unit at the head of Sinclair Inlet (Fig. 1), in the metropolitan Seattle region [Puget Sound], likely include a locally generated tsunami but may also include sand volcanoes, debris flows, or both. The inlet's short fetch and protected location limit the likelihood that storms or wave action generated the deposit.

The steep and complex bathymetry and topography of the densely populated Puget Sound region, coupled with an active fault system, make

this region susceptible to tsunamis, of which historic examples have been landslide-generated.

For example, a landslide following the 1949 Tacoma earthquake generated a locally damaging, 2-m tsunami in Hood Canal. However, in the prehistoric record, there is evidence of larger and potentially more damaging events.

Evidence for one or more earthquakes and subsequent tsunami(s) about 1100 years ago has been documented around Puget Sound (Fig. 1).

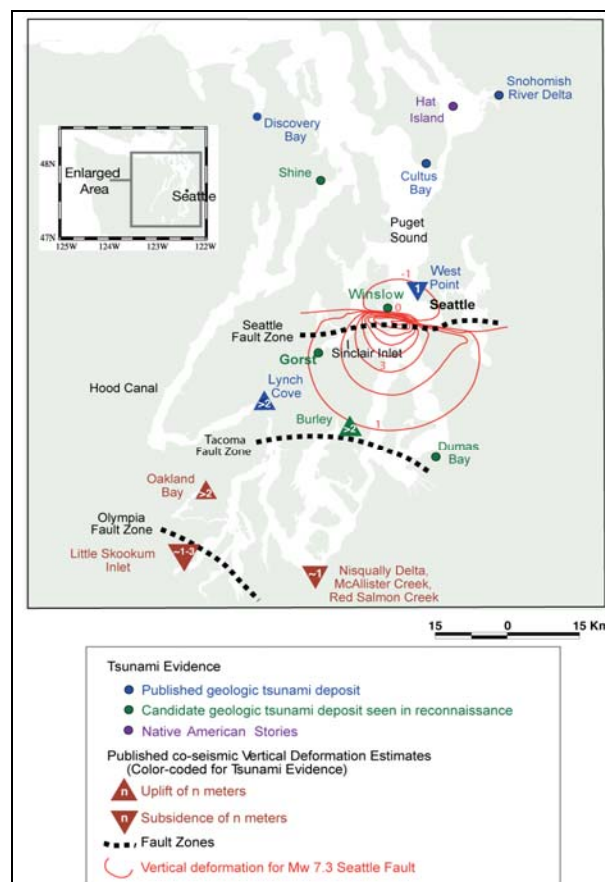


Figure 1. Map of Puget Sound showing the location of the Seattle fault and paleoseismic evidence.

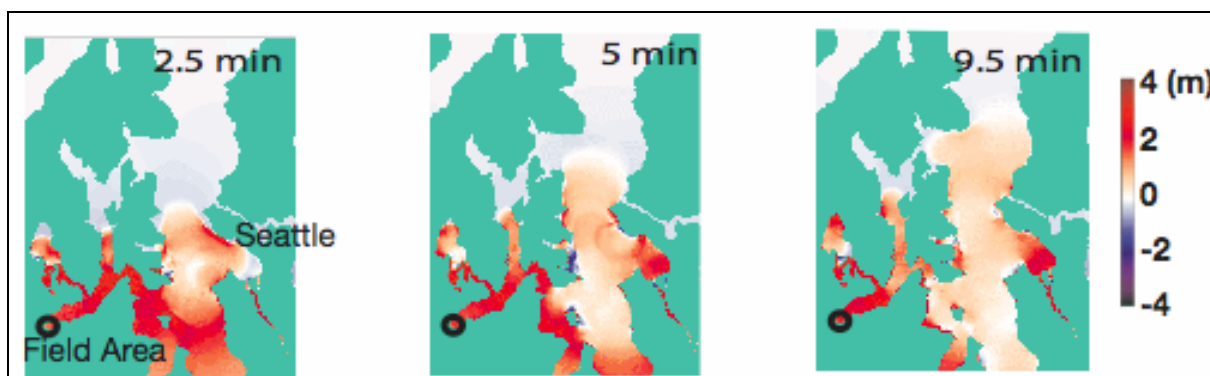


Figure 2. Model of tsunami generated by a Mw 7.3 earthquake on the Seattle fault. Snapshots in minutes after initial uplift and water elevation is in meters. From Koshimura et al., 2002.

The best-documented earthquake, estimated to be a magnitude 7 or larger (Bucknam et al., 1992) caused widespread land level change along the Seattle fault zone (Fig. 1) around A.D. 900-930. Uplift linked to the earthquake of up to 7 m on marine terraces is located 12 km to the east of the Gorst field area (Fig. 1). Another fault south of the field area, the Tacoma fault, has been mapped using LIDAR and dated to have ruptured between A.D. 770 and 1160 (Sherrod et al., 2004).

The tsunami(s) generated by these ruptures deposited sands and silts that are preserved in low-lying marshes in various locations in Puget Sound (e.g. Atwater & Moore, 1992, Bourgeois & Johnson, 2001, Jovanelly & Moore, 2005) (Fig. 1).

South of the Seattle fault but within the zone of coseismic deformation lies Sinclair Inlet (47°31'35.98"N, 122°41'46.11"W). Modelling of an earthquake on the Seattle fault (Fig. 2) indicates high wave heights along Sinclair Inlet (Koshimura et al., 2002).

A branch of Puget Sound 22 km west of Seattle, Sinclair Inlet contains at its head an intertidal mudflat that is fringed by partly urbanized tidal marshes, alder swamps, and higher, forested areas. Much of the valley at the end of the inlet has been developed. The undisturbed marshes and swamps contain a sand layer of variable thickness interpreted to have been at least partially deposited by a tsunami. To determine the extent and source of the deposit at Gorst we are employing various standard field and laboratory methods. Field methods include mapping the extent and thickness of the deposit by coring and excavations. Sediment peels and field descriptions are taken to document sedimentary structures. We are measuring grain size in the lab using a settling column to look for grain size trends in the deposit, such as fining or coarsening upward, and to aid in correlation between locations.

In remnant wetlands in the field area, outcrops, cores and pit excavations reveal an abrupt upward change from tidal flats to freshwater forest that

probably resulted from uplift during the Seattle fault earthquake or possibly an earthquake on the Tacoma fault (pending radiocarbon dating).

The forest peat grades upward into salt marsh peat of the modern depositional environment, indicating subsidence since the uplift event. A complex sand unit lies between the tidal-flat facies and the forest peat (Fig. 3); we interpret at least the lower part of this sand body as a tsunami deposit.

Based on its stratigraphic position, the sand unit formed at or about the time of uplift. The unit consists mainly of silty fine sand up to 1 m in thickness but also can contain fine to medium sand and pebble sized rip-up clasts of silty clay (Fig. 3).

The unit has a sharp contact with shelly mudflat deposits below and a sharp to gradational contact with overlying peat. We found the sand unit, along 0.5 km of the upper inlet's shoreline, beneath modern tidal marshes and alder swamps. Preliminary diatom analysis shows the unit contains diatoms from a brackish environment. The unit can contain at least three parts (Fig. 3): a basal subunit that fines upward from medium and coarse sand to fine sand and silt; a thin, discontinuous (less than 1 cm thick) clay bed, commonly with flame structures; and a capping subunit up to 50 cm thick that is dominated by silty fine to medium sand but which also contains locally derived pebbles.

The lowest portion of the unit is interpreted as a tsunami deposit due to its association with land-level change and its fining-upward texture. The upper two parts of the unit are of more ambiguous origins. The middle, clay layer represents a period of low shear stress, possibly a lull in tsunami waves or a quiet period between two events. The top silty layer could have its origin in a later tsunami wave, tsunami return flow, sand volcanoes, or a debris flow from upstream. To clarify the origin of the top part of the sand unit we made excavations up stream along Gorst Creek. A possibly related sand unit lies 0.8 km inland. Its thickness is in the range 0.2-1.0 m as observed thus far in creek banks and in pits at a nearby park.

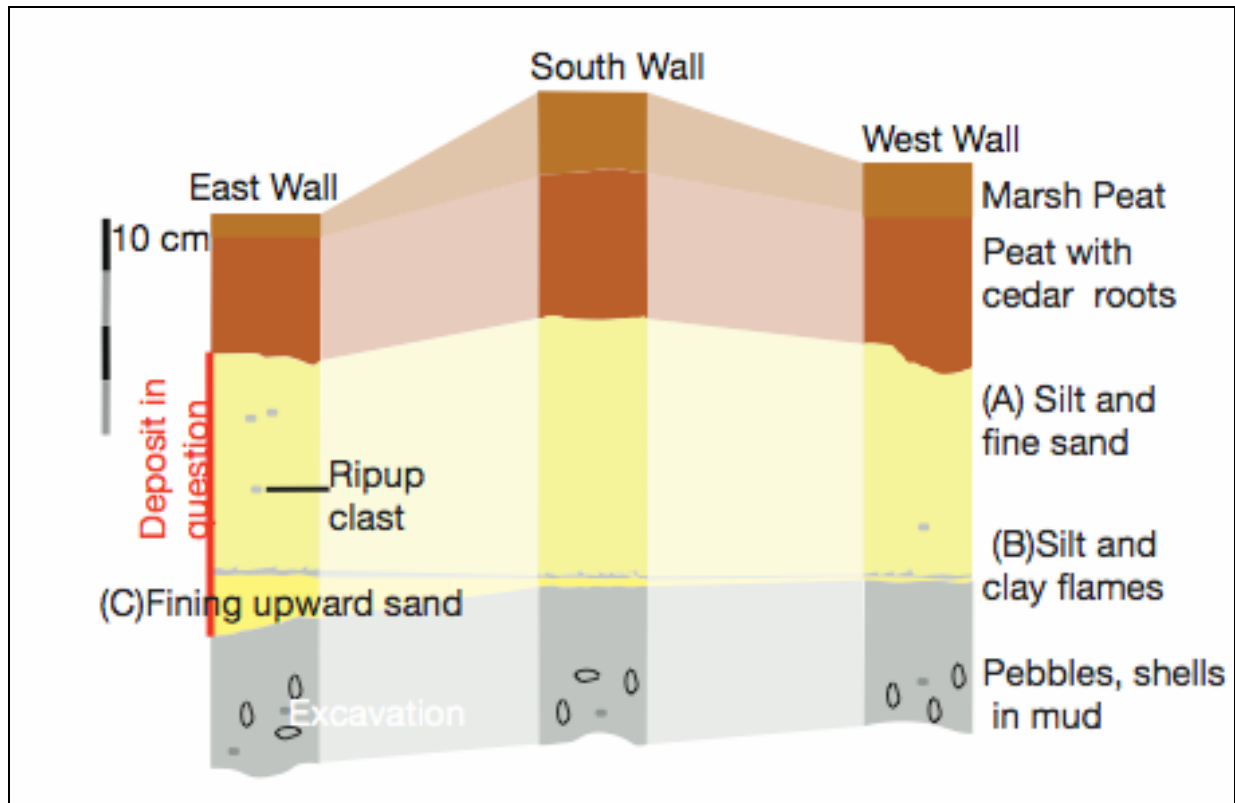


Figure 3. Three walls of an excavation in a salt marsh showing stratigraphic evidence for uplift and three parts of the sandy deposit.

The unit lies above a sandy loam that contains charcoal and fill from a homestead built nearby. Unlike the sand that borders the inlet, the unit in the park contains trough cross-bedding.

We are investigating the relationship between this deposit and the silty sand deposit in the tide flats.

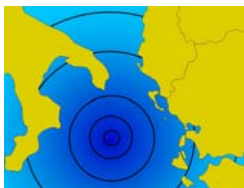
Preliminary diatom analysis did not reveal any diatoms in this deposit.

Further work continues in the park and in creeks draining into the inlet to trace out the extent of the deposits and look for clues to the origin of the sediment. Tracing the deposits will enable us to map changes in thickness of the upper part of the sand unit possibly indicating the direction of the source. Also, further investigations might reveal the shoreline at the time of uplift allowing us to constrain the amount of uplift and provide additional material for dating.

Ultimately, this work will allow us to evaluate models for tsunami propagation in the greater Seattle urban area.

References

- Atwater B. F., Moore A. L. (1992). *A Tsunami About 1000 Years Ago in Puget Sound, Washington*. Science 4 December 1992: Vol. 258. no. 5088, pp. 1614 – 1617.
- Bourgeois J., Johnson, S. (2001). *Geologic evidence of earthquakes at the Snohomish delta, Washington, in the past 1200 yr*. GSA Bulletin; April 2001; v. 113; no. 4; p. 482-494.
- Bucknam R. C., Hemphill-Haley E., Leopold E. B. (1992). *Abrupt Uplift within the past 1700 years at southern Puget Sound, Washington*. Science 4 December 1992: Vol. 258. no. 5088, pp. 1614 – 1617.
- González F., Sherrod B., Atwater B., Frankel A., Palmer S., Holmes M., Karlin B., Jaffe B., Titov V., Mofjeld H., Venturato A. (2003). *2002 Puget Sound Tsunami Sources Workshop Report*. A contribution to the Inundation Mapping Project of the U.S. National Tsunami Hazard Mitigation Program, NOAA OAR Special Report, 34 pp.
- Jovanelly T., Moore A. (2005). *Tsunami origin for an 1,100-year-old enigmatic sand sheet in Lynch Cove, Puget Sound, Washington, USA*. GSA Abstracts with Programs, v. 37, n. 7, p. 65.
- Sherrod B. L., Brocher T. M., Weaver C. S., Bucknam R. C., Blakely R. J., Kelsey H. M., Nelson A. R., Haugerund R. (2004). *Holocene fault scarps near Tacoma, Washington, USA*. Geology; January 2004; v. 32; no. 1; p. 9–12.



2nd International Tsunami Field Symposium

IGCP Project 495

Quaternary Land-Ocean Interactions:
Driving Mechanisms and Coastal Responses

Ostuni (Italy) and Ionian Islands (Greece) 22-28 September 2008



Project 495

Mastronuzzi G.¹, Caputo R.², Di Bucci D.³, Fracassi U.⁴,
Pignatelli C.¹, Sansò P.⁵, Selleri G.⁵

Morphological data and the definition of tsunamogenic areas between Apulia (Italy) and Ionian Islands (Greece)

¹Università degli Studi "Aldo Moro", Dipartimento di Geologia e Geofisica, Bari, Italy
e-mail: c.pignatelli@geo.uniba.it; g.mastrozz@geo.uniba.it;

²Università degli Studi di Ferrara, Dipartimento di Scienze della Terra, Ferrara, Italy; e-mail: rcaputo@unife.it;

³Dipartimento della Protezione Civile, Roma, Italy, e-mail: daniela.dibucci@protezionecivile.it;

⁴Istituto Nazionale di Geofisica e Vulcanologia, Roma, Italy, e-mail: fracassi@ingv.it;

⁵Università degli Studi del Salento, Dipartimento di Scienze dei Materiali, Lecce, Italy
e-mail: paolo.sanso@unile.it; Gianluca.selleri@yahoo.it

Keywords: *tsunami, earthquakes, tsunamogenic area, Apulia, Italy, Ionian Island, Greece*

All around the coastal perimeter of Southern Apulia (Italy), which represents the southernmost part of the emerged Adria foreland (Fig. 1), there are morphological and/or sedimentological evidences of previous sea level stands.

They are represented by raised coastal sediments, extended wave cut platforms and/or abrasional surfaces, or sea cave alignments, associated with notches or algal encrustations (i.e.: Ferranti et al., 2006; and references therein).

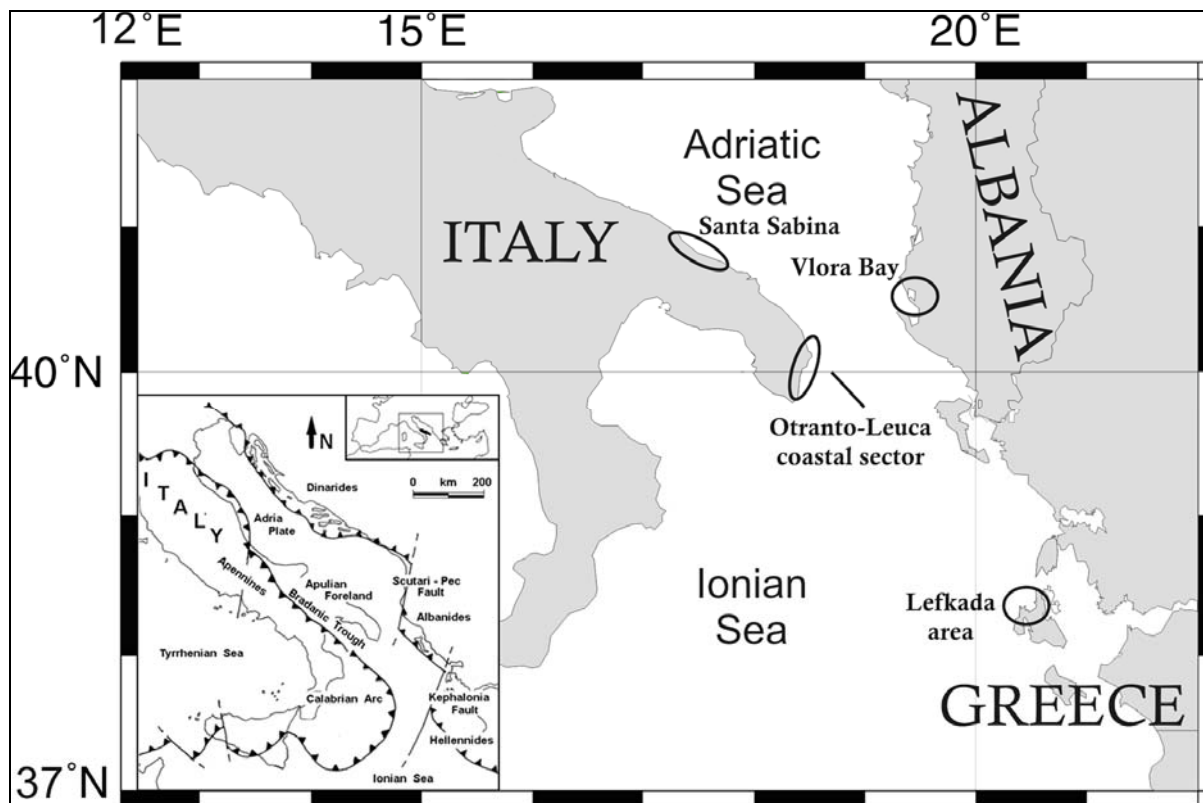


Figure 1. Studied area and localization of mean tsunami deposits in South Adriatic Apulia and Ionian Islands.

This assemblage of coastal landforms testifies a Middle and Late Quaternary geological evolution conditioned by the superimposition of the sea level coastal dynamics on the generalized uplift of the region due to the SW-NE convergence of the Calabrian arc and Dinarides-Albanides-Hellenides chains, and the NW-SE convergence of Eurasia and Nubia (i.e.: Caputo et al., 2008; Di Bucci et al., 2008 and references therein).

MIS 5.5 marine sediments and landforms associated with this eustatic sea level high stand, show decrease in elevation from North to South along the Ionian coast, whereas in the south-easternmost part of Apulia they are located in correspondence with the eustatic elevation (i.e.: Belluomini et al., 2002; Mastronuzzi et al., 2007a). In contrast, along the Adriatic coast, MIS 5.5 marine deposits can be found at lower elevation than the eustatic level (Mastronuzzi & Sansò, 2002; 2003).

Middle-Upper Pleistocene marine coastal sands/calcarenes crop out along the Adriatic side of Apulia and preserve evidence of seismites (Moretti & Tropeano, 1996; Moretti, 2000). Moreover, along the entire coastal perimeter the Lower-Middle and Upper Pleistocene sediments are affected by rare faults, characterized by small displacement, and widespread extension joints, frequently organized in sets (Fig. 2) (Caputo et al., 2008; Di Bucci et al., 2008).

All these data suggest that since the Middle Pleistocene this region has been affected by mild brittle deformation associated with a general although differentiated uplift along the Ionian side and possibly with subsidence along the Adriatic one. In particular, from the quantitative analysis of the joints sets, at least three deformational events of regional significance have been inferred. The last one, that is characterised by a sort of “doming”, is not older than the Late Pleistocene and possibly reflects the active stress field still pervading the entire study area. The mild deformation documented, joined with the lack of major, active, emergent faults (e.g. like the Mattinata fault in the Gargano Promontory) and the scarce historical and instrumental seismicity, do not favour the hypothesis of large seismogenic sources within the study area, whereas the occurrence of moderate earthquakes cannot be ruled out.

However, the entire coastal perimeter of our study area is characterized by morphological evidences of palaeotsunami impact. Some of these palaeotsunamis - constrained thank to morphological surveys, absolute dating and historical investigations -, show a good time correlation with strong earthquakes characterised by epicentres located in the eastern part of the Adriatic Sea (Mastronuzzi & Sansò, 2000; 2004).



Figure 2. Evidences of joints in the Late Pleistocene calcarenite outcropping at Punta Penne near Brindisi (Italy).

New morphological studies carried out along the coasts of Montenegro, Albania and Greece, improved the knowledge of the tectonic behaviour of this part of Adria. In particular, the coasts of Kerkira Island (Corfù) show many evidences of relevant coseismic uplift occurred about 3.0-3.5 ka BP (uncalibrated age) and more recently (Fig. 3) (Pirazzoli et al., 1994; Mastronuzzi et al., in prep).

On the other hand, sedimentological and morphological studies carried out on and near Lefkada Island allowed the identification of different tsunami events occurred 3.0-3.5 ka BP and more recently (Vött et al., 2006; 2007; 2008). Finally, ridges of megaboulders have been identified along the Ionian coast of Salento between Otranto and Leuca (Fig. 4), and ascribed to the strong earthquake occurred on February 20th, 1743 with epicentre generically located in the Ionian Sea between the Ionian Islands and Salento (Mastronuzzi et al., 2007b).

All these data suggest that many of the earthquakes that generated tsunamis impacting the Adriatic coasts of Apulia could be generated to the South of the Otranto Straits, possibly near Kerkira and Lefkada Islands.

Due to the overall geodynamic setting of the region and considering the particular high potential associated with reverse faults cutting the sea bottom,

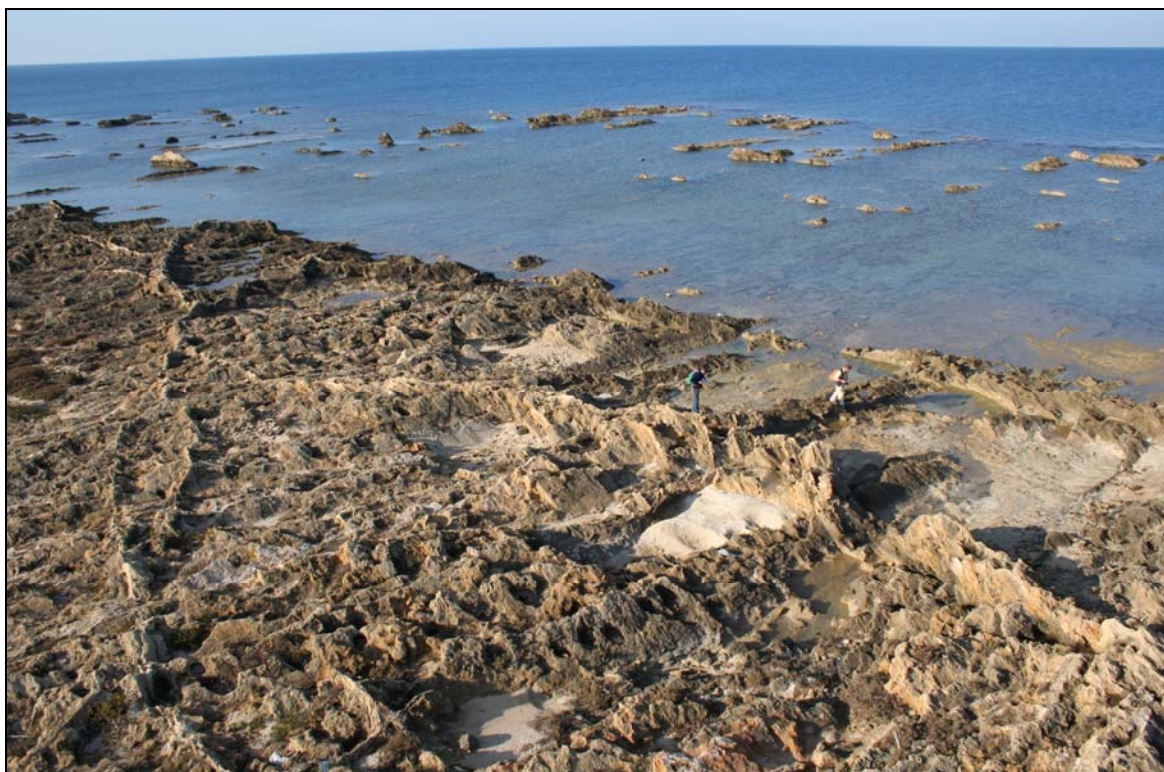


Figure 3. The uplifted beach rock of the southernmost point of Kerkira (Greece).



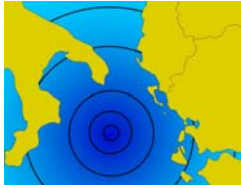
Figure 4. Boulders emplacements near Torre Sant'Emiliano near Otranto (Italy).

the most likely tsunamigenic structures, possibly causative of the observed coastal effects, are related to the still active collision between Adria and the External Hellenides.

References

- Belluomini G., Caldara M., Casini C., Cerasoli M., Mandra L., Mastronuzzi G., Palmentola G., Sansò P., Tuccimei P., Vesica P.L. (2002). *Age of Late Pleistocene shorelines, morphological evolution and tectonic history of Taranto area, Southern Italy*. *Quaternary Science Reviews*, 21, 4-6, 427-454.
- Caputo R., Di Bucci D., Mastronuzzi G., Fracassi U., Sansò P., Selleri G. (2008). *Late Quaternary extension of the southern Adriatic foreland (Italy): evidence from joint analysis*. *Rend. online SGI*, 1 (2008), Note Brevi, www.socgeol.it, 62-67.
- Di Bucci D., Coccia S., Fracassi U., Iurilli V., Mastronuzzi G., Palmentola G., Sansò P., Selleri G., Valensise G. (2007). *Late Quaternary deformation of the Adriatic foreland from*

- mesostructural data (Salento, Southern Italy)*. Boll Soc Geol It, accepted.
- Ferranti L., Antonioli F., Mauz B., Amorosi A., Dai Prà G., Mastronuzzi G., Monaco C., Orrù P., Pappalardo M., Radtke U., Renda P., Romano P., Sansò P., Verrubbi V. (2006) Markers of the last interglacial sea level high stand along the coast of Italy: tectonic implications. *Quaternary International*, 145-146, 30-54.
- Mastronuzzi G., Pignatelli C., Sansò P., Selleri G. (2007b). *Boulder accumulations produced by the 20th February 1743 tsunami along the coast of southeastern Salento (Apulia region, Italy)*. *Marine Geology*, 242, 191-205.
- Mastronuzzi G., Pignatelli C., Stamatopoulos L. (in prep.). *New data on Holocene coseismic uplift in the Kerkira Island (Greece)*.
- Mastronuzzi G., Sansò P. (2000). *Boulders transport by catastrophic waves along the Ionian coast of Apulia (Southern Italy)*. *Marine Geology*, 170, 93-103.
- Mastronuzzi G., Sansò P. (2004). *Large Boulder Accumulations by Extreme Waves along the Adriatic Coast of southern Apulia (Italy)*. *Quaternary International*, 120, 173-184.
- Mastronuzzi G., Sansò P. (2002). *Pleistocene sea level changes, sapping processes and development of valleys network in Apulia region (southern Italy)*. *Geomorphology*, 46, 19-34.
- Mastronuzzi G., Sansò P. (eds) (2003). *Quaternary coastal morphology and sea level changes. Field Guide*. Puglia 2003, Final Conference – Project IGCP 437 UNESCO - IUGS, Otranto / Taranto - Puglia (Italy) 22-28 September 2003, GI²S Coast Coast – Gruppo Informale di Studi Costieri, Research Publication, 5, 184 pp, Brizio srl - Taranto.
- Mastronuzzi G., Quinif Y., Sansò P., Selleri G. (2007a). *Middle-Late Pleistocene polycyclic evolution of a geologically stable coastal area (southern Apulia, Italy)*. *Geomorphology*, 86, 393-408.
- Pirazzoli P.A., Stiros S.C., Laborel J., Laborel-Deguen F., Arnold M., Papageorgiou S., Morhange C., (1994). *Late Holocene shoreline changes related to palaeoseismic events in the Ionian Islands, Greece*. *The Holocene*, 4, 4, p. 397-405.
- Vött A., Brückner H., May M., Lang F., Brockmüller S. (2007). *Late Holocene tsunami imprint at the entrance of the Ambrakian gulf (NW Greece)*. *Mediterranée*, 108, 43-57.
- Vött A., Brückner H., May M., Lang F., Herd S.R., Brockmüller S. R. (2008). *Strong tsunami impact on the Bay of Aghios Nikolaos and its environs (NW Greece) during Classical–Hellenistic times*. *Quaternary International*, 181, 105-122.
- Vött A., May M., Brückner H., Brockmüller S. (2006). *Sedimentary evidence of Late Holocene tsunami events near Lefkada Island (NW Greece)*. *Zeitschrift für Geomorphologie N.F.* 146 (Suppl.), 139–172.



Milella M.¹, Pignatelli C.², Sansò P.^{3*}, Saracino S.⁴

Extreme events frequency and associated coastal damages along the coast of Salento (Southern Italy)

¹Collaboratore esterno, Dip. di Geologia e Geofisica, Università degli Studi "Aldo Moro", Bari, Italy

²Dipartimento di Geologia e Geofisica, Università degli Studi "Aldo Moro", Bari, Italy

³Dipartimento di Scienza dei Materiali, Università del Salento, Lecce, Italy, e-mail: paolo.sanso@unile.it;

⁴Collaboratore esterno, Dip. di Scienza dei Materiali, Università del Salento, Italy

* corresponding author: e-mail: paolo.sanso@unile.it

Keywords: *sea storms, tropical like-cyclones, coastal damages, Salento peninsula, Mediterranean Sea*

In the Mediterranean Sea the development of cyclonic storms is a very usual phenomenon (Petterssen, 1956). Recent studies have reported that some extreme events most likely increase in frequency and/or severity during the last 21st century due to change in the mean and/or variability of climate (Fita et al., 2007; Meehl et al., 2007). In particular, sea storms and gales associated to cyclonic storms seem to enforce becoming more extreme (e.g. Ernst & Matson, 1983; Rasmussen & Zick, 1987; Reale & Atlas, 1998; Pytharoulis et al., 1999). The formation of small scale hurricane-like cyclones are more frequently from statistical point of view; these events are storms, characterised by a life maximum of 2-3 days, attain hurricane intensity and can severely affect coastal area (Emanuel, 2005; Monserrat et al., 2006; Fita et al., 2007).

This implies additional coastal risk specially due to change in the style and density of occupation and utilization of the coastal zone within Mediterranean coastal area.

An analysis of major sea storms which struck the coast of Salento peninsula in the period from 1980 and 1999 has been carried out. Sea storms have been classified in function of coastal damages by means of an appropriate evaluation scale

characterised by 6 different damage classes (Tab. 1).

Results have been plotted as a bar chart whose horizontal-axis reports the 20 years time period while vertical-axis reports damage degree. Wind directions are represented with different bar colours (Fig. 1).

A number of 27 sea storms occurred along the coast of Salento peninsula and three of them caused severe damages (Degree 5). The historical chronicles don't report coastal damages (class 0) caused by five sea storms in the same period.

The analysis points out that the severe sea storms are mainly produced by south-east and south-west winds; minor damage have been produced by events related to W, N and NW winds. During the analyzed time period, NE and E winds did not caused any sea storm event.

Sea storms occurred more frequently from 1982 to 1984 and from 1994 to 1997 while during last years they have been fewer and less powerful. Most severe sea storms occur in November, December and January.

The collated data show that the most damaged costal sites by sea storms are Gallipoli (12 events), S. M. di Leuca and Tricase Porto (5 events) e Porto Miggiano (3 events).

Class	Damage
0	No coastal damages occur during sea storms; sea storms is instrumentally registrated
1	During sea storms, slight navigation discomforts occur
2	During sea storms, the vessels in the harbours suffer slight damages
3	The intensity of sea storms cause severe damages to vessels
4	Some clinched vessels come to sink and slight damages occur to coastal buildings
5	Several clinched vessels come to sink, and severe damages occur to coastal buildings

Table 1. Six different classes of coastal damages in function of sea storms impact.

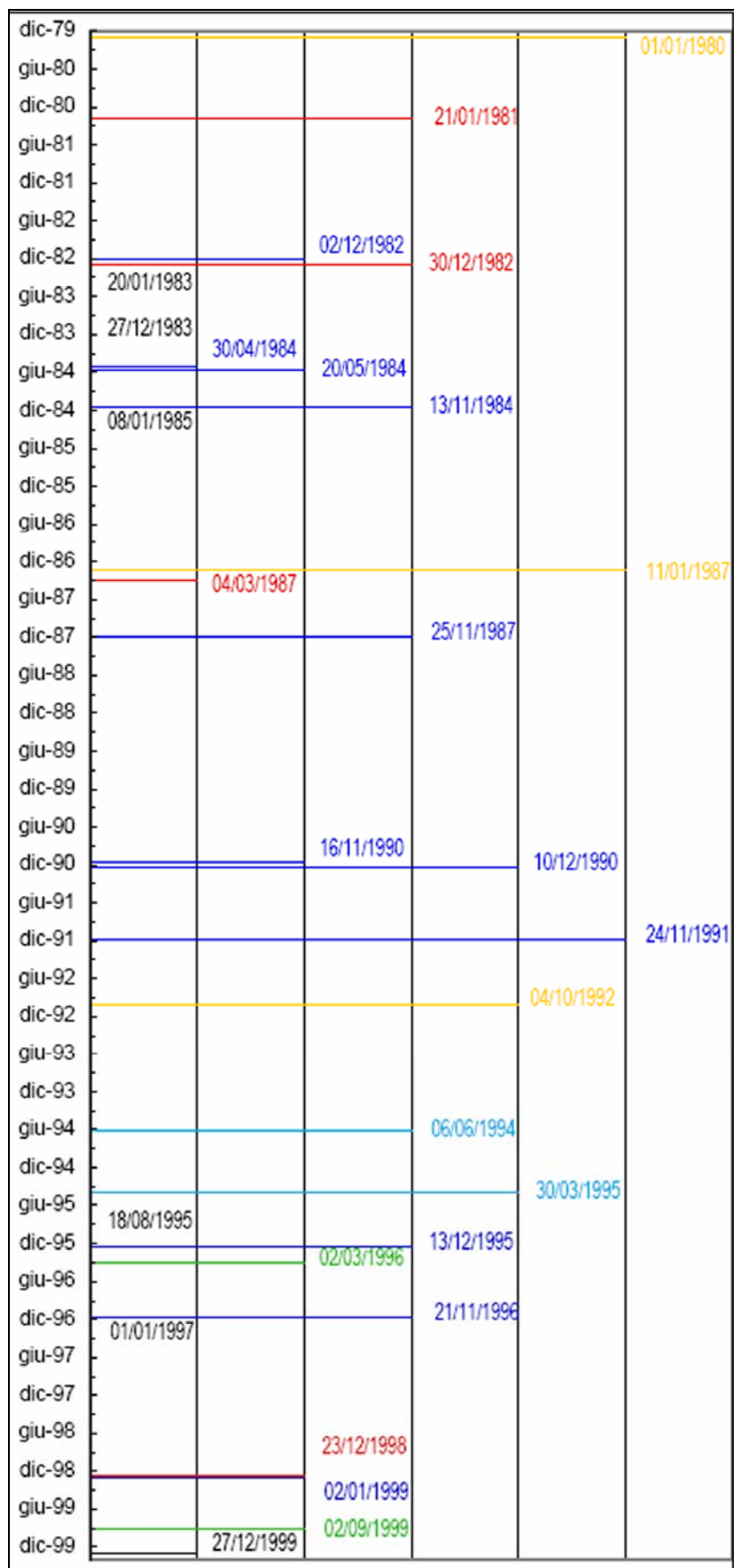


Figure 1. Sea storms trending along the Salento coast in the period between 1989-1999; x axis represents the sea storm time in month; y axis represents the frequency of the sea storm for each month.

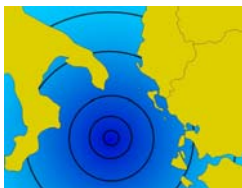
The geomorphological analysis allows four tracts with same bearing to be defined along the coastline of Salento: the Casalabate-Capo d'Otranto tract, NNW-SSE oriented and exposed to NE winds; the Capo d'Otranto-S.M. di Leuca, NNE-SSW oriented and exposed to SE winds; the S.M.di Leuca-Gallipoli tract, NW-SE oriented and mainly exposed to SW winds; the Gallipoli-Punta Prosciutto tract, NNW-SSE oriented and exposed to the SW and NW winds as well.

The analysis of wind climate and coastline orientation points out the coastal tracts from S.Maria di Leuca to Punta Prosciutto are those ones mostly prone to sea storms.

The realized data base comprises extreme sea storm events, wind climate and geomorphological features. These data can be usefully used by planners for the determination of coastal risk in the Salento peninsula and for the definition of mitigation plans.

References

- Ernst J.A., Matson M. (1983). *A Mediterranean tropical storm?*. Weather, 38, 332-337.
- Fita L., Romero R., Luque A., Emanuel K., Ramis C. (2007). *Analysis of the environments of seven Mediterranean tropical-like storms using an axisymmetric, nonhydrostatic, cloud resolving model*. Nat. Hazards Earth Syst. Sci., 7, 41-56.
- Meehl G.A., Stocker T.F., Collins W.D., Friedlingstein P., Gaye A.T., Gregory J.M., Kitoh A., Knutti R., Murphy J.M., Noda A., Raper S.C.B., Watterson I.G., Weaver A.J. and Zhao Z.-C., (2007). *Global Climate Projections*. In: *Climate Change 2007: The Physical Science Basis. Contribution of Working Group I to the Fourth Assessment Report of the Intergovernmental Panel on Climate Change* [Solomon S., Qin D., Manning M., Chen Z., Marquis M., Averyt K.B., Tignor M. and Miller H.L. (eds.)]. Cambridge University Press, Cambridge, United Kingdom and New York, NY, USA.
- Milella M., De Santis V., Pignatelli C., Cacciapaglia G., Selleri G., Fozzati L., Mastronuzzi G., Sansò P., Palmentola G. (2008). *Sensibilità della costa pugliese ad ondate estreme*. Atti del Convegno Nazionale "Coste: prevenire, programmare, pianificare" Maratea 15-17 Maggio 2008.
- Monserat S., Vilibic I., Rabinovich A. B. (2006). *Meteotsunamis: atmospherically induced destructive ocean waves in the tsunami frequency band*. Nat. Haz. Earth Syst. Sci., 6, 1035-1051.
- Petterssen S. (1956). *Weather Analysis and Forecasting*. 2nd McGraw- Hill, New York.
- Pytharoulis I., Craig G. C., Ballard S. P. (1999). *Study of the Hurricane-Like Mediterranean Cyclone of January 1995*. Phys. Chem. Earth (B), 24(6), pp. 627-632.
- Rasmussen E., Zick C. (1987). *A subsynoptic vortex over the Mediterranean with some resemblance to polar lows*. Tellus, 39A, 408-425.
- Reale O., Atlas R. (1998). *A tropical-like cyclone in the extratropics*. International Centre for Theoretical Physics preprint, Trieste, Italy. No. IC98007.



2nd International Tsunami Field Symposium

IGCP Project 495

Quaternary Land-Ocean Interactions:
Driving Mechanisms and Coastal Responses

Ostuni (Italy) and Ionian Islands (Greece) 22-28 September 2008



Project 495

Molfetta M. G.¹, Petrillo A. F.¹, De Girolamo P.², Pratola L.¹,
Di Risio M.², Bellotti G.³, Aristodemo F.⁴, Panizzo A.⁵

Three-dimensional large scale experiments on tsunamis generated by landslide along the coast of a conical island

¹DIAC-LIC, Technical University of Bari, Bari, Italy, e-mail: m.molfetta@poliba.it;

²DISAT-LIAM, University of L'Aquila, L'Aquila, Italy, e-mail: mdirisio@ing.univaq.it;

³DSIC, University of Rome TRE, Rome, Italy, e-mail: bellotti@uniroma3.it;

⁴DDS, University of Calabria, Arcavacata di Rende, Italy, e-mail: aristodemo@dds.unical.it;

⁵DITS, University of Roma "La Sapienza", Rome, Italy, e-mail: andrea.panizzo@uniroma1.it

Keywords: *Tsunami generation and propagation, experimental modeling, landslide, conical island*

This paper describes new three dimensional large scale experiments carried out at the Research and Experimentation Laboratory for Coastal Defence (LIC) of the Technical University of Bari (Italy), aimed at reproducing water waves generated by subaerial landslides sliding down the flank of a conical island. The generated waves in such a situation propagate both offshore and along the curvilinear shoreline.

The research efforts in landslide generated waves has increased in the last decades due to events occurred around the world: the 1958 Lituya Bay event and 2002 Stromboli island one (Tinti et al., 2005), just to mention two of them. Many laboratory experiments have been carried out in order to gain insight about the properties of the landslide generated waves. Most of these studies (Wiegel 1955; Heinrich 1992; Watts 1997, 1998, 2000; Grilli & Watts 2005; Fritz et al. 2003a, 2003b) have focussed on two-dimensional layouts

(1 horizontal, 1 vertical direction) and have provided fundamental information on the process. Panizzo et al. (2005) have studied waves generated in a three-dimensional layout but they employed a flat bottom: their results can be applied to describe the generation process but not the interaction of the waves with the coast. Enet et al. (2003), Enet & Grilli (2005,2007), Liu et al. (2005) and Di Risio et al. (2008) have more recently presented three-dimensional investigations, reproducing landslides sliding along sloping plane beaches. Although several researches have previously addressed landslide generated waves, the only physical model experiments involving tsunamis attacking islands are those by Briggs et al. (1995).

However this pionieristic research reproduced waves attacking the island from offshore, i.e. the waves were generated elsewhere, potentially by an earthquake.

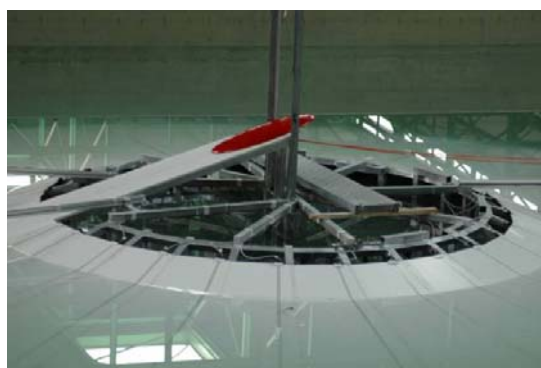


Figure 1. Picture of the conical island placed at the center of the wave tank (left). and a particular of landslide model placed on the ramp (right).

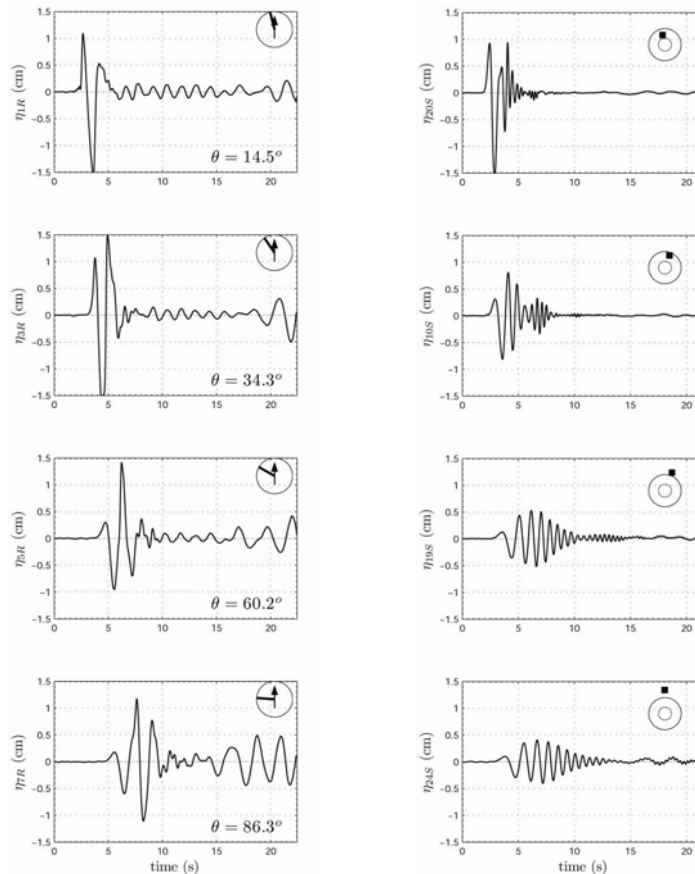


Figure 2. Runup time series - left panels – (figura_2_1.JPG) and surface elevation time series - right panels (figura_2_2.JPG) collected during one of the experiment. The small circle on each plot reproduces the coastline, the arrow indicates where the landslide enters the water and the line (on the left panels) specifies the position of the considered runup gauge and the dark square (on the right panels) specifies the position of the considered wave gauge.

For the case of the Stromboli island, for example, the waves are generated along the coast of the island itself by a large landslide (volume of about $18 \times 10^6 \text{ m}^3$) along the flank of the volcano named “Sciara del Fuoco”, and the generation-propagation-inundation phases cannot be decoupled. For the first time, the experiments described herein are aimed at reproducing water waves generated directly on the flank of the conical island and at measuring both shoreline displacements and radiating waves. The experimental results can be used as benchmark for theoretical and numerical models as the landslide and the island shapes can be easily reproduced. Furthermore the experimental findings can be considered to be of practical interest as they allow insight about the celerity and the height of the wave run-up occurring around the island, a crucial point for the preparation of evacuation maps and for the set up of early warning systems.

The experiments are carried out in a wave tank 30 m long, 50 m wide and 3.0 m high. The maximum water depth is 0.8 m. PVC sheets sustained by steel bars represent an impermeable

beach with slope of 1:3 (see Figure 1) very similar to the “Sciara del Fuoco” flank of the Stromboli island. The conical island diameter at the ground level is of 9.0 m. The landslide is represented by a rigid fibreglass elliptical body (length 0.8 m, width 0.4 m, maximum height 0.05 m) with a total volume of 0.0084 m^3 . The density of the landslide model is 1.83 kg/m^3 for a total mass of 15.4 kg.

Experiments were carried out by keeping constant the landslide properties (i.e. density and shape) and by changing the water depth (ranging from 0.60 m up to 0.80 m) and the falling height of the body (ranging from 0.30 m up to 0.60 m, measured as the distance along the island flank between the lower part of the landslide in its initial position and the undisturbed shoreline). It is important to stress that water depth was also varied in order to change the radius of the undisturbed shoreline that ranged from 2.10 m up to 2.6 m.

The experimental data collected during the tests consisted of (i) time series of surface elevation in the tank, (ii) time series of shoreline position and (iii) time series of accelerations of the landslide model in order to reconstruct its motion.

A series of 22 resistance wave gauges are used to measure the instantaneous surface elevation in the tank and 16 run-up gauges embedded into the PVC of the island flanks measure the displacements of the instantaneous shoreline. A capacitive accelerometer (Metra-Mess CB41) has been placed inside the landslide in order to measure the acceleration during its motion along the slope.

Runup gauges and offshore wave gauges time series (Figure 2) are analyzed in order to detect the

maximum runup along the shoreline and the properties of the waves radiating towards offshore. It has to be stressed that the tank dimensions allow to measure runup before the wall reflected waves come back to the island and affect the measured time series.

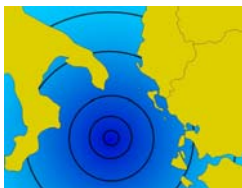
Due to the selected parameters, the overall experimental setup can roughly represent the Stromboli island when a scale reduction factor of about 1:1000 (Froude scaled) is applied.

Acknowledgment

The research described in this paper is funded by the Italian Ministry of Research (MIUR). Thanks are due to the technicians of the LIAM "Umberto Messina" laboratory - Mario Nardi and Lucio Matergia - and LIC laboratory - Giuseppe Intranuovo and Luciano Romanazzi.

References

- Briggs M. J., Synolakis C. E., Harkins G. S., Green D. R. (1995). *Laboratory experiments on Tsunami runup on a conical island*. Pure and Appl. Geophys., 144 (3/4), 569-593.
- Di Risio M., Bellotti G., Panizzo A., De Girolamo, P. (2008). *Three-dimensional experiments on landslide generated waves at a sloping coast*. Submitted for publication to Coastal Engineering.
- Enef F., Grilli S. T., Watts P. (2003). *Laboratory experiments for tsunamis generated by underwater landslides: comparison with numerical modeling*. Proc., 13th Offshore and Polar Engineering Conf., ISOPE03, Vol. 3, Honolulu, ISOPE, Cupertino, Calif. 383, 372-379.
- Enef F., Grilli, S. T. (2005). *Tsunami landslide generation: Modelling and experiments*. Proc., 5th Int. on Ocean Wave Measurement and Analysis, WAVES 2005, Madrid, Spain, IAHR, Paper No. 88.
- Enef F., Grilli, S. T. (2007). *Experimental study of tsunami generation by three dimensional rigid underwater landslides*. Journal of Waterway Port Coastal and Ocean Engineering-ASCE, 133 (6), 442-454.
- Fritz H. M., Hager W. H., Minor H.-E. (2003a). *Landslide generated impulse waves*. 1. Instantaneous flow fields. Experiments in Fluids, 35 (6), 505-519.
- Fritz H. M., Hager W. H., Minor H.-E. (2003b). *Landslide generated impulse waves*. 2. Hydrodynamic impact craters. Experiments in Fluids, 35 (6), 520-532.
- Grilli S. T., Watts P. (2005). *Tsunami Generation by Submarine Mass Failure*. I: Modeling, Experimental Validation, and Sensitivity Analyses. Journal of Waterway Port Coastal and Ocean Engineering-ASCE, 131 (6), 283-297.
- Heinrich P. (1992). *Nonlinear water waves generated by submarine and aerial landslides*. Journal of Waterway Port Coastal and Ocean Engineering-ASCE, 118 (3), 249-266.
- Liu P. L. -F, Wu, T. -R., Raichlen F., Synolakis C. E., Borrero J. C. (2005). *Runup and rundown generated by three-dimensional sliding masses*. Journal of Fluid Mechanics, 536, 107-144.
- Panizzo A., De Girolamo P., Petaccia A. (2005). *Forecasting impulse waves generated by subaerial landslides*. Journal of Geophysical Research-Oceans, 110 (C12), Art. No. C12025.
- Tinti S., Maramai A., Armigliato A., Graziani L., Manucci A., Pagnoni G., Zaniboni F. (2005a). *Observations of physical effects from tsunamis of December 30, 2002 at Strombolivolcano, southern Italy*. Bulletin Of Volcanology, 412 68 (5), 450-461.
- Watts P. (1997). *Water waves generated by underwater landslides*. Ph.D. dissertation, California Institute of Technology, Pasadena, Calif.
- Watts P. (1998). *Wavemaker curves for tsunamis generated by underwater landslides*. Journal of Waterway Port Coastal and Ocean Engineering-ASCE, 124:127.
- Watts P. (2000). *Tsunami features of solid block underwater landslides*. Journal of Waterway Port Coastal and Ocean Engineering-ASCE, 126 (3), 144-152.
- Wiegel R. L. (1955). *Laboratory studies of gravity waves generated by the movement of a submarine body*. Trans., Am. Geophys. Union, 36 (5), 759-774.



Oliveira M. A.¹, Andrade C.¹, Freitas M. C.¹, Costa P.¹

Using the historical record and geomorphological setting to identify tsunami deposits in the southwestern coast of Algarve (Portugal)

¹Centro de Geologia, Departamento de Geologia, Universidade de Lisboa, Faculdade de Ciências,
Campo Grande, Lisboa, Portugal

e-mail: alexandra.oliv@gmail.com; candrade@fc.ul.pt; cfreitas@fc.ul.pt; ppcosta@fc.ul.pt

Keywords: *Tsunami, historical record, geological record, coastal geomorphology, Portugal*

A compilation of historical testimonies of tsunami flooding of the Portuguese Algarve coast was combined with a geomorphological characterization of that coast to produce a data base on locations prone to inundation by such high energy events. Field work has been undertaken in the lowland areas identified by this methodology between Sagres and Lagos in order to characterize the correspondent geological evidences. Results indicate that some locations vulnerable to inundation failed to preserve any sedimentological trace of extreme marine inundation. However, the completeness of the data base on these events significantly increases when the historical record is added by geological information. The sedimentary signature of tsunami inundation of the studied coastal section is varied and it may have been severely damaged by the intense anthropogenic activities that characterize the Algarve coast.

Introduction

The work presented here is currently being developed under the European Project NEAREST (Integrated observations from NEAR shore sourceES of Tsunamis: towards an early warning system), which aims the identification and characterization of potential tsunami sources in the Gulf of Cadiz and the improvement of the current knowledge on the recurrence intervals of these extreme events.

Tsunami deposits can be used to provide an indirect record of former extreme marine events (Dawson, 1999). To obtain a recurrence interval of large earthquakes from such records it is necessary to explore, identify, characterize and date sedimentological evidences of tsunami flooding.

The nature of the onshore sedimentary signature of a tsunami depends firstly of adequate sediment

supply from the nearshore. Sediments deposited there have different characteristics, varying with location and wave parameters: overtopping of coastal dunes or barriers may result in the formation of extensive sand overwash deposits (Dawson & Shi, 2000); small boulders originally sitting in the shallow meso and upper infralittoral zones may be incorporated within sheets of tsunami-deposited sand, as reported by several authors (e.g. da Silva et al., 1996; Hindson et al., 1996; Hindson & Andrade, 1999); in addition, tsunami deposits may also be represented by accumulations of large boulders, including megaclasts (Dawson & Shi, 2000).

Successive tsunami waves may result in the erosion of the deposit of the previous tsunami wave, leading sometimes to complete removal and obliteration of the record shortly after its formation.

This is additionally complicated by the occurrence of episodes of backwash that follow the landward inundation (Dawson, 1999). Thus, preservation of such records in the sedimentary column also requires the existence of accommodation space and that no significant post-depositional sediment removal occurred, promoted by either natural causes (e.g. stream or overland flow) or human activity (e.g. cleaning and eventual replacement of topsoil or repeated ploughing for agriculture).

Deposition of tsunami sediment in low-energy coastal basins such as lagoons or estuaries with high sedimentation rates provides the most favourable contexts to preservation.

Few coastal locations prone to tsunami inundations meet all conditions required for producing a complete long-term record of tsunami activity, and in most cases the geological record should be regarded as incomplete and biased to extreme events.

Nevertheless, space may be used as a replacement of the missing time information, and the survey of a sufficiently long section of coast may yield a compilation of diachronic features that taken together fairly mirror the time-series of generating events. This principle has been used to build a surveying framework of the Algarve coast of Portugal.

Work Development

The Sagres-Lagos 30 km-long section of the Algarve coast was chosen as a study area given the existence of sedimentary record of the 1755 Lisbon tsunami in the lowlands of Boca do Rio and Martinhal (e.g. Andrade, 1992; Dawson et al., 1995; da Silva et al., 1996; Hindson et al., 1996; 1999; Hindson & Andrade, 1999; Andrade et al., 2004; Kortekaas & Dawson, 2007).

The work involved several steps, beginning with a literature review. For this purpose, eyewitness testimonies of tsunami impacts in the Algarve coast reported in the literature, which respect essentially the 1755 event, were collected and analysed (e.g. Relaçam, 1756; Pereira de Sousa, 1919; Costa et al., 2005; GITEC tsunami catalogue). The outcome was a compilation of card files for each place referred in

the documentary sources, containing the transcriptions of the testimonies, relevant observations on the local and regional contexts, material deposited and supporting references. Subsequently, a geomorphological analysis of the coast was undertaken, using geological and topographical maps, aerial photographs and satellite images, to identify and rank sites offering preservation potential of deposits resulting from extreme marine flooding events. To keep the work within reasonable limits, we considered only the coastal section up to 1 km away from the shoreline, less than 10 m above mean sea level (MSL) and displaying evidence of active low energy deposition. After merging together the documentary and geomorphological data, a final guide-document was produced and eight coastal sites elected for field survey (Fig. 1): Sagres, Martinhal (Fig. 1A), Barranco and Zavial (Fig. 1B), Furnas and Figueira (Fig. 1C), Boca do Rio (Fig. 1D) and Luz (Fig. 1E).

Field surveys conducted in 2007 and 2008 to explore these areas for depositional evidence of tsunami flooding lead to the identification of several high-energy sand and boulder deposits displaying characteristics compatible with such events.

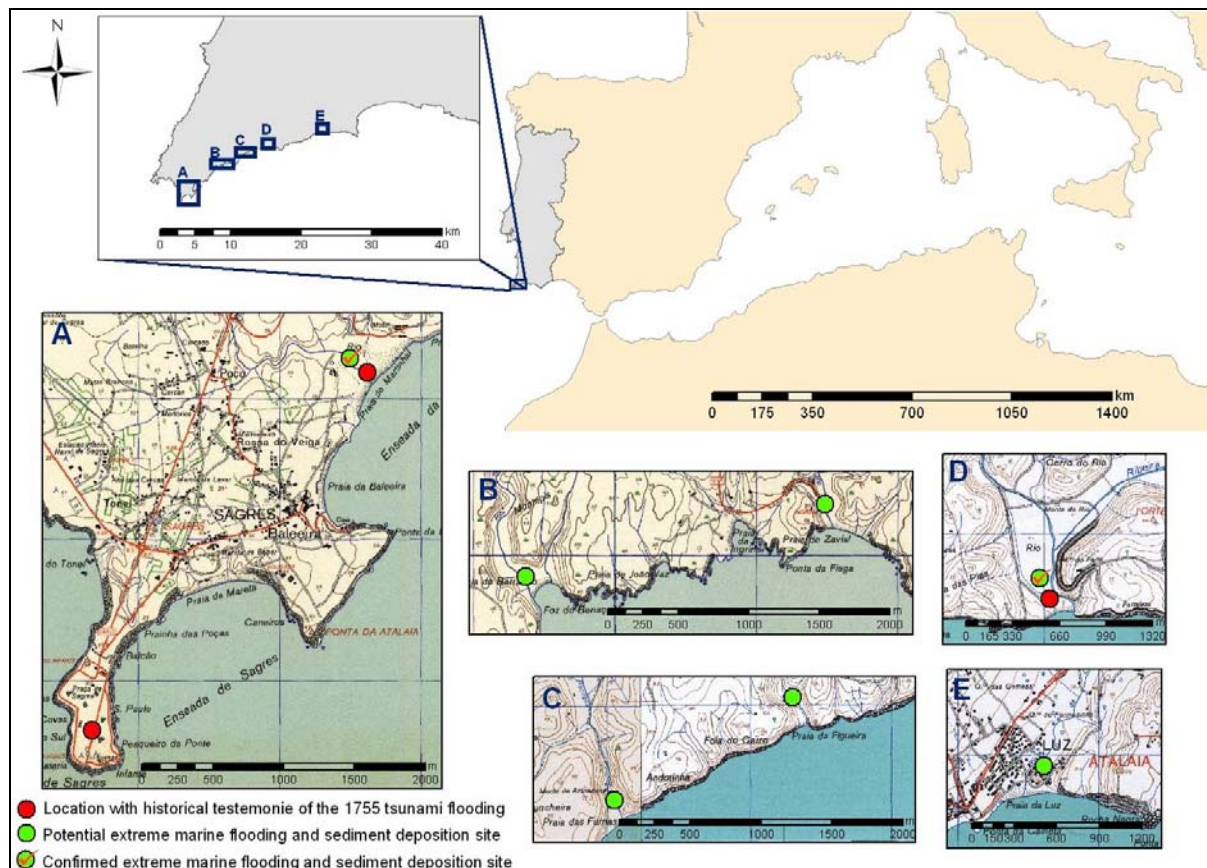


Figure 1. Geographical location of study area. **A** – Sagres and Martinhal; **B** – Barranco and Zavial; **C** – Furnas and Figueira; **D** – Boca do Rio; **E** – Luz. Topographic maps adapted from IGeoE (2005), sheets 601, 602 and 609.

These materials were found either embedded within lagoonal/estuarine muddy sediment (Martinhal, Zavial, Boca do Rio), or sitting upon the present-day surface (Barranco, Furnas), and they were described in the field and sampled. First results are summarized in Table 1, and are expressed as “confirmed” whenever indisputable sedimentary record of tsunami inundation exists, “possible” when attributes of features are compatible with tsunami emplacement and “absent” if no traces at all have been found.

Location	Historical Record of Flooding	Extreme Marine Flooding Deposit
Sagres fort and village	yes	Absent
Martinhal lowland	yes	Confirmed
Barranco lowland	no	Possible
Zavial lowland	no	Possible
Furnas lowland	no	Possible
Figueira lowland	no	Absent
Boca do Rio lowland	yes	Confirmed
Luz lowland	no	Absent

Table 1. Summary of studied locations, historical and depositional records.

Three out of eight locations displaying favourable conditions to the preservation of record of tsunami impacts show at present no clear geological evidence of such flooding, including one site (Sagres) where, a description of the 1755 tsunami impacts exists. In this case the morphological setting on top of a >30m-high promontory added by restoration works following the quake and intensive use of the surface since the 18th century, may well explain the disappearance of any sedimentary evidence (boulders, according to descriptions) left by the 1755 event. If the absence of eye-witness testimonies is quite easily explained given the non-existence of resident people in Figueira lowland, the absence of geological traces may well associate with: a) complete removal of any flood sediment by the backwash, enhanced by the narrowness and steep slope of the valley confining the lowland or b) extensive reworking of

alluvial sediment for farming- the lowlands are in that region the only usable land for agriculture.

The village of Luz is an interesting example of inexistence of both eyewitness and geological records of tsunami flooding (only descriptions of damage by the 1755 earthquake exist), though its geomorphological setting almost excludes the possibility of no tsunami impact; extensive human occupation of the lowland added by intensive agriculture could be responsible for the inexistence of sedimentary record in this case.

Barranco and Furnas show peculiar accumulations of perforated marine boulders extending up to 300m inland; these were most probably emplaced by a tsunami inundation (cf. Costa et al., 2008) and constitute the sole evidence of such a high energy event in these areas. In the case of Zavial, a single patch of marine sand with limited lateral extension may represent the remnant of a larger sand deposit left by the 1755 event; the extensive reworking of the surface for agriculture, may explain the obliteration of most of the original sediment layer. The inexistence of testimonies in these locations may be ascribed to the same reason invoked in the case of Figueira.

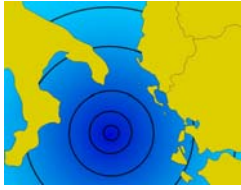
Final remarks

The reconstruction of the inundation history of any region founded on either the historical and/or geological records will most probably produce incomplete data-series, and the results found so far in one test region of the Algarve suggest that about 25% of the locations prone to inundation may fail to produce any record at all. The results indicate that geological evidence may be useful in completing historical information gaps resulting from the inaccuracy of witness descriptions or absence of observers, giving a more complete picture of the impacts. The geological signature is varied in nature even at a small spatial scale and it may be severely damaged by the intense anthropogenic activities that characterize the Algarve coast. Further completion of the data base under construction in the scope of the NEAREST project including relevant bathymetric, morphological and geological data and its processing in GIS environment, associated to lab analyses of the deposits, are expected to highlight reasons explaining the distribution of the geological record of tsunamis in the Algarve.

References

- Andrade C. (1992). *Tsunami generated forms in the Algarve barrier Islands (south Portugal)*. Science of Tsunami Hazards 10,1, 21-33.

- Costa A., Andrade C., Seabra C., Matias L., Baptista M.A., Nunes S. (2005). 1755 – *Terramoto no Algarve*. Centro Ciência Viva do Algarve, Faro, 237pp. Costa P., Andrade C., Freitas M. C., Oliveira M. A., Taborda R., Silva C. M. (2008). *High energy boulder deposition in Barranco and Furnas lowlands, western Algarve (South Portugal)*. *Proceed. 2nd Int. Tsunami Field Symposium*, Ostuni, Italia (this volume).
- da Silva C., Hindson R., Andrade C. (1996). *Bioerosion evidence of extreme marine flooding of Algarve region (Southern Portugal) associated with the tsunami of the AD 1755 Lisbon earthquake. Taphonomic and palaeoecological analysis*. *Proceed. Taphos '96, II Reunion de Tafonomia y Fossilizacion*, Zaragoza, 371-378.
- Dawson A. G., Hindson R., Andrade C., Freitas C., Paris R. (1995). *Tsunami sedimentation associated with the Lisbon earthquake of 1 November AD 1755: Boca do Rio, Algarve, Portugal*. *The Holocene*, 5, 2, 209-215.
- Dawson A. G. (1999). *Linking tsunami deposits, submarine slides and offshore earthquakes*. *Quaternary International*, 60, 119-126.
- Dawson A. G., Shi S. (2000). *Tsunami Deposits*. *Pure and Applied Geophysics*, 157, 875-897.
- Hindson R. A., Andrade C., Dawson A. G. (1996). *Sedimentary processes associated with the tsunami generated by the 1755 Lisbon earthquake on the Algarve coast, Portugal*. *Physical and Chemistry of Earth*, 21, 12, 57-63.
- Hindson R. A., Andrade C. (1999). *Sedimentation and hydrodynamic processes associated with the tsunami generated by the 1755 Lisbon earthquake*. *Quaternary International*, 56, 27-38.
- Hindson R.A., Andrade C., Parish R. (1999). *A microfaunal and sedimentary record of environmental change within the late Holocene sediments of Boca do Rio (Algarve, Portugal)*. *Geol. en Mijnbouw*, 77, 311-321.
- IGeoE (2005). *Carta Militar de Portugal, Série M888 / Escala 1:25000, Sagres (Vila do Bispo), Folha 609*. Edição 4, Instituto Geográfico do Exército, Portugal.
- IGeoE (2005). *Carta Militar de Portugal, Série M888 / Escala 1:25000, Vila do Bispo, Folha 601*. Edição 3, Instituto Geográfico do Exército, Portugal.
- IGeoE (2005). *Carta Militar de Portugal, Série M888 / Escala 1:25000, Lagos, Folha 602*. Edição 3, Instituto Geográfico do Exército, Portugal.
- Kortekaas S., Dawson A. G. (2007). *Distinguishing tsunami and storm deposits: an example from Martinhal, SW Portugal*. *Sedimentary Geology*, 200, 3-4, 208-221.
- Pereira de Sousa F.L. (1919). *O terremoto de 1^o de Novembro de 1755 em Portugal e um estudo demográfico: Distritos de Faro, Beja e Évora, Lisboa*, Tipografia do Comércio, Lisboa, 277pp.
- Relaçam (1756). *Relaçam do terremoto do primeiro de Novembro do anno de 1755 com os efeitos, que particularmente cauzou neste Reino do Algarve*. Biblioteca da Universidade da Coimbra, Manuscrito do Códice 537, fls. 159-163.



2nd International Tsunami Field Symposium

IGCP Project 495

Quaternary Land-Ocean Interactions:
Driving Mechanisms and Coastal Responses

Ostuni (Italy) and Ionian Islands (Greece) 22-28 September 2008



Project 495

Pantosti D.¹, Barbano M.S.², Smedile A.¹, De Martini P.M.¹, Gerardi F.², Pirrotta C.²

Geological evidence of paleotsunamis at Torre degli Inglesi (northeastern Sicily)

¹Istituto Nazionale di Geofisica e Vulcanologia, Sezione Sismologia e Tettonofisica, Gruppo di Tettonica Attiva, Roma, Italy, e-mail: pantosti@ingv.it; alessandra.smedile@ingv.it; paolomarco.demartini@ingv.it;

²Dipartimento di Scienze Geologiche, Università degli Studi, Catania, Italy
e-mail: barbano@unict.it; f.gerardi@unict.it; c.pirrotta@unict.it

Keywords: *historical earthquakes, tsunami deposits, Messina Strait, Sicily*

The recurrence interval for large magnitude earthquakes in Italy is generally longer than 1000 years (e.g. Valensise & Pantosti, 1992; Pantosti et al., 1993; Galadini & Galli, 2004), and largest earthquakes usually have repeat times of the same order as the length of the available historical records. Although the Italian catalogues report earthquakes which occurred in a long time span (461 BC – 2002 AD) (Boschi et al., 2000; Working group CPTI, 2004), the historical data on the earthquake effects are generally sparse at least until the 13-14th century events.

During the 4th century AD southern Calabria and eastern Sicily were hit by an earthquake documented by archaeoseismic analyses, which was interpreted by Guidoboni et al. (2000) as the predecessor of the well-known 1908 earthquake, located in Messina Strait, whereas Galli and Bosi (2002) interpreted this event as the predecessor of the 1783 earthquake.

The purpose of this paper is to find further evidence of these earthquakes in Messina area by a multi-disciplinary study aimed to recognize and date historical and paleo-earthquakes. For this goal we have analyzed historical, archaeological and geological information of excavations performed at Capo Peloro near the Torre del Faro village (Fig. 1) in the Torre degli Inglesi (English Tower), built on an abandoned Roman tower.

Historical earthquakes and tsunamis

There is a little evidence of earthquakes during the first millennium in the area surrounding the Straits of Messina; for the events in 91 BC, 17 AD, around the middle of the 4th century AD (Guidoboni et al., 1994, 2000), and 853 AD (Guidoboni et al., 1994; Boschi et al., 2000) no reliable information of damage is available.

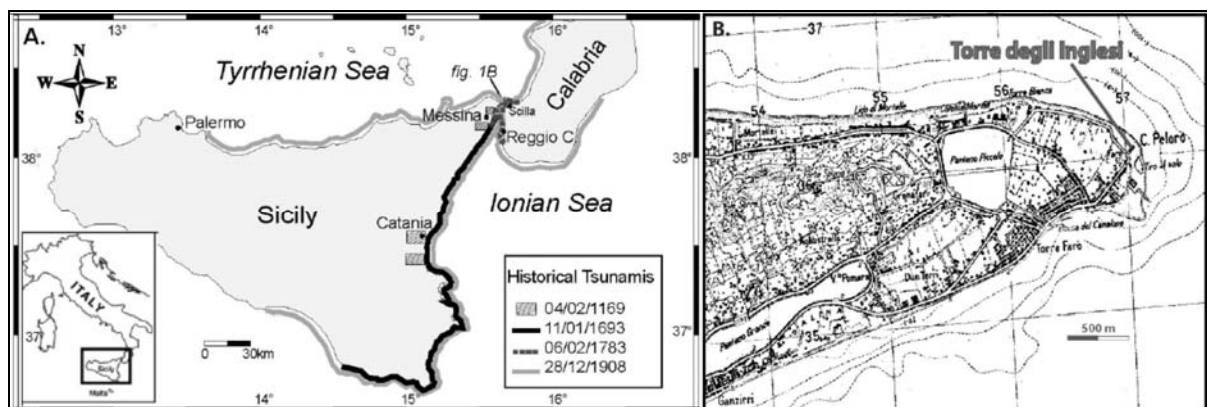


Figure 1. (A) Tsunami inundation in Eastern Sicily: lines with different grey tones and patterns and small striped rectangles indicate the inundated coastal areas. (B) Topographic map of the Ganzirri peninsula with the location of Torre degli Inglesi (arrow) near Capo Peloro, and the village of Torre Faro on the southern coast (from IGM 1:25000 scale topographic maps) (after Pantosti et al., 2008).

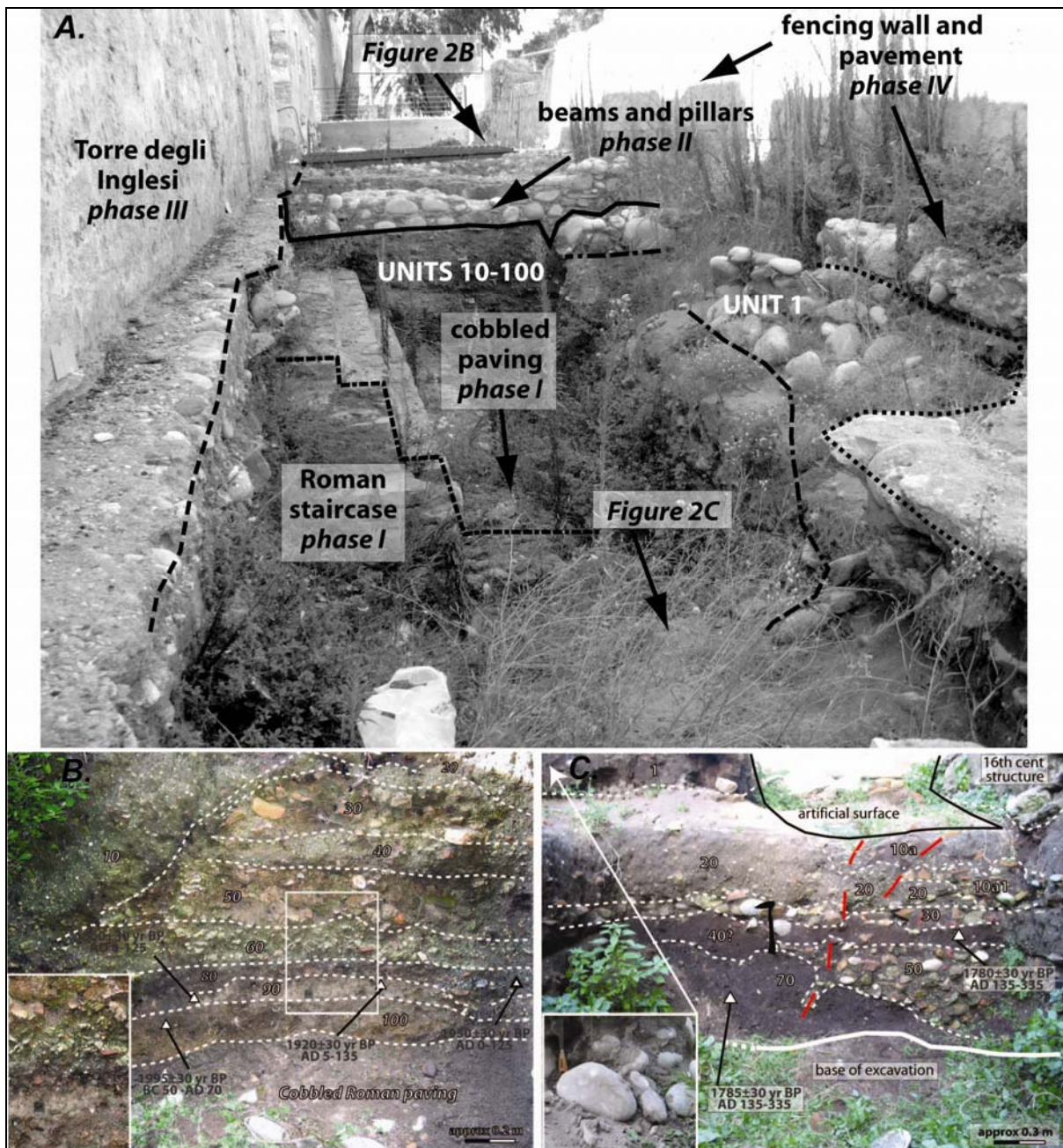


Figure 2. A) View of the archaeological excavation on the NW side of Torre degli Inglesi. The main building phases (i to iv) are visible with the relative chronology. Different patterns highlight the major relationships between features of different age. Labels Fig. 2b and 2c indicate the view of photographs shown in the relative figure (after Pantosti et al., 2008). B) View of the NW wall of the studied excavation at Torre degli Inglesi. Numbers refer to stratigraphic units described in the text, white triangles are location of dated charcoals. Measured and dendrochronologically corrected ages of samples (Stuiver et al., 2006) are reported as yr BP and 2σ intervals, respectively; C) NE wall; dashed black line highlights a fracture probably related to the 1908 earthquake (modified from Pantosti et al., 2008).

Between the end of the fifteenth and the end of sixteen centuries four events damaged some localities near the Messina Straits and the first observation for Torre del Faro refers to the 1509 earthquakes (Boschi et al., 2000). At Torre del Faro the two shocks of 5 and 6 Feb 1783 caused strong damage and the upper part of the Torre degli Inglesi collapsed (Vivenzio, 1783). The earthquake of 28 December 1908 caused four cracks in the new lighthouse of Capo Peloro; cracks E-W and N-S,

and a large fracture E-W which caused disjunction and relative lowering of the northern wall of the Torre degli Inglesi (Baratta, 1910), were also observed.

In the area of Messina Straits tsunamis were observed after the 1169 and 1693 south-eastern Sicily earthquakes, after the two shocks of 5 Feb and 6 Feb 1783, and after the 1908 earthquake. In the Ganzirri Peninsula, where Torre degli Inglesi is located, there is description for only the two most

recent tsunamis with reference to the village of Torre Faro.

At Torre Faro the 6 Feb 1783 tsunami flooded the shore for about 400 steps (~ 400m) inland depositing a large amount of silt and dead fishes (Sarconi, 1784). No direct mention of Torre degli Inglesi is found, but Hamilton (1783) reports that the same warm waves that had caused so much damage to Scilla, having surpassed the tip of lighthouse land at Capo Peloro, swallowed 24 people. Conversely, the 1908 tsunami inundation decreased substantially to the north of the town of Messina and produced a wave that, according to Baratta (1910), flooded inland at Torre Faro only 5m.

Archaeological data

The Torre degli Inglesi is a quadrangular base defence tower located about 40 m from the present shoreline, at an elevation of about 5 m a.s.l. (Fig. 1B). According to archaeological evidence studied by the Superintendence of the Archaeological heritage of Messina, the main building phases (Fig. 2a) of the Torre degli Inglesi, can be summarized as follows: (i) between the 1st century BC and 1st century AD construction of the Roman Tower; (ii) between 3rd-16th century destruction (by an earthquake? a fire?), abandonment and rebuilt of a new undefined structure; (iii) 16th century construction of the Torre degli Inglesi; (iv) end of 19th century construction of facing walls. Finally, the tower was restored after the 1908 earthquake.

Geological evidence

On the basis of the detailed survey of the deposits exposed in the archaeological excavation (Fig. 2 b and c), we found two layers (units 90 and 1) completely different from the deposits exposed at the site and nearby. In fact, these are composed by clean, gray, silicoclastic sands, rounded cobbles and pebbles, substantially contrasting the dark organic colluvia rich in wastes, related to human activity. Micropaleontological analyses confirmed the different origin of the deposits composing units 90 and 1 that are likely marine. The nature of these deposits, coupled to their sharp erosional contacts and their relative infrequency (i.e., if these were storm deposits these should be more frequent), allow us to interpret these layers as paleotsunami deposits (Pantosti et al., 2008).

Radiocarbon dating was performed on 6 charcoals (Fig. 2 b), sampled in the lower bioclastic sandy layer (Unit 90) and in the sandy layers just below and above the same layer, to constrain the age of the lowermost tsunami sand (Pantosti et al., 2008); while the samples (Fig. 2 c) collected in the artificial levelling deposits into two levels to the left

and to the right of the fracture, well predate the younger tsunami deposit, that underlies the facing walls of the 19th century (Fig. 2).

Combining archeological, historical and radiocarbon data we may associate the oldest tsunami layer (unit 90) to the 17 AD earthquake, for which no knowledge and information reported by historical sources existed about tsunamis till now. Conversely, the youngest layer (unit 1) is likely related to the 1783 Feb. 6 earthquake that is well known of the triggered tsunami (Pantosti et al., 2008). No evidence for the famous 1908 Messina tsunami was found.

Conclusion

The sedimentological and archaeological stratigraphy and dating at the site of Torre degli Inglesi contain evidence of the effects of three, possibly four earthquakes, two of which produced also large tsunami inundation. These are:

- The sandy layer (unit 90) deposited by a tsunami between 0 and 125 AD that may be associated to the 17 AD earthquake.

- The pillar and beams of a new construction intervening on the Roman structure but cut by the 16th century tower indicating the abandonment of the Roman tower and re-built of a new structure.

The age of the fill around the tower containing wastes, pottery and charcoal (destruction layer?) is found consistently at AD 135-335 suggesting that the event of destruction occurred in this period of time. This event may be correlated to the 4th cent. event (Guidoboni et al., 2000).

- The sandy layer (unit 1), just below the end of 19th century facing walls that was probably deposited by the Feb 6, 1783 tsunami.

- The north-eastern striking fracture, cutting both the deposits and artefacts, described in the historical accounts for the 1908 earthquake.

These results call for a reconsideration of the historical seismicity of the area and especially on their attribution to seismic sources. This is particularly true for the 17 AD and 4th cent. events for which limited knowledge exists.

In fact, different authors interpret the 4th cent. events as ancestor of the 1908 or 1783 event providing indication on the repetition of large events on the causative faults; whereas the 17 AD earthquake is considered a minor shock, roughly located in the northern side of Mt. Etna with an maximum intensity of VIII-IX MCS and Maw = 5.14 (Working group CPTI, 2004) and information on related tsunami is not reported by historical sources.

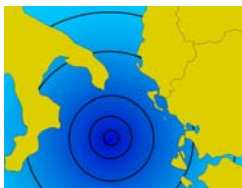
Revising these interpretations on the light of the results of this work is critical for the re-assessment of the seismogenic significance of the faults around the Messina Strait.

Acknowledgements

The authors are grateful to Dr. G. Tigano of the Superintendence of the Archaeological Heritage of Messina that kindly allowed us to scrutinise and sample the excavation walls and for her very useful Archaeological information. This work was funded by the Italian Dipartimento della Protezione Civile in the frame of the 2004-2006 agreement with Istituto Nazionale di Geofisica e Vulcanologia – INGV (Seismological Project S2).

References

- Baratta M. (1910). *La catastrofe sismica calabro messinese* (28 dicembre 1908). 2 voll. Roma.
- Boschi E., Guidoboni E., Ferrari G., Gasperini P., Mariotti D. and Valensise G. (2000). *Catalogue of Strong Italian Earthquakes from 461 a.C. to 1997*. Ann. Geofis. 43 (4), 843-868 and CD-ROM.
- Galadini F., Galli P. (2004). *The 346 A.D. earthquake (Central-Southern Italy): an archaeoseismological approach*. Ann. Geofis., 43 (2/3), 885-905.
- Galli P., Bosi V. (2002). *Paleoseismology along the Cittanova fault: Implications for seismotectonics and earthquake recurrence in Calabria (southern Italy)*. J. Geophys. Res., 107, NO. B3, 2044, 10.1029/2001JB000234.
- Guidoboni E., Comastri A., Traina G. (1994). *Catalogue of ancient earthquakes in the Mediterranean area up to 10th century*. INGV, 504, pp. Roma.
- Guidoboni E., Muggia A. and Valensise G. (2000) *Aims and methods in territorial archaeology: possible clues to a strong fourth-century AD earthquake in the Straits of Messina (southern Italy)*. In: McGuire W.G., Griffiths D. R., Hancock P.L., Stewart I.S. (eds) *The Archaeology of Geological Catastrophes*, Geological Society, London, SP, 171, 45-50.
- Hamilton W. (1783). *Relazione dell'ultimo terremoto delle Calabrie e della Sicilia*, tradotta dall'inglese da Gasparo Sella.
- Pantosti D., Schwartz D.P., Valensise G. (1993) *Paleoseismology along the 1980 Irpinia earthquake fault and implications for earthquake recurrence in the southern Apennines*. J. Geophys. Res., 98, 6561-6577.
- Pantosti D., Barbano M.S., Smedile A., De Martini P.M. (2008). *Geological Evidence of Paleotsunamis at Torre degli Inglesi (northeast Sicily)*. Geophysical Research Letters, 35, L05311doi:10.1029/2007GL032935.
- Sarconi M. (1784) *Istoria de' fenomeni del tremoto avvenuto nelle Calabrie, e nel Valdemone nell'anno 1783 posta in luce dalla Reale Accademia delle Scienze, e delle Belle Lettere di Napoli*. Napoli.
- Stuiver M., Reiner P.J., Reiner R. (2006). Calib 5.0.2. Radiocarbon Calibration.
- Valensise G. and Pantosti D. (1992). *A 125 Kyr-long geological record of seismic source repeatability: in the Messina Straits (southern Italy) and the 1908 earthquake*. Terra Nova, 44, 472-483.
- Vivenzio G. (1783). *Istoria e teoria de' tremuoti in generale ed in particolare di quelli della Calabria, e di Messina del MDCCLXXXII.*, Napoli.
- Working Group, CPTI (2004). *Catalogo Parametrico dei Terremoti Italiani, versione 2004 (CPTI04)*. INGV, Bologna. <http://emidius.mi.ingv.it/CPTI/>



2nd International Tsunami Field Symposium

IGCP Project 495

Quaternary Land-Ocean Interactions:
Driving Mechanisms and Coastal Responses

Ostuni (Italy) and Ionian Islands (Greece) 22-28 September 2008



Project 495

Paris R.¹, Poizot E.², Fournier J.³, Cachao M.⁴, Etienne S.¹,
Morin J.⁵, Lavigne F.⁵, Wassmer P.⁵

Modelling sediment transport and deposition by the 2004 tsunami in Sumatra (Indonesia)

¹Géolab UMR 6042 CNRS – Université Blaise Pascal Clermont-Ferrand, France - contact author:

e-mail: raparis@univ-bpclermont.fr;

²CNAM – Intechmer, Cherbourg, France

³BOME UMR 5178 CNRS – MNHN, France

⁴Department of Geology, University of Lisbon, Portugal

⁵Laboratoire de Géographie Physique UMR 8591 CNRS, Meudon, France

Keywords: *sediment transport modeling, tsunami deposits, Sumatra, Indonesia*

With wave heights of 30 m, runups reaching 51 m a.s.l. and inundation until 6 km inland (Lavigne et al., 2006), the December 26, 2004 tsunami in Sumatra was one of the largest tsunamis in recorded human history. Both inflows and outflow produced extensive erosion, sediment transport and deposition in a few minutes, along hundreds of kilometres of shoreline, and from shallow waters to several kilometres inland (Umitsu et al., 2006; Fagherazzi & Du, 2008; Paris et al., 2008). Thus, large tsunamis are major geomorphic crises. When buried and preserved, tsunami deposits become the geological records of past tsunamis (and most of the time, it is the only record identified). Studies of recent tsunami deposits provide a better understanding of the sedimentary signature of extremely energetic events, to reconstitute historical tsunamis and to better assess tsunami hazard. The interactions between the tsunami itself (flow depth, velocity and direction), the topography and the sediment source seem to dictate the spatial distribution and characteristics of tsunami deposits. A suite of diagnostic characteristics allows palaeo-tsunami deposits to be identified and differentiated from other deposits such as storm deposits (e.g. Dawson, 1994; Goff et al., 2001). These criteria have been confirmed and completed through recent works on 2004 tsunami deposits in Indonesia, Thailand, Sri Lanka and India (e.g. Bahlburg & Weiss, 2006; Goff et al., 2006; Moore et al., 2006; Singarasubramanian et al., 2006; Szczucinski et al., 2006; Hori et al., 2007; Paris et al., 2007; Srinivasalu et al., 2007; Choowong et al., 2008a-b).

Despite considerable progress over the last fifteen years, we cannot deduce actually the

magnitude (or “size”) of past tsunamis after their deposits.

Developing such quantitative tools requires a better understanding and modelling of sediment transport and deposition by tsunamis of distinct magnitudes. As pointed out by Huntington et al. (2007), “inverse models of flow from tsunami deposits and forward models of deposits from flow are relatively new and still under development” (e.g. Jaffe & Gelfenbaum, 2007; Noda et al., 2007).

In our previous publications, we presented descriptions and interpretation of coastal erosion, boulder and sand deposition induced by the 2004 tsunami in the Lhok Nga Bay (Paris et al., 2007 & 2008), located to the West of Banda Aceh (northwest Sumatra).

The aim of this new contribution is to model sediment transport and deposition by the 2004 tsunami in the same area, after new field data collected in August 2006 (side-scan sonar and diving survey), analysis of nannofossils in tsunami deposits, and numerical modelling of the tsunami (provided by the CEA in the framework of the Tsunarisque project).

The very high values of threshold shear velocities (Fig. 1) suggest that most of the sediments deposited inland (Fig. 2) came from offshore, from fine sands to coral boulders. The volume of beach eroded by the tsunami (ca. 150.000 m³) represents less than 10 % of the sediments deposited inland (ca. 1.500.000 m³).

Statistical analysis combining sedimentologic and hydraulic data allow distinguishing several kinds of tsunami deposits and correlations with the characteristics of the tsunami.

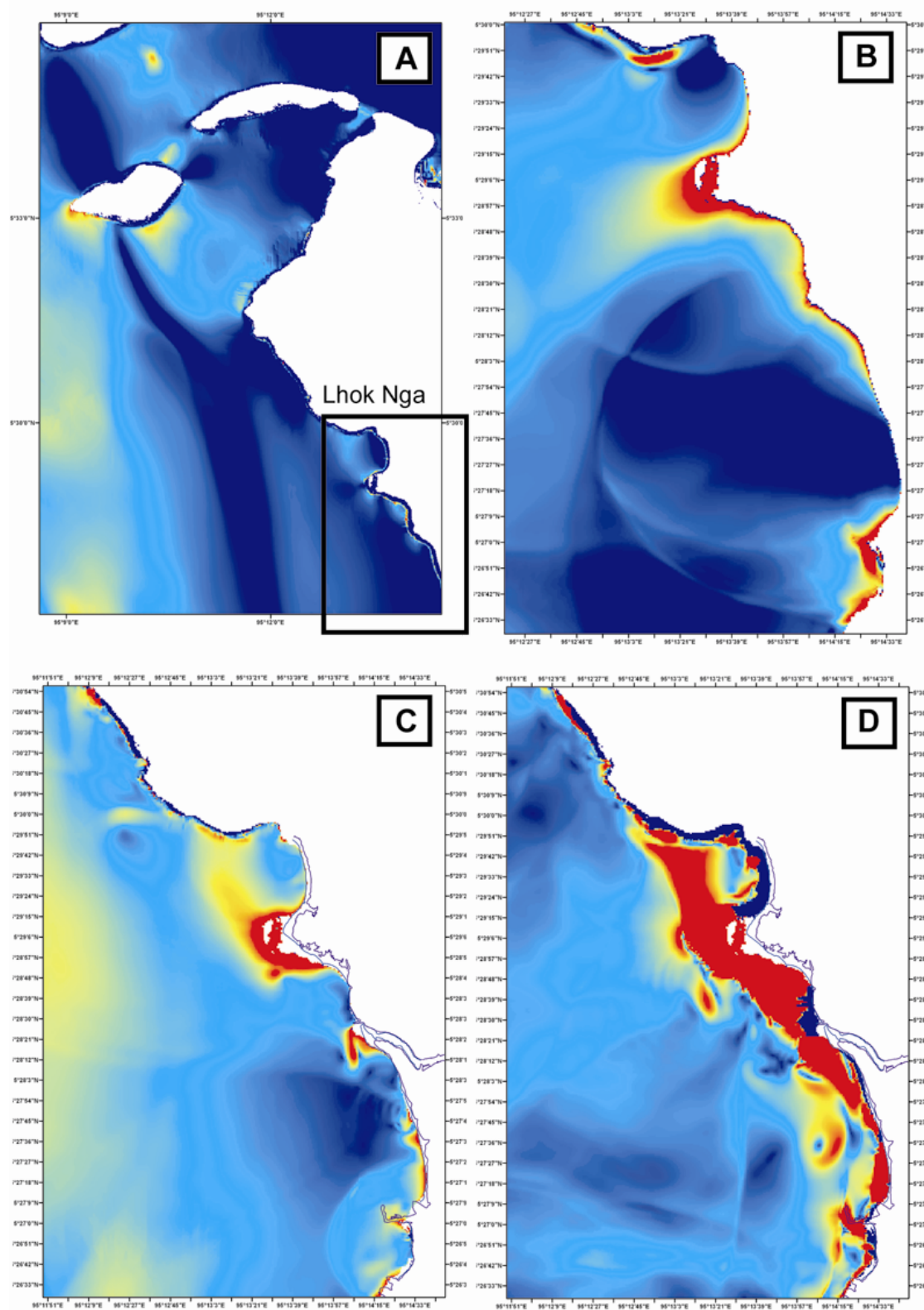


Figure 1. Maps of threshold shear velocity values (U^*) calculated for the 2004 tsunami off Lhok Nga (Northwest Sumatra, Indonesia). Low values appear in blue and high values in red. **A:** 30 minutes after the main earthquake, the tsunami wave train approaches Lhok Nga. U^* at the wave front are already high enough to mobilize submarine sediments. **B:** at 40 minutes, the tsunami has invaded Lhok Nga Bay and very high U^* values are observed at the coast, especially around the fringing reef in Lampuuk. **C:** at 55 minutes, the outflow (backwash) begins, but is channelized by gullies, river beds and coral reefs. A large zone of low U^* values in the south part of the bay corresponds to voluminous deposits identified by side-scan sonar surveys. **D:** at 75 minutes, the extent of the outflow reaches its maximum and very high U^* values suggest that a large volume of sediments were reworked and re-deposited offshore.

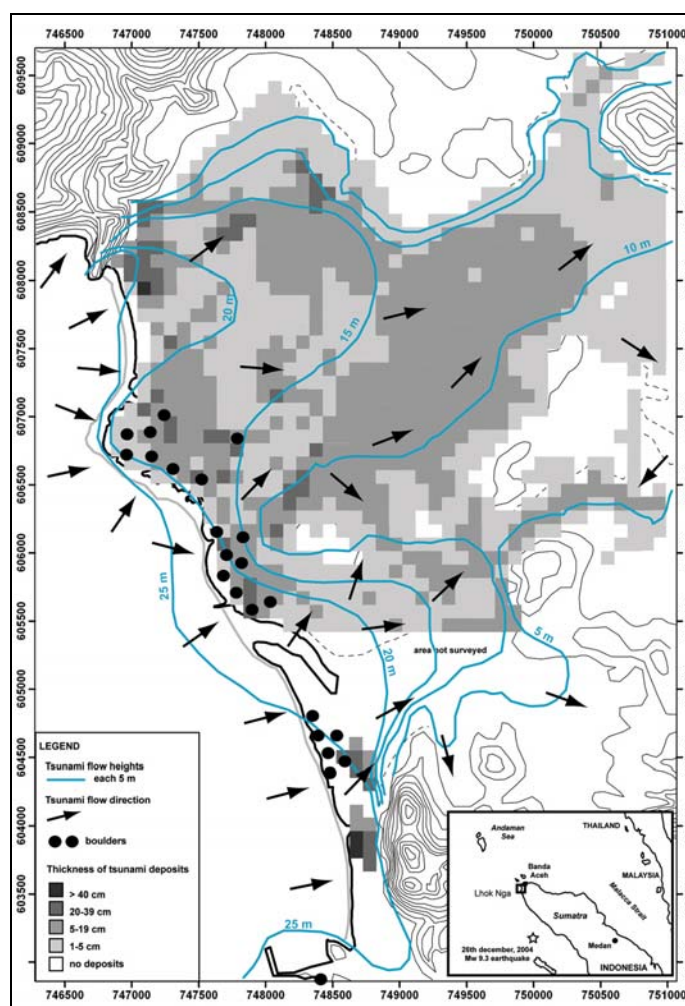


Figure 2. 2004 Tsunami flow heights and direction, related boulder accumulations and thickness of sandy deposits in Lhok Nga Bay (modified after Lavigne et al., 2006, and Paris et al., 2008).

The outflows (or backwash) may also have reworked significant volumes of sediments, re-deposited offshore, especially where inflow deposition was limited by steep slopes near the coast (Fig. 1).

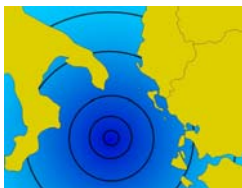
Side-scan sonar images clearly show zones of voluminous backwash deposition, coinciding with zones of low threshold velocity values (Fig. 2).

Thus, a key issue in distinguishing large tsunamis from others may be their geomorphic and sedimentologic impact offshore. The methodology presented here should be applied to next tsunamis in order to progress toward a quantitative model of sediment transport and deposition by tsunamis.

References

- Bahlburg, H., Weiss, R. (2006). *Sedimentology of the December 26, 2004 Sumatra tsunami deposits in eastern India (Tamil Nadu) and Kenya*. International Journal of Earth Sciences 96 (6), 1195-1209.
- Choowong M., Murakoshi N., Hisada K., Charoentitirat T., Charusiri P., Phantuwongraj S., Wongkok P., Choowong A., Subsayjun R., Chutakositkanon V., Jankaew K., Kanjanapayont P. (2008a). *Flow conditions of the 2004 Indian Ocean tsunami in Thailand, inferred from capping bedforms and sedimentary structures*. Terra Nova 20, 141-149.
- Choowong M., Murakoshi N., Hisada K., Charusiri P., Charoentitirat T., Chutakositkanon V., Jankaew K., Kanjanapayont P., Phantuwongraj S. (2008b). *2004 Indian Ocean tsunami inflow and outflow at Phuket, Thailand*. Marine Geology 248, 179-192.
- Dawson A. G. (1994). *Geomorphological effects of tsunami run-up and backwash*. Geomorphology 10, 83-94.
- Fagherazzi S., Du X., (2008). *Tsunamigenic incisions produced by the December 2004 earthquake along the coasts of Thailand, Indonesia and Sri Lanka*. Geomorphology (in press).

- Felton E. A., Crook K. A. W. (2003). *Evaluating the impact of huge waves on rocky shorelines: an essay review of the book 'Tsunami – The Underrated Hazard*. Marine Geology 197, 1-12.
- Goff J. R., Chagué-Goff C., Nichol S. L. (2001). *Palaeotsunami deposits: a New Zealand perspective*. Sedimentary Geology 143, 1-6.
- Goff J., Liu P., Higman B., Morton R., Jaffe B., Fernando H., Lynett P., Fritz H., Synolakis C., Fernando S. (2006). *Sri Lanka field survey after the December 2004 Indian Ocean tsunami*. Earthquake Spectra 22, S155.
- Hori K., Kuzumoto R., Hirouchi D., Umitsu M., Janjirawuttikul N., Patanakanog B. (2007). *Horizontal and vertical variations of 2004 Indian tsunami deposits: an example of two transects along the western coast of Thailand*. Marine Geology 239, 163-172.
- Huntington, K., Bourgeois, J., Gelfenbaum, G., Lynett, P., Yeh, H., Jaffe, B., Weiss, R. (2007). *Sandy signs of a tsunami's onshore depth and speed*. Eos, Transactions, American Geophysical Union 88 (52), 577-578.
- Jaffe B. E., Gelfenbaum G. (2007). *A simple model for calculating tsunami flow speed from tsunami deposits*. Sedimentary Geology, 200, 347-361.
- Lavigne F., Paris R., Wassmer P., Gomez C., Brunstein D., Grancher D., Vautier F., Sartohadi J., Setiawan A., Syahnan Gunawan T., Fachrizal Waluyo B., Mardiatno D., Widagdo A., Cahyadi R., Lespinasse N., Mahieu L. (2006). *Learning from a major disaster (Banda Aceh, December 26th, 2004): a methodology to calibrate simulation codes for tsunami inundation models*. Zeitschrift für Geomorphologie Suppl. Band 146, 253-265.
- Moore A., Nishimura Y., Gelfenbaum G., Kamataki T., Triyono R. (2006). *Sedimentary deposits of the 26 December 2004 tsunami on the northwest coast of Aceh, Indonesia*. Earth Planets & Space 58, 253-258.
- Paris R., Lavigne F., Wassmer P., Sartohadi J. (2007). *Coastal sedimentation associated with the December 26, 2004 in Lhok Nga, west Banda Aceh (Sumatra, Indonesia)*. Marine Geology 238, 93-106.
- Paris R., Wassmer P., Sartohadi J., Lavigne F., Barhomeuf B., Desgages É., Grancher D., Baumert Ph., Vautier F., Brunstein D., Gomez, Ch. (2008). *Tsunamis as geomorphic crisis: lessons from the December 26, 2004 tsunami in Lhok Nga, west Banda Aceh (Sumatra, Indonesia)*. Geomorphology (in press).
- Noda A., Katayama H., Sagayama T., Suga K., Uchida Y., Satake K., Abe K., Okamura Y. (2007). *Evaluation of tsunami impacts on shallow marine sediments: An example from the tsunami caused by the 2003 Tokachi-oki earthquake, Northern Japan*. Sedimentary Geology, 200, 314-327.
- Singarasubramanian S.R., Mukesh M. V., Manoharan K., Murugan S., Bakkairaj D., Peter A. J. (2006). *Sediment characteristics of the M 9 tsunami event between Rameswaram and Thoothukudi, Gulf of Mannar, southeast coast of India*. Sciences of Tsunami Hazards 25 (3), 160-172.
- Srinivasalu, S., Thangadurai, N., Switzer, A.D., Ram Mohan, V., Ayyamperumal, T. (2007). *Erosion and sedimentation in Kalpakkam (N Tamil Nadu, India) from the 26th December 2004 tsunami*. Marine Geology 240, 65-75.
- Szczucinski, W., Chaimanee, N., Niedzielski, P., Rachlewicz, G., Saisuttichai, D., Tepsuwan, T., Lorenc, S., Siepak, J. (2006). *Environmental and geological impacts of the 26 December 2004 tsunami in coastal zone of Thailand – overview of short and long-term effects*. Polish Journal of Environmental Studies 15 (5), 793-810.
- Umitsu, M., Tanavud, C., Patanakanog, B. (2006). *Effects of landforms on tsunami flow in the plains of Banda Aceh, Indonesia, and Nam Khem, Thailand*. Marine Geology 242, 141-153.



Pignatelli C.¹, Damato B.², Mastronuzzi G.¹

A terrestrial laser scanner based method to assess a tsunami wave inland penetration

¹Dipartimento di Geologia e Geofisica, Università degli Studi "Aldo Moro", Bari, Italy

e-mail: c.pignatelli@geo.uniba.it; g.mastrozz@geo.uniba.it;

²Autorità di Bacino della Regione Puglia, e-mail: bartolomeo.damato@adb.puglia.it

Keywords: roughness, LiDAR, flooding, surf bench, Apulia, Southern Italy

When tsunami waves approach the coastline, their features change in two different zones: in the near-shore zone and in the overland zone that they will flood. In the near-shore zone the tsunami surge characteristics are influenced by several local factors as width of the continental shelf, the energy focusing effects, the bathymetry and the actual coastal geometry. Moreover, the impact of a tsunami on coastal belts is greatly influenced by coastal topography and in particular by the

coastline geomorphology. A shoaling effect occurs on a tsunami wave running in a semi enclosed sea and its height increases. This last one can also be increased when impact of the tsunami is concentrated on headlands or when tsunami wave travelling into bays having wide entrances that become progressively narrower.

When the tsunami wave reaches coastline, it may: 1 – flood the landscape without breaking, like a rapidly rising sea level; and/or 2 - arrive as a train

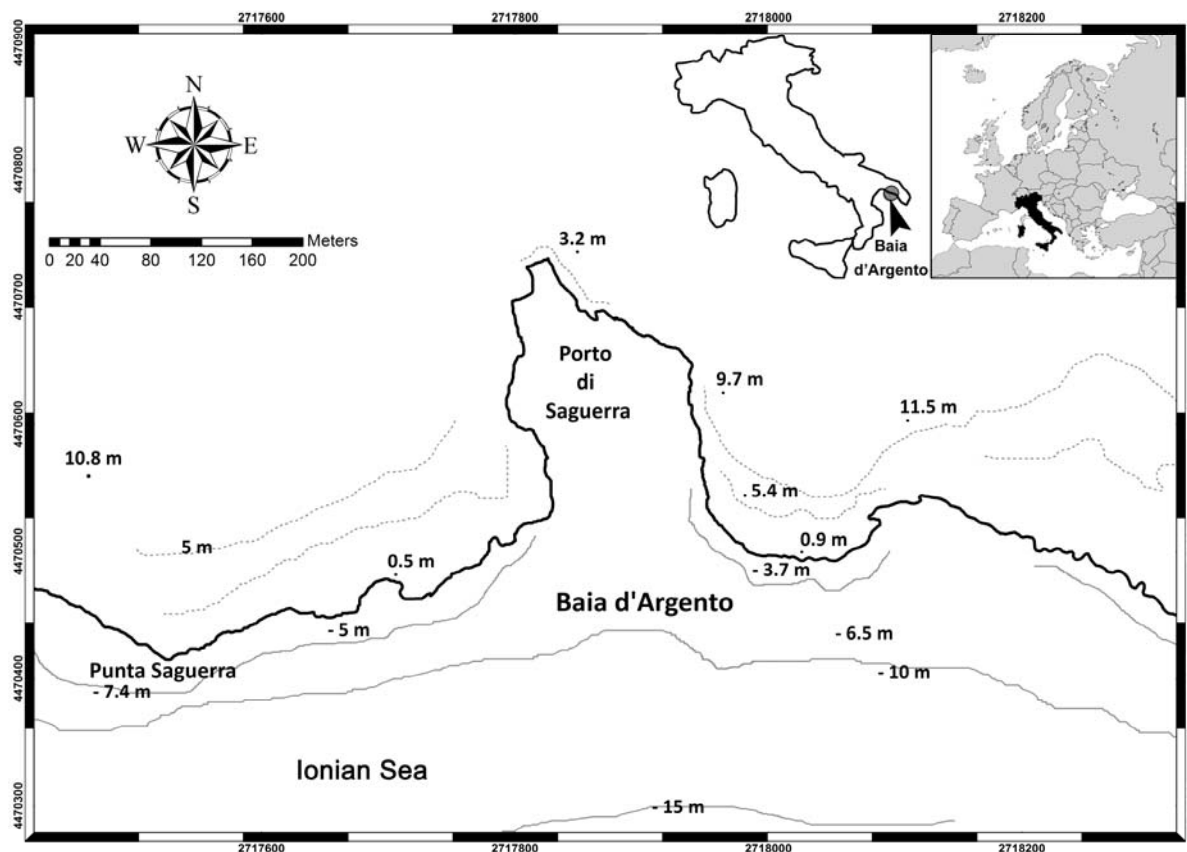


Figure 1. Geographical localisation of the investigated area.

of breaking waves; and/or 3 - become a turbulent water-hammer usually named bore.

The overland propagation of the tsunami surge is influenced by local topography and roughness degree. This latter induce a non-uniform spatial distribution of the sea water flow inland due to coastal morphology, the type of the land use, the density of vegetation, the type and the density of the buildings.

Water level during tsunami inundation is directly connected to the interaction between soil surface micro-topography and the energy of the flow.

In order to obtain inundation limit Hills and Mader (1997) introduced an empirical formula:

$$X_{\max} = (H_{FL}) 1.33 n^{-2} k$$

where: H_{FL} is wave height at the shoreline; n is Manning's coefficient, $k = 0.06$ for many tsunamis (see: Bryant, 2001). To obtain 'n', a semi-empirical equation was developed by Manning in order to simulate open channel water flow. Kay (1998) establishes that n is influenced by morphological features and channel vegetation texture; these characteristics cause difficulty to determine it with a sufficient accuracy degree. Furthermore, the value of n is not constant with time in the same channel due to weed growth and variations of flow conditions over time (Asal, 2003). As consequence, it is possible to obtain an evaluation of the present overland roughness, but it is extremely difficult to infer the past Manning number related to the tsunami impact on the coastal area.

The Hills and Mader (1997) formula is tightly connected to roughness coefficient that is function of small scale features of the surface flooded. According several studies on open channel flows (Aberle et al., 1999; Smart et al., 2002; Smart, 2004) the roughness characteristics of the channel bottom are very well correlated with the standard deviation of the bottom surface, so it is possible to use *in situ* gathered data to calculate Manning's n for given flow conditions.

Smart (2004) provides an equation linking directly Manning's n to the flow conditions and to the bottom surface characteristics:

$$n = \frac{\kappa \sqrt[6]{R}}{\sqrt{g}} \frac{1 - \frac{Z_0}{R}}{\left(\frac{Z_0}{R} - \ln \left(\frac{Z_0}{R} \right) - 1 \right)}$$

where: κ is the Von Karman constant; R is the flow depth and Z_0 is the standard deviation of the bottom surface. It is important to note that with this approach the n value is not absolute but, with a

given bottom surface, it diminishes with the growing of the flow depth.

According to the author, this equation is used for a flow with no lateral limits; the case of a tsunami flooding. Our purpose was to test a method to evaluate a possible future tsunami inundation by the Hills and Mader formula using a Manning's n calculated with the Smart equation on the base of terrestrial laser scanner captured micro-topography data. Tsunami hydrodynamic features are those derived by the study of their deposits.

The selected area for this test is the rocky promontory of Baia d'Argento, located no far from the city of Taranto along the Ionian coast of the Apulia region (Southern Italy) (Fig. 1).

The coastal sector at south of Taranto is characterised by a number of stair-case arranged marine terraces. The entire coastal sector is marked by deep inlet corresponding to fluvial erosive incision produced during the last glacial time with a sea level about 140/150 m lower than present (Mastronuzzi and Sansò, 1998).

Baia d'Argento rocky headland is a low lying coastal area with maximum elevations of 11 m above present sea level (a.s.l.) and has a slightly undulating surface with a mean sloping of about 6-7%. Starting from coastline it is possible to divide them in three different zone: 1 – a terrace surface about 120 m wide; 2 – a ridge of calcareous boulder leaning on a step placed between 2 and 5 meters (a.s.l.) represent a morphological indicator of tsunami impact; 3 – a steeper terrace that reach the top approx 11 m (a.s.l.) (Fig. 2a).

The lowermost terrace is bare of vegetation, is quite flat and bordered seaward by a trottoir approx 3 m wide that marks the biological sea level (*sensu* Lalorel and Laborel Deguen, 1994) and a surf bench marked by spitzkarren and rockpools. Adlitoral zone is characterised by an elevate roughness and a convex profile. Here, surface micro-topography shows small karstic landforms, shaped on the sub-aerially exposed calcareous sandstones are represented mainly by potholes, which became increasingly deeper and wider toward the coastline. In the spray zone potholes are coalescent, giving place to pinnacle-like forms (*Spitzkarren*) separated by wide, flat depressions. Calcareous bedrock presents very long fractures that become wider toward to the coastline.

Baia d'Argento headland is characterised by the presence of sub-vertical longitudinal and transverse fractures resulting from cliff evolution influenced by rock properties and the effects of sea storms on the basal clays. Several of these fractures are parallel to shoreline; some of these are also oriented to SE in relation with more frequent sea storm direction. In this work the field survey has been performed with a HDS3000 by Leica Geosystems.

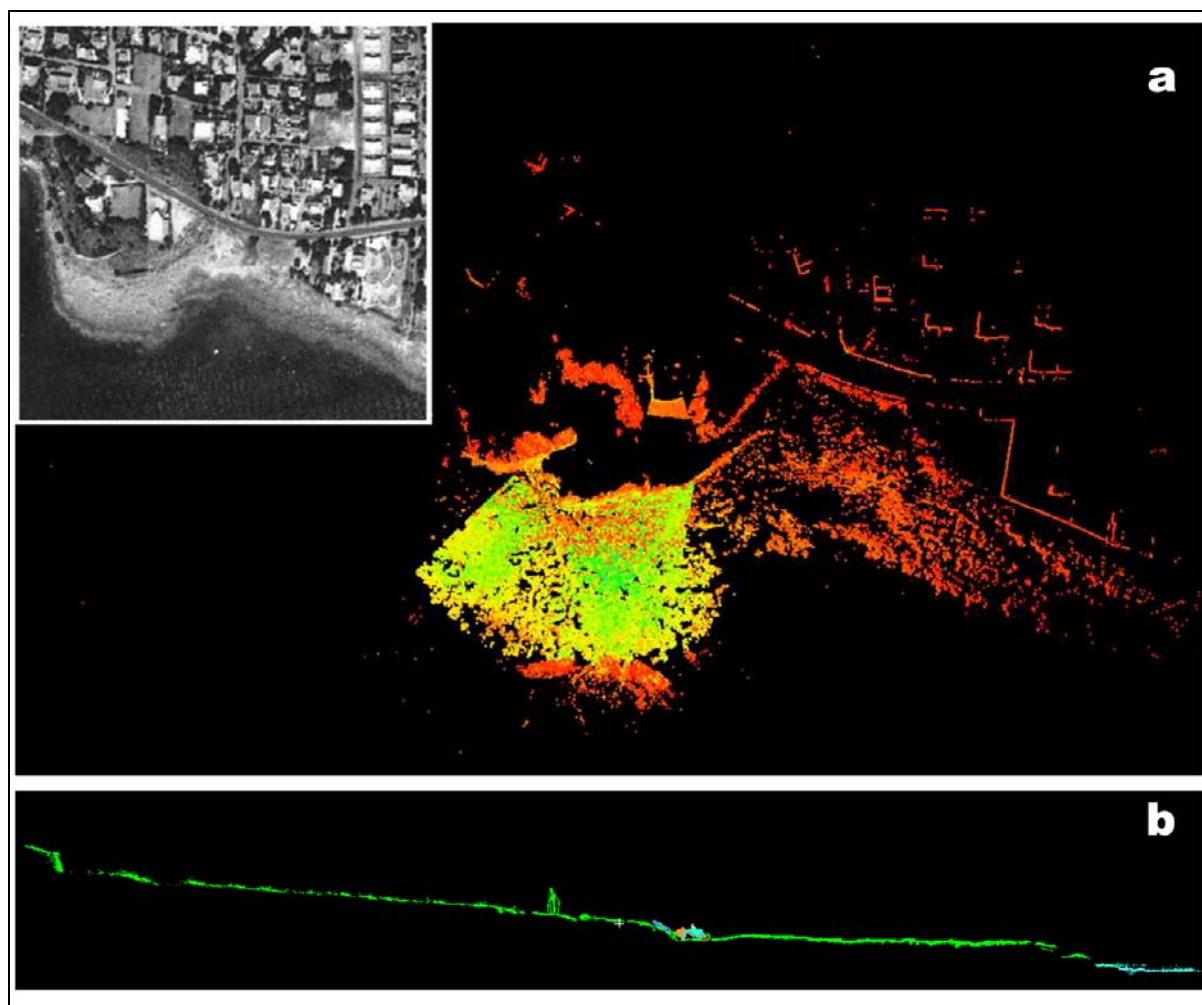


Figure 2. a) Points cloud representing Baia d'Argento headland surface; b) Morphological profile of Baia d'Argento headland obtained by Laser Scanner survey.

The scanner consists of a laser beam generator, a horizontal axis rotating mirror forming a 45° degree with the beam direction and a servomotor making the whole instrument to rotate around the vertical axis; this setting gives the scanner a field of view of $360^\circ \times 270^\circ$. The position of a single point is taken by measuring the angle of incidence and the time of fly of the beam; these two values are used to calculate the cartesian coordinates referred to the centre of the scanner. The instrument can capture 4000 points per second over a maximum range between 200 and 300 m according the reflectivity of the scanned object.

During the field survey seven scans have been performed, three of which covering the whole study area while the remaining four were taken on a restricted part of the surf bench at the toe of the boulder ridge. Five markers were positioned in the survey area in order to overlap all the scans; the exact positions of the three markers were surveyed by GPS in differential static mode to georeference the point cloud.

The laser data were managed with Cyclone 5.3 software; in order to overlap the scans (registering) by the marker points and to georeference the point cloud by importing the right geographic coordinates. Then within the high point density area at the toe of the boulder ridge a square of 100 m^2 was chosen (this dimension being representative, according us, of the roughness characteristics of the surf bench): the whole amount of points in this subset is about 900.000 (about 1 pt/cm^2). These points have been converted to DXF format to be imported in ArcGIS environment where a conversion to "shapefile" (.SHP) was performed.

In order to determine roughness of this terrace we used a Leica HDS3000 terrestrial Laser Scanner to capture a point cloud of studied area and an Ashtech Z-Xtreme Differential GPS to obtain geographical coordinate to georeferencing the point cloud.

Therefore, there is a considerable local roughness variation, hence the studied areas have been subdivided in buffers with constant length and

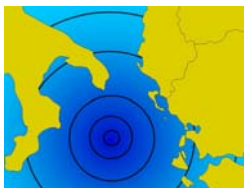
inland depth; this is an approximation useful to simulate open channel flow.

A DEM of the square area was built using the Kriging interpolator (cell size: 1 cm).

Since the data needed to be cleaned by the general slope of the area, the average surface was calculated using the trend tool (same cell size) in order to perform the detrending of the DEM; the latter was accomplished using the raster calculator tool subtracting the cell values of the average surface from the real surface ones. The standard deviation of the resulting raster has been used in equation .

References

- Aberle J., Dittrich A., Nestmann F. (1999). *Description of steep stream roughness with the standard deviations S*. Proc., XXVIII IAHR Biennial Congress, Graz, Austria, on CDROM.
- Asal F. F. F. (2003). *Airborne remote sensing for landscape modelling*. PhD thesis, The University of Nottingham, UK, 317 pp.
- Bryant E. A. (2001). *Tsunami: The Underestimated Hazard*. Cambridge University Press, 320 pp., Cambridge.
- Doglioni C., Mongelli F., Pieri P., (1994). *The Puglia uplift (SE Italy): an anomaly in the foreland of the Apennine subduction due to buckling of a thick continental lithosphere*. Tectonics, 3, 1309-1321.
- Hills J. G., Mader C. L., (1997). *Tsunami produced by the impacts of the small asteroids*. Annals of the New York Accademy of Sciences, 822, 381-394.
- Kay M., (1998). *Practical Hydraulics*. TJ International Ltd, Padstow, UK, Cornwall.
- Laborel J., Laborel-Deguen F. (1994). *Biological indicators of relative sea-level variations and of co-seismic displacements in the Mediterranean region*. Journal of Coastal Research, 10, 395-415.
- Mastronuzzi G., Sansò P. (1998). *Morfologia e genesi delle isole Cheradi e del Mar Grande (Taranto, Puglia, Italia)*. Geografia Fisica Dinamica Quaternaria, 21, 131-138.
- Smart G. M. (2004). *An Improved Flow Resistance Formula*. In: Greco M., Carravetta A., Della Morte R. (Eds) *River Flow 2004*. Proceedings of the second International Conference on Fluvial Hydraulics, 23-25 June, Napoli, Italy, Taylor & Francis, Vol.1, 1455 pp.
- Smart G. M., Duncan M. J., Walsh J. (2002). *Relatively rough flow resistance equations*. Journal of Hydraulic Engineering, ASCE, 128(6), 568-578.



2nd International Tsunami Field Symposium

IGCP Project 495

Quaternary Land-Ocean Interactions:
Driving Mechanisms and Coastal Responses

Ostuni (Italy) and Ionian Islands (Greece) 22-28 September 2008



Project 495

Pignatelli C.¹, Scheffers A.², Scheffers S.³, Mastronuzzi G.¹

Evaluation of tsunami flooding from geomorphological evidence in Bonaire (Netherland Antilles)

¹Dipartimento di Geologia e Geofisica, Università degli Studi di Bari, Italy,

e-mail: c.pignatelli@geo.uniba.it; g.mastrozzi@geo.uniba.it;

²School of Environmental Science and Management, Southern Cross University, Australia,

e-mail: anja.scheffers@scu.edu.au;

³Centre for Environmental Management, Central Queensland University, Australia,

e-mail: s.scheffers@cqu.edu.au

Keywords: *Tsunami, inland penetration, roughness, hydrodynamic equations, Bonaire*

The most dramatic effect of tsunami impact along the coastal areas is its capability to produce widespread inundations. Different coastal area in the world are very close to tsunamogenetic area, so catastrophic waves can reach coastal communities in a short span of time eluding the warnings system. To know the possible limit of tsunami inundation is

important in the alert planning, in the evacuation areas identifying and first aid management. Tsunami flooding, usually, occurs in low-lying region and implies erosion, transport and mixtures of debris/sediment deposit inland; in particular, deposits accumulated by palaeo-tsunami, can be used to recognise past events.

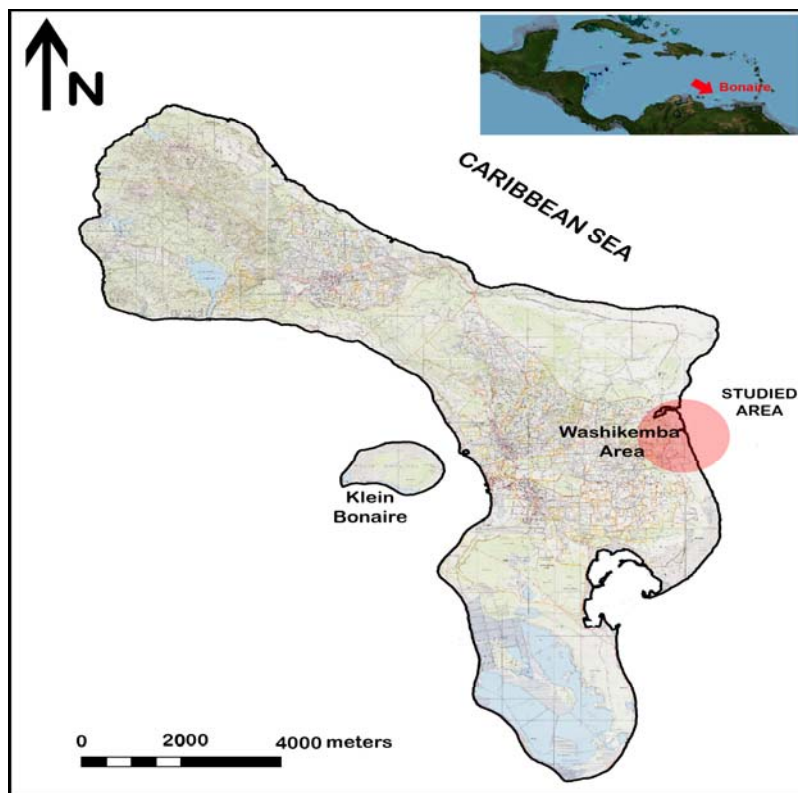


Figure 1. The studied area along the eastern coast of Bonaire (Netherland Antilles).

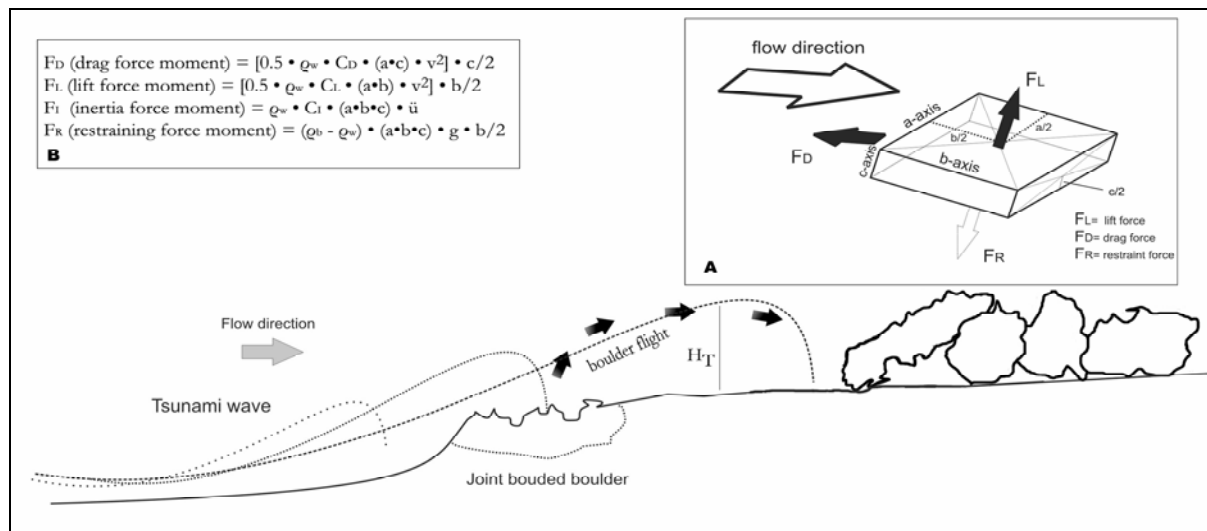


Figure 2. Hydrodynamic of tsunami wave approaching rocky coast: A) Moment forces schemes acting on a rocky boulders; B) Mathematical equations that represent moment forces, where ρ_w = density of the water 1.02 g/cm³, ρ_b = density of the boulder (2.5 g/cm³ for Washikemba), C_D = coefficient of drag = 2 (Helley, 1969), C_L = coefficient of lift = 0.178 (Einstein & El Samni, 1949), C_I = coefficient of inertia = 2 from experimental data by Noji et al. (1985), g = gravitational constant, u = instantaneous flow acceleration, v = flow velocity, the velocity of a tsunami in deep water is $v = \sqrt{gh}$.

Recent studies highlight as tsunami waves are able to detach megaclasts weighting up to hundreds tons from intertidal/adlittoral zone and to transport them onshore at different distances and altitudes above sea level (i.e.: Hearty, 1997; Bryant & Nott, 2001; Scheffers, 2002; Noormets et al., 2004; Williams & Hall, 2004; Kelletat & Scheffers, 2005; Robinson et al., 2006; Hall et al., 2006). When boulders are present along the rocky coasts it is possible to evaluate the intensity of past catastrophic waves; in fact, hydrodynamic equations realized by Nott (1997; 2003) permit to calculate minimum wave height necessary to entrain and transport boulders landward.

This study suggests a methodology to evaluate tsunami inundation limit using both mathematical and morphological approach. In order to test this model has been individuated the coastal site of Boka Washikemba on the eastern side of Bonaire island (Netherland Antilles) (Fig. 1). Here, a detailed analysis of boulders features has been performed.

Boka Washikemba is shaped on a Pleistocene reef; starting from coastline it is possible to recognize three different zones:

- the first one is constituted by a cliff exposed to a trade wind; the intertidal zone close to the cliff shows a well-developed bench with constructive ledges (Scheffers, 2005);
- the second one is characterized by very developed karren and rock pools;
- the last one is a wide surface terrace elevated up to about 4 meters above mean sea level and extended for about 500 meters landward; on this

surface there is a boulder field weighting up to 180 tons.

The boulder dimensions, density of boulder rock, axis alignment, the initial position of the boulders were estimated during surveys.

These features permit to define the pre-transport settings extremely important to choose the opportune hydrodynamic equation useful to calculate tsunami heights (Noormets et al., 2004; Nott, 2003).

The boulders field in Boka Washikemba shows a decreasing sorting starting from coastline and moving inland. Isolated mega-boulders are emplaced at about 50 m from present coastline.

Often, the boulders with same size are aligned and elongated about parallel to shoreline; the smallest boulders, placed about 400 m inland, seem to indicate the inner limit of the inundation. Some megaclasts show well preserved bioerosive rock pools from the supratidal belt and in certain cases are characterised by pieces of notch that indicate an intertidal provenience.

The Washikemba deposit shows the imprints of the impact of numerous sea storms, hurricanes and tsunami; so, it has been necessary focused the surveys on features indicative of tsunami impact.

Morphological and sea climatic studies, permitted to use boulder sizes to suppose the limit between storm and tsunami impact (Scheffers, 2002; Mastronuzzi et al., 2006); therefore, the estimation of the tsunami wave has been performed only on biggest boulders.

When tsunami wave hit a rocky platform edge two phases can occur: *i* – the detachment of boulders; *ii* – the emplacement of boulders. The first phase can occur through two modalities: *i* – a

violent impact that destroy the boulder in numerous pieces; $\dot{\mathbf{u}}$ - the boulder is detached and it surfs until it fell down quite vertically; often, this kind of transport can broken it in little pieces placed very near between them. On the base of this consideration surveys are focused on this type of broken boulders.

When a tsunami strikes a boulder, a set of moment forces acts on a boulder; these moment forces are: $\dot{\mathbf{i}}$ - drag force; $\dot{\mathbf{u}}$ - lift force; $\dot{\mathbf{u}}$ - inertia and restraint force (Fig. 2).

Once surveyed boulders dimension (a = the major axis, b = medium axis, c = minor axis) and rock density, it has been necessary establish the initial position of each surveyed boulders. In the case of Washikemba coasts, boulders derive from the submerged or just emerged part of the cliff; generally they expose directly a face to the wave impact. The difference between our model and that of Nott (2003) is represented by the number of sides along which boulders are jointed (4 in the Nott hypothesis and 3 in the Caribberan cases) and, consequently, drag works. In the Nott's scenario, the only face exposed to the wave impact is the upper one and that is the only area; consequently it is the only face on which the wave forces can act on.

In the cases studied to move a boulder quite disjoined from the rocky surface and placed approx in the inter-tidal zone is necessary that:

$$H_T \geq [0.5 \cdot c \cdot (\rho_b - \rho_w / \rho_w)] / C_L \quad (1)$$

We applied this formula to biggest boulders (see Table 1) recognised in Washikemba area and we calculated a tsunami height $H_T \geq 11$ m

Measure of the maximum flooding

Some assumptions have been adopted in the following elaborations: $\dot{\mathbf{i}}$ - to calculate the inland penetration of the tsunami wave it has been utilised the Hills and Mader (1997) formula:

$$X_{\max} = (H_T)^{1.33} n^{-2} k \quad (2)$$

where: H_{FL} is wave height at the shoreline; n is Manning number, $k = 0.06$ for many tsunami (see: Bryant, 2001); $\dot{\mathbf{u}}$ - to determine inundation limit it has been utilised the value of the tsunami heights H obtained y the analyses of the transported boulders; $\dot{\mathbf{u}}$ - to obtain 'n', a semi-empirical equation was developed by Manning in order to simulate open channel water flow. The value of n is not constant with time in the same channel due to weed growth and variations of flow conditions over time (Asal, 2003). As consequence, it is possible to obtain an evaluation of the present overland roughness, but it is extremely difficult to obtain past Manning number when the tsunami hit the coastal area.

The Hills and Mader (1997) formula is strictly dependent to roughness coefficient that is function of small scale features of the surface flooded. Using Manning's equation and considering morphology and material of which the channel is constituted, some roughness coefficients have been calculated empirically (Chow, 1988). These values have been integrated with some observation obtained during post-event survey performed in numerous locality hit by December 26, 2004 tsunami. These surveys put in evidence that some types of vegetation have been responsible to the deceleration of flow velocity of tsunami wave (Tanaka et al., 2007).

Karsification and fracturation degree of sloping rocky coasts condition Manning number around the value of 0,052 (www.fhwa.dot.gov). Therefore, there is a considerable local roughness variation, hence the studied areas have been subdivided in buffers with constant length and inland depth; this is an approximation useful to simulate open channel flow.

The Hills and Mader formula (1997) gives good estimation for coastal area characterised by overland flat profile.

Therefore, it is important to know the sea water quantity that effectively cause the inundation, this value is represented by water column that reaches the top of the cliff. The wave heights obtained are referred to the boulder transported inland; if a boulder is detached from cliff edge (joint bounded scenario) the height of the water column flooding, can be obtained from this relationship:

$$H_{FL} = H_T - \text{Altitude of the cliff} \quad (3)$$

In fact, at the edge of the cliff – where the boulders initially were placed - the tsunami wave height had to be the minimum able to transport the biggest block. The rampart roughness causes the tsunami wave height decreasing landward and the wave height tend to zero inland. The tsunami wave must be not smaller then minimum wave able to move the biggest boulder.

Moreover, it is possible to deduce:

a) a boulder is dislodged from intertidal zone by a minimum tsunami wave of about H_T ;

b) the minimum lift force need to win the restraint force of this boulder is due to a wave of H_T ; therefore, when this boulder is dropped and broken the wave height must be lesser to H_T ;

c) since a tsunami could be considered a fast sea level rise (Möerner, 1998), the tsunami wave height could be constant for little tracts;

d) the biggest boulder was deposited (and broken in very near pieces) when tsunami wave reduced the energy inland and than the inundation limit must take into account this point.

So, when the boulder is emplaced, the tsunami wave continue to flood but the energy tend to

Block ID	a – axis (cm)	b – axis (cm)	c – axis (cm)	Weight (tons)	distance to coastline (m)	H _T
7.2	850	410	170	149,25	100	6,9
7.3	530	390	200	103,25	140	8,1
7.7	540	400	230	124,20	110	9,4
7.9	600	440	290	178,20	70	11,8
7.11	520	450	260	152,10	80	11

Table 1. Main features of some boulders of boka Washikemba: axis dimensions, weight, distance to coastline, tsunami height calculated using a density of rock $\rho_b = 2,5 \text{ g/cm}^3$, a density of water $\rho_w = 1,02 \text{ g/cm}^3$ and a lift coefficient $C_L = 0,178$.

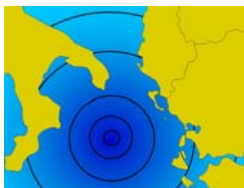
decrease; it is possible to calculate the inundation limit from this point - 70 m landward - where the biggest boulder has been emplaced using a wave height $H_{FL} = 11,8 - 4 = 7,8 \text{ m}$. Using (3) we obtain a limit of the tsunami inland penetration $X_{\max} = 410 \text{ m}$.

In Washikemba area, this obtained inundation limit is often testified by the limit of pseudo-soil stripping and by the accumulation of smallest boulder.

References

- Asal F. F. F. (2003). *Airborne remote sensing for landscape modelling*. PhD thesis, The University of Nottingham, UK, pp. 317.
- Bryant E.A., Nott J. (2001). *Geological indicators of large tsunami in Australia*. Natural Hazards, 24 (3), 231–249.
- Chow V. T. (1959). *Open-Channel Hydraulics*. McGraw-Hill, Inc.
- Einstein H.A., El Samni E.A (1949). *Hydrodynamic forces on a rough wall*. Reviews of Modern Physics, 21-3, 395, 520-524.
- Hall A.M., Hansom J.D., Williams D.M., Jarvis P. (2006). *Distribution, geomorphology and lithofacies of cliff-top storm deposits: Examples from the high-energy coasts of Scotland and Ireland*. Marine Geology, 232, 131-155.
- Hearty J.P. (1997). *Boulder deposits from large waves during the last interglaciation on North Eleuthera Island, Bahamas*. Quaternary Research, 48, 326–338.
- Helley E.J. (1969). *Field measurement of the initiation of large bed particle motion in blue creek near Klamath, California*. U.S. Geological Survey Professional Paper 562-G, 19 pp.
- Hills J.G., Mader C.L. (1997). *Tsunami produced by the impacts of the small asteroids*. Annals of the New York Accademy of Sciences, 822, 381-394.
- Hoerner S.F. (1965). *Fluid-Dynamic Drag*. Published by the author, L.A. Hoerner, Midland Park, NJ, 200 pp.
- Mastronuzzi G., Pignatelli C., Sansò P. (2006). *Boulder Fields: A Valuable Morphological Indicator of Paleotsunami in the Mediterranean Sea*. Zeitschrift für Geomorphologie, NF Suppl.-Bd., 146, 173-194.
- Mörner N.A. (1994). *Recorded sea level variability in the holocene and expected future changes*. Bulletin of the INQUA Neotectonic Commission, 17, 48-53.
- Noji M., Imamura N., Shuto N. (1985). *Numerical simulation of movement of large rocks transported by tsunamis*. Proceedings of the IUGG/IOC International Tsunami Symposium, Wakayama, Japan, pp. 189–197.
- Noormets R., Crook K.A.W., Felton E.A. (2004). *Sedimentology of rocky shorelines: 3. Hydrodynamics of megaclast emplacement and transport on a shore platform, Oahu, Hawaii*. Sedimentary Geology, 172, 41-65.
- Nott J. (1997). *Extremely high wave deposits inside the Great Barrier Reef, Australia; determining the cause tsunami or tropical cyclone*. Marine Geology, 141, 193-207.
- Nott J. (2003). *Waves, coastal boulders and the importance of the pre-transport setting*. Earth and Planetary Science Letters, 210, 269-276.
- Scheffers A. (2002). *Paleotsunami Evidences of tsunami from Boulder deposits on Aruba, Curaçao, and Bonaire*. Science of Tsunami Hazards, 20, 1, 26-37.
- Kelletat D. Scheffers A. (2005). *Tsunami Relics On The Coastal Landscape West Of Lisbon, Portugal*, Science of Tsunami Hazards, 23, 1, 3-16.
- Robinson E., Rowe D.-A.C., Khan S. (2006). *Wave-Emplaced Boulders on Jamaica's Rocky Shores*. In: Scheffers A., Kelletat D. (eds.) (2006). *Tsunamis, Hurricane and Neotectonics as Driving Mechanisms in Coastal Evolution*. Proceedings of the Bonaire Field Symposium, March 2-6, 2006. A contribution to IGCP 495, Zeitschrift für Geomorphologie, NF, Suppl. Volume 146, 39-57.
- Tanaka N. Y., Sasaki M.I.M., Mowjood K.B. Jindasa S.N., Samang Homuchuen (2007). *Coastal vegetation structures and their functions in tsunami protection: experience of the recent Indian Ocean tsunami*. Landscape and Ecological Engineering, 3, 1, 33-45.
- Williams D. M., Hall A. M. (2004). *Cliff-top megaclast deposits of Ireland, a record of extreme waves in the North Atlantic—storms or tsunamis?*. Marine Geology, 206, 101-117.

Website: www.fhwa.dot.gov



Piscitelli A.², Pignatelli C.¹, Mastronuzzi G.¹

Hydrodynamical equations to evaluate extreme meteorological events impact along Adriatic coast of Apulia (Southern Italy)

¹Dipartimento di Geologia e Geofisica, Università degli Studi "Aldo Moro", Bari, Italy

e-mail: c.pignatelli@geo.uniba.it; g.mastrozz@geo.uniba.it;

²Collaboratore esterno al Dip. di Geologia e Geofisica, Università degli Studi "Aldo Moro", Bari, Italy

e-mail: ark.piscitelli@hotmail.it

Keywords: *Sea storm, breakwater, hydrodynamical equations, Torre a Mare, Adriatic Sea*

Many rocky coasts show large lithic boulders - isolated, sparse, arranged in field or in berm - on rocky platforms, and sometimes on top of cliffs tens meters high (i.e.: Williams & Hall, 2004; Hall et al.; 2006; Nott, 2006; Mastronuzzi et al., 2006). Extreme waves like sea storms and/or tsunami can transport and deposit boulders. One of the most important differences between storm and tsunami waves is their respective abilities to transport boulders at the shore. In order to establish a methodology that permit to differentiate storm and tsunami impact, hydrodynamic equations have been

produced (Nott 1997; 2003; Noormets et al., 2004). Nott (1997; 2003) implemented some hydrodynamical equations that permit to calculate minimum wave height able to initiate the transport of boulders; the hydrodynamical equations take into account the size of the boulders, boulders shape, boulders density, axis alignment, the initial position of the boulders. Pignatelli et al. (in prep) are testing these hydrodynamical equations with new boundary hypothesis.

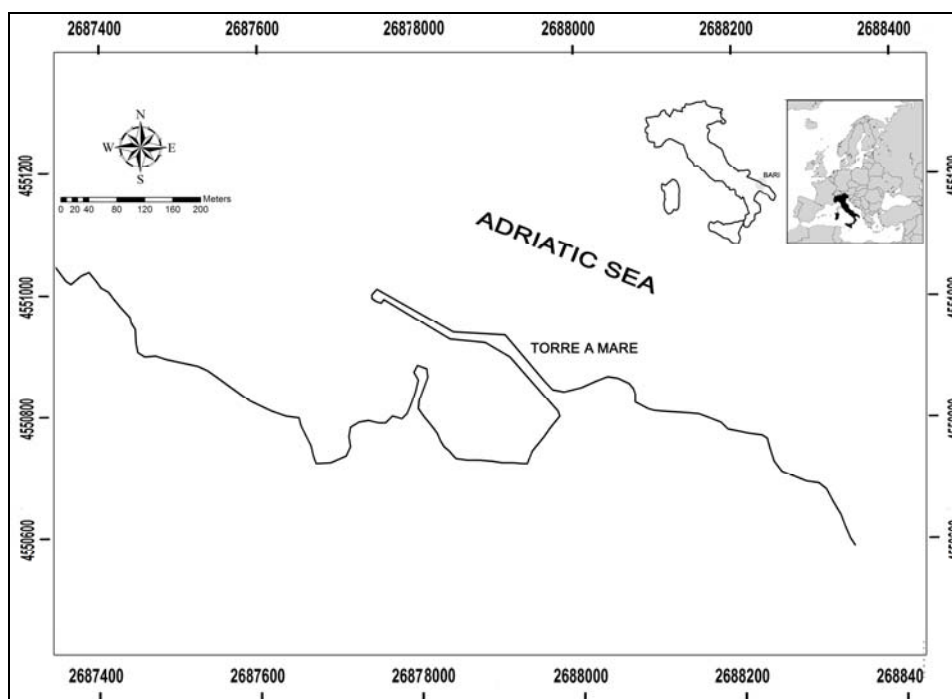


Figure 1. Topographic map of studied area.

Aim of this work is evaluate the accuracy of these hydrodynamical equations starting from a real case occurred some years ago. In particular, we verify the hydrodynamical equations on a shore protection structures in order to define coastal sectors subjected to sea storms and/or tsunami risk.

The studied area is placed on Adriatic coast of Apulia (Southern Italy) between Bari and Brindisi town. (Fig. 1). On the 23-24 December 2003 and 15 January 2004, two exceptional sea storms occurred in the southern Adriatic Sea. These events damaged considerably the harbour of Torre a Mare (Bari). The harbour is mainly constitute by a breakwater elongated for 107 m in 304° N direction; this one is formed by 24 concrete blocks (3,7x1,6x1,5m) and by 5 blocks in cement (5,1x1,6x1,5 m), having

rectangular parallelepiped shape. Considering that technical reports concerning harbour buildings suggest a medium volume weight of about $2,4 \div 2,7 \text{ g/cm}^3$, the first one are 22 tons in weight and the second ones reach about 33 tons. Blocks are connected by means of mortise and tenon joints that permit to align the entire structure.

The impacting sea storms produced the shifting and fracturing of a Torre a Mare breakwater; during this events only the concrete blocks have been moved by waves and a shifting of about 1 meters towards inland has been recorded (See Fig. 2). So, the breakwater has been damaged only in the central section; only 12 blocks have been moved from the initial position.

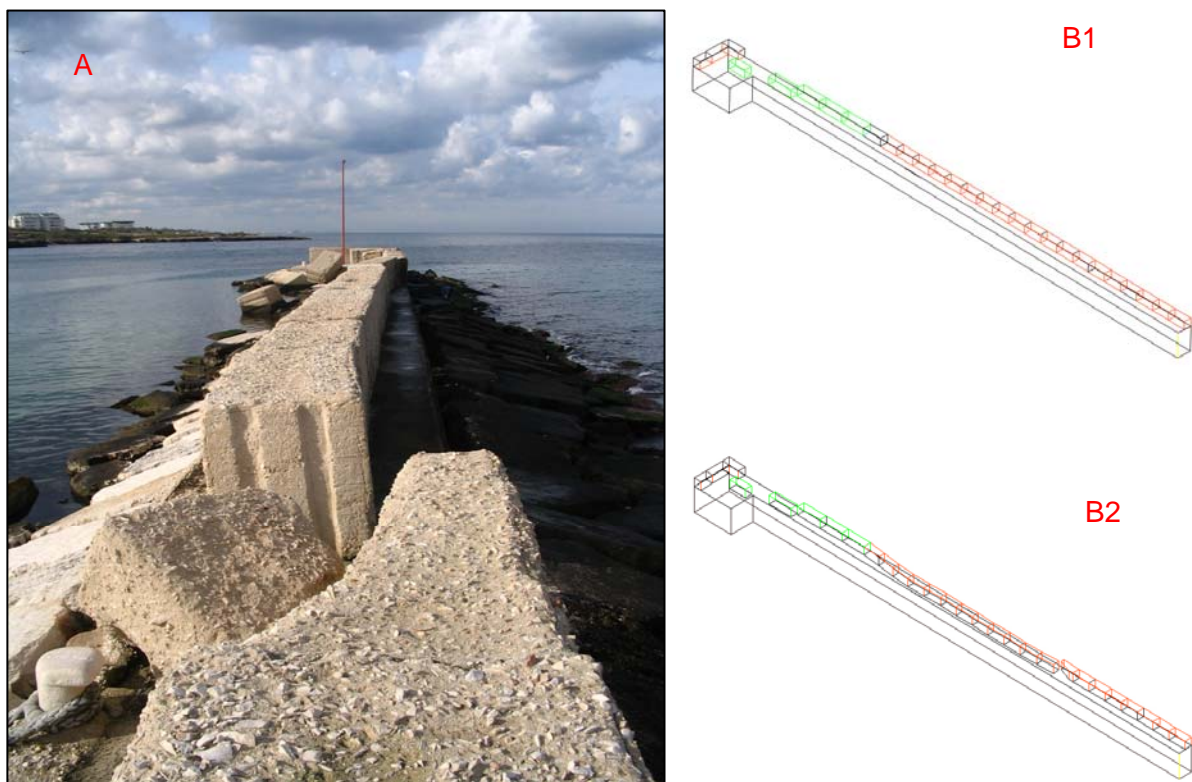


Figure 2. Breakwater along the harbour of Torre a Mare. **A.** Block shifted; **B.** Schemes of the breakwater first (**B1**) and after (**B2**) wave impact.

In order to evaluate these phenomena, mareographic data (essentially sea and wind climate) related to those days have been analyzed. An evaluation from RON - Rete Ondametrica Nazionale records of Monopoli buoy covering the days 23/12/2003, 24/12/2003 and 15/01/2004 of offshore waves has been carried out.

The Monopoli buoy recorded in 23-24 December 2003, about 26 events showing offshore wave heights more than 3 m, with a extreme value of about 4,75 m. On 15 January 2004 the pitch roll recorded 7 events of offshore wave height more than 3 m height and a pick value of about 4,58 m.

For these days wind direction and intensity have been obtained from data recorded in the wind station of RMN - Rete Mareografica Nazionale of Bari.

During these days the main wind directions were: 30° - 45° N (23-24 December 2003) and 105° - 110° N (15 January 2004). Winds intensity were: maximum intensity 20 knots (23-24 December 2003 and 15 January 2004).

In order to calculate the height of wave necessary for the block shifting, Pignatelli et al. (in prep) hydrodynamic equations have been applied, the equation used is:

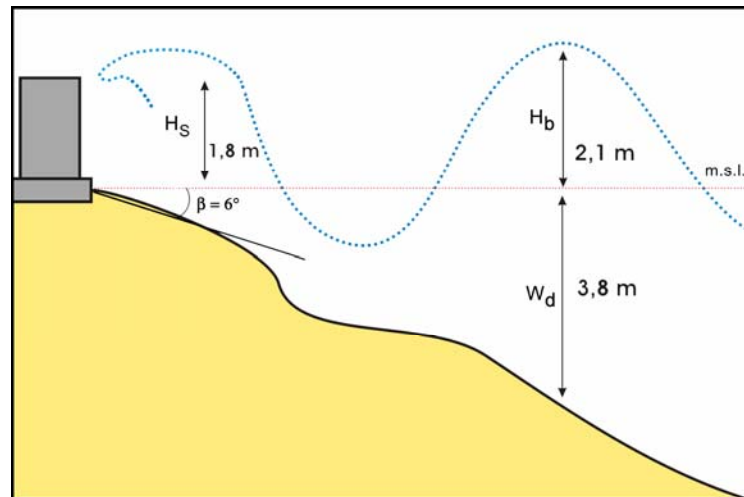


Figure 3. Wind generation wave approaching Torre a Mare harbour.

$$H_s = [b \cdot (\rho_b - \rho_w / \rho_w) - 2 \cdot (C_1 \cdot \ddot{u}) / g] / 0.5 \cdot [(b / c) \cdot C_L + (c / b) \cdot C_D] \quad (1)$$

Where:

- H_s = is height of the storm at the breakwater point;
- a, b, c = are respectively maximum-, medium- and small-axis of each block;
- ρ_b = density of blocks assumed 2.5 g/cm^3 ;
- ρ_w = density of sea water assumed 1.02 g/cm^3 ;
- C_1 = coefficient of inertia = 2 from experimental data by Noji et al. (1985);
- C_D = coefficient of drag = 2 (Helley, 1969);
- C_L = coefficient of lift = 0.178 (Einstein & El Samni, 1949);
- g = gravitational constant;
- \ddot{u} = instantaneous flow acceleration;

To estimate the minimum wave height able to initiate the movement of blocks of the breakwater, we assumed all the shifted blocks, 12 elements, as a unique block. The size of this new block are: $a = 44.40 \text{ m}$, $b = 1.60$ for the height, $c = 1.50 \text{ m}$.

Applying (1) equation, we obtain a wave height $H_s = 1.86 \text{ m}$.

Waves approaching the coast find a decreasing water depth which is used in analytical models with different seafloor slopes; these last ones allow to introduce different empirical coefficients into deep or shallow water wave models. The result is an empirical theory that relies greatly on wave experiments. Apart from the sea surge related to the duration of offshore wind, and wave height of waves approaching the coast in micro-tidal areas, their refraction and reflection are conditioned by local seafloor bathymetry and shoreline configuration.

The calculated value has been compared to that estimated by mean the empirically based wave data

supplied by Monopoli buoy and according to the equation proposed by Sunamura (1992):

$$H_b/H_0 = (\tan \beta)^{0.2} (H_0/L_0)^{-0.2}$$

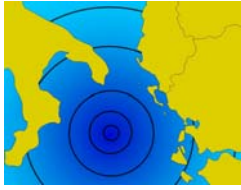
where H_b is the breaking wave height; H_0 is the wave height in deep water; β is the slope of sea bottom; L_0 the wave length in deep water. From Sunamura's equation we have estimated a wave height at the breaking point of $H_b = 2.1$. Using extreme waves recorded at Monopoli buoy and data on the coastal slope in front of studied areas it was possible to estimate the height of the breaking waves. Usually, waves break if the ratio between wave height (H_b) at breaking point and water depth (W_d), H_b/W_d , is approx 0.71–0.78 (Keulegan & Patterson, 1940). For a horizontal bottom, this ratio is smaller: 0.44–0.6 (Massel, 1997), while steeper bottom slopes show ratios between 0.78 and 1.03 (Galvin, 1972). From the comparison of wave heights calculated, data recorded from Monopoli buoy and wave trending nearshore (Tab. 1), it is possible to conclude that wave height calculated ($H_s = 1.87 \text{ m}$) can be considered reliable only with opportune boundary condition: **i** – impacting wave train responsible for the blocks movement perpendicular to breakwater; **ii** – quite regular bottom in front of the breakwater; **iii** – twelve element behaviour as a unique block. In conclusions the Pignatelli et al. equation derived by Nott 1997 and 2003 equations is validated using the Sunamura hydrodynamic theory.

H_0	L_0	β	H_b
4.76 m	1.08	6°	2.1 m

Table 1. The parameters of extreme waves occurred in 23-24 December 2003.

References

- Einstein H. A., El Samni E. A. (1949). *Hydrodynamic forces on a rough wall*. Reviews of Modern Physics, 21-3, 520-524.
- Galvin Jr., C. J. (1972). *Wave breaking in shallow water*. In: Meyer R. E. (Ed.), *Waves on Beaches and Resulting Sediment Transport*. Academic Press, New York, 413-456.
- Hall A. M., Hansom J. D., Williams D. M., Jarvis P. (2006). *Distribution, geomorphology and lithofacies of cliff-top storm deposits: Examples from the high-energy coasts of Scotland and Ireland*. Marine Geology, 232, 131-155.
- Helley E. J. (1969). *Field measurement of the initiation of large bed particle motion in blue creek near Klamath, California*. U.S. Geological Survey Professional Paper 562-G, 19 pp.
- Keulegan G. H. and Patterson G. W. (1940). *Mathematical theory of irrotational translation waves*. Journal of research of the National bureau of standards, 24, 47-101.
- Mastronuzzi G., Pignatelli C., Sansò, P. (2006). *Boulder Fields: A Valuable Morphological Indicator of Paleotsunami in the Mediterranean Sea*. Zeitschrift für Geomorphologie, NF Suppl.-Bd. 146: 173-194.
- Noji M., Imamura N., Shuto N. (1985). *Numerical simulation of movement of large rocks transported by tsunamis*. Proceedings of the IUGG/IOC International Tsunami Symposium, Wakayama, Japan, 189-197 pp.
- Noormets R., Crook K. A. W., Felton E. A. (2004). *Sedimentology of rocky shorelines: 3. hydrodynamics of megaclast emplacement and transport on a shore platform, Oahu, Hawaii*. Sedimentary Geology, 172, 41-65.
- Nott J. (1997). *Extremely high wave deposits inside the Great Barrier Reef, Australia; determining the cause tsunami or tropical cyclone*. Marine Geology, 141, 193-207.
- Nott J. (2003). *Waves, coastal boulders and the importance of the pre-transport setting*. Earth and Planetary Science Letters, 210, 269-276.
- Nott J. (2006). *Extreme events: a physical reconstruction and risk assessment*. Cambridge University Press - New York, 297 pp.
- Massel S. R. (1997). *Prediction of the largest surface wave height in water of constant depth*. In: Saxena N. (Ed.), *Recent Adv. in Marine Science and Technology* 96. PACON International, Honolulu, USA, 141-151.
- Pignatelli C., Mastronuzzi G., Sansò P. (2008). *Evaluation of tsunami flooding along the coast of the southern Apulia (Italy) using geomorphologic evidences*. In prep.
- Sunamura T. (1992). *Geomorphology of Rocky Coasts*. John Wiley and Sons. 302 pp.
- Williams D. M., Hall A. M. (2004). *Cliff-top megaclast deposits of Ireland, a record of extreme waves in the North Atlantic—storms or tsunamis?* Marine Geology, 206, 101-117.



Prabakaran K.¹, Anbarasu K.¹

Modelling of Tsunami inundation for the coastal regions of Tamilnadu, India

¹Department of Geology, National College, Tiruchirapalli-620001, Tamilnadu, India

e-mail: prabageo@gmail.com; anbarasu_gk@yahoo.co.in

Keywords: *Modelling, tsunami, inundation, Tamilnadu, India*

A results of the study of inundation mapping of Tsunami that struck the East Coast of India on Dec 26, 2004 and the mathematical modelling of

Tsunami inundation for predicting the effects of Tsunami form the basis for the paper.

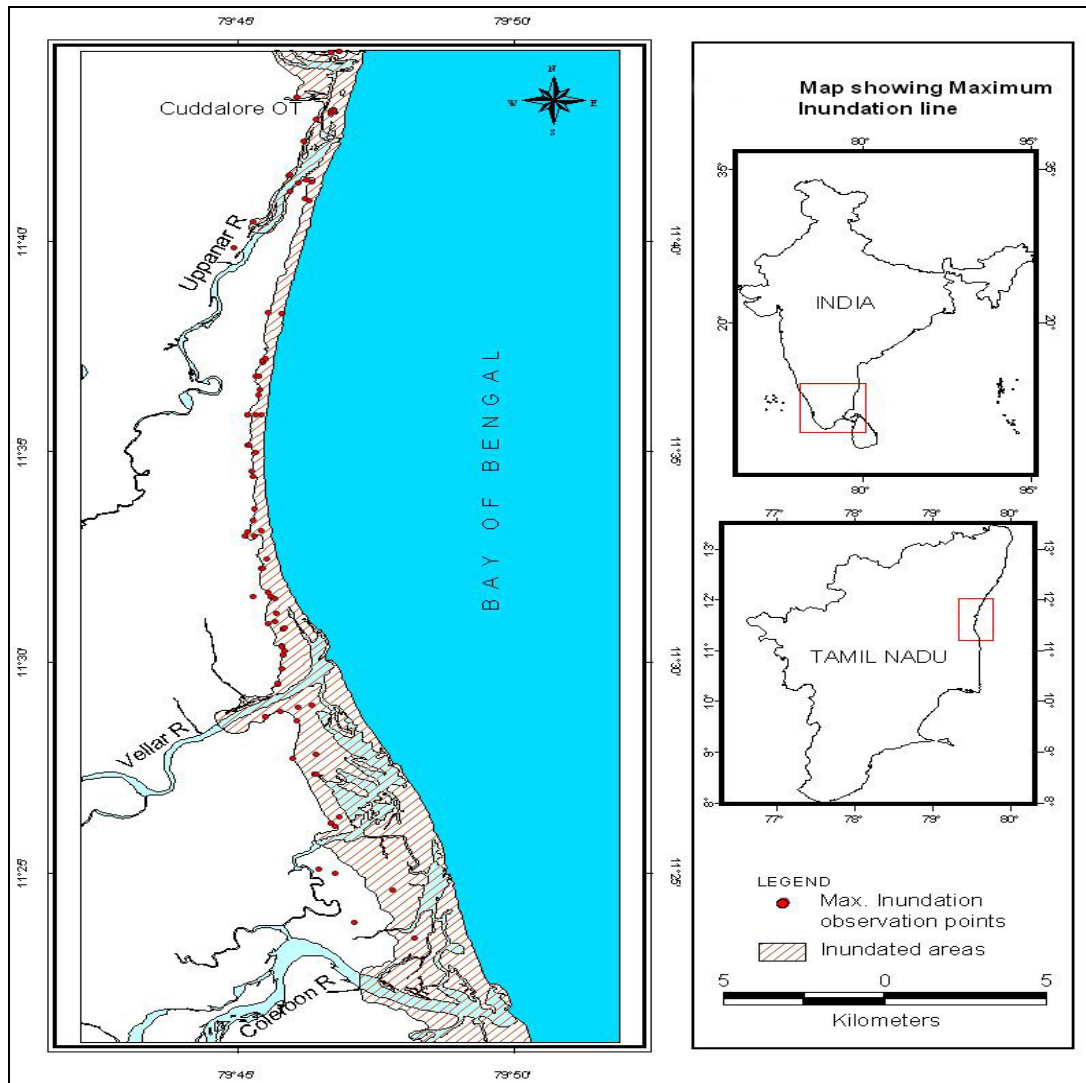


Figure 1. Map showing 26th December 2004 Tsunami Inundation.

Methodology of inundation mapping of 26th Dec 2004 Tsunami

The line of maximum inundation was marked with the help of water mark left by the tsunami waves (Fig 1). Run up elevation was also measured by taking across shore profiles up to the line of maximum inundation using Real Time Kinematic Global Positioning System (RTKGPS).

To understand the effect of Tsunami on landforms and vice versa pre and post tsunami coastal geomorphic maps were prepared using aerial photos and satellite images (IRS P6 LISS III) taken before and after 26th Dec 2004.

To identify the affected cadastral parcel, 44 cadastral maps were procured from the Department of Survey and Land Records, Govt. of Tamilnadu and overlaid with the map of maximum inundation and geo referencing of the maps was done by collecting lat- long positions of the selected points (for each map) in the ground using RTKGPS and survey of India Bench Mark stones.

To collect information about the effect of Tsunami on land use pattern, land use map was prepared and overlaid with the map of maximum inundation.

All these maps were digitized and overlays were made in GIS environment. Since profiling across the coast has been carried for every 200-300 m interval, contours of the area were also drawn and

run up elevation in the contour map was determined by overlaying maximum inundation map over this.

The composite maps showing the extent of inundation in relation to Geomorphology, Landuse, cadastral land parcels and elevation contours were prepared.

Methodology for modelling

Numerical modelling is an excellent tool for understanding past events and simulating future ones. Since the source parameters that triggered the December 2004 tsunami are well known numerical model are first set to capture the past event. Since accurate measurements on inundation and run-up are available for coastal Tamil Nadu, the model results are validated using field observations collected immediately after the tsunami.

Since the predictions of the models are directly related to the quality of the data used to create the bathymetry and topography of the model area, considerable time, resource and effort were made to collect high resolution bathymetry and elevation data of the coastal areas.

The model results were calibrated and validated using field observations. The model once validated can be used for creating different scenarios of extreme inundation and run-up by varying the source parameters that actually trigger the tsunami.

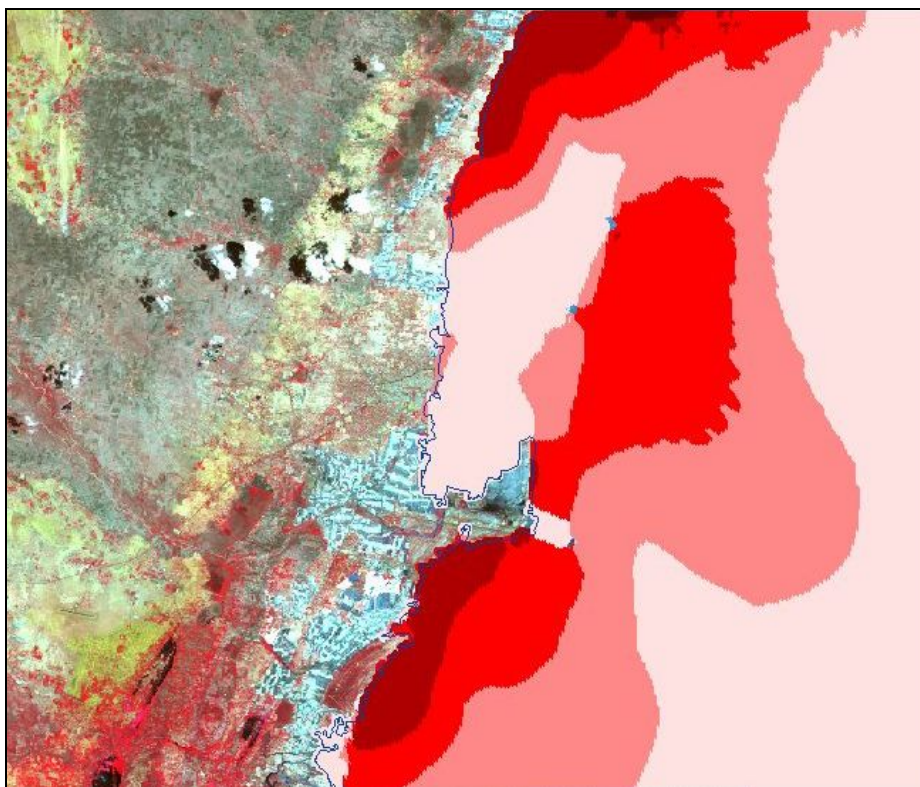


Figure 2. Predicted Inundation for Tuticorin.

Results of inundation mapping

The salient features of the inundation are given below.

The maximum inundation limit in the study area is observed around the mouth of the rivers Gadilam, Uppanar and Vellar and the minimum is observed around Rasapettai and Tammanampettai where the height of the beach ridge occurring along the shoreline ranges between 5-7 m.

In many places inundation has been blocked by beach ridges while the creeks and inlets occurring at the sides allowed the water to encircle the beach ridge.

Run up elevation measured from the watermarks on the walls of the buildings ranges from 3 to 4m from MSL. The composite map containing contour lines and extend of tsunami inundation indicates the coincidence of the line of maximum inundation with 2.5 to 3.5m contour.

The composite map containing land use pattern and extent of tsunami inundation indicates that the barren lands with low elevation have permitted free flow of tsunami while the areas covered by vegetation and sand dunes restrict the inundation process. The phenomenon is observed around Velingarayanpettai, Samiyapettai, Kumarapettai, Madayapallam and Reddiarpettai.

The composite map containing geomorphology and extend of inundation shows that beach ridges and sand dunes restrict the inundation process while swales, creek and other inlets permit free flow. Beach ridges occurring at the berm crest have been

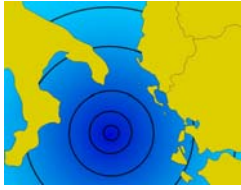
breached at many locations and through which inundation has taken place. In some places beach ridges are not breached or washed away but encircled by water due to the inundation of tsunami through creeks and pooled down in the adjoining swales landward side. The process can be typically noticed around Singarathope and Pudukupam. The people of Singarathope escaped from the fury of tsunami only because the village is located on such a beach ridge.

The school in the Pudukupam village also escaped as it occurs on a beach ridge.

The death toll due to tsunami is found to be maximum only where settlements are close to the shore and the beaches are not bounded by ridges, open without any plantation. The high casualties noticed in Samiyapettai (25 deaths) and Pudukupam (99 deaths) is due to the fact that house are in close proximity to the sea, the beaches are not bordered by beach ridges.

Results of modelling

On the basis of the model prediction, vulnerability maps are prepared in 1: 5000 scale for entire coastal areas of the country which will be useful in disaster management and mitigation activities. These maps help in defining the limits of construction of new essential facilities and special occupancy structures in tsunami flooding zones. A typical inundation map prepared based on 26th December 2004 for Tuticorin is shown Fig. 2.



Pranowo W.^{1,3,5}, Kongko W.^{1,2,4}

Modelling of the Bengkulu Minor Tsunami Event, September 12, 2007, West Of Sumatra, Indonesia

¹United Nations University – Institute for Environment & Human Security, Bonn, Germany

²Danish Hydraulic Institute, Syke, Germany

³Alfred Wegener Institute for Polar & Marine Research, Bremerhaven, Germany

⁴Tsunami Research Group – Agency for the Assessment & Applications Technology (BPPT), Indonesia

⁵Agencies for Marine & Fisheries Research (BRKP), Ministry of Marine Affairs & Fisheries of the
Republic of Indonesia, e-mail: pranowo@ehs.unu.edu

Keywords: *Minor tsunami, TSUNAMI-N1 model, Bengkulu*

Earthquake magnitude of Mw 7.9 – Mw 8.4 was shocking Province of Bengkulu in West Sumatra, Indonesia on September 12, 2007, as reported by BMG-Indonesia, USGS, and GFZ-Potsdam.

This paper is our research documentation which is our modelling results as our quick response to Bengkulu earthquake based on a preliminary estimation of earthquake magnitude (Mw. 8.4) and epicentre (101.00°E, 3.78°S) provided by USGS.

We employ TUNAMI-N1 model to our domain model which has grid resolutions 1,852 meters, for

two scenarios (Mw 8.4 and Mw 8.2) along 4 hours simulation with time step 1 second. Bathymetry data with 1 minute-arc resolution is derived from GEBCO.

We also used water level data derived from real time tide gauge data at stations Padang (IODE-VLIZ, 2007), Cocos Island (UHSLC, 2007), and DART Buoy No. 23401 (NOAA, 2007) for sea surface wave verification.

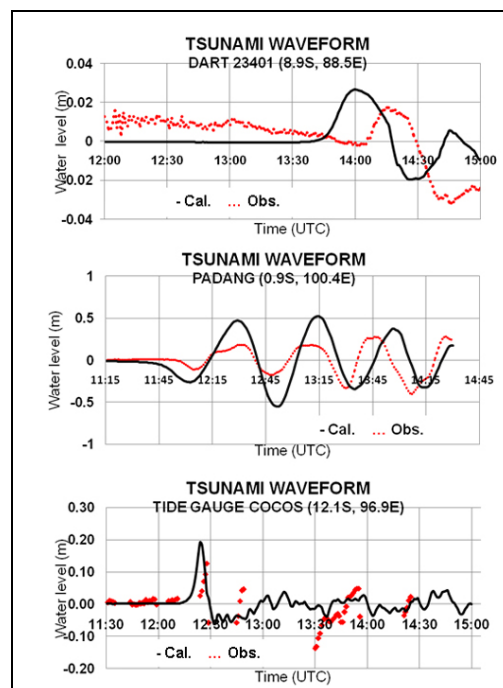


Figure 1. Tsunami modelling results from earthquake Mw 8.4 and its verifications

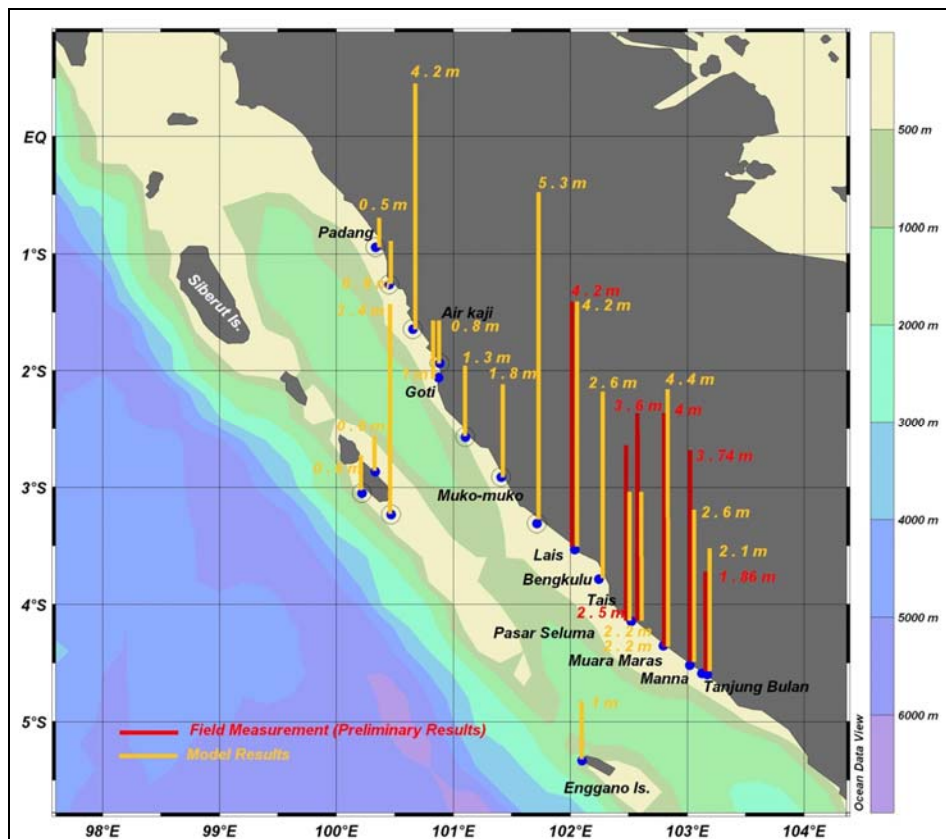


Figure 2. Tsunami maximum wave height modelling results from earthquake Mw 8.4 and its verifications. This verifications data is provided by Jose Borrero et al (2007).

Our modelling results show tsunami wave propagate from its source location then mainly hit Bengkulu and its surroundings, also minor part of Padang. Maximum wave height in Bengkulu and surroundings were varying between 0.5 meters and 5.3 meters.

In general, tsunami wave between modelling results and observations data has similar form, but there's slightly lag of arrival time and differences in wave-form. The best fit of our results is at Padang stations, and then nearly fit at Cocos Islands, which both of them is scenario 1 with earthquake Mw. 8.4. at DART buoy station, from both scenarios, tsunami wave from modelling results is earlier than observations data.

If we compare to the preliminary field survey results of Jose Borrero et al (2007), the maximum wave height in Lais is similar (4.2 meters), but slightly overestimates in Muara Maras and, while slightly underestimates in Tais and Pasar Seluma.

References

Imamura F., Yalciner A., Ozyurt G. (2006). *Tsunami Modelling Manual*. UNESCO IOC International Training Course on Tsunami Numerical Modelling.

Jose C. Borrero, Rahman Hidayat, Suranto. *Field Survey of the Tsunami Generated by the Mw 8.4 Earthquake of September 12, 2007*. Preliminary results survey in September 15 – 18, 2007 at Bengkulu Province, Sumatera.

http://www.usc.edu/dept/tsunamis/2005/tsunami/s/2007_sumatra/index.html

Source parameter data, September 12, 2007. USGS. http://neic.usgs.gov/neis/eq_depot/2007/eq_070912_hear/neic_hear_hrv.html

Tide gauge data at Cocos Island, September 12, 2007. UHSLC.

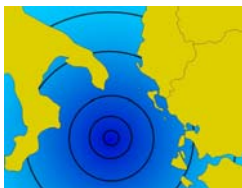
<ftp://ilikai.soest.hawaii.edu/real/>

Tide gauge data at DART Buoy No. 23401, September 12, 2007. NOAA.

http://www.ndbc.noaa.gov/station_page.php?station=23401

Tide gauge data at Padang Station, September 12, 2007. IODE-VLIZ.

<http://www.vliz.be/vmdcdata/iodc/bdata.php?code=pada&fromyear=2007&frommonth=9&fromday=12&fromhour=8&frommin=0&period=1&go=Generate+graph>



Rajamanickam G. V.¹

Distribution of sediments during pre and post-tsunami of 26th Dec. 2004 along the central Tamil Nadu, east coast of India

¹Dept. of Disaster Management, SASTRA University, Thanjavur, Tamil Nadu, India

e-mail: vrajamanickam@hotmail.com; vrajamanickam@carism.sastra.edu

Keywords: Grain size texture, binary plot, CM pattern, Visher's log-normal distribution, Heavy mineral assemblage, Ilmenite, East coast of India

Sediments sample collection was done on eight triangulated stations between Poombukar and Nagoore, Tamil Nadu, East Coast of India from Dec. 2003 to 16th Dec. 2004. After the surprise attack of Tsunami during December 2004 the study of sediments by means of continued sampling from 7th January 2005 has been done (Fig.1).

The intensity of tsunami and the impact of the same can be adjudged from the fact that at Poombukar upper sandy layer of about 3m thickness has been completely removed exposing the underlain layer of sticky clay and at

Kottucherimedu reflect the complete removal of dune of 7m height has been cleanly washed off in such a way, one could not recognized the place of dune after tsunami. From such drastic landform changes, one can easily surmise the influence of the tsunami on the coastal sediments. As there is no record about the occurrence of Tsunami in the historical past and no scientific study has been carried out to any of the past Tsunami, it is decided to utilize this golden opportunity of recording the nature of sediments and the variation during pre and post-Tsunami.

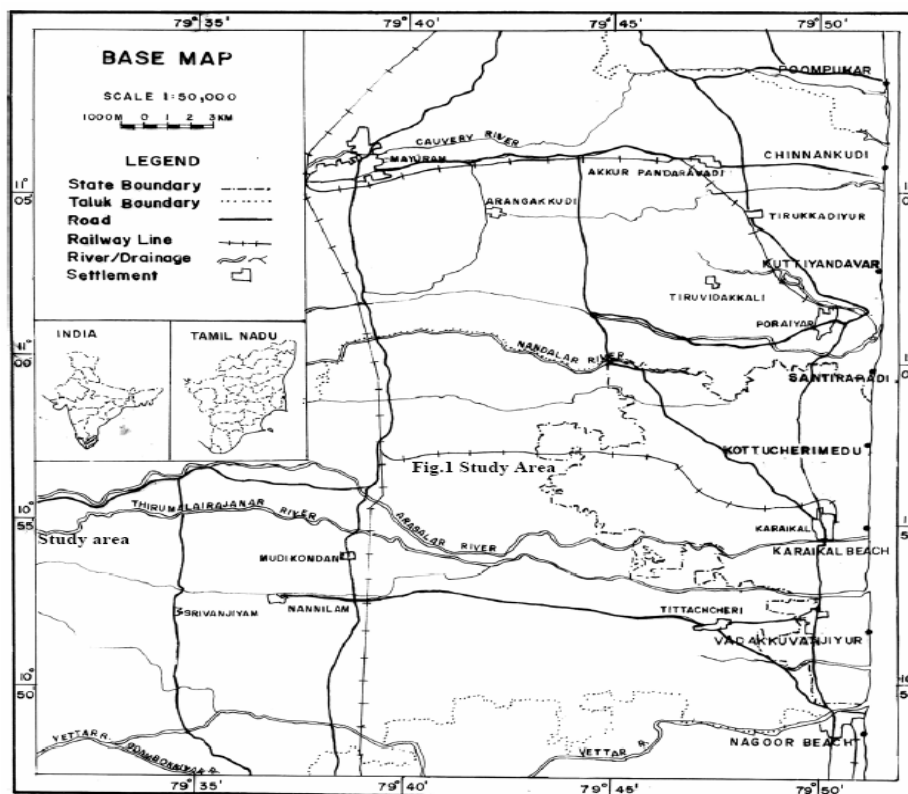


Figure 1. Location map.

Because of the availability of one-year record of triangulated stations' samples just before the Tsunami on a coast in which the highest damages are incurred, the study has been continued.

The sediments were analyzed for grain size with the interval of half phi in all stations, from low tide to dune. The same has been statistically evaluated using both graphic and moment measures, Binary plots Folk & Ward (1957), Mason & Folk (1958), Friedman (1961; 1967; 1979) and Rajamanickam (1983) CM diagram (Passegga, 1964) and Visher's lognormal distribution (Visher, 1969) were prepared. They were showing a very characteristic shift in the nature of sediments.

In the coastal stretch from Poompuhar to Nagoor, surface sediment samples had been collected at an interval of 5 km on 16th December 2004 and 7th January 2005. However, wherever marshy ground near river mouths and bad land

topography block entered on-to the beach, sampling had not been done.

In places where strong lithological differences by virtue of its grain size, black sand enrichment or mixing of other detrital materials were observed, sampling was done in less than 5 km intervals.

Using a hand held Magellan GPS, geographical co-ordinates were fixed for the sample locations. Beach samples were washed and dried. After coning and quartering, carbonates, organic matter and ferruginous coatings were removed from the samples by treatment with 1:10 HCl, 30 %by volume H₂O₂ and SnCl₂, respectively. The dry samples were sieved at Ro-Tap sieve shaker for 15 minutes.

Heavy mineral separation was carried out for all the fractions of each sample from (-16 to +270) using the heavy liquid bromoform as per the standard procedures prescribed by Milner (1962).

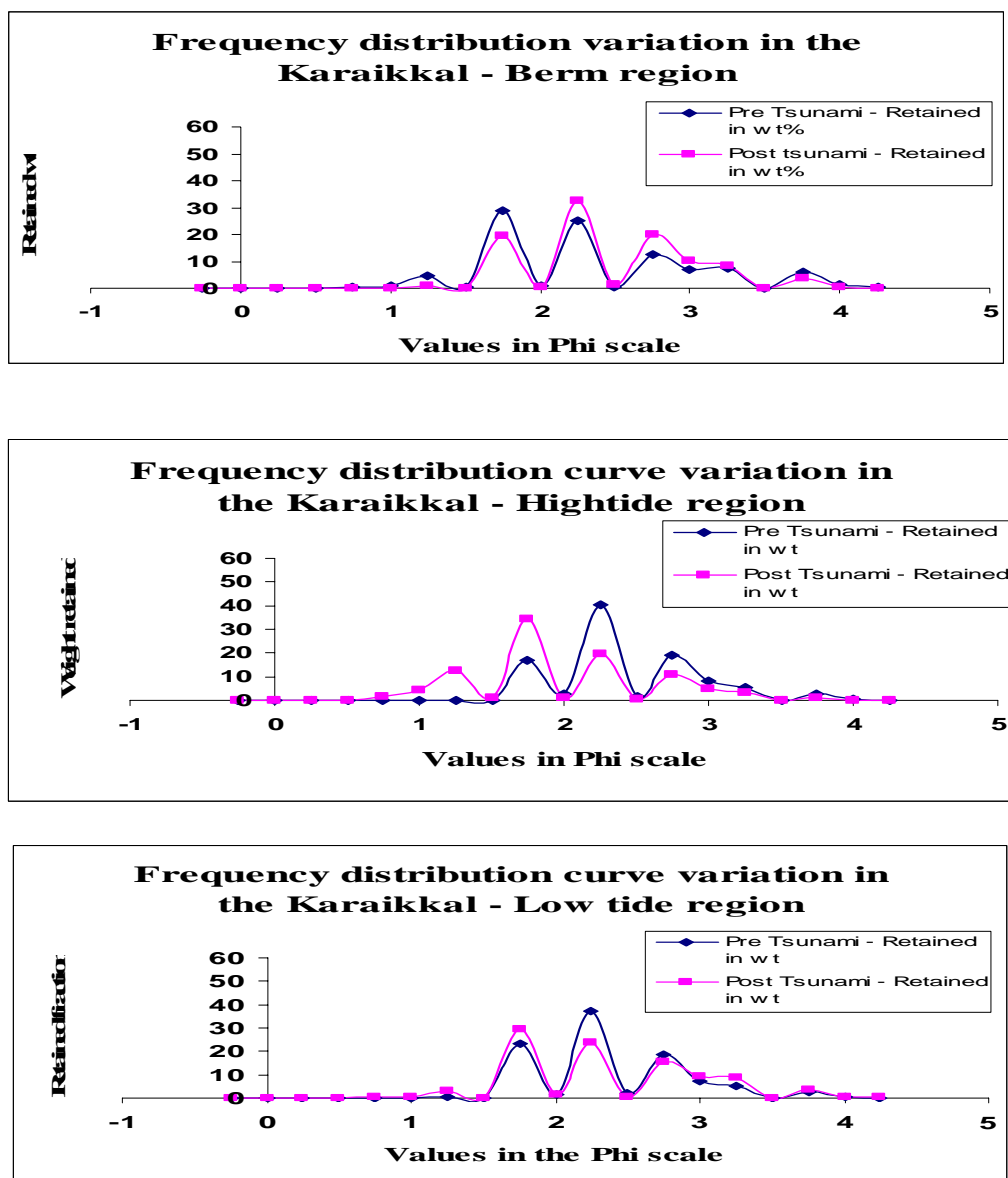
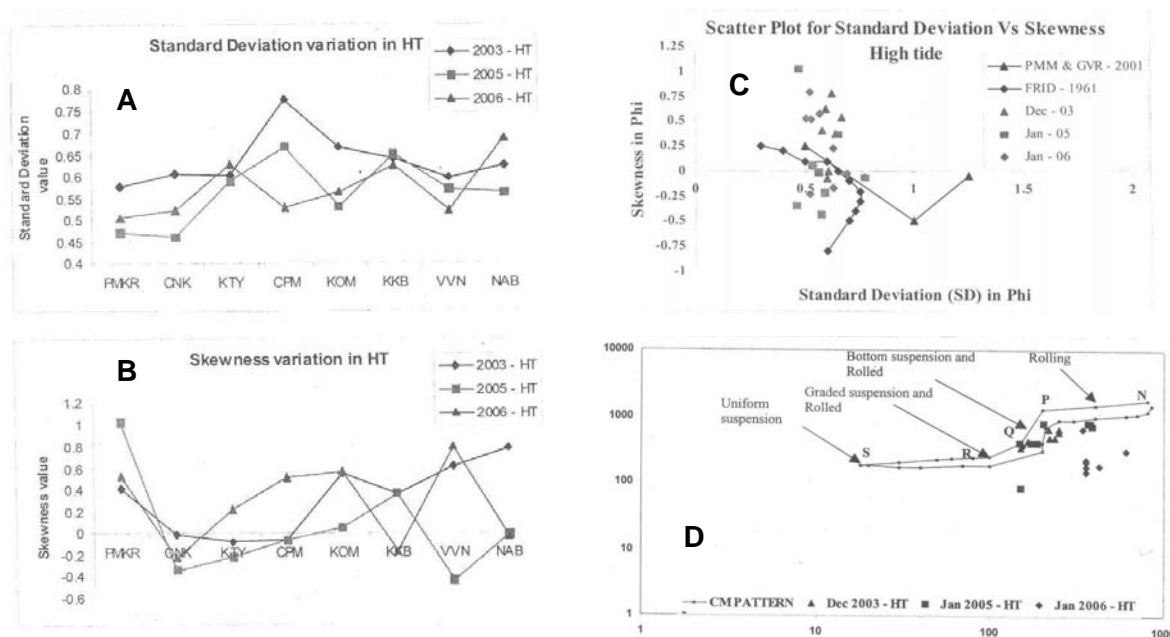


Figure 2. Frequency distribution of sediments.**Figure 3.** A. Standard Deviation variation in HT; B. Skewness variation in HT; C. Standard Deviation (SD) in Phi; D. CM Pattern High tide

The sediment population of clay plus silt has shown a raise in the percentage of distribution in post-Tsunami sediments when compared to pre-Tsunami sediments. The frequency distribution of the grain size study has brought out no difference in the distribution of modal population of being poly modal in nature during both pre and post-Tsunami conditions (Fig.2). However, one has found the shift in the primary peak, in such a way that the post-Tsunami sediments are presenting a shift towards fine. The textural statistics distribution (eg. standard deviation and skewness) clearly projects synchronous distribution of uniform nature of poly modality pre and post tsunami in the studied area (Fig.3A & B). The CM pattern characterizes the presence of graded suspension in both conditions supporting same source of Holocene sediments from the offshore (Fig. 3D). The Visser's sub-population distribution has projected the significant change in the percentage of different populations, not only in adjacent beaches but also from low tide to high tide & dune in the same traverse.

The distribution of grain sizes from the statistical evaluation of texture has projected the presence of grain sizes variation from station to station, though they are very closely placed to each other in spite of receiving the same quantum of Tsunami impact. Variation in structural statistics from station to station is presented in a graphic pattern. The binary plot of sorting vs skewness high tide (Fig. 3C). One can easily observe the drastic shift from pre-tsunami to tsunami whereas the rebuilding of beach after one year in the form of

2006 pattern, one makes to feel the rapprochement by running almost close to 2003.

The statistical parameters are brought in binary form as in case of standard deviation Vs. skewness plot, one can observe that the samples of 2003 and 2006 are seen in the zone whereas the samples of 2005 are found to have been separated out from these two. When the samples are plotted in CM pattern the pre-tsunami samples suggest the dominance of rolling and suspension by being present in the PQ section whereas the samples of 2005 confirm the presence of high turbulence by occupying the zone of NOP. When the samples of 2006 are plotted they are also found still in NOP sector. It suggests that the sediments have not reached the level of pre-tsunami conditions in the distribution of sediments. The role of coastal landforms and relief of near shore bathymetry are presumed to have influenced the same.

The surface structures of the grains indicate concoidal fracture, pitted surface, breakage blocks, furrows, ridge structures, mechanical V shaped pits, upturned plates, fracture plates with shell structures, percussion figures, curve structures and block formation. These features reflect the mechanical impact during the transportation. Features like triangular pits, pitted surface, irregular inundation, adhering particles, overlapping structure, irregular crescentic surface and braided features suggest the chemical action undergone in the depositional basin. Over and above the presence of concoidal features with rounded edges irregular shapes with etching, wavy surfaces with breaking, rounded pitted

surface fracture face, V shaped pits in the Ilmenite grains suggest the strong integrated beach shore environment.

When one considers the data through Visser's table sub-population the zones in the beach like low tide, high tide and berm, behave characteristically different from pre-tsunami to post-tsunami. In depositional site at Poombukar the low-tide saltation population distinctly shifts to higher percentage whereas suspension population and surface creep are much reduced from pre-tsunami.

In the case of depositional sites, the berm projects distinct low in saltation population and surface creep population during post-tsunami and characteristic raise in the suspension population. In other zones, there is not much variation in the distribution of sub-population. The observations suggest that grain size variations during post and pre-tsunami bring out a characteristic change in the berm and low tide whereas high-tide zone remains stable.

The study area from Poombukar to Nagoore, Central Tamil Nadu, East Coast of India, is popular for the distribution of Heavy mineral placers but of fine grain in nature unlike the coarse placers of southern Tamil Nadu Coast. The main minerals are Garnet, Ilmenite and Zircon. They are present to the tune of 30 % by weight in the total sand.

Immediately after the Tsunami when the sediments are analysed for heavy mineral placers, the assemblage of minerals remain almost the same but the percentage distribution of these minerals are found to vary appreciably. For example, in Poombukar the sand recorded 49 % of Pink Garnet instead of 13 % by weight during pre-Tsunami.

Likewise, in Nagoore colourless Garnet is noticed to jump from 1.8 to 21.7 % during post-Tsunami while opaque is observed to vary from 20 to 29 %. When the individual mineral ilmenite is taken into account, it is giving a drastic shift from 0.5 to 20.0 % during post-Tsunami (Table 1). The table shows the shift in the Ilmenite distribution from pre- to post-tsunami. This clearly reflects the strong shift in the southern station when compared to northern stations. It is attributed to the possible influence of nearshore bathymetry in the prevailing slope during the tsunami period.

When the distribution of heavy minerals in those selected eight stations is scanned there is a marginal variation between the Northern and Southern stations. The stations in the middle portion have shown an appreciable raise to the tune of 3 folds. From the distribution of mineral assemblage, the existence of distributional variation for the energy levels in the advancing. The table 3 shows variation of heavy mineral in the beach region between pre- and post- tsunami. It is clearly seen that there is no shift in the assemblage, but only in the relative abundance. In the shift ratio to flaky constituents to

the granular constituents one can easily make out the energy variation prevailing in the respective beach. Low and high energy level variation is noticed alternatively within the adjacent stations.

This type of variation reflects the interaction of near shore bathymetry with coastal landforms. The presence of more flaky constituents in Chandrapadi and Kottucherimedu register low energy and also presence of materials like that. Tsunami waves could be noticed to have low and high-energy presence in the adjacent stations. Total assemblage of heavy minerals has reflected the same source for both pre and post-Tsunami sediments. The Tsunami sediment distribution is confirming that the source of heavy minerals must have been the existing offshore rather than the terrestrial supply.

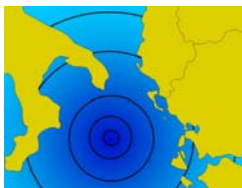
The depositional and erosional sites have reflected the domination of flaky constituents in the depositional sites or other words the heavy heavy minerals like opaque is found to project a reduction in the percentage. Wherever, inlets are present, the domination of the heavy heavy mineral percentage is noted to shoot high.

Taking into account the nature of heavy minerals present and the surface texture of Garnets and Ilmenites, The depositional trend can be tracked in the actual tsunami profile. The break in the nature of sediment distribution as in the case 2004-05 and sudden raise in the percentage of flaky as in the case of Nagoore post-tsunami sediments will be utilized to track the paleo-tsunami records.

Further, the basic data collected about the texture and mineralogy of the sediments immediately after tsunami and comparison with the immediate past conditions of the respective beach may be very useful in recognizing the existence of the past tsunami event in the vertical sampling.

References

- Folk R. L., Ward M. S (1957). *Brazos river bars: A study in the significance of grain size parameters*. Journal of Sedimentary Petrology, 27, 3-27.
- Friedman G. M. (1961). *Distinction between dune, beach and river sands from textural characteristics*. Journal of Sedimentary Petrology, 31, 3-27.
- Friedman G. M. (1967). *Dynamic processes and statistical parameters compared for size frequency distribution of beach and river sand*. Journal of Sedimentary Petrology, 37, 327-354.
- Friedman G. M (1979). *Difference in size distribution of population of particles among sands of various origin*. Sedimentol, 26, pp.3-3.2.
- Mason C. C., Folk R. (1958). *Diffentiation of beach dune, and Aeolian flat environment by size analysis, Mustang Island, Texas*. Journal of Sedimentary Petrology, 28, 211-226.



2nd International Tsunami Field Symposium

IGCP Project 495

Quaternary Land-Ocean Interactions:
Driving Mechanisms and Coastal Responses

Ostuni (Italy) and Ionian Islands (Greece) 22-28 September 2008



Project 495

Regnauld H.¹, Suanez S.², Fichaut B.²

Storms or tsunamis?

The case of boulder accumulations on the coasts of Brittany, western France

¹Laboratoire COSTEL UMR 6554 CNRS and Université Européenne de Bretagne, Rennes 2, Rennes cedex France. e-mail: herve.regnauld@uhb.fr

²Laboratoire GEOMER, UMR 6554 CNRS and Institut Universitaire Européen de la Mer, Plouzané, e-mail: serge.suanez@univ-brest.fr; bernard.fichaut@univ-brest.fr

Keywords: *boulders, storms, tsunamis, coastal morphology, western France*

Tsunamis have most often been seen as events which deliver high energy levels and significant changes in coastal morphology. In many cases tsunamis are identified out of very peculiar deposits, such as pebble sheets (Regnauld et al, 2008) or boulder accumulations. Though the impact of these accumulation on coastal evolution has not been studied very often. Two open questions are at stake. The first one is to decide whether tsunami do actually force coastal evolution or if they are just events, which modify some aspects of the landscape but do not actually interfere with coastal trends that are forced by sedimentary processes such as longshore drift and sediment supply...The second deals with the relative importance of storms and tsunamis (Einsele et al, 1996).

This communication aims at presenting some examples of boulder deposits and gravel landforms which may originate from a tsunami but which more probably are under the present control of severe storms.

Our field work is located on some remote islands off Brittany (the Molène Archipelago, with Banneg and Ouessant islands). These islands are comprised of granite (with some local outcrops of schists) and are low lying plateaux surrounded by coastal cliffs. They are 1 km (Banneg) and 5 km (Ouessant) long and are located on top of a very large submarine rocky platform (about 20 m deep). Their western coast are directly exposed to the Atlantic waves. During severe storms waves 16 to 18 m high have been recorded. Though average waves have a significant height of about 1.5 meter.

On Banneg Island the boulders are located between 7 and 14.5 m of altitude, on top of a west facing cliff. They are grouped into six clusters. The largest cluster is 60 m long and 20 m wide. Each

cluster has the shape of a wall as if the boulders were deposited in lines (or crescent) more or less parallel to the cliff edge. They form continuous boulder ridges. Inside of the clusters the boulder are imbricated and have a seaward dip. The average boulder size is about 0.8x0.6x0.4 m (i.e. about 0.6 tons). The largest one is 5.3x3.9x0.5 m and weighs about 32 tons. All the boulders have an angular shape and show no sign of having been rounded. There is a relation between the decreasing size of the boulder and the distance to the cliff top.

In Ouessant the boulders are located on the two western peninsulas of the island, facing NW. They are lying between 5 and 11 m of altitude on top of sea facing slopes. They are only found on headlands and are not seen in bays: all bays are occupied by gravel barriers/beaches. The barriers are comprised of blocks which may reach 0.6x0.6x0.6 m. Though most of the blocks are about 0.4x0.3x0.2 m. They all are rounded. The boulders are set in heaps (not in lines) and display a very heterogeneous set of sizes. The largest is 1x1x0.9 m and is 10 m inland at 5 m above M.S.L. The average size is about 0.5x0.5x0.4 m. They are not rounded. There is a clear difference between the boulders and the gravel barrier. The blocks which build up the barrier are rounded and rather small. The boulders building up the walls or the heaps are never rounded and are bigger. The first hypothesis which may provide an explanation is that gravel barrier are wave/storms constructed features when boulders are linked to some other processes. A tsunami is a very likely possibility.

In Brittany there is one deposit which has been said to be the result of the 1755 tsunami. It has been found by Haslett et Bryant (2007) in southern western Brittany in Baie des Trépassés.

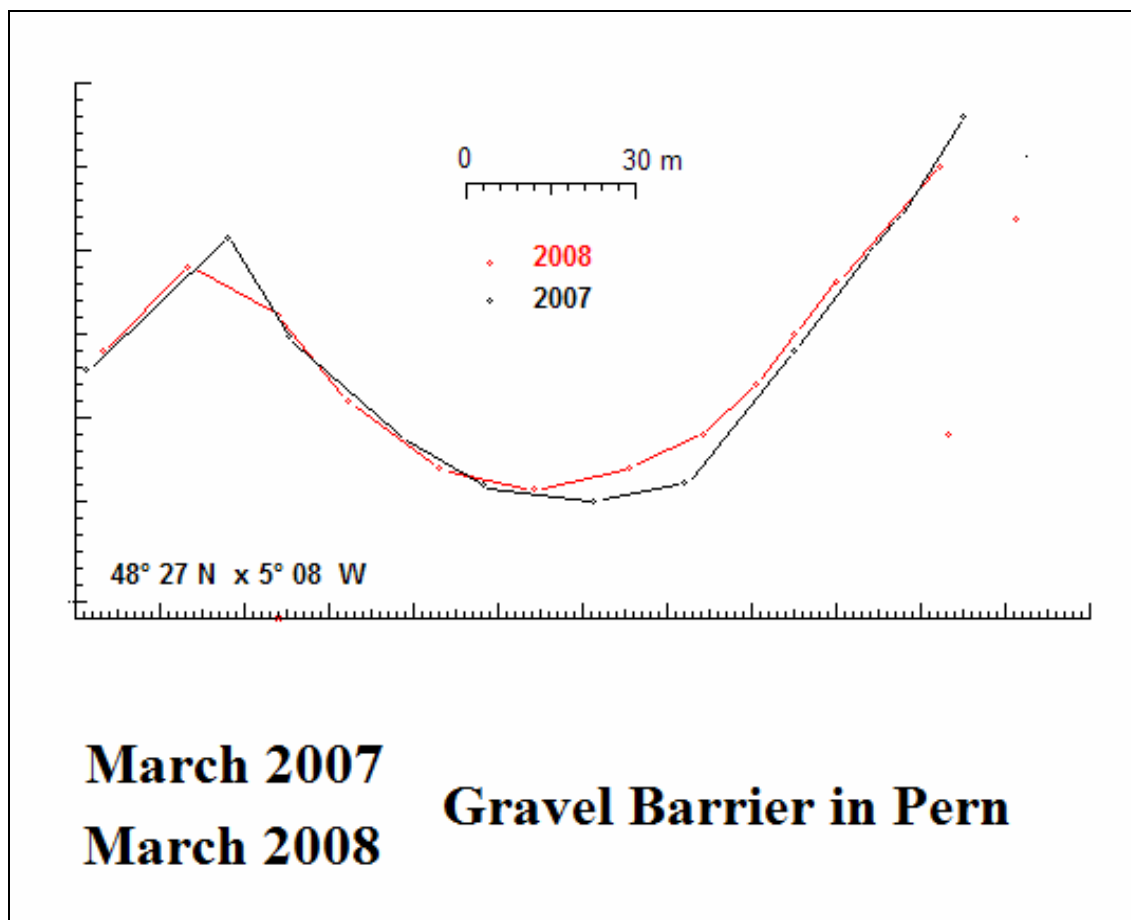


Figure 1. Shows a barrier in Ouessant (the Pern barrier). It has retreated on its western end, where it merges with a low cliff. Some boulders are present in land but they are not rounded and do not come from the destruction of the barrier. This later has gained material and has prograded sea ward in its center. It has also gained enough material to extend farther in land and to gain almost one meter in altitude. This shows that storms are able to mobilise great quantity of rounded boulders and to use them for barrier building.

It is a buried layer inside of a marsh and it doesn't show a very distinct signature from that of a palaeo storm deposit. Though it is a single layer inside of a long core. The basic assumption by Haslett and Bryant is the following one : the "deposits" are unique. If they were laid by storms several such layers would be found along the core. This argument is highly efficient. In south Brittany there are several places (Sucinio for instance) where cores show several storm layers. In Northern Brittany (le Verger) cores do show several storm-related layers (there are three, dated to 2630, 240 and 113 BP). In Baie d'Audierne (Nérizélec) three storm layers are known (2890 2390 and 810 BP). In Baie des Trépassés there is only one event when many storms would be expected there as it is well exposed to the west. Therefore Haslett and Bryant have good reasons to write that the single event is more likely a tsunami than a storm.

In this case it is possible to hypothesise that one large single event has existed in Brittany and it could be the 1755 tsunami. Chronicles do report it and C¹⁴ datations by Haslett and Bryant fit with this

time range. The problem is to decide if this tsunami has also been responsible for the blocks in Banneg and Ouessant (Fichaut & Suanez, 2008). In March 2008 a very severe storm hit western Brittany, during high spring tides. Field work in Ouessant and Banneg after this storm has shown that many blocks have been reworked and that new ones have been added to the previous heaps. The gravel barriers have undergone over-topping and over-washing. They have gained material on their landward side and on their sea ward side. Locally they have gained in height.

The large boulders originate from the submarine abrasion platform and apparently bypass the gravel beach. They are deposited inland of it. Other rocks on the photo are *in situ* tors. This storm seems to have had two different consequences. On one hand it has reworked the barriers (and beaches), which have gained and lost material (with a null balance) and have significantly changed their morphology. On the other hand the storm has been able to move isolated large (and very large) boulders.

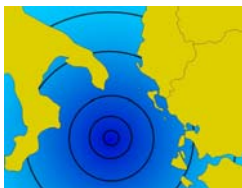


Figure 2. Shows some of the new (and old) non rounded boulders, which are not part of a barrier.

They have been extracted from the submarine areas and have been pushed inland outside of the ordinary location of gravel/ boulders structures (beaches or barriers). This observation leaves entirely open the question of the origin of the boulders. It is very possible that some of the gigantic blocs have been triggered by the 1755 tsunami (or by an other tsunami). But once they have been moved, each violent storm moves them again. But, obviously severe storms may have the same effect. They can remove blocks from the submarine platform and displace them several tens of meter inland. Therefore, though we cannot (and do not) exclude the possibility of a tsunami along these coasts, we do infer that the tsunamis have no large morphological effects and that the coast is storm dependent, not tsunami dependent.

References

- Einsele G., Chough S.K., Shiki T. (1996). *Depositional events and their records-an introduction*. Sedimentary Geology, 104 : 1-9.
- Fichaut B., Suanez S. (2008). *Les blocs cyclopéens de l'Île de Banneg (Archipel de Molène, Finistère) : accumulations supra tidales de forte énergie*. Géomorphologie, 1, 15-32.
- Haslett S. K., Bryant E. A. (2007). *Reconnaissance of historic (post-AD 1000) high-energy deposits along the Atlantic coasts of southwest Britain, Ireland and Brittany, France*. Marine Geology, 242, 1-3, 207-220.
- Regnaud H., Planchon O., Goff J. (2008). *Relative roles of structure, climate, and of a tsunami event on coastal evolution of the Falkland Archipelago*. Géomorphologie, 1, 33-44.



Reicherter K.¹

Tsunami group: Fernández-Steege T., Koster B., Vonberg D., Baer S., Grützner C.

The sedimentary inventory of the 1755 Lisbon tsunami along the Gulf of Cádiz (southwestern Spain)

¹Inst. of Neotectonics and Natural Hazards, RWTH Aachen University, Germany

e-mail: k.reicherter@nug.rwth-aachen.de

Keywords: 1755 Lisbon tsunami, tsunamites, back flow sediments, Gulf of Cádiz

Outcrop evidence and shallow drilling in coastal areas proved sedimentary evidence for paleo-tsunamis along a 50 km long segment of the Atlantic coast of southern Spain. We studied the coast between Barbate and Tarifa (Fig.1), both on top of rocky cliffs as well as in lagunas and along sedimentary beaches (Marismas de Barbate and Zahara de los Atunes, Los Lances N of Tarifa). Also, we focussed on bays (Bolonia, Valdevaqueros), which are most probably sheltered from direct tsunami wave action. However, reflections of the waves may occur and may hit these bays. In these bays, the Roman villages of Baelo Claudia and Mellaria, respectively, have been situated (e.g. Silva et al., 2005, 2006, 2008).

Earlier works provide evidence for the 1755 Lisbon tsunami at the Valdelagrana spit bar near Cádiz, where wash-over fans have been recognized (Luque et al., 2002). Also, Luque et al. (2002) found evidence for an older, Roman tsunami (2.300 yr BP) in the same area. Whelan and Kelletat (2005) described larger boulder deposits at the Cape Trafalgar, and attributed those to the 1755 Lisbon tsunami. The same deposits were interpreted by Gracia et al. (2006) as tsunamites, and they described a run-up height (vertical run-up) of > 19 m in that area.

Further south in the Bolonia Bay, Alonso et al. (2003) described wash-over deposits in the Arroyo de Alpariate with an age of 2.150-1.825 yr BP.

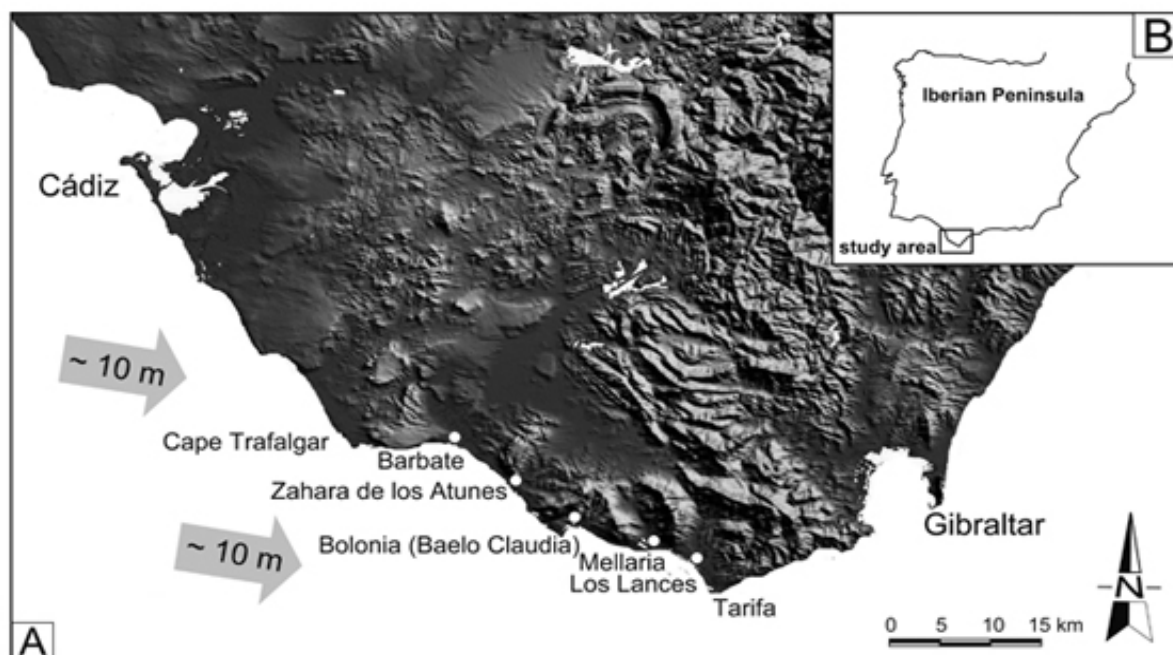


Figure 1. A. Topographic map of the study area in southern Spain and studied localities; arrow indicate direction of tsunami waves of the 1755 Lisbon event, numbers give vertical run-up (modified from Gracia et al. 2006). B. The study area in southern Spain.

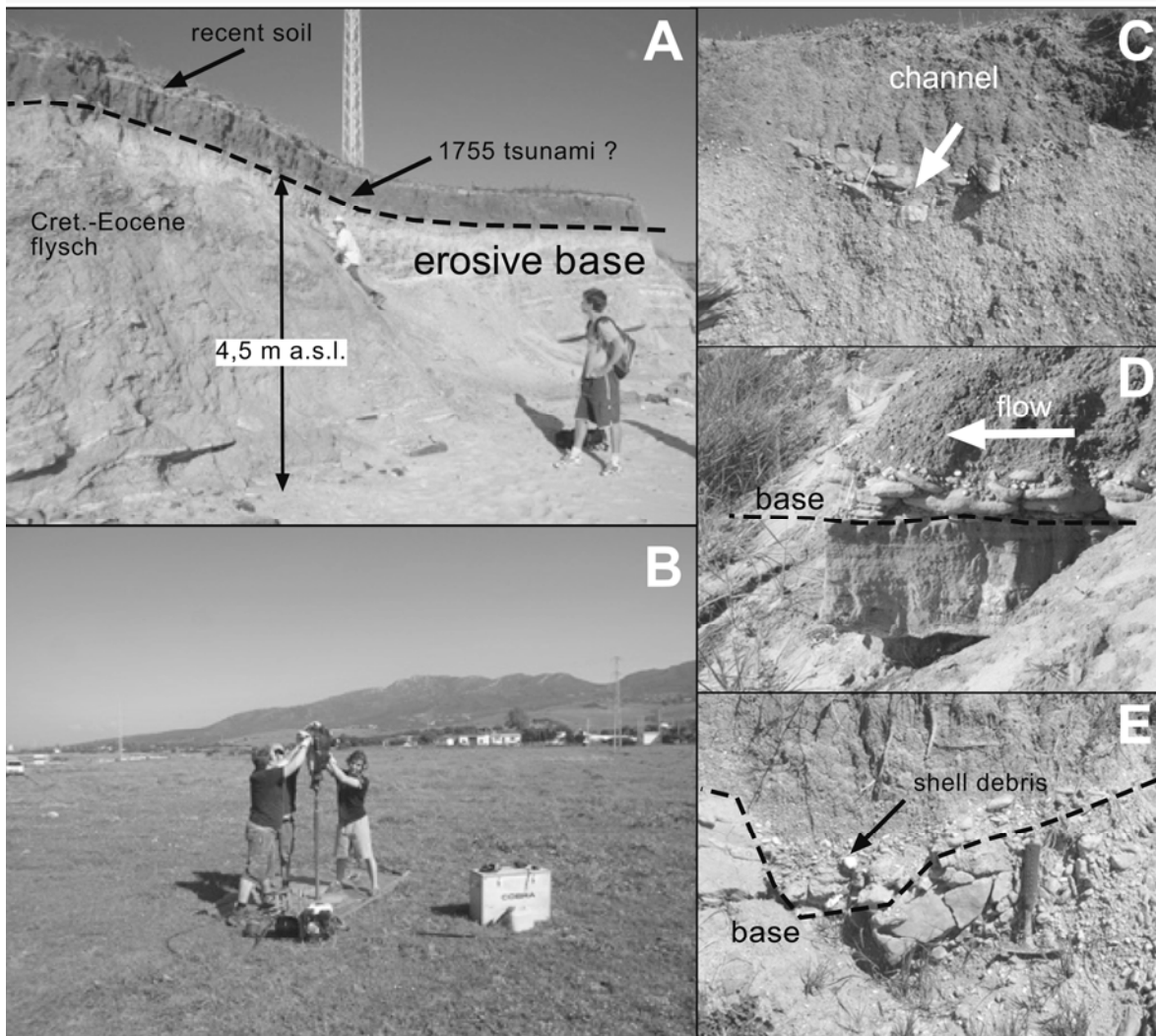


Figure 2. A: Coastal cliff between Barbate and Zahara de los Atunes, dark layer on top of the Cretaceous-Eocene Betic substratum is a tsunami event and represent most probably back flow deposits, possibly that of 1755. Height about 4.5 m above mean sea level. **B:** detail of the location **C:** channelled back flow with coarse-grained basal deposits. **D:** imbricated clasts in the back flow indicate paleocurrent towards the sea (left). **E:** shell debris and conglomerates in the back flow sediments.

Later, Becker-Heidmann et al. (2007) have dated huge sand deposits (at about 4 m above mean sea level) and interpreted those as tsunami sediments. However, the charcoal yielded ages of $455 - 475 \pm 35$ BP, and are approximately 300 years older than the Lisbon event. Possibly, the charcoal has been reworked during wave action. Other tsunami deposits in the Bolonia Bay were described by Gracia et al. (2006), which constitute “block fields”.

These block fields have unfortunately not been dated. Near Tarifa, in the Marismas of the Río Jara, historical damage of buildings (bridges) and geomorphological and geological mapping of Gracia et al. (2006) evidenced as well deposits - here wash-over fans - of the Lisbon tsunami. Also, these deposits were not dated.

Here, we describe new findings of tsunami deposits along the coast between Barbate and Tarifa.

Also, we give an outline of the future research.

Marismas de Barbate: The marshlands of Barbate have only little elevation of about 0 to 1 m above mean sea level and are flooded permanently by the tide. This ideal tsunamite reservoir was probed with percussion coring with an open window sampler. We reached depths of > 5 m. After core description the same site was drilled with a sampler with PVC liners for lab analyses. Cores provided evidence for tsunamigenic layers. Laboratory analyses (see below) are currently in progress.

Beach section between Barbate and Zahara de los Atunes: The 5 km long rock cliff has been mapped, leveled, sampled (including sediment lacquer films). We have surprisingly found only one layer on top of the basement at the cliff, in varying altitudes between 1 and 4,5 m above mean sea level (Fig.2A).

The basement is Cretaceous to Eocene flysch deposits or OIS 5 terraces (Tyrrhenian) of approx. 125 kyr. The dark sandy layer of about 1 m thickness constitutes a fining-up sequence with a coarse-grained base with conglomerates, shell debris and charcoal (Fig.2E). These deposits are channeled (Fig.2C) and clasts are imbricated (Fig.2D), paleo-flow direction is towards the Atlantic. As the beach sands are white to yellowish (Fig.2A), and the layer is dark, organic- and clay mineral-rich, but sandy, we interpret this layer as a back flow. Paleo-current directions endorse these observations and the evidence that only one layer is preserved.

Presumably, former tsunamites were eroded due to multiple wave action and the cliff was “cleaned” to the basement by the waves. The tsunamite has reworked the dark clayey marshlands of Barbate and was deposited as a mixture of beach sands, boulders and shell and the clayey marsh deposits during the back flow of the last major wave. The Flandrian transgression had a maximum at about 7.000-6000 yr BP and reached altitudes of 3-4 m above the present sea level and cannot account for these deposits. Our interpretation of the principal sediment-depositing mechanisms effective in tsunami surges is based on field observations of deposit geometry and internal sedimentary characteristics, which are clearly not related to a beach.

Bolonia Bay: Here, we investigated the Roman ruins of Baelo Claudia. As mentioned above several indicators of tsunami deposits have been published. We are currently investigating deposits in the ruins, which may be tsunami-reworked “post-Roman” colluvium (Silva et al., 2008). Also, the deposits described by Becker-Heidmann et al. (2007) are under examination. The “block fields” of Garcia et al. (2006) are related to small creek mouths into the Atlantic, we regard these as storm deposits reworking fluvial pebbles. They are only found near the creeks and in heights of 2-3 m above the mean sea level along the beach.

Valdevaqueros Bay (Mellaria): In this bay the rests of the Roman village of Mellaria are exposed, they are not excavated and covered by 2 m of sandy, clayey sediments. The laguna of Valdevaqueros yields dark organic-rich marshy sediments, which may possibly be reworked during wave action. We have drilled a profile perpendicular to the coast up to 4 m depth. Laboratory analyses (see below) are currently in progress.

The locality of Mellaria is not the one indicated by Gracia et al. (2006), who put the village in the Los Lances bay. Mellaria was a Roman fishery village directly at the coast.

Los Lances area (Tarifa): The marshlands of the Río Jara north of Tarifa are called Los Lances. Here, wash-over fans of the Lisbon tsunami (without age constraints) and damage of a bridge have been described (Gracia et al., 2006). We have drilled a profile perpendicular and parallel to the coast up to 5 m depth. We have found similar intercalations of tsunamites downhole, which are interpreted as either an expression of repeated earthquake activity or tsunami-like waves induced by submarine slides. Laboratory analyses (see below) are currently in progress.

Future works will include: Sedimentological analyses (sieving, washing, laboratory core description)

Geophysical investigations (magnetic susceptibility on cores)

(Micro)paleontological studies (foraminifera, shells)

Clay mineralogy of tsunamites

Characterisation of organic matter (biomarker studies, terrestrial vs marine)

Dating of the sediments (radiocarbon, mainly charcoal and shells)

Geoarcheological studies in Mellaria and Baelo Claudia (“post-Roman” deposits)

In conclusion, we have found several different distinctive features of tsunamigenic deposits along the Spanish Atlantic coast, which are characterized by:

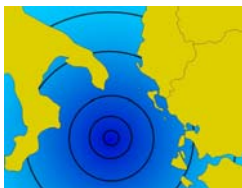
- clast-supported, polymodal, boulder-bearing basal deposits composed mostly of well-rounded clasts and fewer angular clasts, partly imbricated
- normal grading or crude normal grading
- lateral changes in characteristics of depositional facies are common and abrupt (channels)
- clay to sand-sized, bioclastic (and Roman ceramic)-rich matrix is poorly sorted, implying that soft sediments eroded at the lower erosional surface contributed to the tsunami deposit
- mixed sources of sediments (beach and marshes).

These features are interpreted as:

- non-cohesive and sediment-loaded subaquatic density flows
- deposits of successive waves in the tsunami wave train
- back flow or back wash deposits are characterized by the incorporation of sediments derived from mixed sources within the tsunami deposits, such as angular clasts from nearby subaerial settings, rounded clasts reworked from beach gravels, and shell debris and yellowish beach sands eroded from older, and unconsolidated, shoreface deposits.

References

- Alonso C., Gracia F. J., Ménanteau L., Ojeda R., Benavente J., Martínez J. A. (2003). *Paléogeographie de l'anse de Bolonia (Tarifa, Espagne) à l'époque romaine*. In: The Mediterranean World Environment and History. Elsevier S.A.S. Amsterdam, 407-417.
- Becker-Heidmann P., Reicherter K., Silva P. G., (2007). *¹⁴C dated charcoal and sediment drilling cores as first evidence of Holocene tsunamis at the Southern Spanish coast*. Radiocarbon, 49, 2, 827-835. (Proceedings of the 19th International Radiocarbon Conference, Eds Bronk Ramsey C., Higham T. F. G.).
- Gracia F. J., Alonso C., Benavente J., Anfuso G., Del-Río L., (2006). *The different coastal records of the 1755 Tsunami waves along the Atlantic Spanish Coast*. Z. Geomorph. N.F., Suppl. Vol. 146, 195-220.
- Luque L., Lario J., Civis J., Silva P. G., Goy J. L., Zazo C., Dabrio C. J. (2002). *Sedimentary record of a tsunami during Roman times, Bay of Cadiz, Spain*. Journal of Quaternary Science, 17, 623-631.
- Silva P. G., Goy J. L., Zazo C., Bardají T., Lario J., Somoza L., De Luque L., González-Hernández F. M. (2006). *Neotectonic fault mapping at the Gibraltar Strait Tunnel area, Bolonia Bay (South Spain)*. Engineering Geology, 84, 31-47.
- Silva P. G., Reicherter K., Grützner C., Bardají T., Lario J., Goy J. L., Zazo C., Becker-Heidmann, P. (2008). *Surface and subsurface paleoseismic records at the ancient Roman city of Baelo Claudia and the Bolonia Bay area, Cádiz (South Spain)*. In: Eds Reicherter K., Michetti A. M. Silva P. G. Historical and Prehistorical Records of earthquake Ground effects for Seismic Hazard Assessment. J. Geol. Soc. London, Spec. Publ.
- Whelan F., Kelletat D. (2005). *Boulder Deposits on the Southern Spanish Atlantic Coast: Possible Evidence for the 1755 AD Lisbon Tsunami?* Science of Tsunami Hazards, 23, 3, 25-38.



Reicherter K.¹, Becker-Heidmann P.²

Tsunamites in lagunas: remains of the 1522 Almería earthquake (western Mediterranean)

¹Inst. of Neotectonics and Natural Hazards, RWTH Aachen University, Germany

e-mail: k.reicherter@nug.rwth-aachen.de;

²Institut für Bodenkunde, Universität Hamburg, Hamburg, Germany

Keywords: *Tsunamites, lagunas, Gulf of Almería, Western Mediterranean*

Shallow drilling in the laguna and saline of the Cabo de Gata area proved sedimentary evidence for paleo-tsunamis along the Spanish Mediterranean coast. Several coarse grained intervals with fining-up and thinning-up sequences, rip-off clasts, broken shells of lamellibranchs and planktic foraminifera

show erosive bases are interpreted as tsunamites (Fig. 1).

The coarse-grained intervals show up to three sequences divided from each other by a silty layer, as so-called mud drape (Fig. 2).

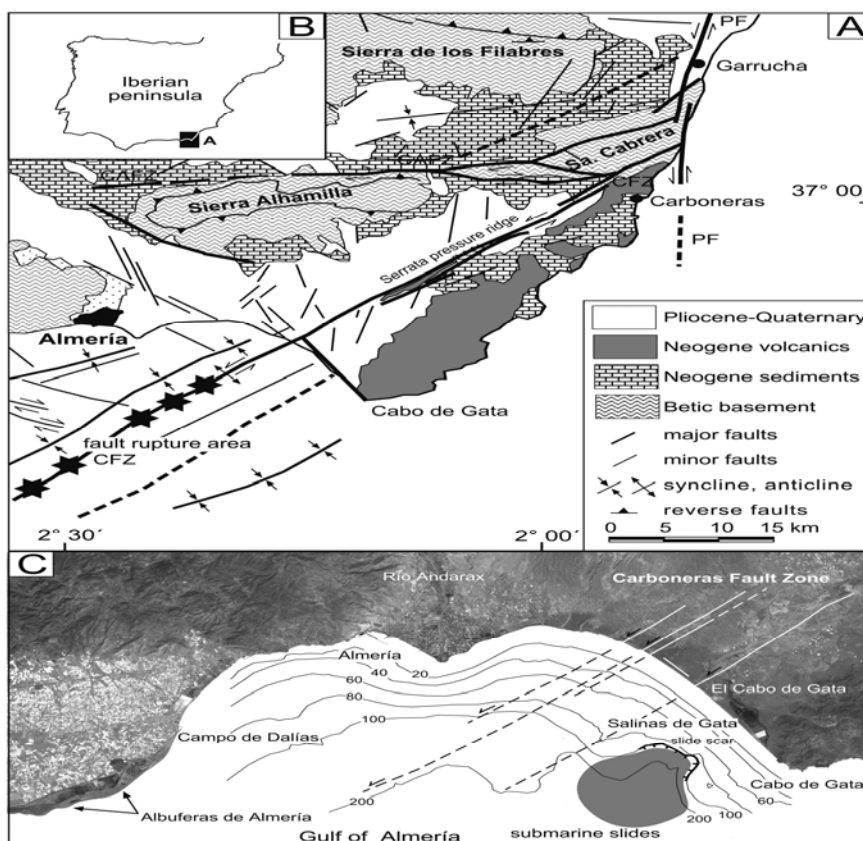


Figure 1. A. Geological sketch map of the study area in the Gulf of Almería, position of the Carboneras Fault Zone (CFZ), and the location of the rupture and epicenter of the 1522 Almería earthquake (stars). PF = Palomares Fault, CAFZ = Corredor de las Alpujarras Fault. B. Study area in Spain. C. Satellite image of the Gulf of Almería with localities and fault strands of the CFZ. Bathymetry (in meters) taken from Sanz et al. (2003). Position of the different strands of the Carboneras Fault Zone, note a submarine slide scar in front of the Salinas of the Cabo de Gata.

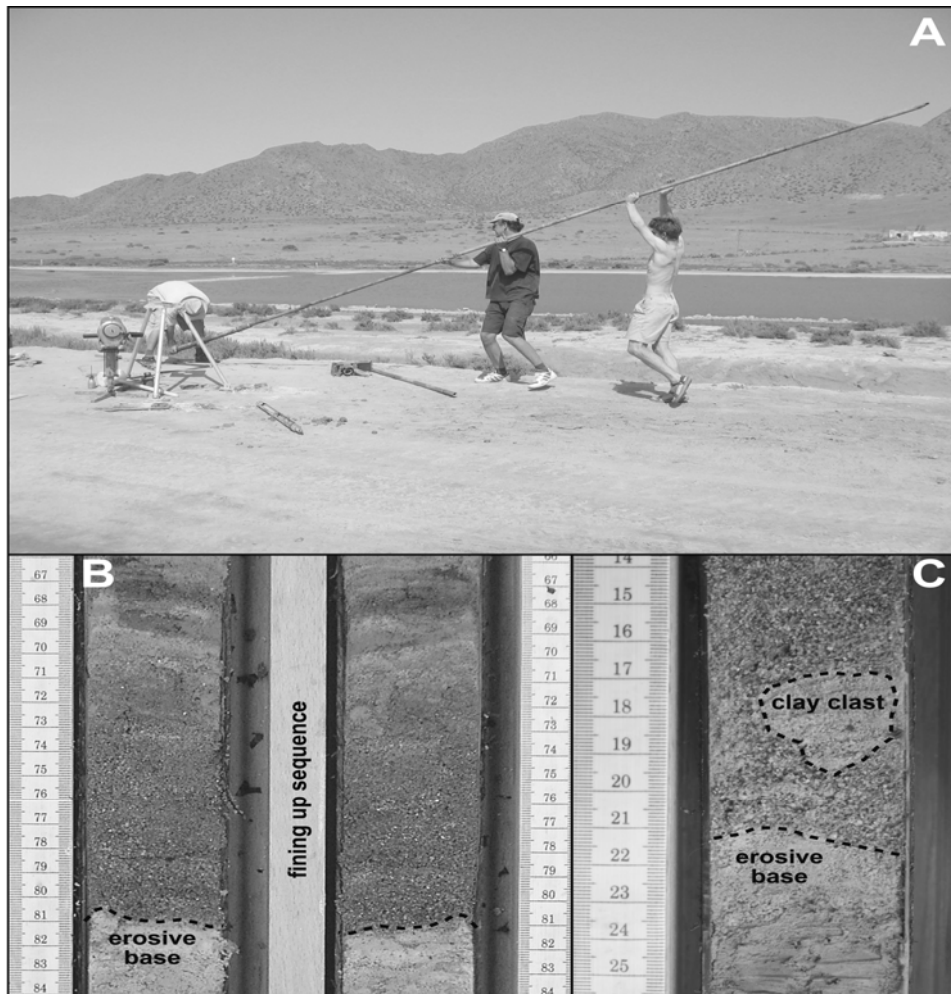


Figure 2. A. Drilling in the Salinas of the Cabo de Gata. B. Detail of core CD G-2, between 69 and 81 cm depth a sequence with erosive base, shell debris, fining-up and thinning is interpreted as tsunami deposit (three cycles – tsunami train), age of the layer below the deposits 680 ± 30 yr BP. C. Detail of core CDG-2, between 92 and 121 cm depth, erosive base, shell debris and rip-off clasts is interpreted as tsunami deposit, age of the layer below the deposits 850 ± 35 yr BP.

These intervals are interpreted as a tsunami train and correspond to three individual waves.

Radiocarbon dating of sediment and shells reveal evidence that these layers can be ascribed to deposition during the 1522 Almería earthquake. The 1522 Almería earthquake ($M > 6.5$) affected large areas in the western Mediterranean and caused more than 1000 casualties. The epicentral area was probably offshore in the Gulf of Almería (southern Spain) along a 50 km long sinistral strike-slip fault, the Carboneras Fault Zone (CFZ, Fig. 1A, C). The potential for tsunami generation along a strike-slip fault is generally small, therefore we assume that seismic shaking triggered submarine slides in the Gulf of Almería and the Cabo de Gata spur, which then caused tsunami waves and due to the geometry of the Gulf also reflections.

We focused our investigations on the Salinas of the Cabo de Gata (Fig. 1C). The laguna is situated at the foot of the San Miguel volcanic hills. Salt production facilities occupy 500 ha, 300 of which

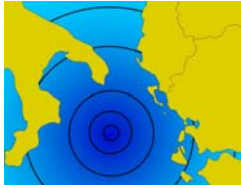
are flooded, favoring the entrance of the sea by gravity. The laguna has a depositional history of about 6000 years BP (Reicherter and Becker-Heidmann, 2008), the sediment logs allowed us to distinguish three periods of the evolution of the laguna. The initial stage is an alluvial fan phase, which commenced already during Pleistocene times, followed by an intermediate beach phase from approximately 5000 yr BP to 3000 yr BP, from then on a marsh laguna developed. The early period is characterized by alluvial fan deposits (Harvey et al., 1999), which consist of reddish unsorted coarse-grained gravels, sands and intercalated paleosols. Sedimentary source is the volcanic Cabo de Gata range, hence, clastic material is exclusively made up of volcanic rocks and some Neogene carbonates. The alluvial fan sequences are cyclic and show fining-up cycles, mostly terminated by a soil development. Upsection, sands with intercalated clays are developed, which point to open marine, and hence beach-like conditions between 5000 to

3000 yr BP. After approximately 3000 years BP a hyper-saline environment typical for a laguna developed with organic-rich clayey and evaporitic layers (i.e. gypsum). In these well-stratified cyclic deposits of the laguna-stage several sandy and coarse-grained layers are intercalated, partly well sorted sand layers are interpreted to be aeolian dunes. Several other coarse-grained intervals with fining-up and thinning-up sequences contain rip-off clasts (Fig.2B, C), shells of lamellibranchs and foraminifera. AMS ¹⁴C- dating of the layer directly below provided an age of 680±30 yr BP, taken into account an erosive base and, hence, some missing (eroded) deposits, we interpret this layer being deposited during a tsunami event accompanying the 1522 earthquake of Almería.

We have also found another intercalation of tsunamites downhole (850±35 yr BP, 92-121 cm depth), which are interpreted as either an expression of repeated earthquake activity or tsunami-like waves induced by submarine slides triggered by seismic shaking in the Gulf of Almería. Our evidence suggests a definite tsunami potential and hazard for offshore active and seismogenic faults in the western Mediterranean region.

References

- Becker-Heidmann P., Reicherter K., Silva P. G. (2007). ¹⁴C dated charcoal and sediment drilling cores as first evidence of Holocene tsunamis at the Southern Spanish coast. Radiocarbon, 49, 2, 827-835. Proceedings of the 19th International Radiocarbon Conference, Eds Bronk Ramsey C., Higham T. F. G.
- Gràcia E., Pallàs R., Soto J. I., Comas M., Moreno X., Masana E., Santanach P., Diez S., García M. Dañobeitia J., HITS cruise party (2006). *Active faulting offshore SE Spain (Alboran Sea). Implications for earthquake hazard assessment in the Southern Iberian Margin*. Earth Planet. Science Letters, 241: 734-749.
- Reicherter K., Becker-Heidmann P. (2008, in press). *Tsunami deposits in the western Mediterranean: remains of the 1522 Almería earthquake?* In: Historical and Prehistorical Records of earthquake Ground effects for Seismic Hazard Assessment. Reicherter K., Michetti A. M., Silva P. G. (eds.). J. Geol. Soc. London, Spec. Publ.,
- Reicherter K., Hübscher C. (2006). *Off-shore evidence for the 1522 Almería earthquake ($M > 6.5$) in the Alborán Sea (southern Spain)*. J. of Seismology, DOI 10.1007/s10950-006-9024-0.
- Sanz J. L., Hermida N., Tello O., Lobato A., Fernández-Salas L. M., González J. L., Bécares M. A., Gómez de Paz R., Godoy D., Alcalá C., Contreras D., Ubiedo J. M., Ramos M., Torres A., Carreño F., Pérez J. I., Alfageme V. M., Redondo B.C., Velasco D., Pascual L., Pastor E. y González (2003): *Estudio de La Plataforma Continental Española. Hoja MC 050 - Cabo de Gata, Serie C, Modelos digitales y geomorfología. Promontorio de Cabo de Gata (Almería)*. Instituto Español de Oceanografía.



2nd International Tsunami Field Symposium

IGCP Project 495

Quaternary Land-Ocean Interactions:
Driving Mechanisms and Coastal Responses

Ostuni (Italy) and Ionian Islands (Greece) 22-28 September 2008



Project 495

Richmond B. M.¹, Jaffe B. E.¹, Gelfenbaum G.², Dudley W. C.³ **Recent Tsunami and Storm Wave Deposits, SE Hawaii**

¹U.S. Geological Survey, Santa Cruz, CA, e-mail: brichmond@usgs.gov; bjaffe@usgs.gov;

²U.S. Geological Survey, Menlo Park, CA, e-mail: ggelfenbaum@usgs.gov;

³University of Hawaii at Hilo, Hilo, e-mail: dudley@hawaii.edu

Keywords: *boulders, tsunami, storms, ridges, coastal morphology, Hawaii*

Deposits formed by extreme waves, such as those from large swells, storms, or tsunamis, leave a sedimentary record that can be useful in elucidating the type and characteristics of the depositional event. The island of Hawaii has been impacted by both storms and tsunamis (Goff and others, 2006) over the last century and is an ideal location to study deposits produced by such events (Fig 1). Basalt flows of known age occur along the southeastern coast of the island of Hawaii and are mantled by several types of extreme wave deposits.

These deposits (Fig. 2) can be characterized as:
1) Scattered gravel fields and occasional thin sand

sheets that extend up to several hundred meters inland. The gravel ranges in size from granules up to boulders (nearly 4 m a-axis) and consists of both angular (common) and rounded (rare) basalt fragments with occasional marine debris such as coral and shell material. The gravel field deposits are attributed to deposition from the locally generated 1975 Kalapana tsunami, and 2) Shore-parallel ridges composed mostly of basalt sand and/or gravel with variable amounts of carbonate detritus. The gravel tends to be mostly well rounded.

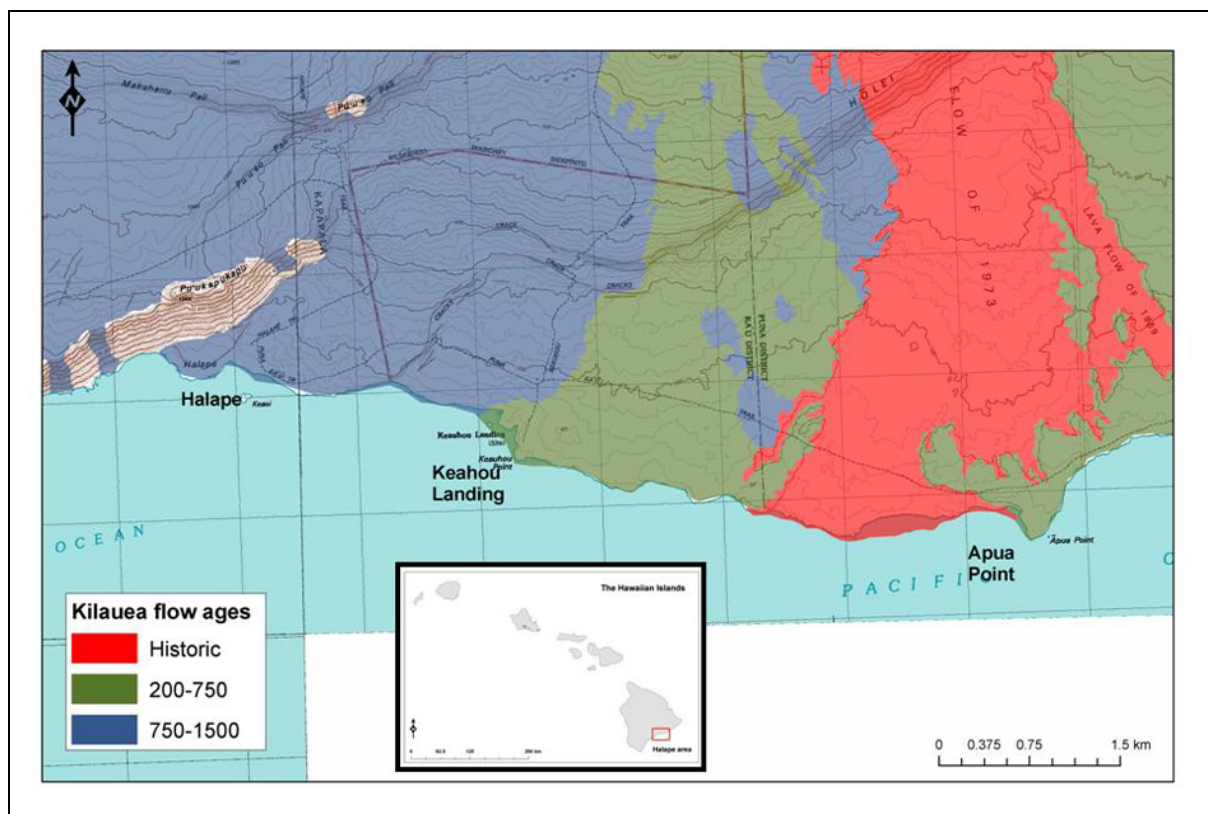


Figure 1. Map of study area on SE Hawaii showing ages of recent lava flows (geology from Wolfe & Morris, 1996).



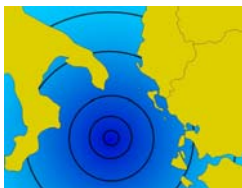
Figure 2. Oblique aerial photograph showing shore-parallel gravel ridge and isolated boulder field deposits (arrows) near Apua Point, SE Hawaii). The boulders rest on a 1973 lava flow and are within the inundation zone of the 1975 Halape tsunami

The ridges range in elevation from about 1 to 3 m and are tens of m wide. They occur either on elevated basalt platforms (1.0-6.5 m above sea level) where the ridges are set back from the cliff edge and separated from the edge by a narrow, sediment-free zone, or, as a supratidal extension of a pocket beach. No major tsunamis have impacted this area since November 1975 and there is photographic evidence that indicates the ridges have formed since the 1975 tsunami and are therefore the product of wave deposition during storms or long distance swell events. Results from this study provide useful information in

differentiating between storm and tsunami deposits in coarse clastic sediment.

References

- Goff J. Dudley W. C., deMaintenon M. J., Cain G., Coney J. P. (2006). *The largest local tsunami in 20th century Hawaii*. Marine Geology, 226, 65-79.
- Wolfe E. W., Morris J. (1996). *Geologic Map of the Island of Hawaii*, U.S. Geologic Survey, Misc. Investigations Series Map I-1-2524-A.



2nd International Tsunami Field Symposium

IGCP Project 495

Quaternary Land-Ocean Interactions:
Driving Mechanisms and Coastal Responses

Ostuni (Italy) and Ionian Islands (Greece) 22-28 September 2008



Project 495

Richmond B. M.¹, Jaffe B. E.¹, Gelfenbaum G.², Watt S.¹, Morton R. A.³

Spatial Characteristics of Coarse-Clast Deposits, Boca Olivia, NE Bonaire

¹U.S. Geological Survey, Santa Cruz, CA, e-mail: brichmond@usgs.gov;

²U.S. Geological Survey, Menlo Park, CA, e-mail: ggelfenbaum@usgs.gov;

³U.S. Geological Survey, Austin, TX, e-mail: rmorton@usgs.gov

Keywords: *boulders, tsunamis, storms, ridges, coastal morphology, Bonaire*

The coast of the island of Bonaire, Netherlands Antilles, contains numerous coarse-clast deposits formed during the Holocene by extreme wave events such as tsunamis and hurricanes (Scheffers 2005, Morton and others, 2006). A field mapping survey was conducted to determine the areal extent, spatial distribution, and origin of a mixed sand, pebble, cobble, and boulder sized sedimentary deposit at Boca Olivia, NE Bonaire (Fig. 1).

The deposit, which rests on an older Pleistocene reef platform approximately 4 to 7 m above present sea level, appears to have been formed by one or multiple extreme wave events (i.e. tsunamis or storms), or a combination of these events over time.

To characterize the deposits, size measurements and orientations were recorded for approximately 600 boulders and georeferenced using GPS and high-resolution aerial photographs collected using a

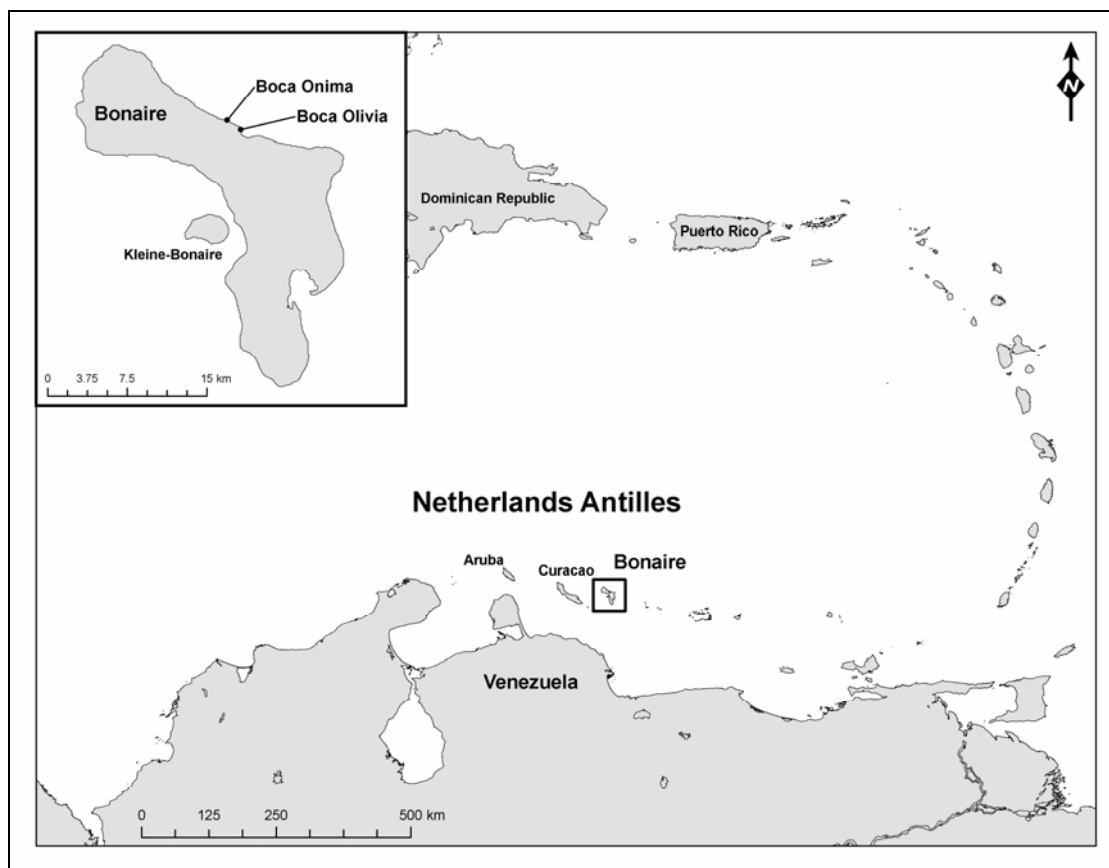


Figure 1. Location map of Bonaire in the southern Caribbean and the primary field site at Boca Olivia.

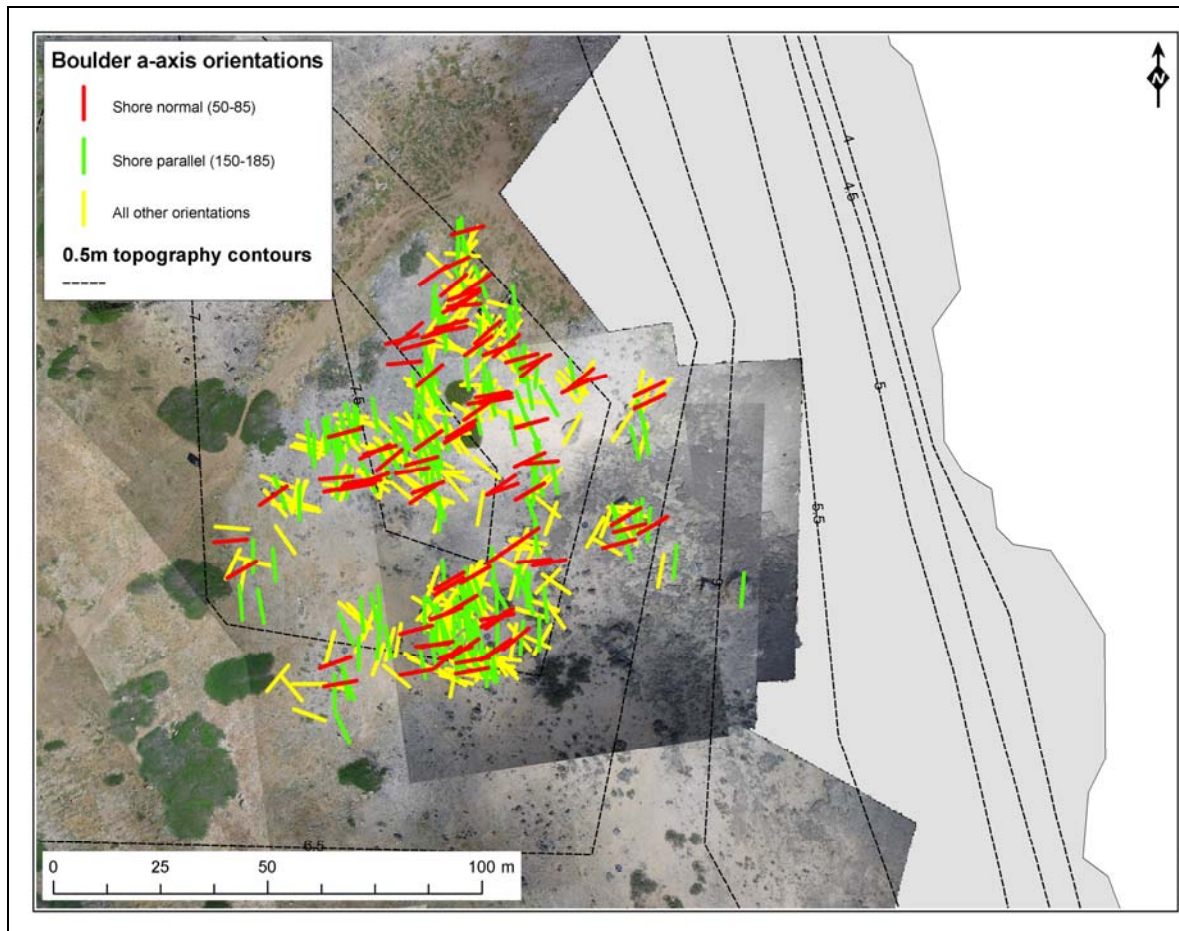


Figure 2. Diagram showing the a-axis orientation for approximately 500 boulders at Boca Olivia, NE Bonaire. Base photomosaic is from imagery collected with the kite cam in November, 2006.

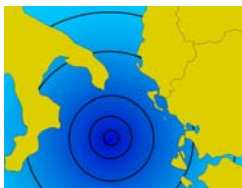
specially designed kite and digital camera system. In addition, topographic profile transects and geologic field observations were recorded. Boulders were mapped over nearly 5 kilometers of coastline with most measurements concentrated along roughly 500 meters in the Boca Olivia area (Fig 2).

Boulders were observed up to 250 meters inland from the shoreline and ranged in volume from 0.01 m³ to 74 m³. Approximately 80% of the boulders measured were smaller than 1.0 m³. The extent and spatial distribution of the boulders at Boca Olivia are similar to tsunami deposits described in Hawaii (Goff and others, 2006), and differ from shore-parallel ridge complexes described elsewhere on Bonaire. Mapping and analyzing spatial distributions of sedimentary deposits formed by past extreme wave events will help develop a greater understanding of the potential tsunami and

extreme storm risk for the Caribbean and other parts of the world.

References

- Goff J. Dudley W. C., deMaintenon M. J., Cain G., Coney J. P. (2006). *The largest local tsunami in 20th century Hawaii*. Marine Geology, 226, 65-79.
- Morton R. A. Richmond B. M., Jaffe B. E., Gelfenbaum G.m(2006). *Reconnaissance investigation of Caribbean extreme wave deposits-preliminary observations, interpretations, and research directions*. U.S. Geological Survey Open-File Report 2006-1293.
- Scheffers A. (2005). *Coastal response to extreme wave events – hurricanes and tsunami on Bonaire*. Essener Geographische Arbeiten 37, 100 pp.



Robinson E.¹, Khan S.¹, Rowe D. A.², Coutou R.¹

Size of shoreline boulders moved and emplaced by recent hurricanes, Jamaica

¹Marine Geology Unit, University of the West Indies, Kingston, Jamaica, e-mail: mgu@uwimona.edu.jm;

²Department of Geography & Development Studies, University of Chester, Park Gate Rd., UK
e-mail: d.rowe@chester.ac.uk

Keywords: boulders, hurricanes, tsunamis, Jamaica, Grand Cayman

Identification of sedimentary deposits on elevated coastal limestone platforms on Jamaica raised questions of origin of these deposits (Robinson et al., 2006; Rowe et al. in press). Based on form and distribution, these deposits were classified into three main categories; debris ridges,

perched beaches and isolated boulder strewns. During the period 2004 to 2007 the south coast of Jamaica was impacted by five hurricanes, all of which reached category 4 in the neighbourhood of Jamaica and three of which reached category 5 near the island (Figure 1).

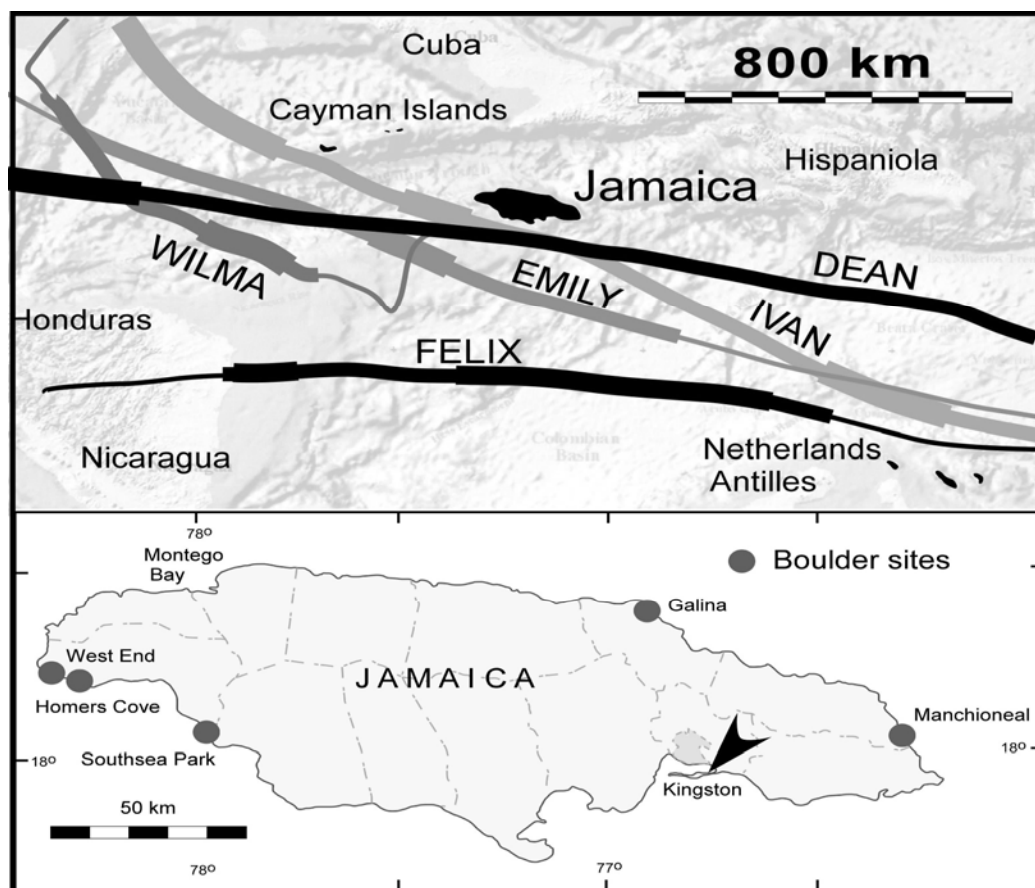


Figure 1. Tracks of five hurricanes passing south of Jamaica are Ivan, September 2004, Emily, July 2005, Wilma, October 2005, Dean August 2007 and Felix September 2007. Width of track indicates intensity: widest, category 5, medium width, category 4, narrowest, less than 4. In addition to the named boulder sites (dots) on the map of Jamaica, the boulder revetment described in the text lies on the Palisadoes peninsula south of Kingston (arrow).

These storms generated surges and wave run-up reaching as much as 5 m above sea-level and penetrated inland to distances exceeding 200 m in places, and surge and waves breaking over 12 m high cliffs in other places. Hurricanes Ivan and Dean generated the most onshore debris. These processes deposited sediments ranging from sand and coral fragments to large boulders and have provided additional insight on the emplacement and transport of debris on shore. Five sites were examined (labeled dots on Figure 1) that include boulders occurring naturally. A sixth site was serendipitously made available when a boulder revetment, constructed to protect the road from Kingston to the airport, was destroyed by hurricane Dean (arrow on Figure 1).

As part of the study we examined methods of estimating boulder mass, as there appear to be few published accounts of such methods. Previously we used an approach based on limiting parameters of geometric shapes using a relative density for limestone of 2.5 (Robinson et al. 2006). Here we developed two approaches. The first is based on volume and relative density determinations (water immersion) using small samples taken from the boulder localities. The second develops volume reconstructions using a graphics programme, based on oriented, calibrated field photographs of large boulders. Constants for both methods were developed to correct the notional volumes provided by measuring the standard a, b, and c axes of large boulders in the field.

For the water immersion method the mean volume correction constant is 0.40 (standard deviation 0.09). This was multiplied by the mean relative density of the limestones, as determined from the samples, (2.0) to calculate the boulder masses in Figure 2 and in the text. The second photographic method provides a similar correction factor but is still undergoing review. The mean relative density of 2.0 for the late Pleistocene limestones of which the boulders are composed, varies slightly from locality to locality, but are all substantially less than the figure of 2.5 used in Robinson et al. (2006), and in some publications on Bonaire (e.g. Scheffers, 2002).

At Galina the boulders were moved by earlier hurricanes, Allen (1980) and Gilbert (1988). At least one (4.5 t; Figure 2) was emplaced from the lower part of the six metre high cliff or as a loose block in the sea on the evidence of serpulids and barnacles dated as post-1950 (Robinson et al. 2006). The others were moved varying distances by Allen as indicated.

At Homers Cove some of the numerous boulders present have been moved repeatedly by storms (Figure 2). At least one (26 t) was emplaced about six metres onshore by hurricane Ivan and

another (12.2 t) by hurricane Dean (Figure 2). One of the largest measured (50 t) was moved 8.5 m by Ivan. At West End nearly all the boulders present were reported to have been moved during hurricane Ivan.

Total distances from the shoreline are indicated on Figure 2. Further work on boulders emplaced at these localities is in progress by one of us (D-AR). Hurricane Wilma emplaced small (0.5 to 1 t) boulders in a hotel on a cliff top at West End while the storm centre was over 600 km to the west (MGU 2008), as well as forming perched imbricated coral rubble beaches near Homers Cove.

At Southsea Park the largest boulder measured (18 t) was reported to have been moved a few metres by hurricane Ivan, when surge, run-up and waves breaking over the cliff top inundated the area for about 40 m inland (MGU, 2008).

At Manchioneal the largest onshore boulder encountered in Jamaica (80 t) was moved about 2 metres during hurricane Dean. It is now located on the limestone platform, 55 m from the top of the 12 m high cliff at this locality. On the cliff face there are scars from other blocks wrenched off by the storm, but none of these were seen on the platform surface.

On the Palisadoes peninsula, Kingston, a revetment was constructed on the ocean side of the peninsula by piling boulders, up to some 4-5 t each, to protect the road to the airport.

This followed massive washovers accompanying hurricane Ivan and, to a lesser extent, hurricane Emily.

In August 2007 Hurricane Dean destroyed the revetment, scattering many of the boulders for distances up to 50 m into the harbour. The sand loss from the 2 m high dunes along the peninsula subsequently allowed frequent minor washovers to recur during spring tides accompanied by NE tradewind-generated swells. Hurricanes Emily and Felix produced extensive washovers on Palisadoes but contributed little in the way of fresh debris.

The distribution of boulders on Grand Cayman was summarized in Robinson et al. (2006, figures 6 & 7) and ones that were probably moved in hurricane Ivan have been added to Figure 2.

We conclude that storm surge, wave run-up and waves breaking over cliff tops from severe hurricanes are able to move the largest coastal boulders (up to 80 t) yet encountered in Jamaica.

At Homers Cove two boulders, of 26 t and 12 t were emplaced on the limestone platform after being torn from the cliff face, respectively, by hurricanes Ivan and Dean. It is not known whether the largest boulders seen were originally emplaced by other giant wave mechanisms, such as tsunamis, and merely moved by hurricanes.

	Shore distance (m)	Mass (t)	Elevation (m)	Remarks
JAMAICA				
GALINA				
	152	5.97		MOVED SEVERAL METRES IN ALLEN
	102	6.36		VERMETIDS INDICATE RECENT EMPLACEMENT
	50	4.03		MAY HAVE MOVED SEVERAL METRES IN ALLEN
	25	4.48		EMPLACED DURING ALLEN OR GILBERT
	91	0.19		POSSIBLY MOVED IN ALLEN
MANCHIONEAL				
	55	79.74	12.0	MOVED 2 m DURING DEAN
		1.44		PROBABLY EMPLACED IN IVAN
HOMERS COVE				
	1	12.20	2.0	EMPLACED DURING DEAN
		11.36		REPORTEDLY EMPLACED IN A 1932 HURRICANE
		4.14		MOVED BY IVAN
		5.51		MOVED BY IVAN
		1.77		EMPLACED IN 1933 HURRICANE MOVED FURTHER BY IVAN
		2.35		EMPLACED IN 1933 HURRICANE MOVED FURTHER BY IVAN
		2.77		EMPLACED IN 1933 HURRICANE MOVED FURTHER BY IVAN
		3.16		EMPLACED IN 1933 HURRICANE MOVED FURTHER BY IVAN
		2.04		EMPLACED IN 1933 HURRICANE MOVED FURTHER BY IVAN
		7.67		EMPLACED BY GILBERT
		4.43		EMPLACED IN 1933 HURRICANE
	about 30 m	50.40		MOVED 8.5 m DURING IVAN
	about 6 m	26.40		EMPLACED BY IVAN
SOUTHSEA PARK				
	11	17.73	2.3	MOVED BY IVAN; UNAFFECTED BY DEAN
WEST END				
	70	0.62		MOST WESTEND BOULDERS WERE MOVED BY IVAN
	64	0.53		
	64	0.46		
	51	2.28		
	53	1.89		
	43	15.40		
	41	3.62		
	41	2.30		
	32	4.26		
	20	8.30		
	24	6.22		
	44	1.93		
	39	3.39		
	25	2.23		
	34	1.07		
	40	5.26		
	34	3.07		
	31	6.73		
	32	3.83		
	31	1.95		
	36	7.22		
	36	5.36		
	21	3.48		
	42	8.14		
	48	6.52		
	49	1.71		
	34	4.71		
	70	0.12		CONCRETE BLOCK FROM SHORELINE STAGE DESTROYED IN IVAN
	63	1.03		
GRAND CAYMAN				
BLOWHOLES				
	53	26.52	8.5	LARGEST MEASURED AT BLOWHOLES; EMPLACED IN IVAN?
PEDRO				
	22	5.39	8.0	OVERTURNED PROBABLY BY IVAN
	19	1.39	8.0	OVERTURNED BY IVAN
	76	0.08	14.0	OVERTURNED BY IVAN

Table 1. Tabulated list of boulders known to have been either moved or emplaced onshore by recent hurricanes on Jamaica and Grand Cayman.

Our documented repeated boulder movements imply that the Transport Figure used by Scheffers & Kelletat (2003) has little value as a measure of energy expended, except for known single event emplacements.

Our evidence suggests that the transport history of many, or most Jamaican boulders is complex, consisting of progressive movement across the coastal platforms by repeated storm action, perhaps extending back some 4000-5000 years, when

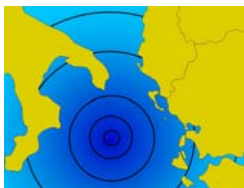
sea-level reached more or less its present elevation. Cumulative movements into zones where storm surge and inundation were reduced in intensity, and coastal forest vegetation increasingly inhibited further movement, have resulted in the boulders forming the debris ridges characteristic of the present coastline (Rowe et al. in press).

Aknowledgments

We thank Monique Johnson for valuable assistance in the field and laboratory. This study was supported by a grant from the Environmental Foundation of Jamaica

References

- Marine Geology Unit (2008). *Physical assessment of post-hurricane Dean shoreline damage and changes, Jamaica*. Open file report to the Environmental Foundation of Jamaica, 121 pages; appended locality maps, 1-16.
- Robinson E., Rowe D. A.C., Khan S. A. (2006). *Wave-emplaced boulders on Jamaica's rocky shores*. Zeitschrift für Geomorphologie, Suppl. Vol. 146, 39-57.
- Rowe D. A. C., Khan S. A., Robinson E. (in press). *Hurricanes or tsunami? Comparative analysis of extensive boulder arrays along the southwest and north coasts of Jamaica: implications for coastal management*. In Macgregor, M., Dodman, D. & Barker, D. (eds), Proceedings of a Conference on Global Change and Caribbean Vulnerability: Environment, Economy and Society at Risk, July 24-28, 2006,
- Scheffers A. (2002). *Paleotsunami in the Caribbean: Field evidences and datings from Aruba, Curaçao and Bonaire*. Essener Geographische Arbeiten, 33, 185 pp.
- Scheffers A., Kelletat D. (2003). *Sedimentologic and geomorphologic tsunami imprints worldwide – a review*. Earth Science Reviews, 63, 83-92.



Rodríguez-Vidal J.¹, Ruiz F.¹, Cáceres L. M.¹, Abad M.¹, Carretero M. I.², Pozo M.³

Morphosedimentary features of historical tsunamis in the Guadalquivir estuary (SW of Spain)

¹Departamento de Geodinámica y Paleontología, Facultad de CC. Experimentales, Campus del Carmen, Universidad de Huelva, Huelva, Spain

e-mail: jrvidal@uhu.es; ruizmu@uhu.es; mcaceres@uhu.es; manuel.abad@dgyp.uhu.es;

²Departamento de Cristalografía, Mineralogía y Química Agrícola, Universidad de Sevilla, Sevilla, Spain

e-mail: carre@us.es;

³Departamento de Geología y Geoquímica, Universidad Autónoma de Madrid, Madrid, Spain

e-mail: manuel.pozo@uam.es

Keywords: *Bioclastic ridge, tsunami, coastal morphology, Holocene, Guadalquivir river, Spain*

The southwestern Spanish coast is a low-probability tsunamigenic zone (Reicherter, 2001). The oldest four historical tsunamis occurred between 218 BC and 209 BC and their effects have been documented in the southern coasts of Spain (Galbis, 1932; Campos, 1991). Nevertheless, the geological record of these high-energy events is still poorly known (Luque, 2002; Ruiz et al., 2004; 2005). The Guadalquivir River (560 km long) is partly blocked in the lower reach by sandy barriers, resulting in a large estuary (1800 km²). On the southwestern sector (Fig. 1), this estuary includes the Doñana National Park, one of the largest wetlands (50,720 ha) in Europe. This area is a UNESCO World Heritage. The main geomorphological features of this area have been analyzed by Rodríguez Ramírez (1996), with the delimitation of the fluvial levees flanking the river and its former courses. They are orientated mainly in north-south and west-east directions. These clay-rich levees have a variable width (300–1500 m) and length (up to 3–5 km), reaching heights of 0.8–1 m above the adjacent marshes. The “hills” (1–2.5 m above the marsh level) are occupied by sandy littoral ridges with a SW–NE orientation (e.g., Vetalengua) and some levees overlain by characteristic accumulations of bivalves, with beach ridge morphologies (Fig. 1). These hills are elongated (3–6 km), with a narrow width (20–30 m) and thickness (0.5–0.7 m).

The geomorphological mapping and new data obtained from two short cores (Fig. 1: A-B) collected and dated in the Vetalengua area (Ruiz et al., 2004; Rodríguez-Ramírez et al., 2004) permit to reconstruct the palaeogeographical evolution of this area in the last 2400 years and to explain the

present geomorphologic features. Grain-size distribution, mineralogy, macrofossil, microfossil and radiocarbon analysis (mollusc shell) of selected samples was carried out. Five phases are distinguished (Fig. 1):

Phase 1 (> 2400 cal. yr BP or > 218 BC). Near the base of core A, the scarce ostracode assemblage extracted (*Cyprideis torosa*, *Loxoconcha elliptica*, *Leptocythere castanea*) and the presence of numerous roots are indicative of a low marsh environment, adjacent to a brackish lagoon (salinity < 25–30‰). These species characterize the inner, shallow areas of recent lagoons with marine connection, located near the lagoon shore and close to a river mouth. This palaeogeographical reconstruction coincides with the first historical description of this estuary, the Roman *Lacus Ligustinus*.

Phase 2 (~ 2400–2200 cal. yr BP or ~218–209 BC). Between 2400 and 2200 cal. yr BP, two erosive periods occurred in this area, both recorded in core A. A first period deposited a bioclastic, silty bed (25 cm thickness) with numerous fragments of bivalves (mainly *Cardium edule*) and gastropods over the previous marshes. This bed has an erosive base and presents high proportions of quartz (75 %), with feldspars and phyllosilicates as accessory components. This event may be assimilated to the tsunamis that occurred at 218–216 BC in this area (Campos, 1991). In a second period, a tsunami (or tsunamis) brooked the Doñana spit and opened a new communication with the sea, with the generation of washover fan deposits represented in the upper part of core A. These washover fans were formed by azoic fine sands (88 % quartz) and proceed from the erosion of the Doñana spit, which

has a similar mineralogical composition. These sands are deposited over the previous bioclastic layer without any intermediate deposits. Consequently, this event may be assimilated to the following historical tsunamis recorded in this area (210-209 BC; Campos, 1991). This bioclastic bed is disposed almost perpendicular to the Doñana spit and show a SW-NE direction, with a southeastern corner that coincides with a clear erosive rupture on the dune systems of this spit. In this corner, the Doñana spit shows a remarkable slimming of its width, passing from almost 5 km (to the northwestern) to 2.5 km (to the southeastern).

Phase 3 (2200-1700 cal. yr BP). This area was progressively isolated, with the creation of a shallow, freshwater lagoon. Massive grey clayey silt was deposited in the bottom lagoon (core B: 100-80 cm depth), with low percentages of sands (< 5 %). The main components of these fines sediments were phyllosilicates (61%), calcite (23%)

and quartz (10%). Microfauna is characterized by abundant populations of the freshwater ostracod *Cypridopsis vidua*, together with scarce oogonia of characeans (*Chara* sp.). In addition, the scarce macrofauna is dominated by marine bivalves (*Donax*, *Diluvarca*, *Spisula*), pulmonate gastropods (*Melanopsis* sp.) and fragments of other marine groups (scaphopods, bryozoans and spines of echinoderms).

The following 20 cm of core B (80-60 cm depth) show a similar lithology, but they are characterized by the absence of marine faunas and the presence of fragmentary specimens of *Cardium edule* and *Melanopsis* sp. The ostracod population is progressively scarcer toward the top, with *Cypridopsis vidua* as dominant species together with other freshwater ostracod species (*Ilyocypris gibba*, *Herpetocypris chevreuxi*, *Cyprinotus salinus*).

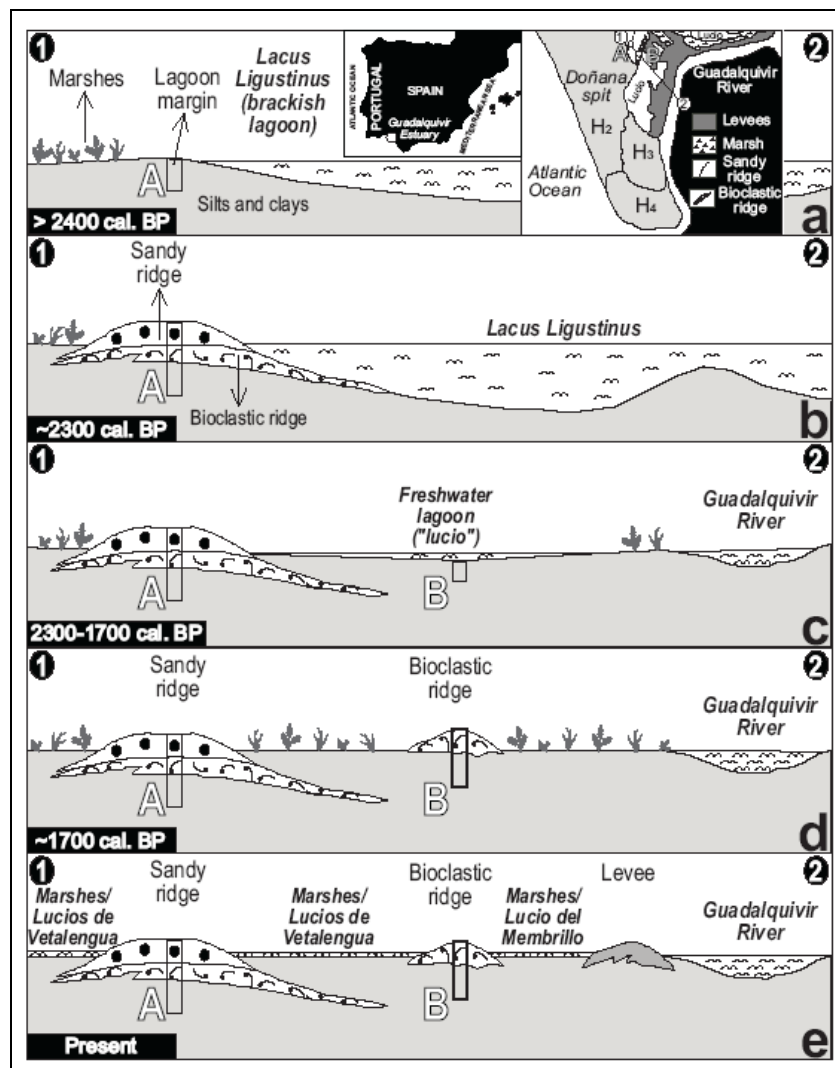


Figure 1. The River Guadalquivir estuary and the studied area. H_{2,4} are Holocene regional phases of spit progradation. 1-2, morphological section and morphosedimentary evolution from 2400 cal. BP to present. A & B, short cores.

In addition, numerous rests of plants and sulphurs were also observed in the upper centimetres, where characeans disappear. These features indicate an increasing subaerial exposure, which causes the sulphur formation. This exposure is a negative factor for the ostracod development and may explain the ostracod decrease. The disappearance of marine faunas may be due to the restriction of the tidal connection. Between 60 and 50 cm depth, this core is formed by sandy silt. They have moderate phyllosilicate contents (46 %) and quartz (21%) dominates over calcite (16%). Fragments of bivalves and gastropods are frequent and explain the aragonite percentages (8 %). Ostracods are very rare (*C. vidua*, *I. gibba*). This facies represents the transition to subaerial conditions, with the predominance of pulmonate gastropods (*Melanopsis*). Consequently, the sedimentological and faunal features of this core reveal a continuous process of emersion in a shallow, freshwater lagoon located near the Doñana spit.

Phase 4 (~1700 cal. yr BP). A new high-energy event was registered, with the presence of a large bioclastic ridge consisting of both lagoon (*Cardium*) and marine (*Diluvaca*, *Donax*, *Spisula*) disposed over the freshwater lagoon deposits in the upper 50 cm of core B. This ridge has a lateral extension up to 4 km, being constituted by bioclastic silts with important percentages of sands (up to 20 %). These sediments exhibit a crude lamination and an erosive base that separated them from the underlying levels. Fragments of reworked marine bivalves (*Diluvaca diluvii*, *Donax vittatus*, *Spisula solida*) and gastropods (*Lemintina arenaria*) are very abundant near the base, being represented mainly by juvenile specimens (< 2 cm length). This abundance of bioclasts explains the high percentages of aragonite (34 %) in comparison with phyllosilicates (20 %), feldspars (20 %) and quartz (16 %). In this basal zone, freshwater ostracods are absent. The upper centimetres of the core are characterized by similar sediments, but they contain freshwater ostracods, sulphurs and fragments of plants. The abundance of bioclasts explains the high percentages of aragonite (34 %), which is dominant over phyllosilicates (20 %), feldspars (20 %) and quartz (16%). The presence of freshwater species may be due to a temporal inundation of this area after the high-energy event.

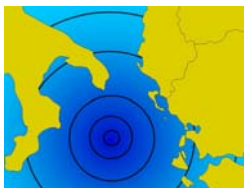
Phase 5 (1700 cal. yr BP-Present). A continuous infilling was observed, with the growing of the fluvial levees and the presence of several freshwater lagoons separated by sandy or bioclastic ridges, which are caused by the high-energy events indicated previously.

Acknowledgments

This work was funded by two Spanish DGYCIT Projects (CTM2006-06722/MAR and CGL2006-01412/BTE) and three Research Groups of the Andalusia Board (RNM-002, RNM-238 and RNM-293).

References

- Campos M. L. (1991). *Tsunami hazard on the Spanish coasts of the Iberian Peninsula*. The Science of Tsunami Hazards, 9, 83-90.
- Galbis R. J. (1932). *Catálogo sísmico de la zona comprendida entre los meridianos 58^o E y 20^o W de Greenwich y los paralelos 45^o y 25^o N*. Dirección General del Instituto Geográfico. Catastral y de Estadística, Madrid, Spain.
- Luque L. (2002). *Cambios en los paleoambientes costeros del sur de la Península Ibérica (España) durante el Holoceno*. PhD Thesis, CSIC-Universidad Complutense de Madrid, Spain.
- Reicherter K. (2001). *Paleoseismological advances in the Granada Basin (Betic Cordilleras, southern Spain)*. Acta Geologica Hispanica, 36, 267-281.
- Rodríguez-Ramírez A. (1996). *Geomorfología continental y submarina del Golfo de Cádiz (Guadiana-Guadalquivir)*. PhD. Thesis. Huelva University, Spain.
- Rodríguez-Ramírez, A., Ruiz, F., Abad, M., Cáceres, L.M., Rodríguez-Vidal, J., Pino, R., Muñoz, J.M. (2004). *Geomorphological and microfaunal evidences of high-energy events in the Holocene record of the Doñana National Park (SW Spain)*. Abstracts International Workshop on Methods for Determining and Representing Coastal Hazards, Faro, Portugal.
- Ruiz F., Rodríguez-Ramírez A., Cáceres L. M., Rodríguez Vidal J., Carretero M. I., Clemente L., Muñoz J. M., Yáñez C., Abad M. (2004). *Late Holocene evolution of the southwestern Doñana National Park (Guadalquivir Estuary, SW Spain): a multivariate approach*. Palaeogeography, Palaeoclimatology, Palaeoecology, 204, 47-64.
- Ruiz F., Rodríguez-Ramírez A., Cáceres L., Rodríguez Vidal J., Carretero M. I., Abad M., Olías M., Pozo M. (2005). *Evidences of high-energy events in the geological record: Mid-Holocene evolution of the southwestern Doñana National Park (SW Spain)*. Palaeogeography, Palaeoclimatology, Palaeoecology, 229, 212-229.



2nd International Tsunami Field Symposium

IGCP Project 495

Quaternary Land-Ocean Interactions:
Driving Mechanisms and Coastal Responses

Ostuni (Italy) and Ionian Islands (Greece) 22-28 September 2008



Project 495

Rössler S.¹, Reicherter K.¹, Papanikolaou I.^{2,3}, Roger J.⁴,

Tsunami Group: Mathes-Schmidt M., Grützner C.

In search of the 479 BC Tsunami and its sediments in the Thermaikos Gulf area (northern Greece)

¹Inst. of Neotectonics and Natural Hazards, RWTH Aachen University, Germany

e-mail: s.roessler@nug.rwth-aachen.de; k.reicherter@nug.rwth-aachen.de;

²Laboratory of Natural Hazards, National and Kapodistrian University of Athens, Greece

³Benfield-UCL Hazard Research Centre, University College London, UK

e-mail: i.papanikolaou@ucl.ac.uk;

⁴CEA-DASE, Bruyères-le-Châtel, France, e-mail: jean.roger@cea.fr

Keywords: *Tsunamites, Aegean Sea, Thermaikos Gulf, Greece*

The Herodotus Histories report on a series of large waves and sea withdrawals occurring in 479 BC during the Persian-Greek war. Large portions of the Persian troops perished by drowning near Potidaea, western Chalkidiki peninsula (e.g. Papazachos & Papazachou, 1989) (Fig. 1A, Fig. 2A). Therefore, Herodotus's report is regarded as the first description of a historical tsunami (e.g. Bolt, 1978). Our Greek-German project involves the extraction and study of sediment cores from coastal deposits of the Thermaikos Gulf in Northern Greece, in order to identify paleotsunami deposits and to correlate them to the activity of faults from the North Aegean Basin (Fig. 1B). We concentrated on three localities along the eastern coast of the Thermaikos Gulf between Thessalonica and Chalkidiki peninsula. These areas are exposed towards the South, where the possible tsunami source is situated. Spit bars and lagunas serve as archives for tsunamites as their topography allows the conservation of a tsunami record. Furthermore, we probed two sites on the western shore of the bay.

About 200 m of cores were drilled during the field campaign in fall 2007, which have been analyzed and sampled in the lab (Fig. 1C). Sedimentological analyses include sieving, washing, and laboratory core description. Magnetic susceptibility on cores has been measured and micropaleontological samples have been picked (foraminifera, shells) (Fig. 1C).

As a preliminary result, we have found several coarse clastic layers intercalated in fine-grained laguna deposits. Those have erosive bases, show fining-up and thinning up sequences, and include shell debris and rip-up clasts of laguna sediments.

Multiple intercalations of these layers downhole are interpreted as either paleotsunamis of repeated earthquake activity or tsunami-like waves induced by submarine slides triggered by seismic shaking in the Thermaikos Gulf.

In a second campaign in fall 2008 will help to intensify our net of tsunami information, with drilling and – for the first time – tsunami trenching, along the northern Aegean coast. Other future tasks are:

Clay mineralogy of tsunamites;

Characterization of organic matter (biomarker studies, terrestrial vs. marine);

Dating of the sediments (radiocarbon, mainly charcoal and shells);

Geoarcheological studies in Potidea, Kassandra (deposits of the Greek epoch);

This project aims to: a) to verify whether a tsunami occurred in 479 BC, b) to identify whether other unknown tsunami deposits can be traced in the Thermaikos Gulf coastal sediments, c) to assess the tsunami hazard, d) to assess the seismic hazard by calculating the recurrence interval of the oblique normal fault located in the southwestern part of the North Aegean Basin, indirectly through the tsunami recordings.

Recent offshore studies have underpinned the possibility of a tsunami generation that could affect the Thermaikos Gulf, caused by an activation of an oblique normal fault located in the western part of the North Aegean basin (Fig. 2B).

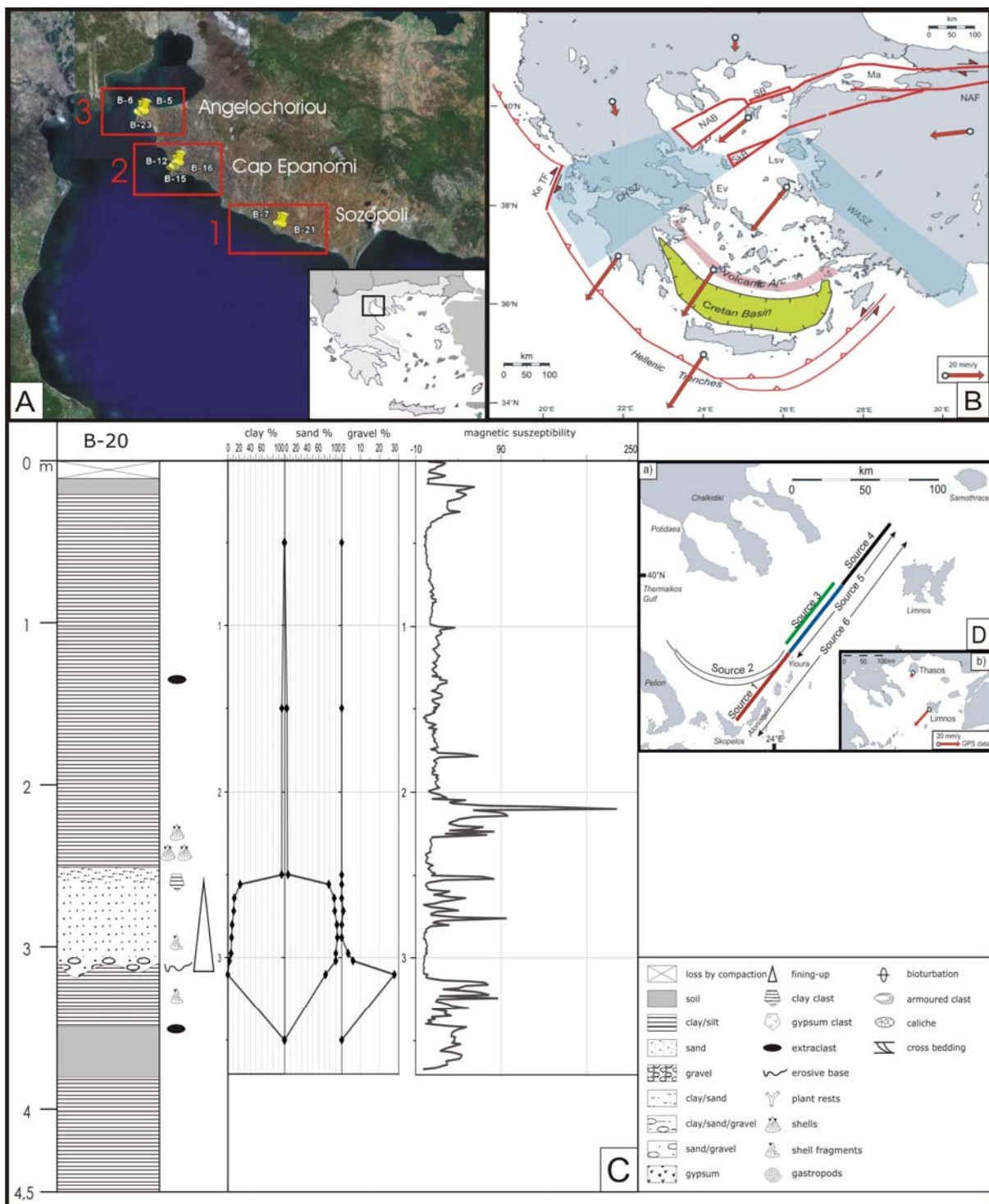


Figure 1. **A.** Working area in the Theraikos Gulf in the northernmost part of the Aegean Sea. **B.** Tectonic setting of the North Aegean Basin (NAB). **C.** Core-log of B-20 in Sozopol, stratigraphy, magnetic susceptibility and grain size variation (clay/silt < 63 μm, sand 63 μm–2 mm and gravel > 2 mm). **D.** (a) sketch map of the different seismic sources used for the tsunami modelling. (b) GPS rates show a remarkable difference of velocity values northwards and southwards of the NAB. Based on the measurements of McClusky et al. (2003) and references therein, the slip-rate difference between the islands of Thasos and Limnos is 16 ± 2 mm/yr. Source 1 represents a ~55 km long oblique normal fault segment, accommodating a vertical and horizontal displacement that might generate a $M=7.1$ event, producing a maximum vertical offset of up to 3–4 m, posing also a tsunami threat apart from submarine landslides. The other seismic sources mainly represent strike-slip faults. The dominant structure is a 160 km long NE-SW trending fault (source 6), comprising a multi-rupture segment.

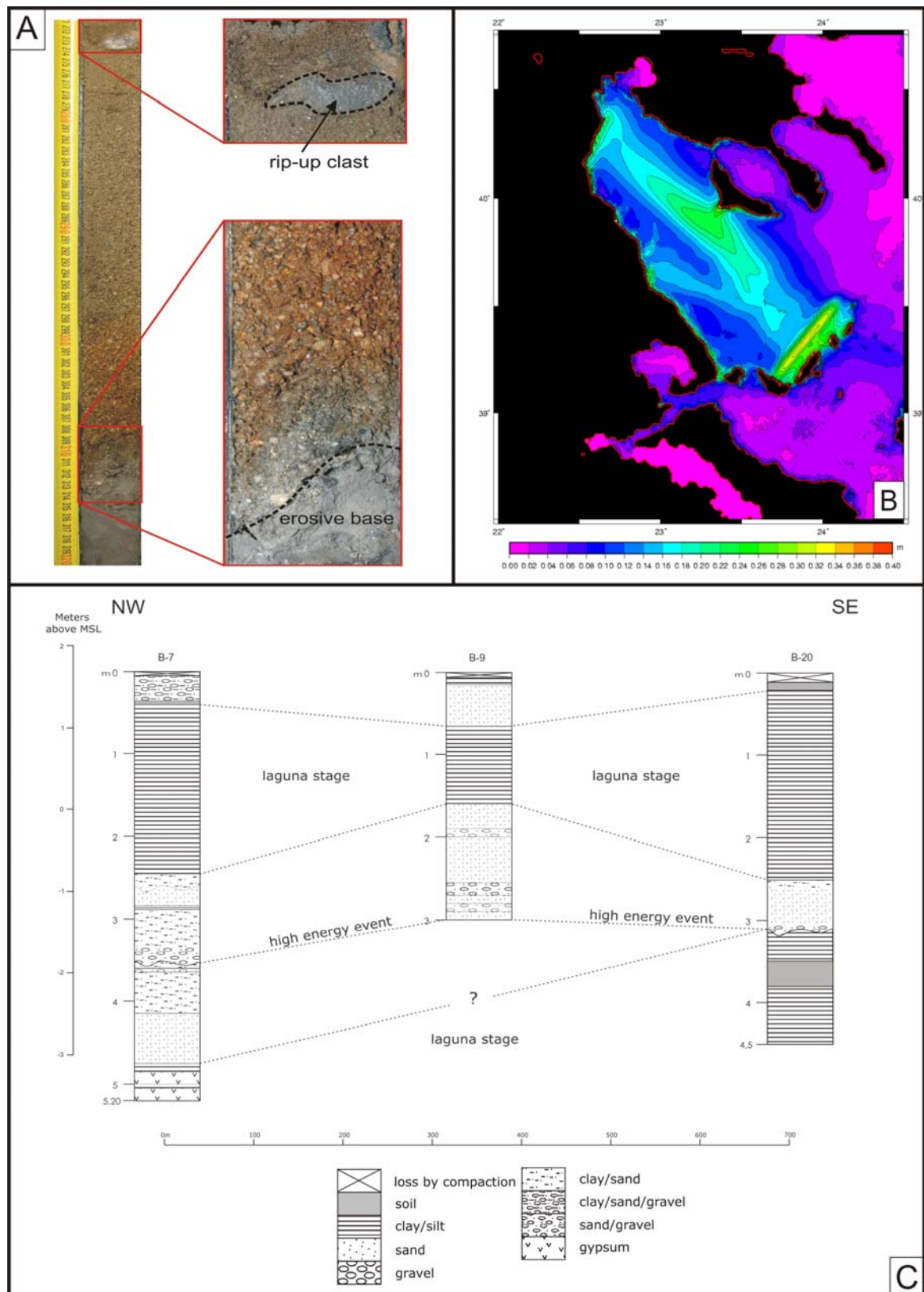
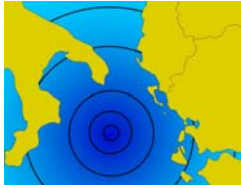


Figure 2. **A.** Tsunami modelling of the propagating wave fronts including all seismic sources and data (by Jean Roger): length 160 km, width 5 km, dip 60°, coseismic slip 4m, and rake 180° of the fault plane. **B.** Photo and details of core B-20 from the southernmost location (Sozopoli, see Fig.1A) with a sandy interval within laguna deposits, about 25 km NW of the place of the Herodotus' descriptions. This interval is interpreted as a paleo-tsunami with a coarse-grained erosive base forming a distinct fining-up sequence including rip-up clasts and open marine shell debris. **C.** Drill logs of all Sozopoli cores. The section is approximately 100 m from the parallel beach at the eastern part of the Thermaikos Gulf. Evidence for one high-energy event (up to 24 cm thick layer) in 2 cores close to the beach and also in a more distal drill hole.

The geodynamic framework in the study area is dominated by the western termination of the North Anatolian Fault Zone with steep normal faults with strike-slip, separated in several segments, which can host an M 7 earthquake associated with a vertical displacement of approx. 3 m (Papanikolaou and Papanikolaou, 2007) (Fig. 2C).

References

- Bolt B.A., (1978). Earthquakes. Freeman and Company, San Francisco, 241pp.
- McClusky S., Reilinger R., Mahmoud S., Ben Sari D., Tealeb A. (2003). *GPS constraints on Africa (Nubia) and Arabia plate motions*. Geophys. J. Int. 155, 126-138.
- Papanikolaou I., Papanikolaou D. (2007). *Seismic hazard scenarios from the longest geologically constrained active fault of the Aegean*. Quat. Int., 171-172, 31-44.
- Papazachos B. C., Papazachou C. B. (1989). *The Earthquakes of Greece*. Ziti Publications, Thessalonica, 356 pp. (in Greek).



2nd International Tsunami Field Symposium

IGCP Project 495

Quaternary Land-Ocean Interactions:
Driving Mechanisms and Coastal Responses

Ostuni (Italy) and Ionian Islands (Greece) 22-28 September 2008



Project 495

Rowe D. A.¹, Degg M.¹, France D.¹, Miller S.¹

Tsunami Hazard Mapping, SW Jamaica

¹Department of Geography and Development Studies, University of Chester, United Kingdom,
e-mail: d.rowe@chester.ac.uk

Keywords: *Tsunami, hazard mapping, vulnerability, hazard perception, Jamaica*

Historical records show that the island of Jamaica in the northwestern Caribbean has been affected by significant tsunami impacts during the period 1688-1907 (Lander *et al.*, 1999, 2002). Some of the largest of these are now known to have been generated close to the island (Fig. 1), most probably through nearshore submarine landsliding (Lander *et al.*, 2002), but significant events have also originated further afield along the active tectonic zones of the eastern Caribbean. Notable documented tsunami impacts in the island's history include those at Port Royal on the south coast in 1692 and at Annotto Bay on the north coast in 1907 (Lander *et al.*, 2002). In addition wave-emplaced boulder fields along the island's northern and western coastal margins (Robinson *et al.* 2006) may reflect the impact of larger pre-historical tsunami events during the Holocene.

Miller (2005) produced the first generalised tsunami hazard map for the island and showed that significant areas of existing and proposed coastal development are potentially at risk from small to moderate tsunami wave impacts (Fig. 2). This paper

reports on the first two years of a PhD project aimed at characterising the nature of the tsunami hazard and risk in one of these areas – along the island's SW coastal margin where a number of communities with contrasting demographic and socio-economic profiles are potentially at risk (Fig. 1). The work has included:

- mapping of (wave-emplaced) boulder assemblages along parts of the coastal margin, to extend work of this nature conducted elsewhere on the island;
- coring of low-lying (morass) coastal areas to seek sedimentary traces of historical tsunami/storm surge events;
- use of a Geographical Information System (GIS) to model possible tsunami run-up distances in low-lying coastal areas and possible impact on communities
- a questionnaire survey of local people's perception of (and response to) tsunami hazard, in relation to the perceived threat posed by other natural hazards such as hurricane.



Figure 1. Map of fieldwork locations in Jamaica and historical tsunami events (after Miller, 2005).

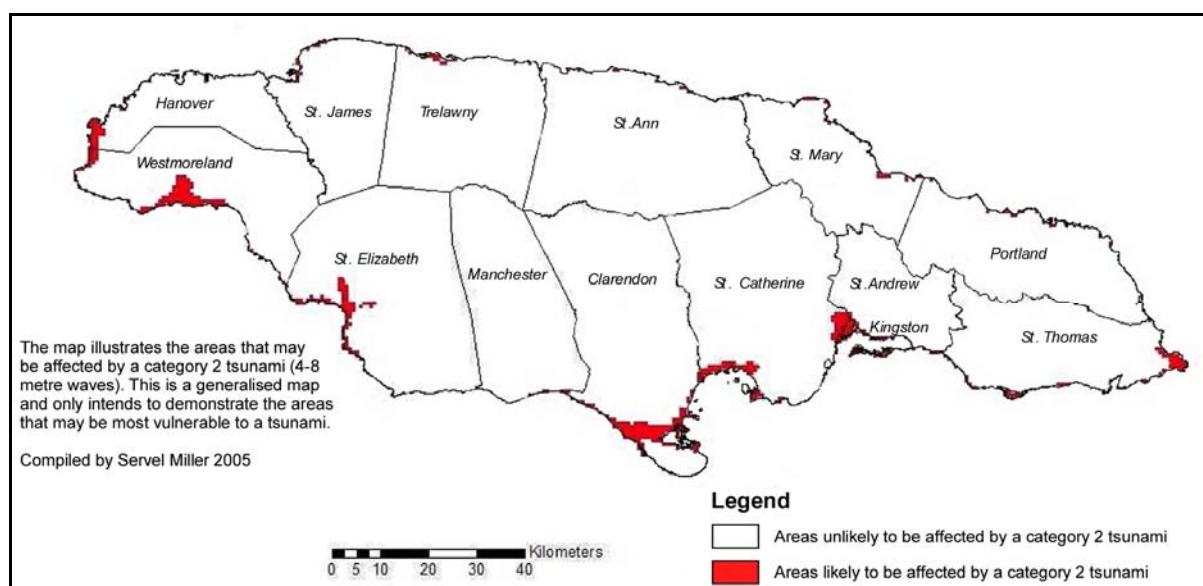
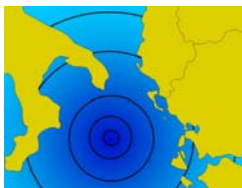


Figure 2. Generalised tsunami hazard map of Jamaica.

The paper reports on progress to date and, in particular, on the findings as they pertain to the communities at risk within the study area. The applicability of the work to other parts of the island is also considered.

References

- Lander J. F., Whiteside L., O'Loughlin K. (1999) *Proceedings Tsunami Symposium*. Honolulu, Hawaii USA, (May 25-27).
- Lander J. F., Whiteside L. S., Lockridge P. A. (2002). *A brief history of tsunamis in the Caribbean*. Science of Tsunami Hazards, 20, 2, 57-94.
- Miller S. (2005). *Preliminary tsunami hazard mapping for Jamaica*. 17th Caribbean Geological Conference, San Juan, Puerto Rico, July 17-24, 2005.
- Robinson E., Rowe D. A., Khan S. (2006). *Wave-emplaced boulders on Jamaica's rocky shores*. Z. Geomorph. N.F., Suppl.-Vol. 146, 39-57.



2nd International Tsunami Field Symposium

IGCP Project 495

Quaternary Land-Ocean Interactions:
Driving Mechanisms and Coastal Responses

Ostuni (Italy) and Ionian Islands (Greece) 22-28 September 2008



Project 495

Sansò P.¹, Bianco F.², Cataldo R.², Vitale A.³

A web site for historical tsunamis of Salento (Apulia, Italy)

¹Osservatorio di Chimica, Fisica e Geologia ambientale, Dip. di Scienza dei Materiali, Università del Salento, Italy, e-mail: paolo.sanso@unile.it;

²Dip. di Scienza dei Materiali, Università del Salento, Italy, e-mail: rosella.cataldo@unile.it;

³Collaboratore esterno presso l'Osservatorio di Chimica, Fisica e Geologia ambientale, Dip. di Scienza dei Materiali, Università del Salento, Italy, e-mail: vitaleandrea@inwind.it

Keywords: boulders, tsunamis, MapServer, vulnerability, Salento

Out-of-size landforms occurring in a coastal landscape can be used to prove the occurrence of paleotsunamis. This is especially true for regions dominated by a low-energy wave climate, such as Salento coast which is marked by the presence of large boulder accumulations. Boulder accumulations studied along the rocky coast of Salento suggest the occurrence of three recent tsunamis, most likely related to the strong earthquakes of the 5th December 1456 (Mastronuzzi & Sansò, 2000), 6th April 1667 (Mastronuzzi & Sansò, 2004), 20th February 1743 (Mastronuzzi & Sansò, 2004; Mastronuzzi et al., 2007)

The growing urbanization of the coastal area raises the risk linked of low frequency - high magnitude events, like tsunamis. These phenomena are rarely taken into account by planners, with the exception of particular high-developed areas where the high frequency and intensity of these phenomena have imposed the realization of structures and procedures for the mitigation of the tsunami risk.

Consequently, an interactive application that can be accessed on the web has been developed to raise awareness of the phenomenon of tsunami.

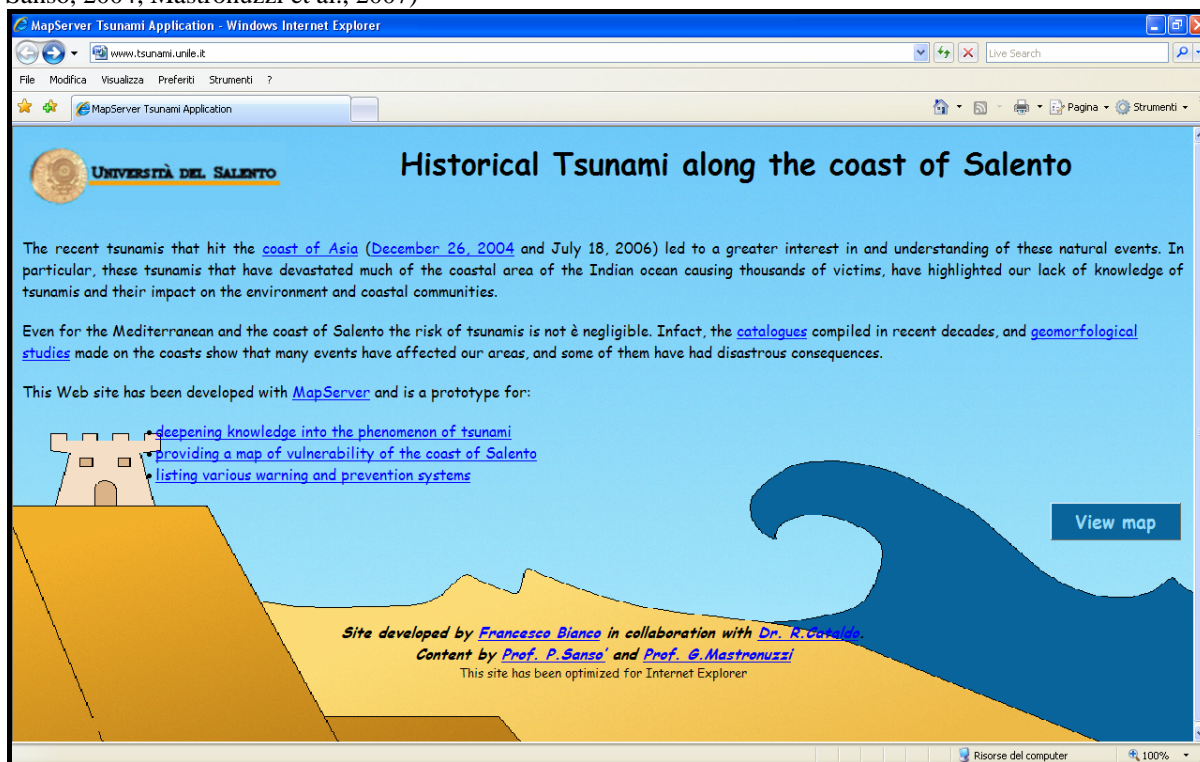


Figure 1. Home page of historical tsunami along the coast of Salento.

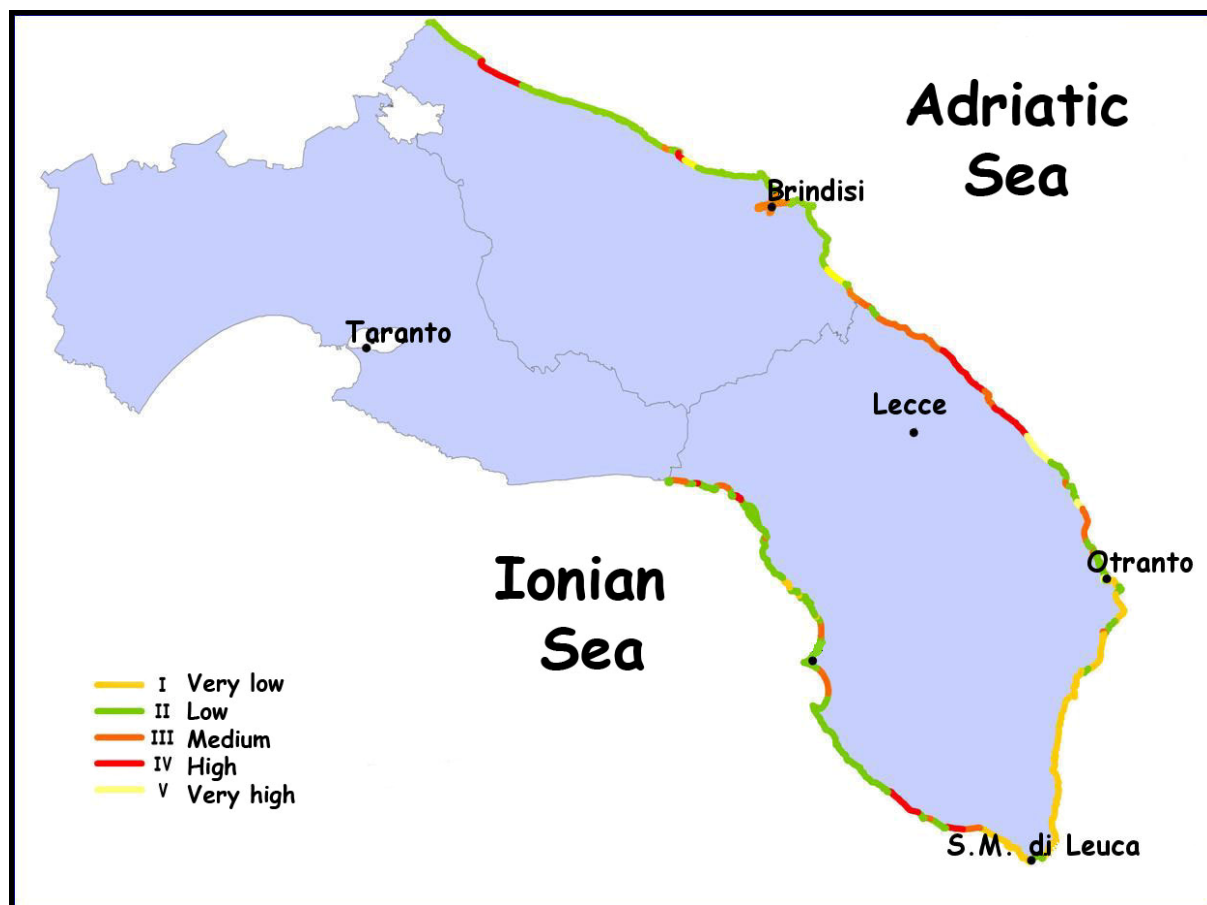


Figure 2. Vulnerability of Salento coasts to tsunami action.

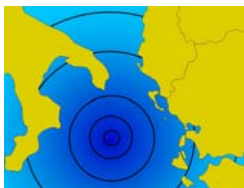
A WebGIS software has been used to produce this application. GIS is the acronym that stands for Geographic Information System; it is a set of tools for collecting, storing, retrieving at will, transforming and displaying spatial data from the real world for a particular set of purposes (Burrough P.A., 1986). A WebGIS is a GIS application made available through a common web browser. The software that has been used is MapServer: it is an Open Source development environment for building spatially-enabled internet applications; it allows you to create "geographic image maps", i.e. maps that can direct users to content. MapServer was originally developed by the University of Minnesota with support from NASA, which needed a way to make its satellite imagery available to the public.

The prototype produced (Fig. 1) contains several information on the phenomenon of tsunami (what they are and how they are generated) along with a catalog of tsunami that occurred in the world and in Italy. Moreover a number of photos about boulder accumulations studied in Salento and a map

of vulnerability (Fig. 2) of the coast of Salento are provided.

References

- Burrough P.A. (1986). *Principles of geographical information systems for land resource assessment*, Clarendon Press, Oxford, U.K, 194.
- Mastronuzzi G., Sansò P. (2000). *Boulders transport by catastrophic waves along the Ionian coast of Apulia (southern Italy)*. Marine Geology, 170, 93-103.
- Mastronuzzi G., Sansò P. (2004). *Large boulder accumulations by extreme waves along the Adriatic coast of southern Apulia (Italy)*. Quaternary International, 120, 173-184.
- Mastronuzzi G., Sansò P., Selleri G., Pignatelli C. (2007). *Boulder accumulation produced by the 20th of February 1743 tsunami along the coast of southernstern Salento (Apulia region, Italy)*. Marine Geology, 242, 191-205.



2nd International Tsunami Field Symposium

IGCP Project 495

Quaternary Land-Ocean Interactions:
Driving Mechanisms and Coastal Responses

Ostuni (Italy) and Ionian Islands (Greece) 22-28 September 2008



Project 495

Scheffers A.¹, Kelletat D.², Browne T.³

Wave-emplaced Coarse Debris and Mega-clasts in Ireland and Scotland: A Contribution to the Question of Boulder Transport in the Littoral Environment

¹School of Environmental Science and Management, Southern Cross University, Lismore Campus,
Australia, e-mail: anja.scheffers@scu.edu.au;

²Geographisches Institut der Universität Köln, Germany, e-mail: dieter.kelletat@t-online.de;

³ School of Environmental Science and Management, Southern Cross University, Lismore Campus,
Australia, e-mail: tony.browne@scu.edu.au

Keywords: *boulder transport, storms, tsunamis, dating, Ireland, Scotland*

Coastal boulder deposits had never found specific scientific interest in earlier years. They only came into discussion with the developing of paleo-tsunami field research more than 20 years ago, but this discussion is still highly controversial regarding the processes involved (storms or tsunamis). Some authors argue that former storms may have had much more power than those of today's category 5 hurricanes, which has been rejected by others because of physical restrictions. Task forces to inspect modern strong tsunamis nearly exclusively deal with fine sediments, and so do review articles on "tsunami deposits". While tsunamis cannot be excluded for any kind of coastal deposits, storms may well be, in particular if the clasts are too large for storm-wave dislocation.

The situation now is that we observe a large group of coastal researchers in the section of 'tempestologists' as well as a rising number of fellow scientists in the group of 'tsunamiists' (similar to the 'neptunists' and 'plutonists' among geologists around 1800 AD). In this dispute on storm or tsunami transport of very large boulders (20–50 t and more) field work from Ireland and northern Scotland has been published (Williams, 2004; Williams & Hall, 2004; Hansom, 2004; Hall et al., 2006) with observations on mega-clasts along steep and high coastlines, deposited up to 50 m asl in places (so-called cliff-top mega-clasts) by extreme storm waves, as the authors conclude.

All the deposits (with clasts up to several hundred tons in weight in the lower parts and several tons near 50 m asl) are said to be modern in age and in harmony with contemporary storm processes. Williams (2004) additionally argues that cliff retreat and coastal abrasion, is, on average, 0.4

m/year, or 1 km since the Iron Age. No one, however, argues with objective physical calculations for boulder transport, or supports his arguments by direct observation of extremely large boulders transported by storm waves at high places and far from the shoreline – evidently because this kind of observation does not exist!

Jonathan Nott (2003) has tried to fill the gap by equations concerning boulder movements from a subaerial, submerged or joint-bound position. The equations result in wave heights deserved 'to overturn boulders' of certain forms and weights. For the joint-bound scenario (which is the normal case in cliff destruction in Ireland and Scotland) he generally found that a storm wave has to be 4 times as high as a tsunami wave to result in the same transport. Although Nott's calculations are a first approximation to the general problem, this certainly is an important step forward in the question of boulder transport by waves, and it gives weight to arguments of the "tsunamiists", because for the transport of a 50-t boulder storm-wave heights would be required that simply do not exist on our planet. The overall aim must be to find the threshold of boulder sizes transported by storm waves, and the level from which storms definitely have to be excluded, even at deep-water coasts with plunging cliffs. Certainly there will be some overlap of both categories, but at the end figures for practical use in field geology and geomorphology may arise.

During decades of field work along exposed coastlines of the world, the present authors never have found (or overlooked?) massive accumulations of large boulders, evidently late Holocene in age, after big storms or hurricanes

except for single boulders of limited size. Where we have found extremely large boulders up to several hundreds of tons outside of the surf, far inland and high above the shoreline, which could be dated as Holocene littoral deposits, we concluded that they were moved by tsunamis. The distribution of absolute data from these deposits has shown their rarity in the Late Holocene in comparison with regularly occurring hurricanes or other extreme storms.

Our research is based on the extended literature on the coastal geomorphology of Ireland and Scotland as well as on historical documents on storm events in this region. Valuable information concerning environmental change could be gained from publications on the coastal archaeology from Neolithic up to Medieval times.

Assuming strong abrasion in the order of 0.4m/year like Williams (2004), means, that older coastal forms and deposits must have disappeared or constantly reworked by moving onshore over a wide area. There are, however, a lot of arguments against strong abrasion during the last millennia, like a large number of shell middens from Neolithic times directly at the coast, Neolithic and Bronze Age coastal settlements (Skara Brae on the Orkneys and Jarlshof in southern Shetland) still preserved, nearly 200 Promontory Forts from Iron Age times (2500-2000 BP) on steep coastal headlands, boats houses from Viking times immediately at the upper part of winter storm surf, or Medieval castles and

monasteries built on stacks, very exposed and nearly inaccessible but still existing. Arguments against a strong Late Holocene abrasion can also gained from the existence of coarse coastal deposits like boulder ridges and boulder clusters, which not only show all signs of an intensive weathering at their crests and landward slopes, but also are covered by vegetation, soil or even peat as documents for a longer persistence at the same place. Numerical age dating with ages from the 18th century back into Bronze Age times (see Figure 1) support the conclusion, that most of the boulder deposits are not in harmony with modern storm wave regimes. These are important facts because they allow to compare the modern situation of bathymetry, exposure and general topography with conditions hundreds or thousands of years ago. The age of a deposit, however, says nothing about the processes responsible. We agree with Williams & Hall (2004) and Hall et al. (2006), that the high boulder deposits and very large boulders occur where water depth and exposure both are great.

However, boulders up to more than 100 tons in weight can also be found at protected places with shallow water conditions and at sheltered sides of islands like in the case of the Galway-Aran region in central western Ireland (Fig. 1).

Another argument against the storm wave hypothesis for the coarse coastal deposits in western Ireland and Scotland is the fact, that, the extremer the storms, the larger the areas affected.

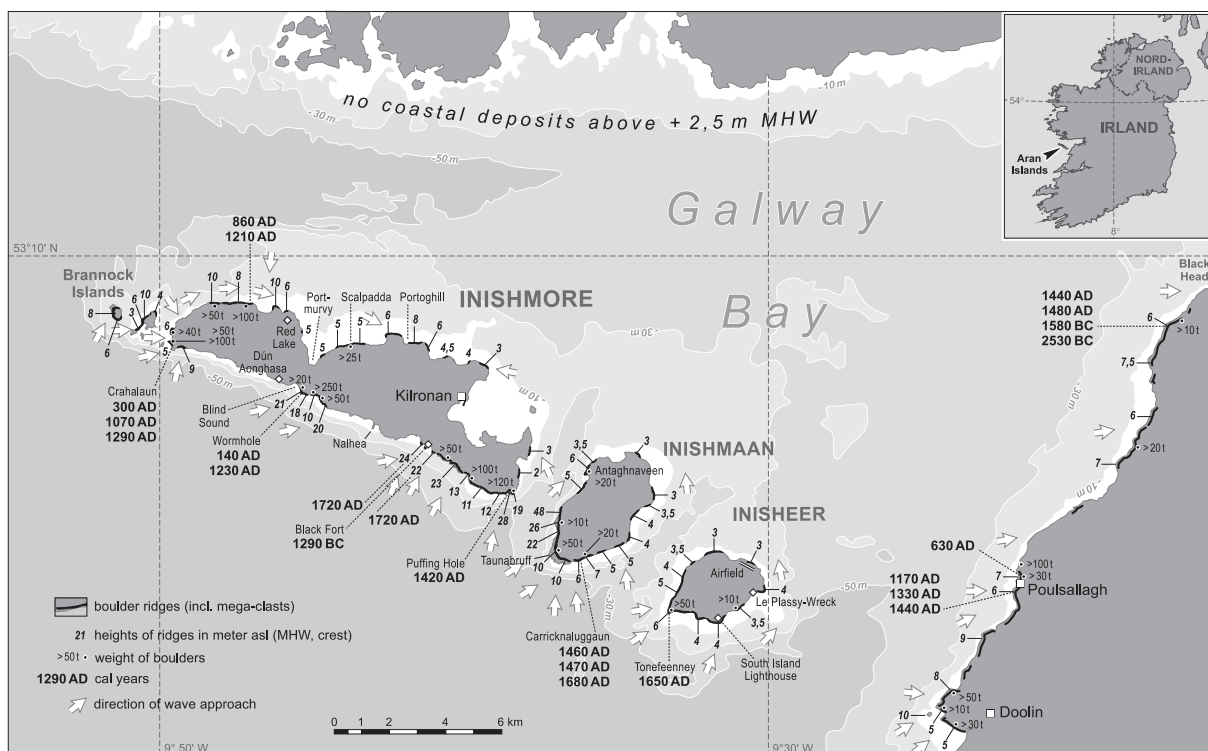


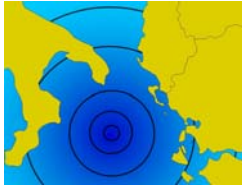
Figure 1. Distribution of boulder ridges including heights and boulder weights as well as ages at the Aran Islands and Galway Bay, central west coast of Ireland.

The deposits to discuss, however, are restricted to single places (e.g. Esha Ness on mainland Shetland, Annagh Head in county Mayo, or the Galway area in central western Ireland), and even along exposed deep water coasts nearby, boulder deposits are missing (e.g. along the Connemara coast immediately north of Galway Bay).

From all field observations (boulder ridges in very high positions, apart from the modern coastline, with extremely large clasts) and datings (clustering in particular for medieval times and the 18th century) we only can conclude, that several tsunamis of different energy and a more regional impact occurred during the last millennia. The tsunami history of the northern Atlantic Ocean is just in the beginning of its deciphering (see also Bondevik et al., 2005; Dawson et al, 2006; Haslett & Bryant, 2007).

References

- Bondevik S., Mangerud J., Dawson S., Dawson A., Lohne O. (2005). *Evidence for three North Sea tsunamis at the Shetland Islands between 8000 and 1500 years ago*. Quaternary Science Reviews, 24, 1757–1775.
- Dawson A., Dawson S., Bondevik S. (2006). *A late Holocene tsunami at Basta Voe, Yell, Shetland Isles*. Scottish Geographical Journal, 122 (2), 100–108.
- Hall A. M., Hansom J. D., Williams D. M. Jarvis J. (2006). *Distribution, morphology, and lithofacies of cliff-top storm deposits: Examples from the high-energy coasts of Scotland and Ireland*. Marine Geology, 232, 131–155.
- Hansom J. (2004). *The Impact of Extreme Waves on the Atlantic Coast of the British Isles*. Oral presentation, International Geographical Congress, Glasgow, August 17, 2004.
- Haslett S. K. Bryant E. A. (2007). *Reconnaissance of historic (post-AD 1000) high-energy deposits along the Atlantic coasts of southwest Britain, Ireland and Brittany, France*. Marine Geology, 242, 207–220.
- Nott J. (2003a). *Waves, coastal boulders and the importance of the pre-transport setting*. Earth and Planetary Science Letters, 210, 269–276.
- Williams D. M. (2004). *Marine erosion and archaeological landscapes a case study of stone forts at cliff-top locations in the Aran Islands, Ireland*. Geoarchaeology, 19, 167–175.
- Williams D. M., Hall A. M. (2004). *Cliff-top megaclast deposit of Ireland, a record of extreme waves in the North Atlantic – storms or tsunamis?* Marine Geology, 206, 10–11.



Scicchitano G.¹, Costa B.¹, Di Stefano A.¹, Longhitano S.², Monaco C.¹

Tsunami deposits in the Siracusa coastal area (south-eastern Sicily)

¹Dipartimento di Scienze Geologiche, Università di Catania, Italy, e-mail: gscicchi@unict.it;

²Dipartimento di Scienze Geologiche, Università della Basilicata, Campus Universitario di Macchia Romana, Potenza, Italy

Keywords: *Tsunami, coastal morphology, Holocene, Sicily, Southern Italy*

Eastern Sicily is one of the most seismically active areas of the central Mediterranean. Normal faulting accommodates WNW-ESE oriented extension, active along the Siculo-Calabrian rift zone (Fig. 1a; Monaco & Tortorici, 2000).

In eastern Sicily the normal faults are mostly located offshore and controls the Ionian coast from Messina to the eastern lower slope of Mt. Etna, joining southwards to the system of the Malta Escarpment. It is marked by a high level of crustal seismicity producing earthquakes with intensities of up to XI-XII MCS and $M \sim 7$, such as the 1169,

1693 and 1908 events (Postpischl, 1985; Boschi et al., 1995). Several earthquake-generated tsunamis struck the Ionian coast of south-eastern Sicily in historical times (AD 365, 1169, 1329, 1693, 1818, 1908, 1990; Soloviev et al., 2000; Tinti et al., 2004). According to published geological data and numerical modelling, the seismogenic source of most of these events should be located in the Messina Straits and in the Ionian offshore (the Malta Escarpment) between Catania and Siracusa (Monaco & Tortorici, 2007 and references therein).

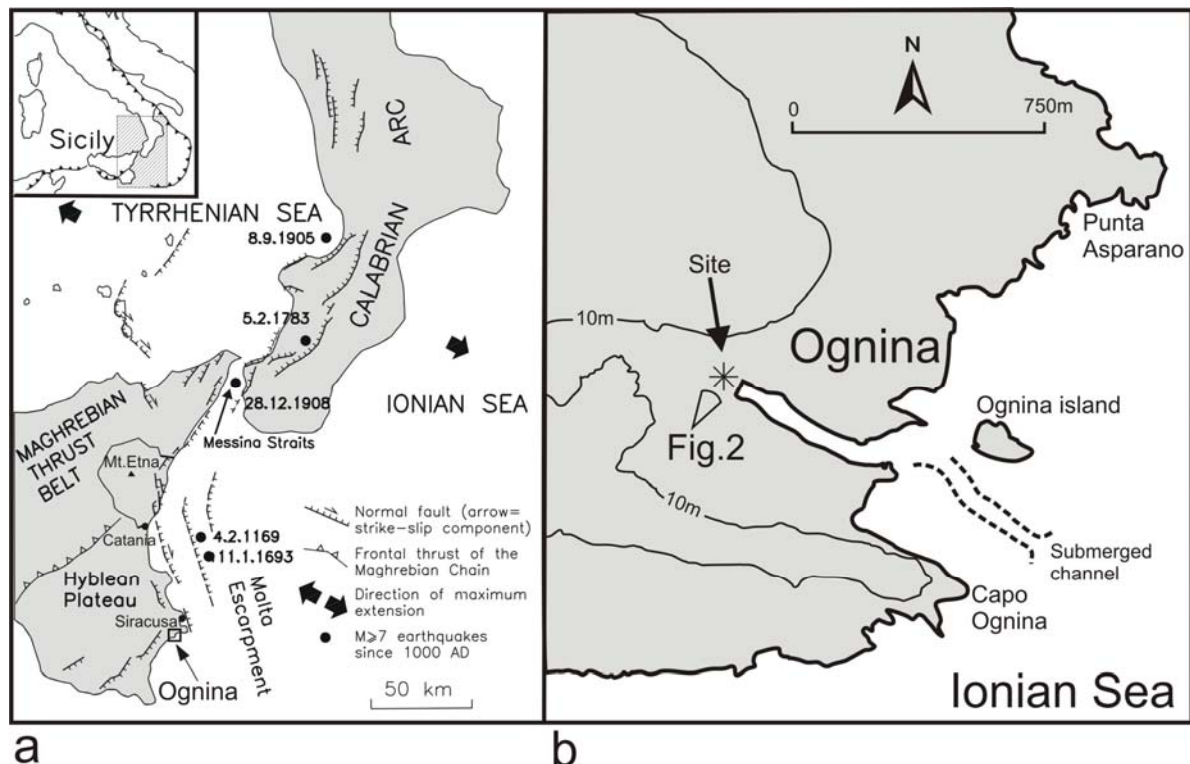


Figure 1. a) Tectonic sketch map of the Siculo-Calabrian rift zone (from Monaco & Tortorici, 2000). **b)** Geographical position of the studied area.

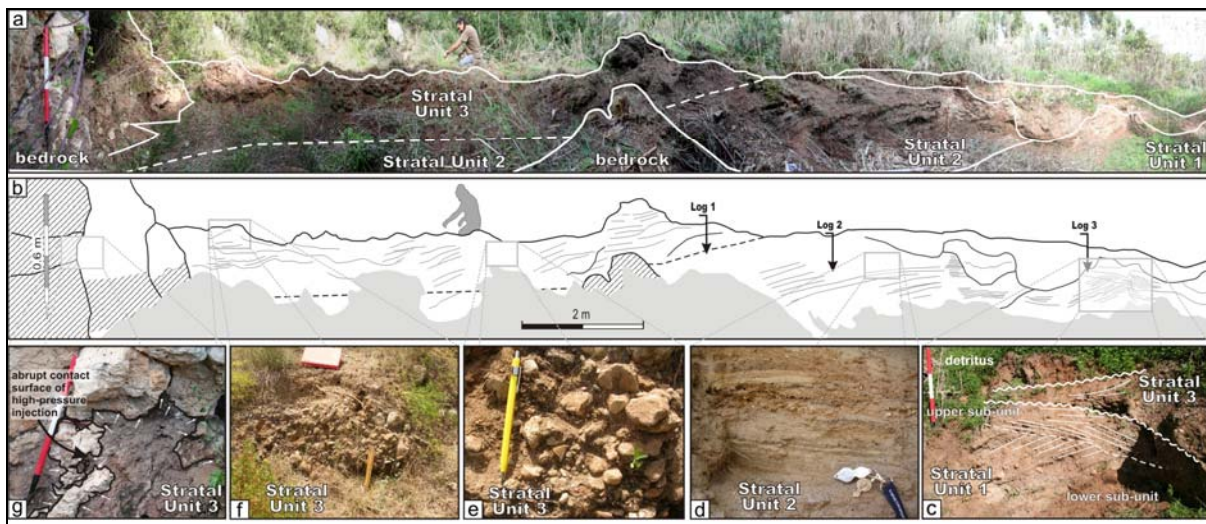
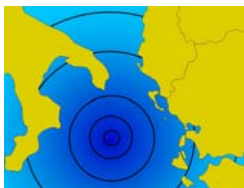


Figure 2. a) Photomosaic of the Ognina section (see Fig. 1 for location) showing the three main stratal units and their spatial relationship; b) line drawing showing the main depositional surfaces and log position of the Fig. 3; c) detail of the Stratal Unit 1, showing the two component sub-units and the contact with the overlying Stratal Unit 3; d) Plain-parallel lamination characterising the Stratal Unit 2; e) and f) details of the Stratal Unit 3; g) sedimentary dikes of sands infilling pre-existing open fractures within the calcareous bedrock, indicating high-energy sediment injection.

The effects of the 1169, 1693 and 1908 tsunamis are still recognizable in the Siracusa coastal area where boulders up to 182 ton in weight, encrusted by dated marine organisms, were removed and transported inland at a distance of up to 70 m (Scicchitano et al., 2007). New tsunami deposits have been discovered in the narrow embayment of Ognina, located about 20 km south of Siracusa (Fig. 1). These deposits fill the back edge of a ria incised within Miocene limestones and are composed of three main stratal units characterized by distinct sedimentological features (Fig. 2). The two lower units, formed by cross-bedded sands and laminated clays, recorded the development of a small confined beach-barrier depositional system, influenced by frequent high-energy events. The upper unit, represented by chaotic coarser sediments, can be attributed to a destructive marine event. Absolute dating and archaeological determinations allow to correlate the latter deposit to a tsunami wave triggered by the 1693 A.D. catastrophic earthquake.

References

- Boschi E., Ferrari G., Gasperini P., Guidoboni E., Smriglio G., Valensise G. (1995). *Catalogo dei forti terremoti in Italia dal 461 a.D. al 1980*. Istituto Nazionale di Geofisica, S.G.A., Roma.
- Monaco C., Tortorici L. (2000). *Active faulting in the Calabrian arc and eastern Sicily*. *Journal of Geodynamics*, 29, 407-424.
- Monaco C., Tortorici L. (2007). *Active faulting and related tsunamis in eastern Sicily and south-western Calabria*. *Bollettino di Geofisica Teorica e Applicata*, 48 (2), 163-184.
- Postpischl D. (1985). *Catalogo dei terremoti italiani dall'anno 1000 al 1980*. CNR, P.F. Geodinamica, Graficoop, Bologna, 239 pp.
- Scicchitano G., Monaco C., Tortorici L. (2007). *Large boulder deposits by tsunami waves along the Ionian coast of south-eastern Sicily*. *Marine Geology*, 238, 75-91.
- Soloviev S. L., Solovieva O. N., Go C. N., Kim K. S., Shchetnikov N. A. (2000). *Tsunamis in the Mediterranean Sea 2000 B.C.–2000 A.D.* Kluwer Academic Publishers, Dordrecht, 237.
- Tinti S., Maramai A., Graziani L. (2004). *The new catalogue of Italian Tsunamis*. *Natural Hazards*, 33, 439-465.



2nd International Tsunami Field Symposium

IGCP Project 495

Quaternary Land-Ocean Interactions:
Driving Mechanisms and Coastal Responses

Ostuni (Italy) and Ionian Islands (Greece) 22-28 September 2008



Project 495

Smedile A.¹, De Martini P. M.¹, Barbano M. S.², Bellucci L.⁴, Del Carlo P.³, Gerardi F.²,
Pantosti D.¹, Pirrotta C.², Gasperini L.⁴, Polonia A.⁴

Paleotsunami deposits in the Augusta Bay area (Eastern Sicily, Italy): combining onshore and offshore data

¹Istituto Nazionale di Geofisica e Vulcanologia, Sezione di Roma 1, Italy

e-mail: alessandra.smedile@ingv.it; paolomarco.demartini@ingv.it; pantosti@ingv.it;

²Dipartimento di Scienze Geologiche, Università degli Studi di Catania, Italy

e-mail: barbano@unict.it; f.gerardi@unict.it; c.pirrotta@unict.it;

³Istituto Nazionale di Geofisica e Vulcanologia, Sezione di Catania e Sezione di Pisa, Italy,

e-mail: delcarlo@ct.ingv.it; delcarlo@pi.ingv.it;

⁴Istituto di Scienze Marine, Sezione di Geologia Marina di Bologna, CNR, Italy

e-mail: luca.bellucci@bo.ismar.cnr.it; luca.gasperini@bo.ismar.cnr.it; alina.polonia@bo.ismar.cnr.it

Keywords: *tsunami deposits, marine geophysics, Eastern Sicily, Southern Italy*

Introduction

Eastern Sicily has been affected in historical time by large earthquakes (CPTI Working group, 2004) and, in particular, its southern sector, also inundated in 1693 and 1169 by devastating tsunamis. The Augusta Bay area is one of the locations where the information available from historical reports on tsunami effects (hit localities, inundated areas and run-up distribution) stimulated our curiosity in searching for the geological signature of tsunamis. In this paper we present the

evidence of multiple tsunami deposits found within onshore sedimentary deposits, together with preliminary results of a marine geophysical/geological study of the shallow offshore. A tentative correlation between onshore and offshore records is also discussed. The research was carried out through a multi-theme approach consisting of historical studies, geomorphological and geological surveys, coring campaigns, laboratory analyses (paleontological, radiometric, X-Ray, petro-geochemical petrophysical, magnetic, etc.).

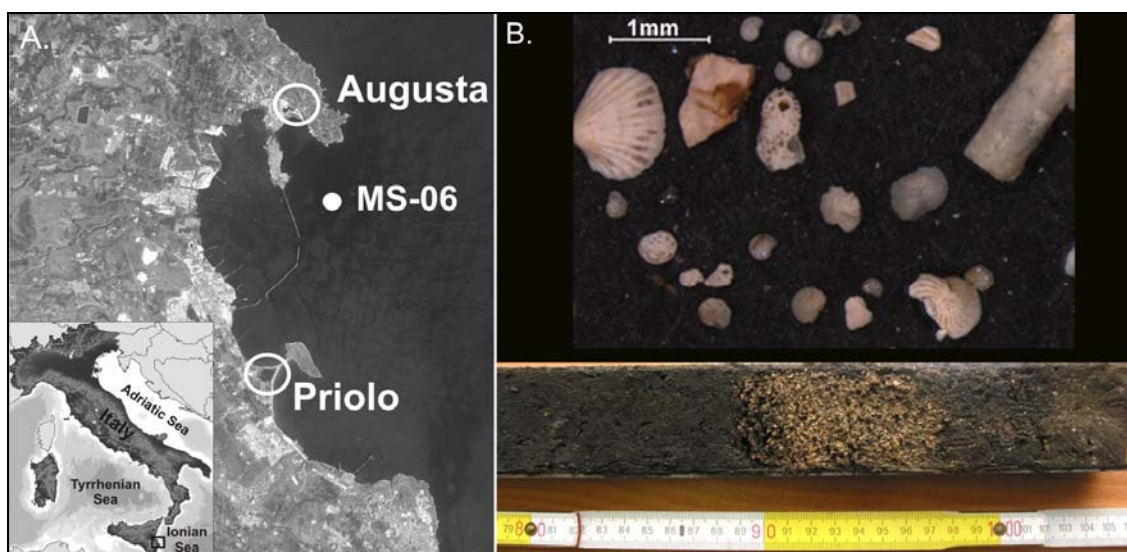


Figure 1. (A) Location map of the study area. (B) Augusta site: picture of the OSA-S6 core yellowish bioclastic layer (below); macro and micro paleontological assemblage from the same layer (above).

Onshore data

We mainly concentrated our study on marshes or lagoons because in these environments the preservation potential of episodic events such as tsunami deposits in the sedimentary sequence, is high as well as the possibility of finding datable material. The preliminary work was based on a detailed geomorphological study of the Augusta Bay coast, through aerial-photographs and satellite image interpretation, in conjunction with field surveys. Augusta and Priolo were selected as the most favorable sites based on geomorphological and historical evaluations (De Martini et al., 2006; Gerardi et al., 2006) (Fig. 1a).

In both sites we carried out coring campaigns using both hand auger equipment and a vibracoring (gasoline powered percussion hammer). A first stratigraphic and sedimentological description, together with photographs of the core deposits were performed directly in the field (Smedile et al., 2006; 2007). Once an interesting stratigraphic sequence was found, we were properly equipped to collect 100 cm long undisturbed sample (within specific pvc tubes) down to 5 m maximum depth.

Micropaleontological analyses were carried out on samples collected in all the performed cores, to detect the possible marine component of a tsunami deposits within a marsh/lagoonal sequence (e.g planktonic foraminifera, that are exclusive of the marine realm, and/or benthic forams exclusive of peculiar marine depth range). Tephra identification and radiocarbon analyses were used to constrain the age of the sediments, to estimate sedimentation rates and to correlate potential paleotsunami deposits with historical earthquakes. Magnetic and X-ray analyses were also performed on selected cores to look for susceptibility variations and peculiar small-scale sedimentary structures (e.g. sharp contacts, convoluted layers, etc.).

Augusta site. We collected 9 cores down to a maximum depth of 4.3 m, at a maximum distance from the sea of 460 m. The stratigraphic sequence is mainly composed by fine-grained sediments, ranging from clay to silt, with the exception of some gravel layers (up to 10 cm thick) and one peculiar bioclastic deposit found at 190 cm in depth. The micropaleontological analyses show the occurrence of a high energy event (bioclastic layer) within a brackish lagoonal environment (Fig. 1b).

In detail, the yellowish bioclastic layer found at about 190 cm depth is composed by few entire gastropods (*Hydrobia* spp., *Pirenella conica*), abundant shell fragments (mollusks, corals and echinoderms), few ostracods, often broken benthic (*Ammonia* spp., *Bolivina* sp., *Cassidulina laevigata*, *Cibicides lobatulus*, *Haynesina germanica*, miliolidae, *Pullenia bulloides*, *Rosalina* spp.) and

few badly preserved planktonic (*Globigerina* spp., *Globigerinoides* spp., *Globorotalia inflata*, *Turborotalita quinqueloba*) foraminifera (Fig. 1b).

This layer was found within a gray to dark-gray fine silt deposit (20-30 cm thick) characterized by abundant ostracods (*Cyprideis torosa*), several entire gastropods (*Hydrobia* spp., *Pirenella conica*) and few species of benthic foraminifera (*Ammonia parkinsoniana*, *A. tepida*, *Haynesina germanica*). It showed a sharp, possibly erosional, basal contact. The erosional character of this bioclastic layer coupled with striking micropaleontological results allowed us to interpret it as a tsunami deposit, with a high level of confidence.

Radiocarbon dating was performed on 3 samples, collected just above, within, and below this bioclastic layer; these ages gave coherent results, constraining the paleotsunami age to the interval 1000-800 BC. Being this age interval very narrow, it points toward a sharp change, such as a sudden inundation rather than a gradual transition to higher energy environment. **Priolo site:** We collected 17 cores down to a maximum depth of 4.2 m, as far as 530 m from the sea. The stratigraphic sequence is composed mainly by fine sediments, from clay to silt, with two distinctive bioclastic layers (A and B found at 10-15 and 30- 40 cm depth, respectively), one detritic deposit (C at 90 cm depth) and one peculiar sand layer (D at 160 cm depth). Combining micropaleontological and X-ray analyses we found that: a) the entire stratigraphic sequence appears characteristic of lagoonal environment; b) both bioclastic layers show a sharp basal contact, as well as an anomalous concentration of shell fragments and entire gastropods (all arranged in a chaotic pattern); c) the B layer shows an increment in the benthic foraminifera specific diversity; d) the detritic deposit C (2-3 cm thick) shows a anomalous assemblage made by macromammal bone fragments together with rare and badly preserved benthic (*Cassidulina carinata*, *Cibicidoides pseudoungerianus*, *Melonis barleeianum*, *Planulina ariminensis*) and planktonic (*Globigerinoides* sp.) foraminifera; e) the marine microfauna of D layer appear well preserved, differently from the association characterizing the fine to very fine deposits above and below. Thus, we interpret the four layers A-B-C-D as tsunami deposits, although with different level of confidence. We assign to A and B a medium-high level, whereas a lower level of confidence should be attributed to the detritic deposit C and the peculiar sand layer D. Moreover, magnetic, petro-chemical and morphoscopic analyses on a normally graded black volcanic coarse sand found in 6 cores at about 70 cm of depth, allowed us to correlate it with the 122 BC Etna tephra (Coltelli et al., 1998).

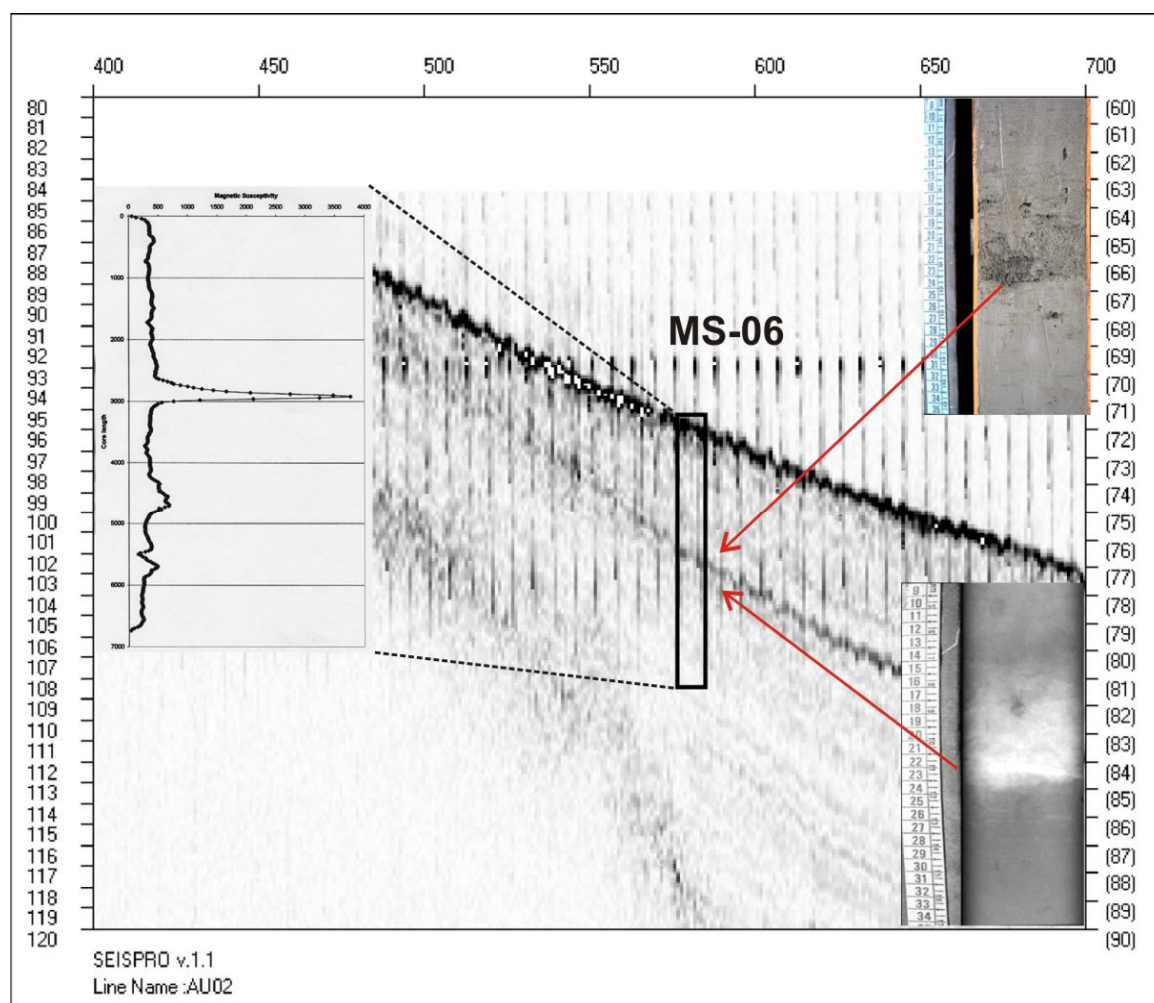


Figure 2. Chirp-sonar profile over the MS-06 core location. On the left, magnetic susceptibility of the MS-06 core, close-up containing photograph and X-ray image of the 122 BC tephra on the upper and lower right, respectively.

Radiocarbon dating was performed on 2 shell specimens: the uppermost one collected just below the A bioclastic layer, while the second comes directly from the lowermost tsunami sand. Combining tephrostratigraphic and C14 data, we may estimate an average sedimentation rate of 0.35–0.45 mm/yr for the past 4000 yrs. Moreover, we tentatively associate the A and B bioclastic deposits to 1693 and 1169 historical tsunamis, respectively. The age of the C and D layers, found at 90 and 160 cm depth, could be constrained in the time intervals 570–122 BC and 2100–1635 BC.

Offshore data

Since marine environment is in general more preservative than the littoral one, showing a sedimentary record more continuous and potentially highly sensible to anomalous events like earthquakes and tsunamis, we decided to follow our tsunami markers in the shallow offshore on the Augusta Bay

Unpublished seismostratigraphical data from the

Augusta offshore showed the presence of a main reflector, within a transparent, homogeneous unit as thick as several tens of meters below the sea bottom. Due to its acoustic character (amplitude and continuity) and its position within the sedimentary sequence we considered this reflector as a good target for further investigations as potential signature of an historical tsunami. About 200 km of high resolution chirp-sonar and bathymetric profiles, together with one 7 m long piston core (MS-06) were collected in the area to better constrain this hypothesis (Fig. 2).

The MS-06 core was collected at 70 m of water depth, few kilometers from the Augusta site, at the foot of a small morphological step. Stratigraphic analysis confirmed the presence of a homogeneous sequence of fine-grained dark gray deposits interrupted at -3 m by a volcanic sandy layer, 3–4 cm thick. Time to depth conversion of the seismic profile, as well as geometrical corrections carried out to compensate the effect of differential compressions within the core during the sampling using a specific software (Dal Forno & Gasperini, 2008), allowed us to correlate the volcanic sandy

layer to the prominent reflector observed in the seismic profiles.

Magnetic petro-chemical and morphoscopic analyses of the ash fall deposit enabled a correlation of this level with the 122 BC plinian Etna eruption (Fig. 2). MS-06 sedimentation rate was derived from radiocarbon datings, magnetostratigraphy and radioactive tracers (^{210}Pb and ^{137}Cs), the latter method only for the uppermost part of the sequence. Results from these independent methods were in good agreement suggesting sedimentation rates ranging from 0.7 mm yrs^{-1} to 2 mm yrs^{-1} for the past 4500 yrs.

The benthic foraminifera paleoenvironmental analysis highlighted at least six peaks marked by high percentages of displaced epiphytic specimens (species which grows common in vegetated substrates like the *Posidonia* prairies) from the infralittoral zone. This anomalous distribution of the microfauna was also confirmed by high amount of vegetal remains in the washed fraction and by corresponding darker stripes in the X-Ray films.

These peaks could be interpreted either as the primary effect of tsunami waves (back-wash) or as secondary effects of significant *Posidonia* remobilization due to earthquake shaking, that made available an extra amount of material from the uppermost infralittoral zone.

More cores and extra C14 datings are needed to substantiate these preliminary interpretations and to contribute to the discrimination of the causative sources (local vs regional) responsible for the evidence collected so far.

Conclusions

The study of onshore costal deposits in selected sites of the Augusta Bay allowed us to recognize two tsunami deposits at Priolo associated to the 1693 and 1169 earthquakes. We also collected interesting evidence for three paleoinundations occurred about 570-122 BC (Priolo), 1000-800 BC (Augusta) and 2100-1635 BC (Priolo).

The study of the uppermost sedimentary sequence offshore Augusta Bay suggests the presence of at least six anomalous peaks in the past 4500 yrs, possibly triggered by tsunamis or earthquakes. A distinctive reflector and its gentle seaward deepening was also detected as the well known Etna tephra (122 BC) and so used as stratigraphic marker.

Identification and characterization of geological evidence of historical- and paleo-tsunamis (useful to obtain tsunami recurrence time, maximum inundation distance, elapsed time since the last tsunami event, etc) may have a significant relevance for Civil Protection applications. These data are also directly usable in the field of tsunami scenario and modeling, especially taking into

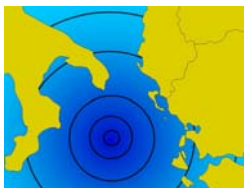
consideration the fact that the Augusta Bay area has an important role as main national industrial and military site.

Acknowledgements

This work was funded by the Italian Dipartimento della Protezione Civile in the frame of the 2004-2006 agreement with Istituto Nazionale di Geofisica e Vulcanologia – INGV (Seismological Project S2).

References

- Coltelli M., Del Carlo P., Vezzoli L. (1998). *The discovery of a Plinian basaltic eruption of Roman age at Mt. Etna*. *Geology*, 26, 1095-1098.
- CPTI Working group 2004. *Catalogo Parametrico dei Terremoti Italiani, version 2004 (CPTI04)*. INGV, Bologna. <http://emidius.mi.ingv.it/CPTI/>.
- Dal Forno G., L. Gasperini. (2008). *ChirCor: A new tool for generating synthetic chirp-sonar seismograms*. *Computers & Geosciences*, 34, 2, 103-114.
- De Martini P. M., Pantosti D., Barbano M., Gerardi F., Smedile A., Azzaro R., Del Carlo P., (2006). *Joint contribution of historical and geological data for tsunami hazard assessment in Gargano and eastern Sicily (Italy)*. *100th Anniversary Earthquake Conference Commemorating the 1906 San Francisco earthquake. April 18-22, San Francisco, CA*. Abstracts of the Centennial Meeting of the Seismological Society of America. Nr. 609.
- Gerardi F., Smedile A., Del Carlo P., De Martini P.M., Barbano M.S., Pantosti D., Azzaro R., Pirrotta C., Mostaccio A., (2006). *Integration of historical and geological data to identify tsunami deposits in eastern Sicily*. "EGU General Assembly 2006", 02-07 April - Vienna, Austria. *Geophysical Research Abstracts*, Vol. 8, 04356.
- Smedile A., Barbano M.S., De Martini P.M., Gerardi F., Pantosti D., Pirrotta C., Azzaro R., Cosentino M., D'Addezio G., Del Carlo P., Guarnieri P. (2006). *Multidisciplinary study to identify tsunami deposits in eastern Sicily, XXV Convegno GNGTS*. Riassunti estesi delle comunicazioni, Roma, 28-30 November 2006, 325-328.
- Smedile A., Barbano M.S., De Martini P.M., Pantosti D., Del Carlo P., Gerardi F., Guarnieri P., Pirrotta C., Cosentino M. (2007). *In search of tsunami deposits along the eastern coast of Sicily (Italy)*, IUGG XXIV 2007, Perugia, July 2-13.



Spiske M.^{1*}, Piepenbreier J.¹, Benavente C.², Kunz A.³, Bahlburg H.¹

Historical tsunami events along the coast of Peru – sedimentology and dating

¹Westfälische Wilhelms-Universität, Geologisch-Paläontologisches Institut, Münster, Germany

²Instituto Geológico, Minero y Metalúrgico INGEMMET, Lima, Peru

³Institut für Geowissenschaftliche Gemeinschaftsaufgaben GGA, Hannover, Germany

* corresponding author: e-mail: spiske@uni-muenster.de

Keywords: *tsunami, sedimentary structures, optically stimulated luminescence dating, Peru*

The coasts of Peru are greatly endangered by tsunami events. The subduction of the Nazca Plate below the South American active margin triggers strong submarine earthquakes that are capable of causing tsunami. Even though there is no voluminous riverine sediment input from the Andes along the coasts of Peru, submarine mass movements on the continental slope can occur due to seismic events. The greatest historical tsunami impacts are the two Arica tsunamis on 24th November 1604 and 13th August 1868, and the Chile tsunami on 22nd May 1960 (Berninghausen, 1962; Lockridge, 1985). The greatest local tsunami

events of the last 15 years are the Chimbote tsunami on 21st February 1996 (with a 5 m runup; Kulikov et al., 2005) and the Camaná tsunami on 23rd June 2001 (with a 9 m runup; Jaffe et al., 2003). The latest event was the tsunami of 15th August 2007 which was triggered by a magnitude 8.0 earthquake located 150 km SSE of Lima (USGS, 2007). The highest runup of 10 m occurred at the Paracas Peninsula (Fritz et al., 2007).

In order to learn about the tsunami history of Peru, we visited about 1400 km of the Peruvian coastline from Chimbote in the north to Boca del Rio in the south (Fig. 1).

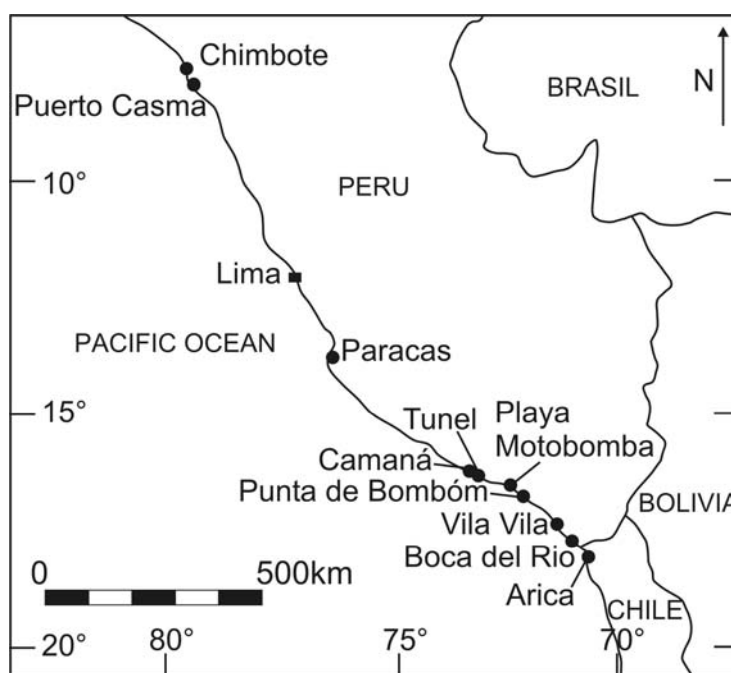


Figure 1. Study locations along the coast of Peru.

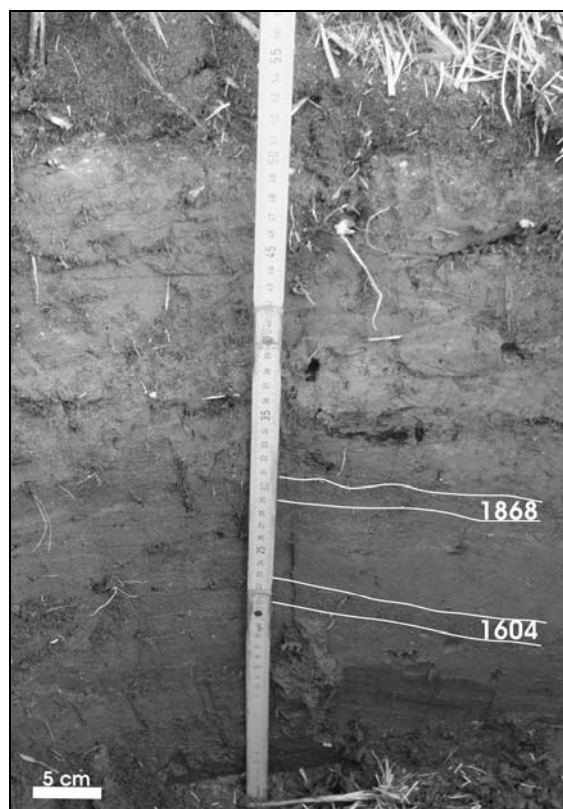


Figure 2. Outcrop in the marsh of Boca del Rio probably showing the sandy deposits of the two Arica tsunamis in 1604 and 1868.

The encountered sediments were dated by using optically stimulated luminescence. This contribution presents preliminary data of sedimentology and age determination of these deposits.

Tsunami deposits are present as (1) layers of coarse sand, optionally with shell fragments or pieces of rock, (2) shell layers, (3) heavy mineral accumulations and (4) mud caps or mud balls.

At Puerto Casma a 2 cm thick coarse sandy layer with an erosive base cuts into the finer grained beach sediments. Heavy minerals occur above the erosional contact. Shell fragments and pieces of rock of up to 1 cm are incorporated. Normal graded shell layers of up to 17 cm in thickness are present at Vila Vila. Biggest shells are 9 cm in diameter, biggest incorporated stones 7 cm. Unfortunately these deposit cannot be proven to be of tsunamigenic origin due to the lack of additional sedimentary structures and unsuccessful electron spin resonance dating.

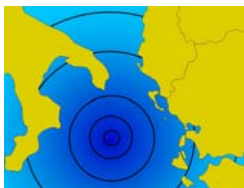
A possible back-wash sediment was found at Punta de Bombón where a irregular brownish mud layer of 4-6 cm occurs within the beach sand and thins out seawards. In a distance of 18 m from the sea, the layer ends and gives way to mud balls with a maximum diameter of 5.5 cm. These balls could be consistent with tsunami rip up balls caused by the back-wash. The muddy material was very likely

derived from agricultural fields adjacent to the beach. The sediments of the 2001 Peru tsunami were studied by Jaffe et al. (2003) within the Camaná region. We revisited these locations and realized that the preservation potential of these sediments seems to be very low. Only some remaining mud caps resembling the tsunami deposit were left. All other structures seem to have disappeared due to erosion or bioturbation. At Tunel, a small settlement 30 km south of Camaná, an eyewitness reported a ca. 10 m high wave that followed a 200 m withdrawal of the sea on an afternoon in June 2006. The water reached about 350 m inland, flooding a street and houses for approximately one hour. People were injured by floating debris. Unfortunately no distinctive sediments have been preserved. Since this tsunami seems to be a very local one, we assume a local submarine slide to have been the trigger.

Most tsunami sediments described in this study are relicts of the two regional tsunami that hit the Chimbote and Camaná regions in 1996 and 2001, respectively. The oldest tsunami sediments, most likely connected to the two Arica tsunami of 1604 and 1868, occur at Boca del Rio close to the boarder to Chile.

References

- Berninghausen W. H. (1962). *Tsunamis reported from the west coast of South America from 1562-1960*. Bulletin of the Seismological Society of America, 52(4), 915-921.
- Fritz H. M., Kalligeris N., Ortega E., Broncano P., (2007). *15 August 2007 Peru tsunami runup and inundation*.
http://www.eeri.org/lfe/pdf/peru_coast_tsunami.pdf
- Jaffe B., Gelfenbaum G., Rubin D., Peters R., Anima R., Swensson M., Olcese D., Anticono, L. B., Gomez J. C., Riega P. C. (2003). *Identification and interpretation of tsunami deposits from the June 23, 2001 Peru tsunami*. Proceedings of the International Conference on Coastal Sediments 2003, CD-ROM published by World Scientific Corp and East Meets West Production, Corpus Christi, Texas, USA.
- Kulikov E. A., Rabinovich A. B., Thomson R. E., (2005). *Estimation of tsunami risk for the coasts of Peru and Northern Chile*. Natural Hazards, 35, 185-209.
- Lockridge P. A. (1985). *Tsunamis in Peru-Chile*. World Data Center A for Solid Earth Geophysics, Report SE-39, 97 pp.
- USGS (2007):
<http://earthquake.usgs.gov/eqcenter/eqinthenews/2007/us2007gbcv/>



2nd International Tsunami Field Symposium

IGCP Project 495

Quaternary Land-Ocean Interactions:
Driving Mechanisms and Coastal Responses

Ostuni (Italy) and Ionian Islands (Greece) 22-28 September 2008



Project 495

Switzer A. D.¹

20 years of palaeotsunami studies on coastal sandsheets: a review

¹Department of Earth Sciences, The University of Hong Kong, Hong Kong SAR, China

e-mail: aswitzer@hku.hk

Keywords: *sandsheets, boulders, Tsunami, coastal morphology, sediments*

20 years after the publication of key initial studies on sandy tsunami deposits from the Scottish and western north American coasts the palaeotsunami research community has expanded considerably. The field now incorporates not only geologists and geomorphologists but computer and mathematical modellers, geophysicists, chronology experts, palaeontologists, hydrologists and ecologists. The 20 year anniversary of these initial studies presents a good opportunity to reflect on the progress made in the field, evaluate some recent criticisms and highlight knowledge gaps for future study.

Introduction - the early days

Until the late 1980's the study of tsunami predominantly involved seismologists, numerical modellers, geophysicists and historians. In particular, historians played a valuable role by providing detailed documentary information on former tsunamis from around the world (Dawson & Shi, 2000). Often, historical accounts would provide estimates of frequency-magnitude relationships for past tsunami events and hence provide information on future tsunami risk for different areas. Geologists paid little attention to tsunami records in recent coastal stratigraphy until 1987 and 1988, when two papers were published one from the United States west coast (Atwater, 1987) and another from the Scottish coast (Dawson et al., 1988). The paper by Atwater (1987) linked prehistoric earthquakes with geological evidence from the outer coast of Washington State, U.S.A. This evidence included sheets of marine sediment visible in coastal stratigraphic sequences that were interpreted as prehistoric (palaeo-) tsunami deposits. Around the same time Dawson et al. (1988) in a study of uplifted coastal sedimentary sequences in Scotland, described an unusual sand deposit which they linked to a prehistoric tsunami event. They

hypothesized the event was the result of the Storegga slide, one of the world's largest submarine slides that took place approximately 7100 ¹⁴C years ago on the continental shelf edge west of Norway.

The last 20 years

Although geological investigations of former tsunami remain a relatively new research area, the last twenty years has seen a plethora of academic papers on the topic. A wide range of sedimentary evidence from different locations has been attributed to a series of former tsunami (see reviews by Dawson & Shi, 2000; Goff et al., 2001; Bryant, 2001; Scheffers & Kelletat, 2003; Kortekass & Dawson, 2007). Many authors have argued that tsunami are frequently associated with the deposition of continuous and discontinuous sediment sheets across large areas of the coastal zone, provided that there is an adequate sediment supply (e.g., Dawson, 1999; Goff et al., 2001). Although tsunami deposits are mostly characterised by sheets of sediment, they are also frequently represented by boulder accumulations (see reviews of Scheffers & Kelletat, 2003; Kelletat, *in press*). In addition, microfossil assemblages of diatoms and foraminifera contained within tsunami-deposited sandsheets may provide additional information on the nature of onshore transport of sediment from deeper water (Dominey-Howes, 1996; Hemphill-Haley, 1996). Other aspects such as mineralogy (Switzer et al., 2005) and sediment chemistry (Chague-Goff, et al., 2000; Chague-Goff & Goff, 1999; Szczuciński et al., 2005) may also be effective proxies for tsunami dynamics.

Distinguishing between storm and tsunami deposits in sandsheets

The generation, propagation and run up of tsunami and storm surge are characteristically

different. Tsunami waves propagate away from the source region where disturbance of the water column generates waves with small amplitude, long period and long wavelength that travel at high velocity (Geist, 1999).

At the coast tsunami waves slow in velocity and rise in amplitude before inundating the coastline with high velocity. In contrast severe low pressure systems such as tropical cyclones can induce long-wavelength, low-amplitude sea surface displacements called storm surges. A storm surge migrates with the storm and is the result of a combination of wind stress and falling atmospheric pressure (McInnes & Hubbert, 2001). The water elevation (inundation) caused by storm surges at a coastal location involves four components: (1) the storm surge, (2) storm waves, (3) wave setup and (4) the astronomical tide (Cheung, et al. 2003).

In the open ocean the wavelength and amplitude can be similar for storm surge and tsunami with both being markedly longer in wavelength than wind generated waves. The difference in velocity, wave set-up, period and water volume at the coast mean tsunami and storm surge can be differentiated in terms of velocity, period and repetition of inundation, likely bed shear stress and back flow characteristics. For example Dawson (1994) and Dawson & Stewart, (2007) proposed that it is the unique characteristics of tsunami run-up wave behaviour (with respect to storm waves) that produces a distinctive style of sedimentation across the coastal zone, although this has recently been challenged by Bridge (in press). The long period between tsunami waves (often 20 minutes to more than an hour) mean the time period between inundation of a coastline can vary from hours to days (Dawson, 1994). This long period often allows for alternate periods of tsunami inflow and outflow which can deposit sedimentary beds that contain distinct sedimentary features indicative of alternating landward and seaward flow (Nanayama & Shigeno, 2006).

Sandsheets found in low energy back-barrier environments are often indicative of washover deposition by storm surge, large waves or tsunami (Witter et al. 2001). Differentiating between these deposits in geological sequences can only be accomplished by developing well-defined facies models that incorporate mineralogical and sedimentological features from deposits of known origins. Recent research into modern tsunami and storm events (Goff et al 2001; Nanayama et al. 2000; Gelfenbaum & Jaffe, 2003; Sedgwick & Davis, 2003; Switzer et al. 2004; Switzer & Jones, 2008a; Morton et al., 2007) has provided several key identifiable and differentiating sedimentary features that may assist the investigation of older sequences. In particular storm and tsunami deposits can be reportedly differentiated by comparing and

contrasting the contact with the underlying sediments (recently challenged by Bridge, in press); the range of identifiable source sediments; the degree to which the sediments are sorted; the presence and thickness of graded beds; and evidence for directional flow changes (Kortekaas, 2002; Switzer & Jones, 2008b).

In back barrier environments storms overwash events are usually non-erosional events that cause little erosion of the back barrier substrate. In direct contrast tsunami deposits often contain rip-up clasts of the underlying stratigraphy (Gelfenbaum & Jaffe, 2003; Kortekaas, 2002). Direct contrasts also exist in sediment source, with storm deposits eroding mainly beach face and dune material whereas tsunami erode material from a much larger range of environments (Nanayama et al., 2000; Switzer et al., 2005; Switzer & Jones, 2008b). Other diagnostic criteria such as sediment sorting characteristics and the presence and nature of graded beds, are inherently related to the source area of sediments. Differential sorting and graded beds require a range of grain sizes; it is apparent that in some cases a restricted grain size range can make it difficult to use these criteria with any interpretive confidence (Switzer & Jones, 2008b). Finally the presence of sedimentary features that indicate uni-directional or bi-directional flow has been cited as definitive of storm or tsunami with storms characterised by uni-directional flow (Nanayama et al., 2000; Nanayama & Shigeno, 2006).

There are no globally applicable tsunami criteria obtainable from sedimentological studies (Kortekaas, 2002; Switzer and Jones, 2008b). What can be compiled for the many deposits attributed to tsunami is a suite of sedimentary features or commonalities, often called signatures (Bryant, 2001; Kortekass, 2002; Goff et al., 2001, 2004; Kortekaas & Dawson, 2007; Switzer & Jones, 2008b). These signatures must be considered in terms of the local setting as they are very much site dependant. Palaeo-washover deposits can only be attributed to an event type through careful analysis of spatial features such as the elevation, lateral extent and run-up of the deposit along with sedimentary features such as grading, the presence of intraclasts, and particle size distribution of the sediments. These analyses when combined may lead to a suite of evidence that can point to storm or tsunami as the likely depositional agent. Unfortunately when considered alone many of the characteristics are equivocal. In fact most of the signatures presented, including the presence of marine diatoms (Hemphill-Haley, 1996; Dawson & Smith, 2000) or increases in particular elemental concentrations (Chague-Goff & Goff, 1999; Goff & Chague-Goff, 1999; Chague Goff et al. 2000; Goff et al., 2001) only indicate the marine origin of the sediments and inundation by ocean water. Hence

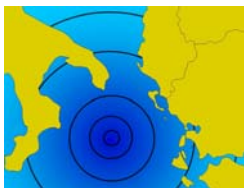
storm surges, sea level change or regional subsidence may show similar sedimentological characteristics (Witter et al., 2001).

Recent work by Witter et al. (2001), Kortekaas (2002), Switzer et al. (2004), Switzer (2008b) and Bridge (in press) have recognized the equivocal nature of many so called tsunami signatures found in sandsheets. This stated, there remain many cases in the literature where a tsunami or storm origin is stated with little consideration given to alternative interpretations. Although work continues on the differences between tsunami and storm deposits, their preservation and recognition in the geological record remains subject to much uncertainty and conjecture.

References

- Atwater B.F. (1987). *Evidence for great Holocene earthquakes along the outer coast of Washington State*. Science 236, 942-944.
- Bridge J.S. (2008). *Discussion of articles in "Sedimentary features of tsunami deposits"*. Sedimentary Geology, in press.
- Bryant E.A. (2001). *Tsunami: The Underrated Hazard*. Cambridge University Press, Stanford, 350 pp.
- Chague-Goff C., Goff J.R. (1999). *Palaeotsunami: now you see them now you don't*. Tephra 10, 10-12.
- Chague-Goff C., Nichol S.L., Jenkinson A.V., Heijnis H. (2000). *Signatures of natural catastrophic events and anthropogenic impact in an estuarine environment, New Zealand*. Marine Geology, 167, 3, 285-301.
- Cheung K.F., Phadke A.C., Wei Y., Rojas R., Douyere Y.J.M., Martino C.D., Houston S.H., Liu P.L.F., Lynette P.J., Dodd N., Liao S., Nakazaki E. (2003). *Modeling of Storm-Induced Coastal Flooding for Emergency Management*, Ocean Engineering, 30, 1353-1386.
- Dawson A.G. (1994). *Geomorphological effects of tsunami runup and backwash*. Geomorphology 10, 83-94.
- Dawson A.G. (1999). *Linking tsunami deposits, submarine slides and offshore earthquakes*. Quaternary International 60, 119-126.
- Dawson A.G., Shi S.Z. (2000). *Tsunami deposits*. Pure and Applied Geophysics 157, 875-897.
- Dawson A.G., Stewart I. (2007). *Tsunami deposits in the geological record*. Sedimentary Geology 200 166-183.
- Dawson A.G., Long D., Smith D.E. (1988). *The Storegga slides: evidence from eastern Scotland for a possible tsunami*. Marine Geology, 82, 271-276.
- Dawson S., Smith D. E. (2000). *The sedimentology of Middle Holocene tsunami facies in northern Sutherland, Scotland, UK*. Marine Geology 170 1-2, 69-79.
- Dawson S. (2007). *Diatom biostratigraphy of tsunami deposits: Examples from the 1998 Papua New Guinea tsunami*. Sedimentary Geology 200, 238-335.
- Dominey-Howes D. (1996). *The Geomorphology and Sedimentology of Five Tsunami in the Aegean Sea Region, Greece*. PhD thesis, Coventry University, Coventry, 272 pp. (unpublished).
- Geist E. L. (1999). *Modeling the Natural Complexities of a Local Tsunami*. International Tsunami Society Proceedings, 7, 7-5, 751-758.
- Gelfenbaum G., Jaffe B. (2003). *Erosion and sedimentation from the 17 July, 1998, Papua New Guinea tsunami*. Pure and Applied Geophysics, 160, 1969-1999.
- Goff J.R., Chague-Goff C. (1999). *A late Holocene record of environmental changes from coastal wetlands: Abel Tasman National Park, New Zealand*. Quaternary International, 56, 39-51.
- Goff J.R., Chague-Goff C., Nichol S. (2001). *Palaeotsunami deposits: a New Zealand perspective*. Sedimentary Geology, 143, 1-6.
- Goff J.R., McFadgen B.G., Chague-Goff C. (2004). *Sedimentary differences between the 2002 Easter storm and the 15th-century Okoropunga tsunami, southeastern North Island, New Zealand*. Marine Geology, 204, 235-250.
- Hemphill-Haley E. (1996). *Diatoms as an aid in identifying late-Holocene tsunami deposits*. The Holocene, 6, 439-448.
- Kelletat D. Comments to Dawson A.G. and Stewart I. (2007). *"Tsunami deposits in the geological record"*. Sedimentary Geology, in press.
- Kortekaas S. (2002). *Tsunamis, storms and earthquakes: Distinguishing coastal flooding events*. Ph.D. thesis, University of Coventry, Coventry, 179pp. (unpublished).
- Kortekaas S., Dawson A.G. (2007). *Distinguishing tsunami and storm deposits: An example from Martinhal, SW Portugal*. Sedimentary Geology 200 208-221.
- McInness K.L., Hubbert G.D. (2001). *The impact of eastern Australian cut-off lows on coastal sea levels*. Meteorological Applications, 8, 229-24.
- Morton R. A., Gelfenbaum G., Jaffe B. E. (2007). *Physical criteria for distinguishing sandy tsunami and storm deposits using modern examples*. Sedimentary Geology, 200, 184-207.
- Nanayama F., Shigeno K., Satake K., Shimokawa K., Koitabashi S., Mayasaka S., Ishii M. (2000). *Sedimentary differences between 1993 Hokkaido-Nanseioki tsunami and 1959 Miyakojima typhoon at Tasai, southwestern Hokkaido, northern Japan*. Sedimentary Geology, 135, 255-264.

- Nanayama N., Shigeno K. (2006). *Inflow and outflow facies from the 1993 tsunami in southwest Hokkaido*. *Sedimentary Geology*, 187, 139-158.
- Scheffers A., Kelletat D. (2003). *Sedimentologic and geomorphologic tsunami imprints worldwide - a review*. *Earth Science Reviews*, 63, 83-92.
- Sedgwick P.E., Davis R.A. (2003). *Stratigraphy of washover deposits in Florida: implications for recognition in the stratigraphic record*. *Marine Geology*, 200, 31-48.
- Switzer A.D., Jones B.G. (2008a) *Setup, Deposition, and Sedimentary Characteristics of Two Storm Overwash Deposits, Abrahams Bosom Beach, Southeastern Australia*. *Journal of Coastal Research*, 24, sp1 pp. 189–200.
- Switzer A.D., Jones B.G. (2008b). *Large-scale washover sedimentation in a freshwater lagoon from the southeast Australian coast: tsunami or exceptionally large storm*. *The Holocene*, 18(4), 633-649
- Switzer A.D., Jones B.G., Bristow C.S. (2004). *Geological evidence for large-scale washover events from coastal New South Wales, Australia: implications for management*. In: *Delivering Sustainable Coasts: Connecting Science and Policy Littoral 2004 Proceedings*, Volume 1, 390-395. Cambridge Publications, Cambridge.
- Switzer A.D., Pucillo K., Haredy R.A., Jones B.G., Bryant E.A. (2005). *Sea-level, storms or tsunami: enigmatic sand sheet deposits in a sheltered coastal embayment from southeastern Australia*. *Journal of Coastal Research*, 21, 655-663.
- Szczuciński W., Niedzielski P., Rachlewicz G., Sobczyński T., Zio'a A., Kowalski A., Lorenc S., Siepak J. (2005). *Contamination of tsunami sediments in a coastal zone inundated by the 26 December 2004 tsunami in Thailand*. *Environmental Geology*, 49(2), 321-331.
- Witter R.C., Kelsey H.M., Hemphill-Haley E. (2001). *Pacific Storms, El Niño and Tsunamis: Competing Mechanisms for Sand Deposition in a Coastal Marsh, Euchre Creek, Oregon*. *Journal of Coastal Research*, 17, 563-583.



2nd International Tsunami Field Symposium

IGCP Project 495

Quaternary Land-Ocean Interactions:
Driving Mechanisms and Coastal Responses

Ostuni (Italy) and Ionian Islands (Greece) 22-28 September 2008



Project 495

Vött A.¹, May S. M.², Masberg P.³, Klasen N.², Grapmayer R.², Brückner H.²,
Bareth G.¹, Sakellariou D.⁴, Fountoulis I.⁵, Lang F.⁶

Tsunamite findings along the shores of the Eastern Ionian Sea – the Cefalonia case study (NW Greece)

¹Department of Geography, Universität zu Köln (Cologne), Germany
e-mail: voett@staff.uni-marburg.de;

²Faculty of Geography, Philipps-Universität Marburg, Deutschhausstr. Marburg, Germany

³Mineralogical Museum, Philipps-Universität Marburg, Firmaniplatz, Marburg, Germany

⁴Hellenic Center for Marine Research, Institute of Oceanography, Athens, Greece

⁵Department of Dynamic, Tectonic and Applied Geology, National and Kapodistrian University of
Athens, Panepistimiopoli, Athens, Greece

⁶Department of Classical Archaeology, Technische Universität Darmstadt, Darmstadt, Germany

Keywords: *tsunamite, dislocated blocks, Holocene, Ionian Islands, NW Greece*

The northwestern Greek coast between the Ambrakian Gulf and the southern Peloponnese is exposed to the highly tsunamigenic Hellenic Trench where the African Plate is being subducted by the overriding Aegean Plate (Sachpazi et al., 2000; Doutsos & Kokkalas, 2001).

Tsunami catalogues show that the eastern Ionian Sea is characterized by the highest number of tsunami events reported from all over the Eastern Mediterranean. The statistical re-occurrence interval for tsunami events is 8-11 years only (Soloviev et al., 2000; Schielein et al., 2008).



Figure 1. High-energy event deposits at the western coast of Paliki Peninsula on Cefalonia Island and location of Cefalonia in NW Greece.

In 2005, for the first time for northwestern Greece and the Ionian Islands, a series of (palaeo-)tsunami deposits were discovered (Vött et al., 2006, 2007a, 2007b, 2007c, 2008a; May et al., 2008). These sediments, partly interrelated, attest to multiple tsunami landfall since the mid-Holocene. Tsunamite types comprise dislocated mega-blocks both on land and under water, washover fan deposits (chevrons), runup/backwash layers, a breakthrough channel and suspension deposits in a near-coast freshwater lake environment. Recent studies along the shores of the quiescent lagoonal waters of the nearby Sound of Lefkada revealed geo- and bio-scientific evidence of multiple tsunami influence since, at least, around 3000 cal BC and document strong impact on the long-term coastal evolution (Vött et al., 2008b). Tsunami findings from the inner sound correlate well with those known from the Preveza-Lefkada outer-sound area.

A number of comparative studies were carried out in order to bring these results in a wider supra-regional context.

The area around Cape Gerogombos shows a cliff-top stripe which runs parallel to the present coast. The stripe is 150-200 m wide and void of soil or vegetation. It is characterized by different zones. Zone I, closest to the sea, is made up of bedrock which is completely free of any loose material.

The adjacent zone II shows dislocated mega-blocks (boulders) and zone III, following landward, thick rubble ridges out of smaller blocks and stones.

The elevation of the stripe ranges from 10-15 m a.s.l. near the cliff, up to 20 m a.s.l. further inland. Dislocated mega-blocks encountered in zone II are up to 10 m³ large and partly arranged in the form of imbrication trains. The blocks derive from the (supra-)littoral zone as indicated by rock pool structures and show an inclined, locally even upside-down position.

Here, we present selected results from the Cefalonia case study. On Cefalonia Island, geomorphological research was carried out on the western coast of Paliki Peninsula.

We found mega-blocks up to 5-10 m³ large at elevations of up to 10 m a.s.l., partly characterized by imbrication and locally occurring as imbrication trains. High-energetic dislocation is documented by the fact that bio-erosive rock pools found in the massive limestone blocks were tilted or even rotated upside-down (Fig. 1). Impact of extreme events is also reflected by thick rubble ridges, several dozens of meters long, which were encountered at elevations of up to 20 m a.s.l.

Most bizarre is a 2.5 m-thick conglomeratic tsunamite out of gravel clasts of different size including numerous fossil fragments found at around 2 m a.s.l. at the western coast of Paliki Peninsula (Fig. 2).

The conglomerate is made up of several layers with a seaward inclination of 10-15° and is adhesively stuck on the adjacent limestone cliff. Its uppermost part lies at 3.20 m a.s.l.

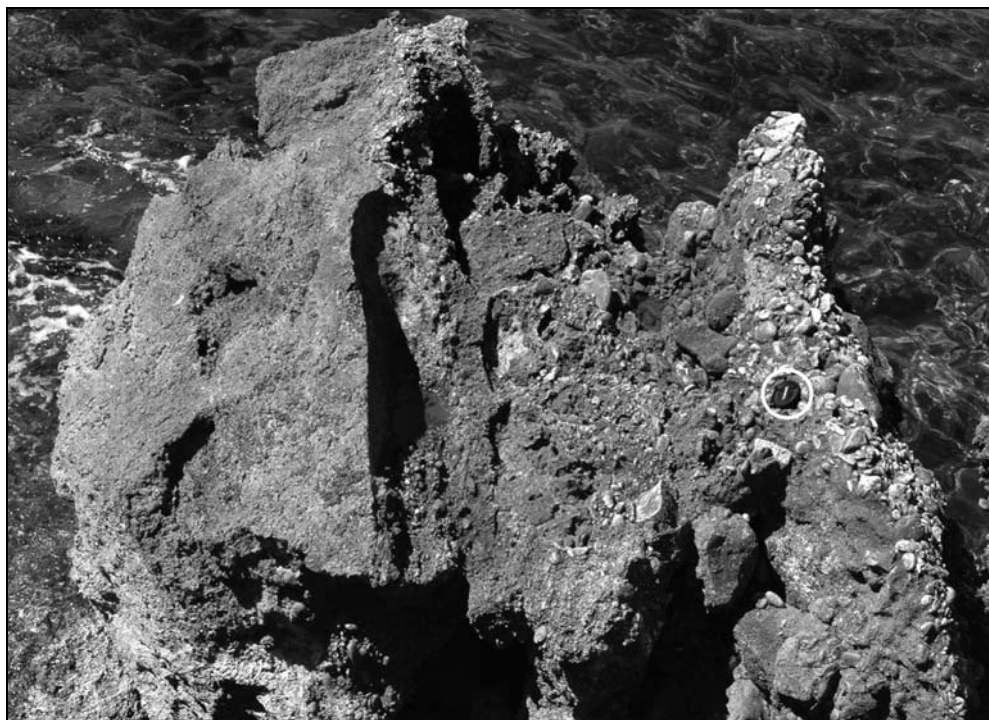


Figure 2. Tsunamigenic conglomerate encountered at the western coast of Paliki Peninsula on Cefalonia Island. The block is broken off the tsunamite covering an area of approximately 400 m². The block's left side shows the underlying limestone bedrock, its right side the high-energy deposit. The camera cap is 6.7 cm in diameter.

The sequence shows a number of sedimentological features characteristic for tsunami deposits such as (i) a distinct erosional unconformity at its base, (ii) rip-up clasts of the underlying material incorporated into the high-energy deposits, (iii) a distinct layering as well as (iv) an upward increase in sorting and (v) a general fining-upward sequence. Radiocarbon dating of three macrofossils encountered in the conglomerate yielded dates of around 24,000 cal BP, 22,000 cal BP, and 16,000 cal BP. X-ray diffraction analyses showed that the dated material is not re-crystallized and the ages have to be considered as reliable (maximum) ages. The conglomerate thus is of late Pleistocene or even Holocene age.

The conglomerate shows features typical of tsunami deposits such as (i) an erosional unconformity at its base, (ii) numerous incorporated rip-up clasts of the underlying bedrock, up to 0.5 m in diameter, (iii) a clearly laminated overall structure, (iv) well sorted to very badly sorted grain size distribution, and (v) a fining-upward and thinning-landward appearance (for detailed lists of criteria see Dominey-Howes et al., 2006; Kortekaas and Dawson, 2007; see also Moore et al., 2006; Hawkes et al., 2007; Morton et al., 2007; Paris et al., 2007 for characteristics of the 2004 Indian Ocean tsunami). Three radiocarbon dates of macrofossil remains out of the conglomerate, accomplished by Prof. Dr. P.M. Grootes, Leibniz-Labor für Altersbestimmung und Isotopenforschung, Christian-Albrechts-Universität zu Kiel, rendered around 24,000 cal BP, 22,000 cal BP, and 16,000 cal BP. X-ray diffractometric analyses of the samples yielded around 99% aragonite. Thus, major re-crystallization of the fossil carbonate can be excluded meaning that the given ages are to be considered as reliable dates. Taking into account that the high-energy conglomerate contains a lot of reworked older material and fossils, we consider 16,000 cal BP as maximum age of the event.

This tsunamite finding offers two intriguing scenarios both of which have not yet been discussed for the Mediterranean: (i) if the 16,000 cal BP age is correct, the palaeo sea level stand at that time implies a tsunami runup of at least 70-80 m; (ii) if the true age is Holocene, the 2.5 m-thick deposits document tremendous high-energy input and subsequent cementation sometime during the past millennia. Further detailed analyses will be carried out within the framework of a tsunami research project during 2009-2011 focussing the eastern Ionian Sea.

Moreover, vibracores were retrieved from along the shores of the inner Argostoli Gulf to the east of Paliki Peninsula in order to look for distal effects of tsunami impact. Vibracore LIX 1 in the Livadi coastal plain revealed a sequence of more than 4 m of strongly consolidated, probably allochthonous

middle sand including numerous gravel and large bedrock fragments on top of well sorted in-situ fine sandy to silty foreshore deposits. Vibracore LIX 2, drilled some 800 m to the northeast of LIX 1 in the same coastal plain, yielded a layer of ex-situ unsorted sandy gravel including numerous marine shell fragments in between silty mud of an autochthonous swampy environment. Similar stratigraphies were found, for instance, in core KRA 3 in the Koutavos coastal plain near Argostoli where a palaeosol sequence shows an erosional unconformity at its top and is covered by a 40-cm-thick stratum of unsorted sand and gravel including bedrock and ceramic fragments. This unit is followed by muddy silt of a swampy environment.

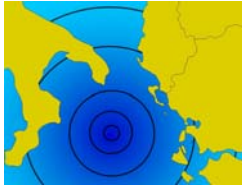
Our cores thus corroborate high-energy impacts on the Argostoli Gulf during the Holocene which are probably associated to those tsunami events which left their sediments along the outer Paliki coast. However, detailed vibracore studies and dating efforts are required to clarify the extent and characteristics (runup, inundation) of tsunami influence on Paliki Peninsula and the adjacent Argostoli Gulf.

This paper gives the first report on tsunami evidence from Cefalonia Island, the most touristic of all Ionian Islands. Considering our results, tsunami hazard in the eastern Ionian Sea must not be underestimated and risk assessment plans are highly required.

References

- Dominey-Howes D.T.M., Humphreys G.S., Hesse P.P. (2006). *Tsunami and palaeotsunami depositional signatures and their potential value in understanding the late-Holocene tsunami record*. The Holocene, 16/8, 1095-1107.
- Doutsos T., Kokkalas S. (2001). *Stress and deformation patterns in the Aegean region*. Journal of Structural Geology, 23, 455-472.
- Hawkes A.D., Bird, M., Cowie S., Grundy-Warr C., Horton B.P., Shau Hwai A.T., Law L., Macgregor C., Nott J., Eong Ong J., Rigg J., Robinson R., Tan-Mullins M., Tiong Sa, T., Yasin Z., Wan Aik L. (2007). *Sediments deposited by the 2004 Indian Ocean Tsunami along the Malaysia-Thailand Peninsula*. Marine Geology, 242, 169-190.
- Kortekaas S., Dawson A.G. (2007). *Distinguishing tsunami and storm deposits: An example from Martinhal, SW Portugal*. Sedimentary Geology, 200, 208-221.
- May S.M., Vött A., Brückner H., Brockmüller S. (2008). *Evidence of tsunamigenic impact on Actio headland near Preveza, NW Greece*. In: Gönner G., Pflüger B., Bremer J.-A. (Eds.), *Von der Geoarchäologie über die*

- Küstendynamik zum Küstenzonenmanagement*. Coastline Reports, 9, 115-125.
- Moore A., Nishimura Y., Gelfenbaum G., Kamataki, T., Triyono R. (2006). *Sedimentary deposits of the 26 December 2004 tsunami on the northwest coast of Aceh, Indonesia*. Earth Planets Space, 58, 253-258.
- Morton R.A., Gelfenbaum G., Jaffe B.E. (2007). *Physical criteria for distinguishing sandy tsunami and storm deposits using modern examples*. Sedimentary Geology, 200, 184-207.
- Paris R., Lavigne F., Wassmer P., Sartohadi J. (2007). *Coastal sedimentation associated with the December 26, 2004 tsunami in Lhok Nga, west Banda Aceh (Sumatra, Indonesia)*. Marine Geology, 238, 93-106.
- Sachpazi M., Hirn A., Clément C., Haslinger F., Laigle M., Kissling E., Charvis P., Hello Y., Lépine J.-C., Sapin M., Ansorge J. (2000). *Western Hellenic subduction and Cephalonia Transform: local earthquakes and plate transport and strain*. Tectonophysics, 319/4, 301-319.
- Schielein P., Zschau J., Woith H., Schellmann G. (2008). *Tsunamigefährdung im Mittelmeer – Eine Analyse geomorphologischer und historischer Zeugnisse*. Bamberger Geographische Schriften, 22, 153-199.
- Soloviev S.L., Solovieva O.N., Go C.N., Kim K.S., Shchetnikov N.A. (2000). *Tsunamis in the Mediterranean Sea 2000 B.C. – 2000 A.D.* Kluwer, Dordrecht, The Netherlands, 237 pp.
- Vött A., Brückner H., Brockmüller S., May M., Fountoulis I., Gaki-Papanastassiou K., Herd R., Lang F., Maroukian H., Papanastassiou D., Sakellariou D. (2008a). *Tsunami impacts on the Lefkada coastal zone during the past millennia and their palaeogeographical implications*. In: Papadatou-Giannopoulou H. (Ed.), Proceedings of the International Conference Honouring Wilhelm Dörpfeld, August 6-9, 2006, Lefkada, in press.
- Vött A., Brückner H., Brockmüller S., Handl M., May S.M., Gaki-Papanastassiou K., Herd R., Lang F., Maroukian H., Nelle O., Papanastassiou D. (2008b). *Traces of Holocene tsunamis across the Sound of Lefkada, NW Greece*. Global and Planetary Change (in press).
- Vött A., Brückner H., May M., Lang F., Herd R., Brockmüller S. (2007a). *Strong tsunami impact on the Bay of Aghios Nikolaos and its environs (NW Greece) during Classical-Hellenistic times*. Quaternary International (available online – <http://dx.doi.org/10.1016/j.quaint.2007.02.017>).
- Vött A., Brückner H., May M., Lang F., Brockmüller S. (2007b). *Late Holocene tsunami imprint on Actio headland at the entrance to the Ambrakian Gulf*. Méditerranée, revue géographique des pays méditerranéens, 108, 43-57.
- Vött A., Brückner H., Georg C., Handl M., Schriever A., Wagner H.-J. (2007c). *Geoarchäologische Untersuchungen zum holozänen Landschaftswandel der Küstenebene von Palairos (Nordwestgriechenland)*. In: Lang F., Schwandner E.-L., Funke P., Kolonas L., Jahns S., Vött A. (Eds.): Interdisziplinäre Landschaftsforschung im westgriechischen Akarnanien. Archäologischer Anzeiger, 1/2007: 191-213. Berlin.
- Vött A., May M., Brückner H., Brockmüller S. (2006). *Sedimentary evidence of late Holocene tsunami events near Lefkada Island (NW Greece)*. In: Scheffers A., Kelletat D. (Eds.), Tsunamis, hurricanes and neotectonics as driving mechanisms in coastal evolution. Zeitschrift für Geomorphologie N.F., Suppl. Vol., 146, 139-172.



Wassmer P.¹, Schneider J.-L.², Lavigne F.¹, Paris R.³

Sedimentary signature of the December 26th 2004 tsunami along the north eastern shore of Banda Aceh: anisotropy of magnetic susceptibility (AMS) contribution to a better understanding of the tsunami wave train dynamic

¹Laboratoire de Géographie Physique UMR 8591 CNRS - Université Panthéon-Sorbonne (Paris 1), Meudon Cedex. e-mail: wassmerpat@aol.com; lavigne@univ-paris1.fr;

²UMR 5805 EPOCH CNRS, Université de Bordeaux 1, Talence Cedex
e-mail: j.l.schneider@epoch.u-bordeaux1.fr;

³Géolab UMR 6042 CNRS-Université Blaise-Pascal, Clermont-Ferrand Cedex 1
e-mail: raparis@univ-bpclermont.fr

Keywords: *Sedimentary signature, Tsunami, Anisotropy of Magnetic Susceptibility, Wave train dynamic, Sumatra, Indonesia*

The tsunami that struck the Indian Ocean shores on December 26, 2004 was triggered by an earthquake of exceptional magnitude ($M_z = 9.15$)

with disastrous consequences for the northern littoral of Sumatra close to the epicentre, where more than 170,000 people died.

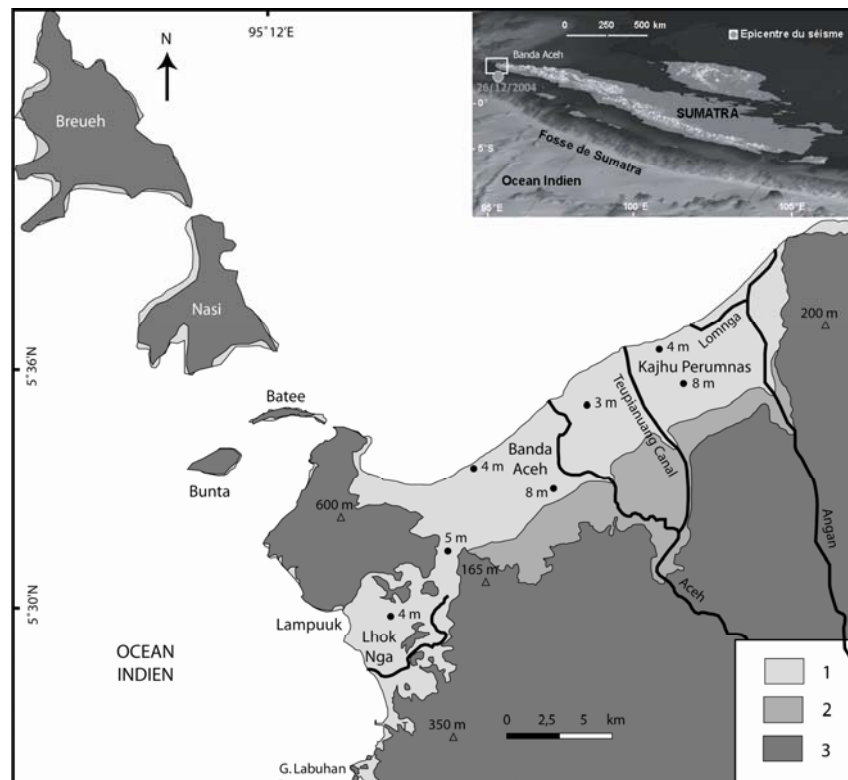


Figure 1. Location map of the Banda Aceh region. 1: coastal plains flooded by the tsunami; 2: non flooded coastal plains; 3: uplands. Insert 3D-map showing the Sumatra Island, the studied area, and the epicentre of the 26/12/2004 earthquake.

This event is an unprecedented human disaster but offers a unique opportunity to improve our knowledge of such devastating natural hazards. The environmental impact of huge tsunamis like this one, with waves heights reaching up to 34 m on the south-western coast and 15 m on the north-western coast of Aceh Province (Lavigne et al., 2006), varies with coastal morphology.

On the coast of Banda Aceh, only the lowest areas, i.e. 20 to 30 m above sealevel, were scoured. Due to conditions causing a wave trap, however, a maximal height of 51 m was recorded in the small bay of Labuhan (Lavigne et al., 2006). In other locations such as Lhok Nga Bay and Banda Aceh Bay, the extremely flat topography allowed wave penetration as far as 5 km inland.

The district of Kajhu, located northeast of Banda Aceh (Fig. 1), is a wide flat area where the ten waves constituting the December 26, 2004 tsunami wave train totally uprooted the trees, planed off the sea front dunes, destroyed all the buildings.

The topography was locally modified by the turbulent wave front and then buried by a layer of sediment translocated from the beaches and dunes of the seafront.

An investigation led on 150 holes dug to the previous soil, with a 7 m mesh size on a sub horizontal surface shows a variation of the deposit thickness from 0 to 71 cm and indicates that the sediments levelled the former topography.

In order to better understand the link between wave dynamics and sediment facies in that particular context, the sedimentary deposits were studied in the light of direct and indirect evidence concerning the number and behaviour of the waves involved (tree trunks oriented by the waves, eyewitnesses testimonies).

Profiles were excavated along transects realized according to the main wave direction. Sediment translocation was practically instantaneous during the event.

Stacked layers of normal graded sequences have commonly been reported in the context of tsunami deposits (Dawson et al., 1996; Dawson and Shi, 2000; Hawkes et al., 2007; Hori et al., 2007; Morton et al., 2008).

However, this study reveals a sharp facies differentiation between the deposits located near the shoreline (proximal zone) and those located far inland (distal zone). Near the sea, the deposits were found to be coarse and ungraded, whereas inland the frequency of stratified normal graded sequences increases (Fig. 2).

1: fine-grained grey sand; **2:** roughly laminated grey sand; **3:** medium-grained beige sand; **4:** beige medium- to coarse-grained sand; **5:** coarse-grained sand; **6:** thin layer of fine black sand; **7:** rustcoloured thin layer; **8:** pre-tsunami brownish soil; **9:** pre-tsunami brownish soil with abundant roots; **10:** identified sequences; **11:** samples; **12:** distance from the former shoreline.

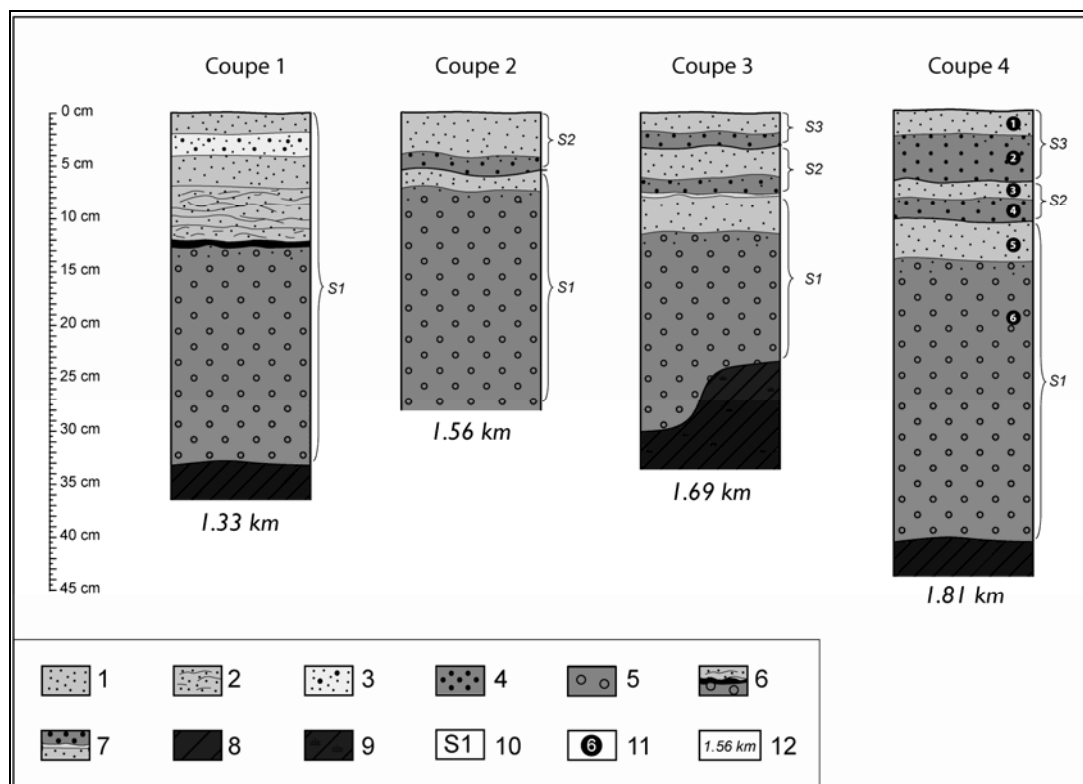


Figure 2. Sedimentary differentiation exhibits progressively more accentuated stratification and grading within the tsunami deposits along a landward transect from the coastline.

Sedimentary profiles coordinates:

Log 1: 46 N 0763815 / UTM 0620350;

Log 2: 46 N 0764049 / UTM 0620318;

Log 3: 46 N 0764202 / UTM 0620272;

Log 4: 46 N 0764300 / UTM 0620224.

As many as seven sequences were observed. Each one corresponds to the sediment mass brought by one wave. These deposits are well preserved because the power generated by the movements from and to the sea (end of the run-up and beginning of the backwash movements) was too low in this distal zone to enable removal of the material deposited by the previous waves (Wassmer et al., 2007). The respective roles of the run-up and backwash on the sedimentary signature were also studied. Only the first wave was followed by a backwash but the second wave which was the strongest, wiped out the previous deposited sediments. The following waves pushed inland during about 45 minutes without intermediary backwash. After the last wave, the retreat occurs. Slow in the distal zone, the speed of the water increased seaward allowing the erasing of the previous deposited material (Wassmer et al., 2007). As macroscopic fabric is poorly developed in the deposits, we have conducted a study of the anisotropy of the magnetic susceptibility (AMS) in order to test the possible contribution of this method to a better understanding of the tsunami wave train dynamic. AMS allows assessment of the overall fabric of the deposits. It is an aid to reconstruction of transport direction and mechanisms (Schneider et al., 2004). AMS studies have not been applied previously to tsunami deposits. The goal of this approach is to obtain data about wave train flow in terms of dynamics and directions. Undisturbed and oriented samples used for this study were collected in the field on vertical profiles using 19 mm cubic plastic box. In each identified layer, a box was plugged horizontally in the moist sediments (with unconsolidated material, the sampling must be done in humid conditions). As it can be seen on Fig. 3 profile, five fining upwards sequences can be observed.

Samples were taken in each sequence at the base (coarser material), and at the top (finer material). Measurements of the AMS were done with a Kappabridge KLY-2 device. Magnetic susceptibility was measured for each sample in 15 directions in order to determine the ellipsoid of AMS. The geometry of the AMS ellipsoid (Hrouda, 1982; Tarling & Hrouda, 1993) can be established by the characteristics (azimuth and plunge) of its main axis (K_{\max} , K_{int} , K_{\min}). K_{\max} generally parallels the mean long axis of the magnetic particles, and is often imbricated in respect to the vector of transport, even if Hamilton and Rees (1970) shown that, in

some cases, rolling effects can induce an orientation of the K_{\max} axis perpendicular to the flow direction. For each sample, anisotropy rate P (K_{\max}/K_{\min}), foliation rate F (K_{int}/K_{\min}) and lineation rate L (K_{\max}/K_{int}) have been calculated.

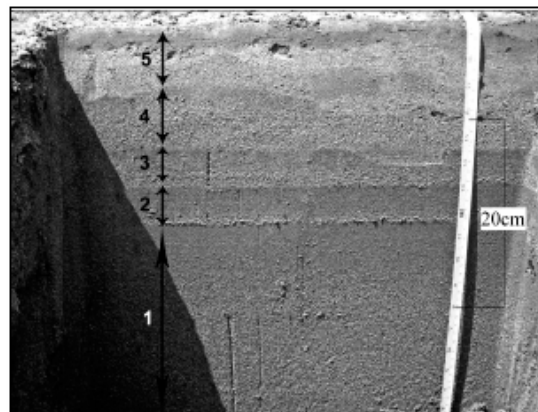


Figure 3. Sedimentary profile n° 5 (see Fig. 1) Showing five stratified fining upward sequences.

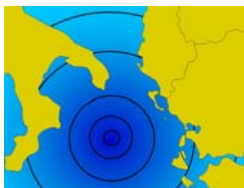
The petrofabrics can be visualized by binary diagrams, in which F and L are reported. The results show a clear differentiation for each sequence between the base, where the measure indicates that traction was the main process when the material emplaced, and the top, where decantation dominated during the emplacement of the fine upper material. This confirms the previous observations and the link between observed sequences and sediment mass brought by waves within the tsunami wave train.

Each fining upward sequence reflects the progressive slowing down of a single wave. The traction predominates during the emplacement of the coarse material while decantation of the fine sediments occurs when the water, at the end of the uprush, is quite at rest. Unfortunately the K_{\max} axis plunge is generally insignificant and, as it can be related to errors during sampling, it cannot be used, on this site, as a flow indicator.

References

- Dawson A.G., Shi S. (2000). *Tsunami Deposits*. Pure and Applied Geophysics, 157, 875-897.
- Dawson A.G., Shi S., Dawson S., Takahashi T., Shuto N. (1996). *Coastal Sedimentation Associated with the June 2nd and 3rd, 1994 Tsunami in Rajegwesi, Java*. Quaternary Sciences Review, 15, 901-912.
- Hamilton N., Rees A.F. (1970). *The use of magnetic fabric in paleocurrent estimation*. In: Runcorn, S.K. (Ed.), *Paleogeophysics*. Academic, San Diego, pp. 445-464.
- Hawkes A.D., Bird M., Cowie S., Grundy-War C., Horton B.P., Shau Hwai A.T., Law L.,

- Macgregor C., Nott J., Ong J.E., Rigg J., Robinson R., Tan-Mullins M., Sa T.T., Yasin Z. Aik L.W. (2007). *Sediment deposited by the 2004 Indian Ocean Tsunami along the Malaysia-Thailand Peninsula*. Marine Geology, 242 (1), 169-190.
- Hori K., Kuzumoto R., Hirouchi D., Umitsu M., Janjirawuttikul N., Patanakanog B. (2007). *Horizontal and vertical variations of 2004 Indian tsunami deposits: An example of two transects along the western coast of Thailand*. Marine Geology, 239 (3), 163-172.
- Hrouda F. (1982). *Magnetic anisotropy of rocks, and its applications in geology and geophysics*. Geophys. Surv. 5, 37-38.
- Lavigne F., Paris R., Wassmer P., Gomez C., Brunstein D., Grancher D., Vautier F., Sartohadi J., Setiawan A., Syahnan, Gunawan T., Fachrizal, Waluyo B., Mardiatno D., Widagdo A., Cahyadi R., Lespinasse N., Mahieu L. (2006). *Learning from a major disaster (Banda Aceh, December 26th, 2004): a methodology to calibrate simulation codes for tsunami inundation models*. Zeitschrift für Geomorphologie N.F., Suppl.-vol. 146, 253-265.
- Morton R.A., Goff J. R., Nichol S. L. (2008). *Hydrodynamic implications of textural trends in sand deposits of the 2004 tsunami in Sri Lanka*. Sedimentary Geology, doi: 10.1016/j.sedgeo.2008.03.008
- Tarling D.H., Hrouda F. (1993). *The Magnetic Anisotropy of Rocks*. Chapman & Hall, London, 218 pp.
- Wassmer P., Baumert Ph., Lavigne F., Paris R., Sartohadi J. (2007). *Sedimentary facies and transfer associated with the December 26, 2004 tsunami on the north eastern littoral of Banda Aceh (Sumatra, Indonesia)*. Géomorphologie, 4, 335-346.
- Schneider J.L.M., Pérez Torrado F.J., Gimeno Torrente D., Wassmer P., Cabrera Santana M. C., Carracedo J.C. (2004). *Sedimentary signature of the entrance of coarse-grained volcaniclastic flows into the sea: the example of the breccias units of the Las Palmas Detritic Formation (Mio-Pliocene, Gran Canaria, eastern Atlantic, Spain)*. Journal of Volcanology and Geothermal Research, Vol. 138, 3-4, 295-323.



2nd International Tsunami Field Symposium

IGCP Project 495

Quaternary Land-Ocean Interactions:
Driving Mechanisms and Coastal Responses

Ostuni (Italy) and Ionian Islands (Greece) 22-28 September 2008



Project 495

Weiss R.¹, Bourgeois J.²

“Chevrons” are not mega-tsunami deposits – a sedimentologic assessment

¹JISAO-UW and NOAA Center for Tsunami Research, PMEL, Seattle, WA, USA

e-mail: weisrz@u.washington.edu;

²Department of Earth & Space Sciences, University of Washington, Seattle, WA, USA

e-mail: jbourgeo@u.washington.edu

Keywords: chevrons, tsunami, bedforms, sedimentology, mega-tsunami, parabolic dunes

The term “chevron” was originally used for large, v-shaped, sublinear to parabolic landforms on islands in the eastern, windward Bahamas. The paleo-activity of these forms is generally associated

with Quaternary stage 5e, the last interglacial sea-level highstand, which was 4-6 m higher than present.

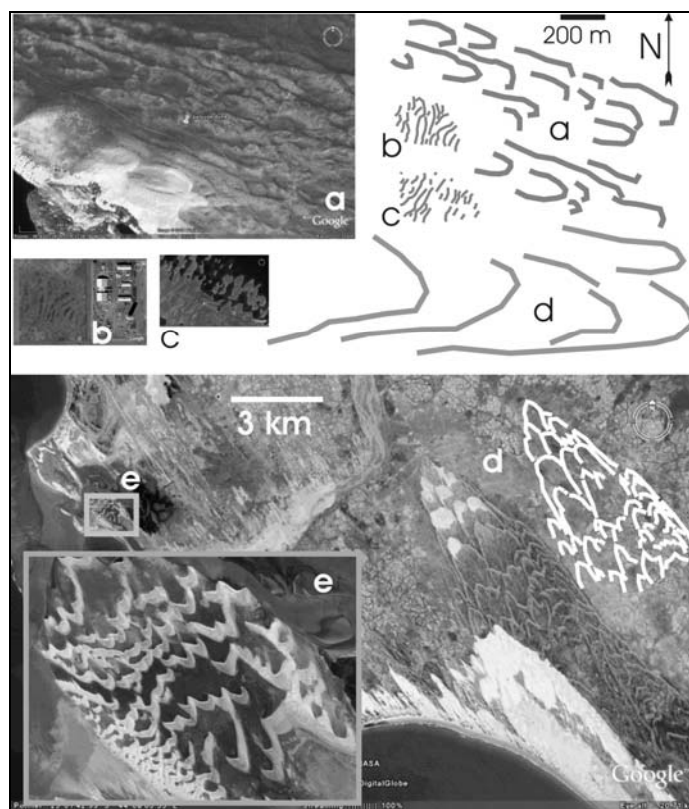


Figure 1. Large bed forms in eastern Washington State (above, shown at same scale) and southern Madagascar (below, with inset). Sketch outlines of bed forms (upper right) are also all shown at the same scale. Images are from Google Earth. Above: **a**—parabolic dunes in the Palouse region, eastern Washington, just east of the Columbia River; **b**—giant current ripples near Spokane, eastern Washington; **c**—giant current ripples in the Palouse region of eastern Washington. Below: **d,e**—coast of southern Madagascar showing “chevrons,” sand streaks, and barchans (enlarged inset).

These features have been variously interpreted as eolian bed forms, as storm-related features, and as large-wave (possibly tsunami) deposits (Hearty et al., 1998; Kindler & Strasser, 2000, 2002; Hearty et al., 2002).

In any case, it is clear from cross-bedding within these features that they are deposits associated with bed-load transport; all these Bahamas forms are composed of locally generated carbonate grains principally of sand size (0.063 – 2 mm diameter). In scale and geometry, they resemble modern shallow-water bed forms on the Bahamas platform associated with “spillover” of currents focused between islands (cays). They also resemble parabolic dunes, most of them demonstrably eolian, from around the world. However, the Bahamas chevrons typically do not repeat regularly, with predictable wavelengths, as ripples and dunes do. Since the introduction of the term “chevron” for large v- or u-shaped bed forms, the term has also been adopted by several authors (e.g. Bryant, 2001 and earlier papers; Kelletat & Scheffers, 2003; Abbott et al., 2007) to describe large-scale coastal bed forms in Australia, Madagascar, and elsewhere. These authors interpret these “chevron” bed forms as mega-tsunami deposits of Holocene age and suggest that they

point to oceanic asteroid impacts (e.g., Masse, 2007). They liken the forms to giant swash marks and tend to reject an eolian, parabolic-dune interpretation based on associated larger clasts and incorporated marine fossils, though definitive cases are lacking.

Are these features parabolic eolian dunes, mega-tsunami bed forms, or something else? Recently, in a brief essay, Pinter and Ishman (2008) challenged the interpretation of “chevrons” as mega-tsunami deposits, based essentially on the principle of Occam’s rule, arguing that an eolian interpretation is simpler and more reasonable.

We argue herein that they are NOT mega-tsunami deposits by taking a physical approach of modeling tsunami behavior and evaluating sediment-transport conditions under which these features formed. While our strongest argument is that these chevrons are *not* mega-tsunami deposits, we also agree with Pinter and Ishman (and others) that these features are mostly eolian, parabolic dunes.

In order to assess the mega-tsunami interpretation, we summarize the basic physical characteristics of the “chevron” bed-form cases where such an interpretation has been invoked, in particular, Australia and Madagascar (Fig. 1).

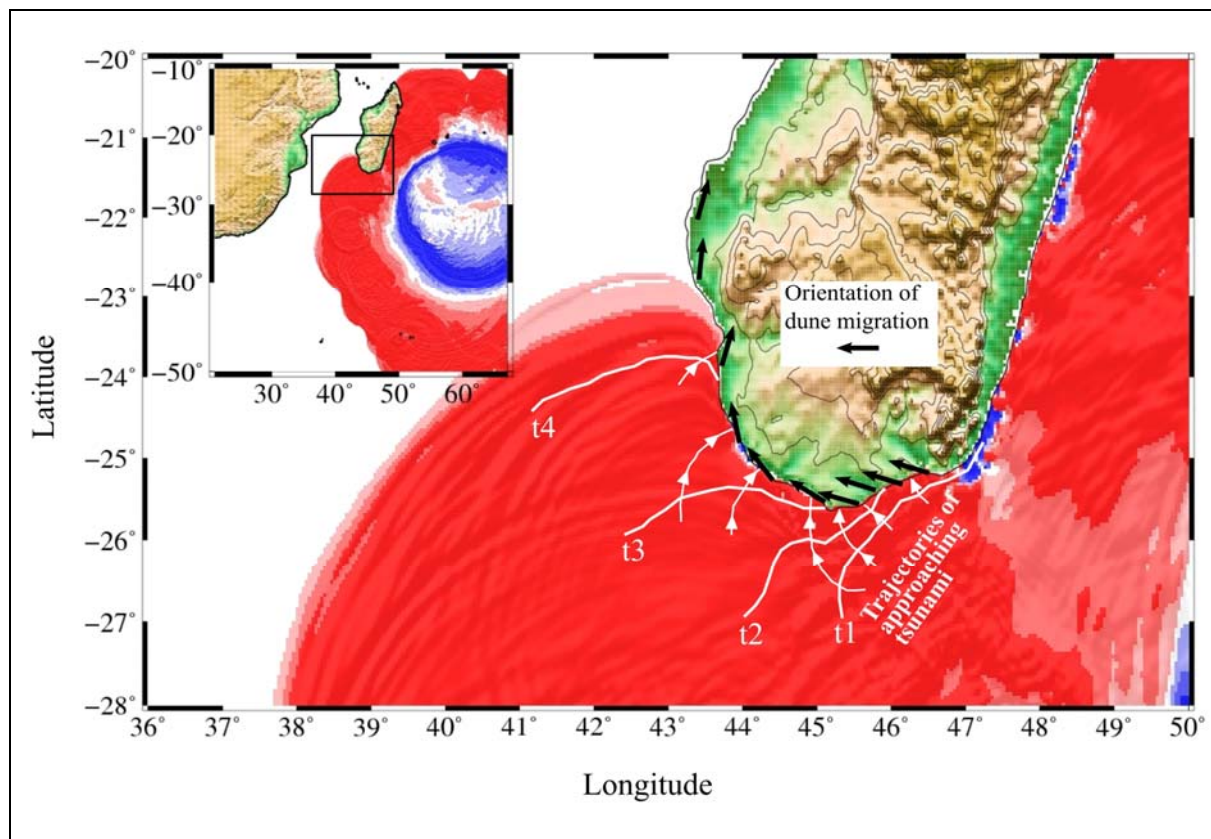


Figure 2. Modeled tsunami propagation from a point source located in the area specified by Masse (2007) and suggested in abstracts by others (e.g., Abbott et al.). Time lines of wave crests in white, with wave approach at right angles. Orientation of large bed forms shown in black (see also Figure 1d,e).

Authors who have worked in the Bahamas have not invoked impact-generated tsunamis. Bed-form parameters of interest include: orientation (provides transport direction; not tabulated), bed-form height (provides minimum flow depth), component grain size (for modeling sediment transport), and elevation of the “chevrons” above sea level (for maximum flow depths). For elevation above sea level, we do not take into account that for the earlier Holocene, e.g., sea level was 10s of m lower than present. Few of these bed forms have been dated.

Impact-tsunami assessment

We initially choose the southern Madagascar case as an example to test the tsunami hypothesis by modeling tsunami behavior—at what angle would the tsunami approach the coast? Long axes of the bed forms are assumed to be (or to have been) parallel to the flow. We modeled a tsunami with a circular source located at the proposed impact site (Fig. 2).

We used an initial wave shape that corresponds to a small impact in deep water (as in Ward & Asphaug, 2000; also see Weiss & Wunnemann, 2007). The source wave was propagated over regional bathymetry, using MOST code (Titov & Synolakis, 1998). In modeling, we considered only relative wave amplitudes, as we were more interested in the pattern of wave approach to the coast. From our analysis, it is clear that modeled wave approach is inconsistent with chevron orientation.

Sediment transport assessment

The authors cited above have postulated that chevrons are bedforms developed under flow conditions of mega tsunamis, e.g., tsunamis generated by meteoritic impacts.

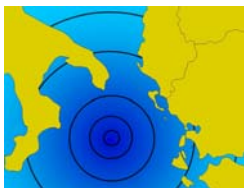
If these structures are regular bedforms with cornice structure, which all on-the-ground described cases are, then they must have been developed in flow that met physical conditions allowing bedload transport. That is, the Rouse number $p = Ws/kU_*$ must exceed 2.5. With the help of the Rouse number, we can test the postulate that “chevrons” are tsunami deposits, that is, do bedload conditions exist in overland flows of the scale suggested? For the postulated flows and given grain sizes, we investigate transport regimes by varying flow depth, roughness, and Froude number. In our analysis, none of the conditions specified generate pure bedload transport ($p > 2.5$), which is the condition for ripple and dune stability. Most of the conditions specified result in pure suspended load transport ($p < 0.8$). For example, if we take a “chevron” made of 1 mm sand, having a bedform

height of 10 m (therefore a minimum flow depth of 20 m) and assume a roughness of 1 m, the Rouse number for $F = 1$ is 0.7 and for $F = 2$ is 0.4. Many of the “chevrons” are found at elevations of more than 50 m (up to 200 m) above sea level. If these “chevrons” really were subaqueous, under such flow depths bedload transport is not possible.

References

- Abbott D., Bryant E.A., Gusiakov V., Masse W.B., Raveloson A., Razafindrakoto H. (2006). *Report of International Tsunami Expedition to Madagascar*: www.ldeo.columbia.edu/users/menke/slides/madagascar06/report.pdf
- Abbott D., Bryant T., Gusiakov V., Masse W. (2007). *Megatsunami of the world ocean: Did they occur in the recent past?* Eos (Transactions American Geophysical Union), 88(23), Joint Assembly Supplement, Abstract PP42A-04.
- Bryant E. (2001). *Tsunami. The Underrated Hazard*. Cambridge University Press, 320 pp.
- Hearty P.J., Neumann A.C., Kaufman D.S. (1998). *Chevron ridges and runup deposits in the Bahamas from storms late in oxygen isotope substage 5e*. Quaternary Research, 50, 309-322.
- Hearty P.J., Tormey B.R., A.C. Neumann (2002). *Discussion of “Palaeoclimatic significance of co-occurring wind and water-induced sedimentary structures in the last-interglacial coastal deposits from Bermuda and the Bahamas”* (Kindler & Strasser, 2000, *Sedimentary Geology*, 131, 1-7). *Sedimentary Geology*, 147, 434-436.
- Kelletat D., Scheffers A. (2003). *Chevron-shaped accumulations along the coastlines of Australia as potential tsunami evidences?* Science of Tsunami Hazards, 21 (3), 174-188.
- Kindler P., Strasser A. (2000). *Palaeoclimatic significance of co-occurring wind- and water-induced sedimentary structures in last-interglacial coastal deposits from Bermuda and the Bahamas*. Sed. Geol., 131, 1-7.
- Kindler P., Strasser A. (2002). *Palaeoclimatic significance of co-occurring wind- and water-induced sedimentary structures in last-interglacial coastal deposits from Bermuda to the Bahamas: response to Hearty et al.’s comment*. *Sedimentary Geology*, 147, 437-443.
- Masse W. B. (2007). *The archaeology and anthropology of Quaternary Period cosmic impact*, in Bobrowsky, P.T. and Rickman, H., eds., *Comet/Asteroid Impacts and Human Society*. Springer-Verlag, Berlin, 25-70.
- Pinter N., Ishman S.E. (2008). *Impacts, megatsunami, and other extraordinary claims*. GSA Today, January 2008, 37 pp.

- Titov V.V., Synolakis C.E. (1998). *Numerical modeling of tidal wave runup*: J. Waterway, Port & Coastal Engineering, 124, 157-171.
- Ward S.N., Asphaug E. (2000). *Asteroid impact tsunamis: a probabilistic hazard assessment*, Icarus, 145, 64–78.
- Weiss R., Wünnemann K. (2007). *Large waves caused by oceanic impacts of meteorites*. In: Kundu A (ed) *Tsunamis and Nonlinear Waves*, Springer-Verlag, Berlin, 235-260.



2nd International Tsunami Field Symposium

IGCP Project 495

Quaternary Land-Ocean Interactions:
Driving Mechanisms and Coastal Responses

Ostuni (Italy) and Ionian Islands (Greece) 22-28 September 2008



Project 495

Zahibo N.¹, Pelinovsky E.², Didenkulova I.³, Nikolkina I.¹

Tsunamis in the French West Indies, Lesser Antilles, Caribbean

¹Laboratoire de Physique Atmosphérique et Tropicale, Département de Physique, Université Antilles
Guyane, Pointe-a-Pitre, France, e-mail: narcisse.zahibo@univ-ag.fr;

²Department of Nonlinear Geophysical Processes, Institute of Applied Physics, Nizhny Novgorod, Russia
e-mail: Pelinovsky@hydro.appl.sci-nnov.ru;

³Institute of Cybernetics, Tallinn University of Technology, Tallinn, Estonia, e-mail: ira@cs.ioc.ee

Keywords: *Tsunami, French West Indies, Lesser Antilles, Caribbean*

The tsunami catalogue has been recently created for the Caribbean Sea (Lander et al, 2002; HTDB/ATL, 2002; O'Loughlin & Lander, 2003; NGDC, 2006) and in particular, for the Lesser Antilles (Zahibo & Pelinovsky, 2001, 2006). In the past 500 years this region has had devastating tsunamis that caused damage in many states of the Caribbean Basin. According to Lander et al (2002), totally 91 waves reported might have been tsunami. Of these, 27 are judged by the authors to be true verified tsunamis; and the additional nine are considered to be very likely true tsunamis. The tsunami list for the 20th century contains 33 events, thus one every three years.

The present paper has a goal to revise the historical data of tsunamis for the French West Indies (Guadeloupe, Martinique, St Martin and several small islands) using all available publications and results of numerical simulations.

In this paper only true and almost true events are represented, which classification corresponds to the validity 4 ("**Definite tsunami**. Tsunami did occur.

Data corroborated or deemed valid information") and 3 ("**Probable tsunami**. Likely or probable tsunami occurrence. Reliable observations for corroboration are few") according to the definition of O'Loughlin and Lander (2003). Totally, eighteen events are selected as true and almost true. Ten events have been generated by underwater earthquakes in the Caribbean (06.04.1690, 24.04.1767, 30.11.1823, 30.11.1827, 11.01.1839, 07.05.1842, 08.02.1843, 18.11.1867, 16.03.1985, 21.11.2004); seven events - by the volcano eruptions (05.05.1902, 08.05.1902, 18.05.1902, 30.06.1902, 26.12.1997, 12.07.2003, 20.06.2006), and one is a teletsunami from Portugal after the Lisbon earthquake (01.11.1975). The geographical distribution of tsunami events is presented in Fig. 1, and the detailed information of tsunami characteristics for Guadeloupe Department is presented in Fig. 2.

Data of the tsunami field surveys after the Montserrat volcanic eruption occurred in 2003 and in 2006, Les Saintes earthquake in 2004, and Martinique earthquake in 2007 are presented.

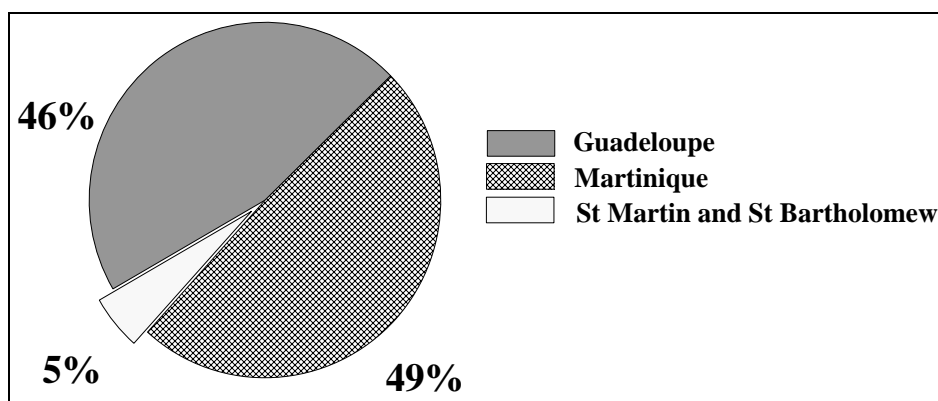


Figure 1. Geographic distribution of tsunamis in French West Indies.

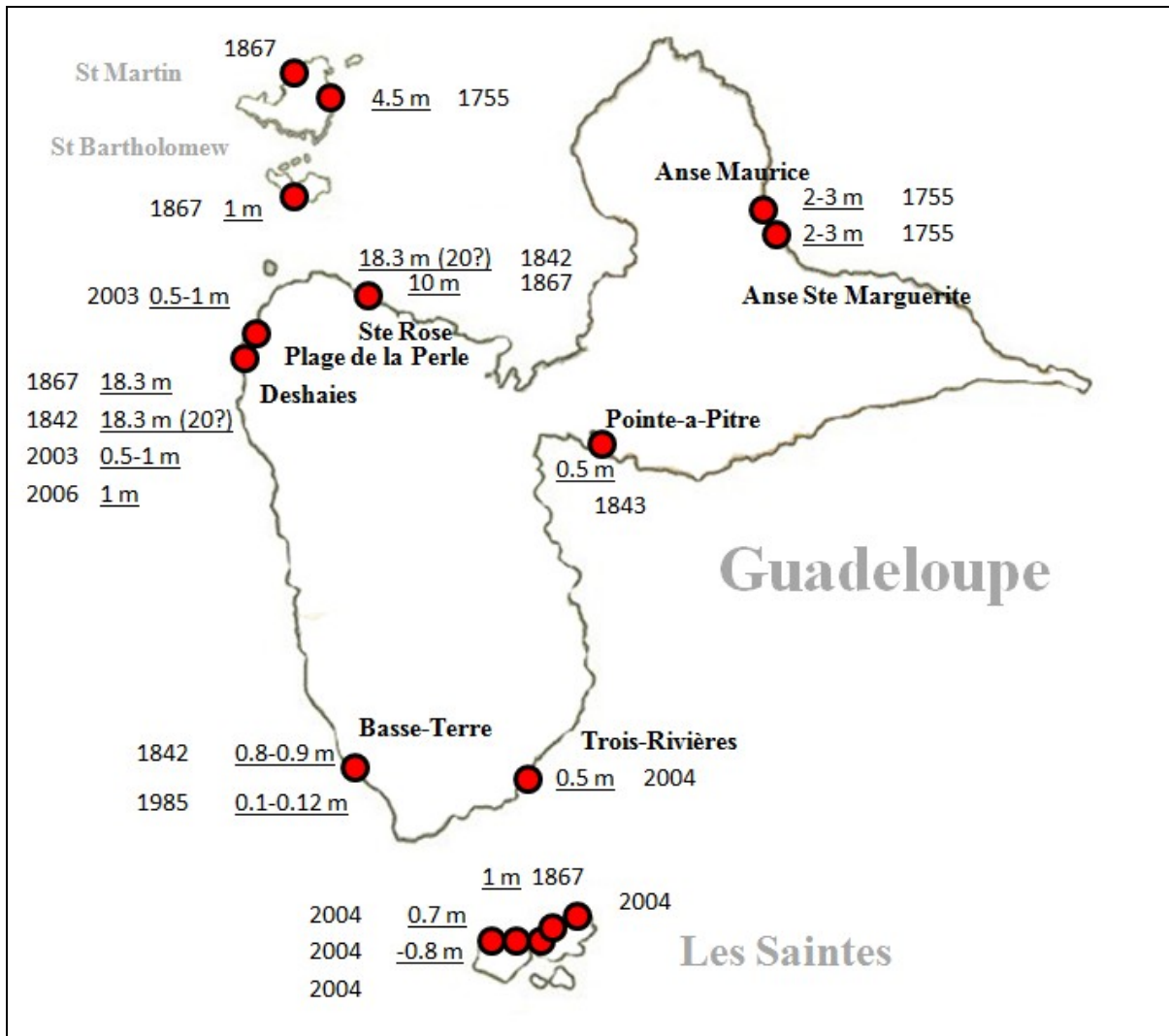


Figure 2. Runup locations in Guadeloupe department (runup locations are shown by circles).

References

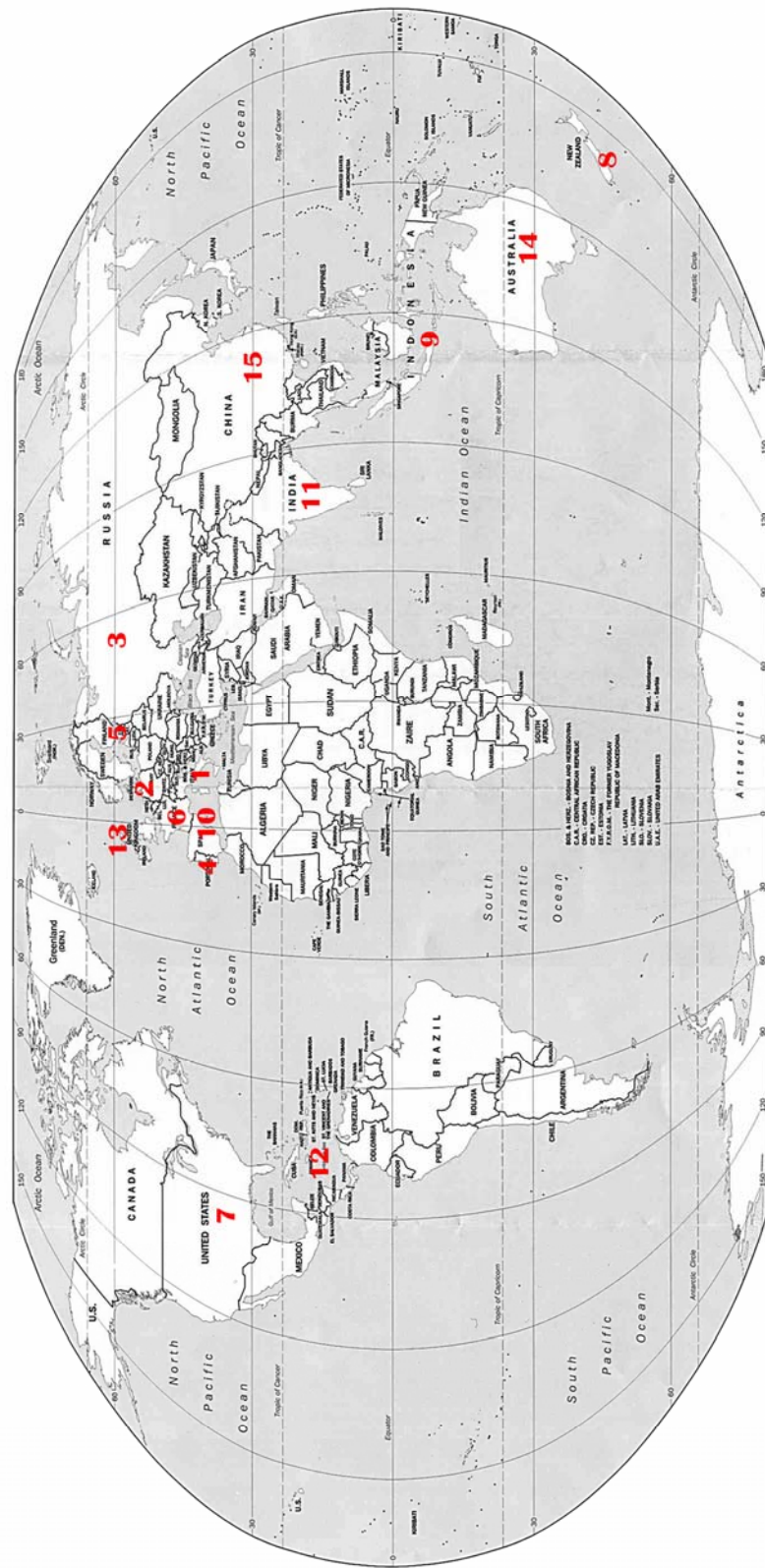
- HTDB/ATL (2002). *Expert Tsunami Database for the Atlantic. Version 3.6 of March 15, 2002.* Tsunami Laboratory, Novosibirsk, Russia.
- Lander J.F., Whiteside L.S., Lockridge P.A. (2002). *A brief history of tsunami in the Caribbean Sea.* Science of Tsunami Hazards, 20, 57-94.
- NGDC (National Geophysical Data Center) Tsunami Database, (2006). http://www.ngdc.noaa.gov/seg/hazard/tsu_db.shtml
- O'Loughlin K.F., Lander J.F. (2003). *Caribbean Tsunamis: A 500-Year History from 1498–1998.* Advances in Natural and Technological Hazards Research, 20, Kluwer.
- Zahibo N., Pelinovsky E. (2001). *Evaluation of tsunami risk in the Lesser Antilles.* Natural Hazard and Earth Sciences, 3, 221-231.
- Zahibo N., Pelinovsky E. (2006). *Tsunamis in the Lesser Antilles.* Caribbean Tsunami Hazard (Eds. Mercado-Irizarry A., Liu P.). World Sci., Singapore, 244-254.

Author's Index

- Abad M., 139
 Abramson H., 23
 Amijaya H., 13
 Anbarasu K., 109
 Andrade C., 19, 85
 Aristodemo F., 81
 Armigliato A., 9
 Baer S., 123
 Bahlburg H., 13, 161
 Barbano M. S., 41, 89, 157
 Bareth G., 167
 Becker-Heidmann P., 127
 Bellotti G., 81
 Bellucci L., 157
 Belousov A., 15
 Belousova M., 15
 Benavente C., 161
 Bianco F., 149
 Borja C., 57
 Borja F., 57
 Bourgeois J., 61, 69, 175
 Brizuela B., 49
 Browne T., 151
 Brückner H., 29, 167
 Burrato P., 23
 Cabero A., 57
 Cáceres L. M., 139
 Cachao M., 93
 Caputo R., 73
 Carretero M. I., 139
 Cataldo R., 149
 Civis J., 57
 Costa B., 155
 Costa P., 19, 85
 Coutou R., 135
 da Silva C. M., 19
 Dabrio C., 57
 Damato B., 97
 De Girolamo P., 81
 de Luque L., 57
 De Martini P. M., 23, 41, 89, 157
 Degg M., 147
 Del Carlo P., 157
 Di Bucci D., 73
 Di Risio M., 81
 Di Stefano A., 155
 Didenkulova I., 27, 179
 Dudley W. C., 131
 Engel M., 29
 Etienne S., 33, 93
 Federici P. R., 37
 Fernández-Steeger T., 123
 Fichaut B., 119
 Fountoulis I., 167
 Fournier J., 93
 Fracassi U., 73
 France D., 147
 Freitas M. C., 19, 85
 Gallazzi S., 9
 Gasperini L., 157
 Gelfenbaum G., 39, 131, 133
 Gerardi F., 41, 89, 157
 Goff J., 45
 González-Delgado J. A., 57
 Goy J. L., 57
 Grapmayer R., 167
 Graziani L., 23, 49
 Grützner C., 123, 143
 Jaffe B. E., 39, 131, 133
 Kelletat D., 29, 151
 Khan S., 135
 Khomarudin M. R., 51
 Klasen N., 167
 Kongko W., 51, 55, 113
 Koster B., 123
 Kravchunovskaya E. A., 61
 Kunz A., 161
 Lang F., 167
 Lario J., 57
 Lavigne F., 55, 93, 171
 Longhitano S., 155
 Ludwig R., 51
 MacInnes B. T., 61
 Manucci A., 9
 Maouche S., 65
 Maramai A., 23, 49
 Marsico A., 67
 Martin M. E., 69
 Masberg P., 167
 Mastronuzzi G., 9, 73, 97, 101, 105

- Mathes-Schmidt M., 143
 May S. M., 167
 Meghraoui M., 65
 Milella M., 77
 Miller S., 147
 Molfetta M. G., 81
 Monaco C., 155
 Moore A., 39
 Morhange C., 65
 Morin J., 93
 Morton R. A., 39, 133
 Nikolkina I., 179
 Oliveira M. A., 19, 85
 Pagnoni G., 9
 Panizzo A., 81
 Pantosti D., 23, 41, 89, 157
 Papanikolaou I., 143
 Paris R., 33, 55, 93, 171
 Pelinovsky E., 27, 179
 Petrillo A. F., 81
 Piepenbreier J., 13, 161
 Pignatelli C., 9, 67, 73, 77, 97, 101, 105
 Pinegina T. K., 61
 Pirrotta C., 89, 157
 Piscitelli A., 105
 Poizot E., 93
 Polonia A., 157
 Post J., 51
 Pozo M., 139
 Prabakaran K., 109
 Pranowo W., 51, 113
 Pratola L., 81
 Rajamanickam G. V., 115
 Regnauld H., 119
 Reicherter K., 123, 127, 143
 Richmond B. M., 131, 133
 Robinson E., 135
 Rodolfi G., 37
 Rodríguez-Vidal J., 139
 Roger J., 143
 Rössler S., 143
 Rowe D. A., 135, 147
 Ruiz F., 139
 Sakellariou D., 167
 Sansò P., 9, 73, 77, 149
 Saracino S., 77
 Schäbitz F., 29
 Scheffers A., 29, 101, 151
 Scheffers S., 101
 Schneider J. L., 171
 Scicchitano G., 155
 Selleri G., 73
 Smedile A., 89, 157
 Spencer C., 57
 Spiske M., 13, 161
 Strunz G., 51
 Suanez S., 119
 Switzer A. D., 163
 Taborda R., 19
 Tinti S., 9, 49
 Tonini R., 9
 Vitale A., 149
 Vonberg D., 123
 Vött A., 29, 167
 Wassmer P., 93, 171
 Watt S., 133
 Weiss R., 13, 175
 Wille M., 29
 Willershäuser T., 29
 Zahibo N., 179
 Zaniboni F., 9
 Zazo C., 57
 Zoßeder K., 51

- 1 Italy (Armigliato et al.; Barbano et al.; De Martini et al.; Federici & Ridolfi; Gerardi et al.; Graziani et al.; Marsico & Pignatelli; Mastronuzzi et al.; Milella et al.; Molfetta et al.; Pignatelli et al.; Sansó et al.; Scicchitano et al.; Smedile et al.)
- 2 Germany (Bahlbarg et al.; Engel et al.; Khomarudin et al.; Reicherter et al.; Rossler et al.; Spiske et al.; Vott et al.)
- 3 Russia (Belousov & Belousova)
- 4 Portugal (Costa et al.; Oliveira et al.)
- 5 Estonia (Didenkulo & Pelinovsky)



- 6 France (Etienne & Paris; Maouche et al.; Paris et al.; Regnaud et al.; Wassmer et al.; Zahibo et al.)
- 7 USA (Geiffenbaum et al.; McInnes et al.; Martin & Bourgeois; Richmond et al.; Weiss et al.)
- 8 New Zealand (Goff)
- 9 Indonesia (Kongko et al.)
- 10 Spain (Lario et al.; Rodriguez-Vidal et al.)
- 11 India (Prabakaran & Anbarasu)

- 12 Jamaica (Robinson et al.)
- 13 UK (Rowe et al.)
- 14 Australia (Scheffers et al.)
- 15 China (Switzer)

Index

Introduction	7
The 20 th February 1743 tsunamigenic earthquake in Apulia, Italy: investigation on the source from numerical tsunami modelling and geological evidences	9
Sedimentological characteristics of the July 17, 2006 tsunami in South Java.....	13
Deposits and effect of tsunamis generated by the 1996 underwater explosive eruption in Karymskoye Lake, Kamchatka, Russia	15
High energy boulder deposition in Barranco and Furnas lowlands, western Algarve (south Portugal)	19
Identification of tsunami deposits and liquefaction features in the Gargano area (Italy): paleoseismological implication.....	23
Analysis and modelling of the 1883 Krakatau volcanic tsunami	27
Traces of Holocene extreme wave events within sediment traps along the coast of Bonaire (Netherlands Antilles)	29
Boulder accumulations related to storms on the south coast of the Reykjanes Peninsula (Iceland).....	33
Traces of an ancient tsunami event on the Archangelos coast (Southern Peloponnese, Lakonia, Greece)	37
Variations in Tsunami deposit thickness: the role of pre-existing topography.....	39
Discrimination of tsunami sources (earthquake or landslide) on the basis of historical data in Eastern Sicily and Southern Calabria	41
Local, regional, and nationwide palaeotsunamis – a comprehensive database refocuses ongoing and future palaeotsunami research (New Zealand).....	45
Four tsunami events in the Euro-Mediterranean region: analysis and reconstruction of the effects	49
People exposure and land-use damage estimation causes by tsunami using numerical modelling and GIS approaches (case study: South Coast of Java – Indonesia).....	51
Investigation on colliding wave of tsunami run-ups in December 26th 2004 Indian Ocean Tsunami	55
A review of the high energy events in the Gulf of Cadiz: tsunami vs. storm surges	57
A comparison of sediment eroded vs. deposited by the 15 Nov 2006 Kuril Island tsunami	61
Large boulder accumulation on the Algerian Coast. Evidence catastrophic tsunami events in the Western Mediterranean.....	65
Laser Scanner survey to rebuild large boulder accumulated by extreme event in Torre Squillace (Southern Apulia – Italy)	67
Candidate tsunami deposit near Seattle, Washington state, USA.....	69
Morphological data and the definition of tsunamogenic areas between Apulia (Italy) and Ionian Islands (Greece)	73
Extreme events frequency and associated coastal damages along the coast of Salento (Southern Italy)	77

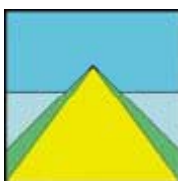
Three-dimensional large scale experiments on tsunamis generated by landslide along the coast of a conical island	81
Using the historical record and geomorphological setting to identify tsunami deposits in the southwestern coast of Algarve (Portugal).....	85
Geological evidence of paleotsunamis at Torre degli Inglesi (northeastern Sicily).....	89
Modelling sediment transport and deposition by the 2004 tsunami in Sumatra (Indonesia)	93
A terrestrial laser scanner based method to assess a tsunami wave inland penetration	97
Evaluation of tsunami flooding from geomorphological evidence in Bonaire (Netherland Antilles)	101
Hydrodynamical equations to evaluate extreme meteorological events impact along Adriatic coast of Apulia (Southern Italy).....	105
Modelling of Tsunami inundation for the coastal regions of Tamilnadu, India.....	109
Modelling of the Bengkulu Minor Tsunami Event, September 12, 2007, West of Sumatra, Indonesia.....	113
Distribution of sediments during pre and post-tsunami of 26 th Dec. 2004 along the Central Tamil Nadu, east Coast of India.....	115
Storms or Tsunamis? The case of boulder accumulations on the coasts of Brittany, western France	119
The sedimentary inventory of the 1755 Lisbon tsunami along the Gulf of Cádiz (southwestern Spain).....	123
Tsunamites in lagunas: remains of the 1522 Almería earthquake (western Mediterranean)	127
Recent tsunami and storm wave deposits, SE Hawaii	131
Spatial characteristics of coarse-clast deposits, Boca Olivia, NE Bonaire	133
Size of shoreline boulders moved and emplaced by recent hurricanes, Jamaica	135
Morphosedimentary features of historical tsunamis in the Guadalquivir estuary (SW of Spain).....	139
In search of the 479 BC Tsunami and its sediments in the Thermaikos Gulf area (northern Greece).....	143
Tsunami hazard mapping, SW Jamaica	147
A web site for historical tsunami of Salento (Apulia, Italy)	149
Wave-emplaced coarse debris and mega-clasts in Ireland and Scotland: A contribution to the question of boulder transport in the littoral environment	151
Tsunami deposits in the Siracusa coastal area (south-eastern Sicily)	155
Paleotsunami deposits in the Augusta Bay area (Eastern Sicily, Italy): combining onshore and offshore data ..	157
Historical tsunami events along the coast of Peru – sedimentology and dating	161
20 years of palaeotsunami studies on coastal sandsheets: a review	163
Tsunamite findings along the shores of the Eastern Ionian Sea – the Cefalonia case study (NW Greece)	167

Sedimentary signature of the December 26 th 2004 tsunami along the north eastern shore of Banda Aceh: anisotropy of magnetic susceptibility (AMS) contribution to a better understanding of the tsunami wave train dynamic	171
“Chevrons” are not mega-tsunami deposits – a sedimentologic assessment	175
Tsunamis in the French West Indies, Lesser Antilles, Caribbean	179
Author’s Index.....	181
Index.....	185

Publication designer and art copy editor:

Dr. Arcangelo Piscitelli

GDS – Geo Data Service, Taranto, Italy



Copyright 2008

GI²S Coast – gruppo Informale Interuniversitario di Studi Costieri

Part of this publication may be reproduced if the source is clearly reported.
This book is out of print. It is available from editors.

Leica ScanStation 2 Exceptional Speed, Outstanding Versatility



- when it has to be **right**

Leica
Geosystems

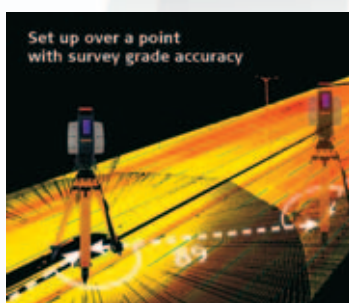
- 
- The main image shows a Leica ScanStation 2 total station, a grey and black surveying instrument with a red handle and a red vertical stripe. It is mounted on a black tripod. The background is a blue sky with white clouds.
- Very-High Speed, Pulsed Laser**
 Excellent range, up to 10-times faster than other pulsed scanners, and capable of single point surveying
 - Integrated High-Resolution Camera**
 For fast scene selection and compelling, auto-rectified photo overlays
 - HI Marks, Tribrach Mount, Carry Handle, and QuickScan™ Button**
 Standard procedures and accessories make ScanStation 2 easy to learn
 - Advanced Timing Electronics**
 Integrated with a patented microchip laser to deliver accurate, low-noise distance measurements
 - X-function Compatibility**
 Interoperable with Leica System 1200
 - Advanced Scripting Controls**
 SmartScan™ firmware allows automated sequencing of scans and unattended operation
 - Integrated, Dual-Axis Level Compensator**
 For survey-grade traversing and stakeout
 - External Bubble Level**
 Conveniently located on back of rotating scan head

A New Level of As-built & Topographic Surveying ... And More



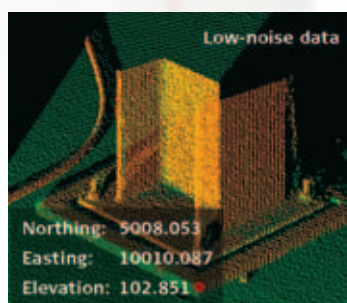
1. Full Field-of-view

One of its four (4) fundamental total station features, the full dome field-of-view lets users capture overhead, vertical, horizontal, and sub-level geometry with equal ease.



2. Survey-grade Dual-axis (Tilt) Compensation

Like a total station, users can setup ScanStation 2 over control, traverse, resection, and even stakeout and point with it.



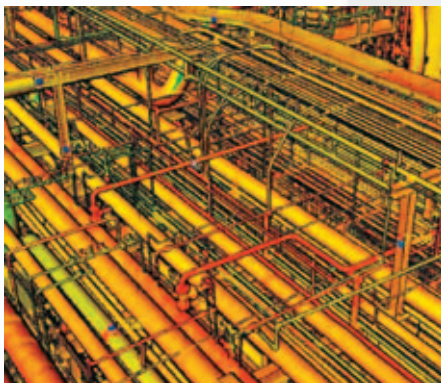
3. Survey-grade Accuracy

As part of the ScanStation instrument category, ScanStation 2 delivers survey-grade accuracy for each point. Ultra-fine scanning with a small beam at long range also enables optimal project control & registration.



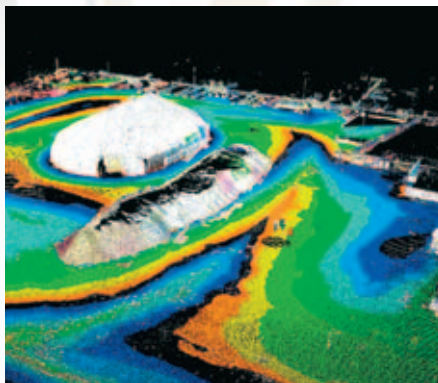
4. Excellent Range

ScanStation 2's detection range (300 m @ 90 % reflectivity), high accuracy, small beam, and ultra-fine scanning combine for a "useful range" that addresses many typical sites.



Plants

From a single vessel to entire plants and factories – accurate as-built data makes retrofit projects and maintenance/operations go more smoothly.



Volumes

With its high scan speed, 300 m (max) reflectorless range, and survey accuracy, ScanStation 2 is more cost-effective, more precise and safer for many pile and pit surveys.



Variety

ScanStation 2 provides unobtrusive, fast and complete surveys for a wide range of accident scenes, archaeology sites, heritage structures, and more.

Leica ScanStation 2 Performance Specifications

Instrument type	Pulsed, dual-axis compensated, very-high speed laser scanner, with survey-grade accuracy, range, and field-of-view		
User interface	Notebook or Tablet PC		
Camera	Integrated high-resolution digital camera		
Accuracy of single measurement	Position*	6 mm	
	Distance*	4 mm	
	Angle (horizontal/vertical)	60 μrad/60 μrad	
		(3.8 mgon/3.8 mgon) **	
Laser spot size	From 0 – 50 m: 4 mm (FWHH-based); 6 mm (Gaussian-based)		
Modeled surface precision/noise	2 mm **		
Target acquisition	2 mm std. deviation		
Dual-axis compensator	Resolution 1", dynamic range +/- 5'		
Data integrity monitoring	Periodic self-check during operation and start-up		
Laser scanning system	Range	300 m @ 90 %; 134 m @18 % albedo	
	Scan rate	Maximum instantaneous: up to 50,000 points/sec	
		Average: dependent on specific scan density and field-of-view	
	Scan density	<1 mm max, through full range; fully selectable horizontal and vertical spacing; single point dwell capability	
Laser class	3R (IEC-60825-1), visible green		
Lighting	Fully operational between bright sunlight and complete darkness		
Power supply	36V; AC or DC; hot swappable		

Specifications subject to change without notice

See Leica ScanStation 2 Product Specifications for full technical data

* At 50 m range, one sigma

** One sigma

Illustrations, descriptions and technical specifications are not binding and may change.
Printed in Switzerland – Copyright Leica Geosystems AG, Heerbrugg, Switzerland, 2007.
760368en – VI.07 – RDV



Total Quality Management –
Our commitment to total
customer satisfaction

Ask your local Leica Geosystems
dealer for more information
about our TQM program.

Laser class 3R in accordance with
IEC 60825-1 resp. EN 60825-1



Leica ScanStation 2
Product information
and specifications



Leica HDS6000
Product information
and specifications



**Leica Cyclone 5.8
MODEL, SURVEY**
Product information



**Leica Cyclone 5.8
REGISTER**
Product information



**Leica Cyclone 5.8
SCAN**
Product information



Colagem Ufficio Immagine Lorenza comunicazione e pubblicità - foto: philar

Our values for building the future



Our corporate culture is the result of shared values, a heritage that represents the company's strength and our commitment to the future. It has always been our policy to **protect the environment**, through the restoration and reutilization of the land; to develop our ideas by investing in **research** and **technology**; and to establish relations based on trust, constantly maintaining professional standards and **guaranteeing the excellency of our products**.

At present, Colacem is one of the most important industrial groups in Italy: progress and corporate culture are encouraged, helping our communities to grow up and develop.

COLAGEM
GRUPPO FINANCO

Colacem company profile

Colacem currently represents an avant-garde Italian industrial group, which has been able to grow and transform itself during the years, thanks to an always modern and innovative company policy and philosophy.

The company is present all across Italy with 7 full-cycle production plants: Caravate (VA), Rassina (AR), Ghigiano-Gubbio (PG), Sesto Campano (IS), Galatina (Le), Ragusa and Modica (Rg); 2 grinding centers: Acquasparta (TR) and Limatola (BN); 1 production plant for pre-mixed products : Salone (Roma), 2 terminals: Savona and Mestre (VE) and 3 warehouses in Ravenna, Ancona and Ascoli Piceno.

The 3 full-cycle plants located in Tunisi (Tunisia), Sabana Grande de Palenque (Dominican Republic) and Kilmar-Grenville sur la Rouge (Canada), and the terminals of Alicante and Cartagena in Spain , well represent the international dimension of the whole Group.

The 2007 turnover exceeded 493 million Euro (the consolidated aggregated turnover of the Financo Group is equal to 866 million Euro), with an increase of over 2% compared to the year 2006.

The number of employees exceeds 1450 people.

The entrepreneurial history of the Colaicovo Family is the result of hard working, new ideas and expertise : the Colaicovo brothers, Pasquale, Giovanni, Franco and Carlo, have been able to create such a company in a few decades, which is now among the first Italian producers and distributors of cement.

Colacem style is clear: a firm commitment aimed to enabling any division and department of the Company to grow and develop. This has led the company to attain very prestigious goals in the technologic and innovation field, which are recognized internationally: future-oriented dynamics; a unique know-how that has allowed the company to achieve important organization and technological results even in the design, construction and management of their production plants.

A winning strategy constantly marked by success, thanks to a company policy that has always seen the research activity as the basis of its development process. It resulted in a highly valuable background of knowledge and experience aimed to performing a correct management of both natural and human resources .

An active and reliable approach towards social and environmental subjects , centered around industrial purposes that combine ecologic preservation with economic growth.